Chem Soc Rev

REVIEW ARTICLE

Cite this: DOI: 10.1039/c9cs00720b

Advances in covalent kinase inhibitors

Ayah Abdeldayem,†[ab] Yasir S. Raouf,†[ab] Stefan N. Constantinescu,[c] Richard Moriggl[d] and Patrick T. Gunning*[ab]

Received 21st October 2019

DOI: 10.1039/c9cs00720b

rsc.li/chem-soc-rev

Over the past decade, covalent kinase inhibitors (CKI) have seen a resurgence in drug discovery. Covalency affords a unique set of advantages as well as challenges relative to their non-covalent counterpart. After reversible protein target recognition and binding, covalent inhibitors irreversibly modify a proximal nucleophilic residue on the protein *via* reaction with an electrophile. To date, the acrylamide group remains the predominantly employed electrophile in CKI development, with its incorporation in the majority of clinical candidates and FDA approved covalent therapies. Nonetheless, in recent years considerable efforts have ensued to characterize alternative electrophiles that exhibit irreversible or reversibly covalent binding mechanisms towards cysteine thiols and other amino acids. This review article provides a comprehensive overview of CKIs reported in the literature over a decade period, 2007–2018. Emphasis is placed on the rationale behind warhead choice, optimization approach, and inhibitor design. Current FDA approved CKIs are also highlighted, in addition to a detailed analysis of the common trends and themes observed within the listed data set.

Introduction

The emergence of covalent molecules as viable therapeutics can be largely attributed to the salicylate revolution and the development of acetylsalicylic acid (ASA, Aspirin) in the 19th century. Studies into the mechanism-of-action revealed that a nucleophilic serine hydroxyl on cyclooxygenase (COX-1, COX-2) enzymes irreversibly modifies the electrophilic acetyl within ASA (Fig. 1). Inactivation of COX function

[a] *Department of Chemical & Physical Sciences, University of Toronto, 3359 Mississauga Road, Mississauga, ON L5L 1C6, Canada. E-mail: patrick.gunning@utoronto.ca*

[b] *Department of Chemistry, University of Toronto, 80 St. George Street, Toronto, ON M5S 3H6, Canada*

[c] *Ludwig Institute for Cancer Research, Avenue Hippocrate 74, Brussels, Belgium*

[d] *Institute of Animal Breeding and Genetics, University of Veterinary Medicine, 1210 Vienna, Austria*

† These authors contributed equally to this work.

Ayah Abdeldayem

Ayah Abdeldayem obtained her Honours Bachelor of Science degree in Chemistry and Biology from the University of Toronto in 2017. She is currently pursuing her PhD degree under the supervision of Prof. Patrick Gunning at the University of Toronto. Her research interests combine aspects of chemical biology, proteomics and activity-based protein profiling (ABPP) as well as medicinal chemistry efforts. Currently, she is focused on the development of novel covalent probes to aid in the design of selective kinase inhibitors. Outside of her research, she is an active member of the graduate student association and serves on several university councils.

Yasir S. Raouf

Yasir received his Honours Bachelor of Science degree in Chemistry and Biology from the University of Toronto, Canada (2016). He then embarked upon a direct-entry PhD at the University of Toronto under the supervision of Prof. Patrick Gunning. As a medicinal chemist, his interest lies at the interface of synthetic, biological and computational chemistries. His research focuses on developing isozyme-selective lead compounds (reversible or covalent) with efficacy against various oncology targets (e.g. kinases, histone deacetylases). Yasir is also the recipient of a provincial Ontario Graduate Scholarship and a recent nationwide grant to initiate studies in Duchenne Muscular Dystrophy.

disrupts Prostaglandin synthesis, inducing an anti-inflammatory effect.[1,2] Following global commercial success, ASA remains an extensively investigated molecule with >700 clinical trials conducted annually on varying salicylate scaffolds, within various indications (*e.g.* cancer,[3] strokes,[4] cardiovascular or chronic inflammatory and autoimmune disease).[5] To date, it remains the most successful covalent therapeutic.

Traditionally, small molecules (ligands) achieve a biological response *via* reversible (non-covalent) binding to disease-implicated targets (receptors). This concept was first pioneered by Ehrlich[6] and Langley,[7,8] before seminal work on adrenergic receptors by Ahlquist[9] and methods of target identification by Lefkowitz *et al.*[10] An overview by Limbird[11] details the

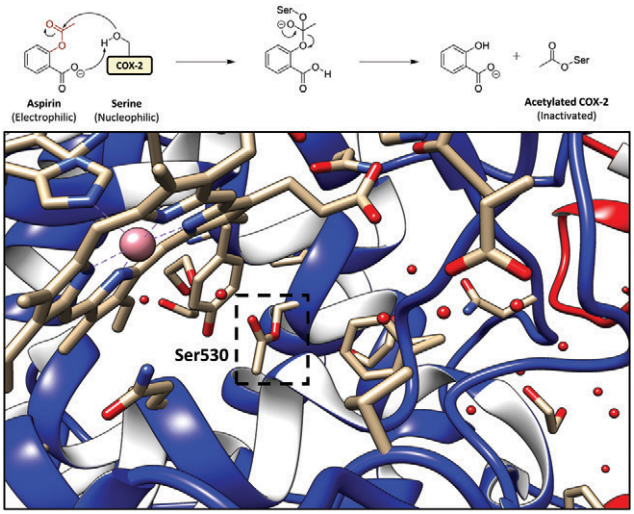

Fig. 1 (top) Covalent mechanism of aspirin (ASA) mediated inactivation of COX-2 *via* serine modification. The electrophilic motif is shown in maroon. (bottom) Crystal structure of acetylated COX-2 (PDB 5F19), highlighting O-acetyl Ser530.

Stefan N. Constantinescu

Stefan Constantinescu (MD, PhD) is Professor at the Université catholique de Louvain, de Duve Institute and Member of the Ludwig Institute for Cancer Research in Belgium. After attaining his MD, PhD, Prof. Constantinescu completed Post-doctoral studies at the Whitehead Institute in MIT with Prof. Harvey Lodish. His research has contributed to the discovery of the JAK2 V617F mutation in myeloproliferative neoplasms (MPNs), reported the first JAK1 and TYK2 active mutants in T-cell leukemias and identified the activation of thrombopoietin receptors by W515 mutants. He is currently a Member of the Royal Academy of Medicine of Belgium.

"Receptor" concept. Non-covalent drug receptor interactions are driven by enthalpic (*e.g.* hydrogen bonding) and entropic (*e.g.* hydrophobic effect) forces.

Receptors [R] are in dynamic equilibrium with inhibitors [I], forming a reversible complex [RI], characterized by an inhibitory equilibrium constant (K_i). In the special case of a covalent binder, this process involves two interrelated but discrete steps. The formation of an initial reversible complex is followed by a typically irreversible covalent bond, between an electron-deficient moiety (electrophile) on the ligand and an electron-rich residue (nucleophile) on the receptor (Fig. 2).

While selective covalent modification was historically serindipitious (*e.g.* ASA), as the field progressed, rationally

Richard Moriggl

Dr Richard Moriggl graduated in Molecular Biology (1997) at the University of Freiburg, Germany before postdoctoral studies at St. Jude Children's Research Hospital, USA and the Institute of Molecular Pathology, Austria. He served as cancer research director for 14 years and is currently Professor for Functional Cancer Genomics, University of Veterinary Medicine, Austria. His research studies core cancer pathway activation, with specific interest in the JAK–STAT pathway. He performs comparative pathology studies and pioneers targeted therapy in transgenic mouse models mimicking human cancer progression. Identifying Lead compounds targeting transcription factors or relevant kinases is also a primary research focus lab.

Patrick T. Gunning

Patrick T. Gunning is full Professor of chemistry and Canada research Chair in Medicinal Chemistry at the University of Toronto (UofT). Patrick received his BSc (2001) and PhD (2005) from the University of Glasgow before pursuing post-doctoral studies with Professor Andrew D. Hamilton (Yale). He then established a research group (2007) at UofT focused on small molecule inhibitors of protein–protein interactions, namely STAT3/STAT5. In this field, Dr Gunning has >100 publications with several awards and honours including, 2015 Rose Winer Levin Lectureship (Dana-Farber Cancer Institute), 2012 RSC MedChemComm Emerging Investigator Lectureship and 2016 Canadian Society for Chemistry's Bernard Belleau award.

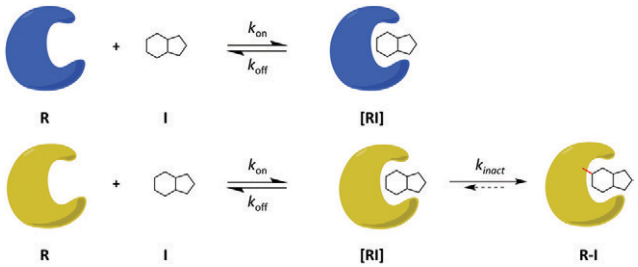

Fig. 2 General schematic of a non-covalent (blue) and covalent (yellow) binding event between a receptor [R] and inhibitor [I]. Adapted from R. A. Bauer,[12] with permission from Elsevier, copyright 2015.

designed molecules were designed to selectively modify a particular target of interest.

$$k_{on}[R][I] = k_{off}[RI] \quad (1)$$

$$K_i = \frac{[R][I]}{[RI]} = \frac{k_{off}}{k_{on}} \quad (2)$$

As seen in eqn (1); [R], [I] represent receptor and inhibitor equilibrium concentrations while k_{on}, k_{off} describe binding and dissociation kinetics, respectively.

By ensuring [R] ≪ [I] and measuring the first-order rate constant (k_{obs}) as a function of $[I]_{total}$, reaction kinetics can be described in a linear form (eqn (3)) to find the rate of target inactivation (k_{inact}).

$$\frac{1}{k_{obs}} = \frac{k_{inact}}{K_i}\left(\frac{1}{[I]}\right) + \frac{1}{k_{inact}} \quad (3)$$

While K_i describes non-covalent binding, k_{inact} defines the covalent bonding event. Note, true irreversibility is highly dependent on the motifs involved. While certain electrophiles form irreversible adducts (*e.g.* epoxides), others can form reversible-covalent interactions (*e.g.* disulphides).[13]

Long lived target inactivation tends to enhance potency and extend duration of action. This allows for smaller and less frequent dosing regimens while reducing idiosyncratic toxicities (IDTs), which generally improves both compliance and patient outcome.[14] Although covalent inhibitors are theoretically very attractive, there are several challenges to this approach.

One common example is off-target reactivity and subsequent cytotoxicity, which previously hindered the progress of covalent binders relative to reversible scaffolds. Historically, ASA paved the way for many successful covalent therapeutics; including penicillin (1928), omeprazole (1989), and ibrutinib (2013) (Fig. 3). It was estimated in 2011, a value of 33 billion USD was generated in total sales between 26 covalent drugs. As of 2017, >40 drugs covalently modify their target, against varying indications (*e.g.*, neurological disease, cancer) with many more small molecules in clinical development.[15]

In this article, we aim to comprehensively review the past 10 years (2007–2018) of covalent kinase inhibitors and the recent advancements in electrophilic warheads. General methods toward CKI design and lead identification are described along with considerations for nucleophilic target residue selection (Section 2). This is followed by reviewing reported CKIs utilizing acrylamide, α,β-unsaturated, α-halo-substituted electrophiles as well as other warheads (Section 3). The compounds are detailed

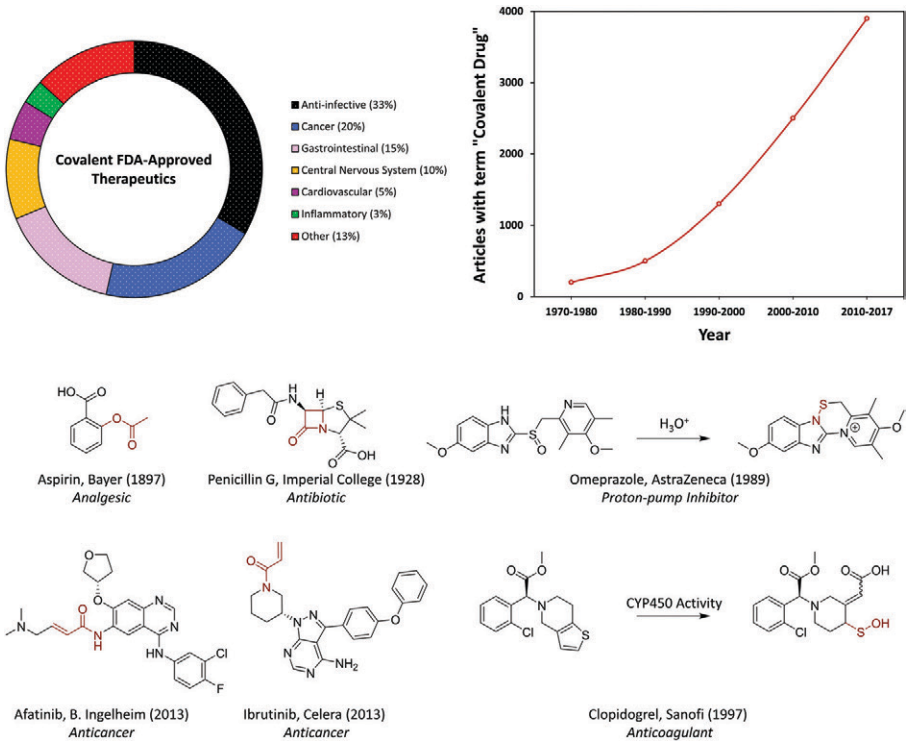

Fig. 3 (left) Percentage of FDA-approved covalent drugs by therapeutic indication (n = 39). (right) Exponential rise in articles containing the term "Covalent drug" between 1970–2017. (bottom) Chemical structures of clinically successful covalent drugs.

with a focus on electrophile used, target kinase, potency achieved, and current stage of preclinical/clinical development.

Kinases represent a highly investigated family of enzymes, which regulate protein phosphorylation. They play diverse regulatory roles within signalling pathways, controlling many key cellular processes. Perturbation of kinase activity is known to be implicated in many diseases, notably cancer, making them an attractive therapeutic target.[16] However, due to structural homology, selectivity is a challenge and kinases were initially deemed undruggable. Nonetheless, they have evolved into a key target in therapy development. In this regard, we will review the 6 FDA approved CKIs (as of late 2018); namely afatinib, osimertinib, neratinib, dacomitinib, ibrutinib and acalabrutinib, with an emphasis on their successes and challenges in the clinic (Section 4). Finally, the data presented within this article is consolidated, analysed, and the underlying trends described (Section 5). In this analysis, many aspects of inhibitor development were considered, such as, but not limited to; scaffold design, physicochemical properties, spatial distribution of nucleophilic residues, warhead design and recent developments in tuning electrophile reactivity.

Emergence of kinase-targeting in drug discovery

The human kinome comprises >500 kinases, with >400 Ser/Thr and >100 Tyr-specific isoforms along with ~ 50 pseudokinases[17] and ~ 25 atypical kinases.[18] As one of the largest gene families, they catalyze γ-phosphate transfer from adenosine triphosphate (ATP) to various cellular macromolecules (Fig. 4). Protein phosphorylation regulates a range of important cellular processes, such as protein localization, stability, protein folding properties, signal transduction and protein activity,[19] with implications in cellular homeostasis and disease. ATP is mainly synthesized in normal cells in the mitochondria *via* the electron transport chain (ETC).

Importantly, cancer cells have alternative ways to generate energy (in the form of ATP) during disease situations, complicating the picture of energy supply and kinase action. Thus, metabolism, proliferation and survival in conjunction with kinase action and ATP synthesis together with transcription, operate as tightly interwoven processes.

The value of kinases as drug targets was recognized after discovering the oncogenic potential of the SRC gene in coding for cancer-causing tyrosine kinases (c-Src proto-oncogene).[20] Subsequent research implicated aberrant kinase activity (generally due to genomic instability) in various diseases, such as immunogenic ailments, inflammations and cancer.[21] Tumorigenesis is typically sustained by several signal transduction pathways, thus inhibiting any one cascade may only partially alleviate cancer progression due to compensatory mechanisms. Counter wise, certain tumours develop a dependence on specific signalling oncogenes for their survival (a trait known as oncogene addiction).[22] Selective inhibition of these particular oncogenic drivers can abrogate disease progression. Thus, a concerted effort to develop kinase-selective molecules began in earnest.

Imatinib (Glivec),[23] an orally bioavailable, once daily-dosing 2-phenylaminopyrimidine and reversible inhibitor of fusion-gene product, Breakpoint cluster region (BCR)-Abelson murine leukaemia (ABL) kinase, was approved in 2001 for Philadelphia chromosome-positive chronic myelogenous leukaemia (Ph^+-CML). Imatinib is ATP-competitive, occupying the kinase catalytic domain, and potently inhibiting phosphorylation, blocking subsequent signal transduction thereby inducing leukemic cell apoptosis (Fig. 5).[24]

Imatinib was a major milestone in kinase drug discovery. High-throughput Screening (HTS) methods followed by extensive Structure–activity relationships (SAR) identified this small molecule as one of the first examples of *targeted* kinase inhibition. It demonstrated *in vivo* efficacy and unprecedented clinical success against a previously lethal pathology.

To date, it remains a gold standard for Ph^+-CML patients and has since been approved for >10 indications.[25] Following this success, kinase inhibition has grown to become one of the most well studied fields in drug discovery. Currently, >45 drugs are bonafide kinase inhibitors, almost all of which are small molecules. In 2017 alone, six novel molecules were FDA approved, excluding those compounds in development, pre-clinical or clinical trials.[26] Notably, while most molecules function as reversible ATP competitive inhibitors, kinase inhibition can be achieved in a variety of ways.

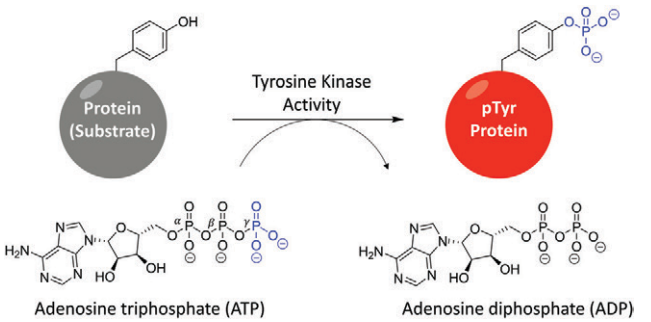

Fig. 4 Schematic describing the catalytic phosphorylation of substrate proteins by tyrosine kinases using ATP.

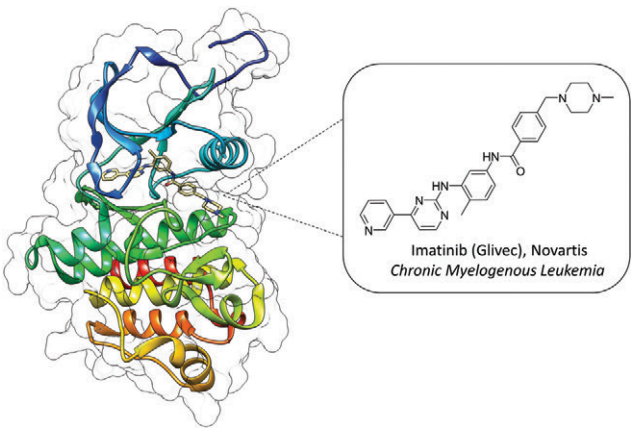

Fig. 5 Co-crystal structure of Imatinib (beige) bound to ABL kinase (PDB 1IEP), shown as coloured ribbon representation.

Types of kinase inhibitors

The classification of kinase inhibitors is centered around the enzyme-ligand complex. As bi-lobal structures, kinases contain a generally β-stranded amino-lobe (N-lobe), which mediates ATP binding and an α-helical carboxy-lobe (C-lobe), which is important for substrate binding. These domains are linked together by a short and flexible stretch of conserved residues known as the hinge region. A Gly-rich loop within the N-lobe is known as the ATP binding loop (P-loop) and it interacts with ATP α and β phosphates. A second, more variable region (in size and sequence) called the activation loop (A-loop), plays a regulatory role in kinase activity. The A-loop exists in two conformations (open/closed), which characterize an active kinase state, (open A-loop) allowing substrate binding and an inactive kinase state (closed A-loop), blocking the active site.

The N-terminus of the A-loop also contains a conserved Asp-Phe-Gly sequence (DFG motif) which is also important in ATP binding (Fig. 6).[27]

Kinase inhibitors were first categorized by Dar and Shokat[28] into three classes: I, II and III. Type I molecules bind the active kinase conformation within the ATP pocket. Type II bind the inactive kinase conformation and type III are non-ATP competitive inhibitors, which bind proximal to the active site (*i.e.* allosteric). To extend this further, molecules binding more distal were defined by Gavrin and Saiah as type IV inhibitors.[29] Active and inactive kinase conformations are defined relative to the positioning of the DFG motif. In the active state, the Phe residue is buried inwards towards the hydrophobic pocket in the groove between the two kinase lobes (DFG-in). Conversely, in the inactive state, a 180°-flip reorients the Phe residue outwards, forming the DFG-out conformation. Zuccotto *et al.*,[30] proposed type I 1/2 inhibitors, which bind the DFG-in (a feature typically seen in active kinases) within the ATP pocket of inactive kinases. Lamba and Gosh[31] introduced type V inhibitors as bivalent molecules which bind two distinct regions within the catalytic domain. Finally, type VI inhibitors bind through permanent/long-lived covalent attachments. These classes represent an expanded and thorough representation of different binding modes by a kinase–ligand pair (Table 1).

Covalent target engagement: irreversible *vs.* reversible

Fundamentally, a covalent bond occurs *via* the equal sharing of electron pairs between atoms. In the context of CKI development, this typically involves, a ligand electrophile (*e.g.* acrylamide) and a target nucleophile (*e.g.* a cysteine sulfhydryl). However, achieving selective kinase targeting is challenging and cytotoxicity through extended or permanent off-target modifications is possible. Such concerns of irreversibility, non-specific hyperreactivity and IDTs have lately catalyzed the development of long-lived reversible covalent inhibitors.[32–35] While the development of such inhibitors has progressed tremendously, reversible covalent chemistry was first observed in the 1960s by Pritchard *et al.*[36] It was found that thiols react rapidly with 2-cyanoacrylates at physiological pH, yet the product could not be isolated. Recently, in work by Serafimova *et al.*,[35] this was hypothesized to result from rapid equilibration and reversibility.

Covalent reversibility is characterized by the lifetime of a protein–ligand complex and rate of covalent dissociation (k_{-2}). This description introduced the notion of ligand-residence time (τ), first reported by Tummino and Copeland.[37] Defined as the period of time a molecule resides within a binding site, it is generally represented (in a two-state binding model) as the reciprocal of k_{-2} (Scheme 1). Studies have shown molecules can span a broad range of residence times.[37] For instance, in the human dipeptidyl exopeptidase IV (DPP IV) inhibitors, vildagliptin and sitagliptin (used as potential therapies for type II diabetes), while the first is entirely reversible (τ = 0.1 h), the second is reversible covalent (τ = 5.0 h).[38,39]

Assessing true covalent inhibition is quantitatively determined by the second order rate constant (k_{inact}/K_i). A larger ratio typically indicates higher potency. In order to delineate individual contributions of covalent reactivity (k_{inact}) and binding affinity (K_i), it is common to plot these parameters (independently) to generate a quadrant scale (Fig. 7). Ideally, a compound should reside within Q3, which includes high affinity structures (K_i < 10 nM) with moderate-weak covalent reactivity (k_{inact} < 0.05 s^{-1}). In contrast, Q1 contains highly reactive, low affinity compounds (non-specific alkylators), Q2 describes high reactivity scaffolds with good affinity (also desirable) while Q4 defines low affinity, weakly reactive inhibitors.

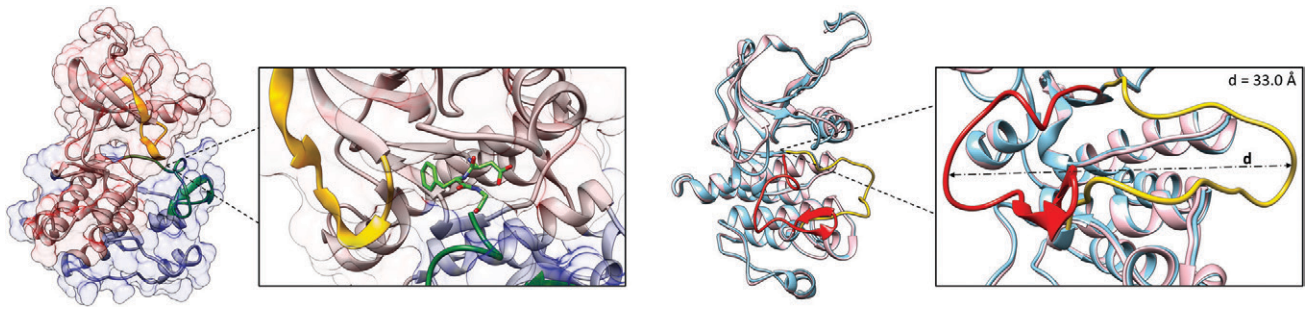

Fig. 6 (left) Crystal structure of ABL kinase in the inactive conformation (PDB 1IEP), amino-lobe (red) surface, carboxy-lobe (blue surface), P-loop (yellow ribbon), A-loop (green ribbon). Left inset displays the DFG motif. (right) Superposition of inactive and active (PDB 2GQG) conformations of ABL kinase. Active kinase A-loop (red ribbon), inactive kinase A-loop (yellow ribbon). Right inset shows translational distance between both A-loop conformers.

Table 1 Types of kinase inhibitors and specific distinguishing attributes. PDB IDs retrieved from (http://www.rcsb.org)

Type	Binding mode	DFG	ATP-competitive	Reversible	Ligand-kinase (PDB)
I	Active kinase-ATP pocket	In	Yes	Yes	Dasatinib-ABL (2G2Q)
$I_{1/2}$	Inactive kinase-ATP pocket	In	Yes	Yes	Crizotinib-MET (2WGJ)
II	Inactive kinase-ATP pocket	Out	Yes	Yes	Imatinib-ABL (1IEP)
III	Allosteric (proximal)	Varies	No	Yes	TAK733-MEK1 (3PP1)
IV	Allosteric (distal)	Varies	No	Yes	GNF2-ABL (3K5V)
V	Bivalent	Varies	Varies	Yes	Lenvatinib-VEGFR2 (3WZD)
VI	Covalent	Varies	No	Varies	Afatinib-EGFR (4G5J)

Scheme 1 General reaction scheme of a covalent binding interaction between a receptor (R) and inhibitor (I). Inset image describes the relationship between ligand residence time (τ) and covalent bond reversibility (k_{-2}).

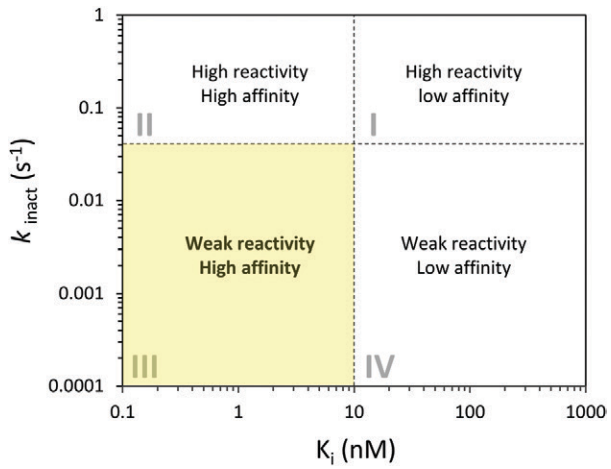

Fig. 7 Covalency quadrant scale to classify covalent binders by comparing the rate of covalent bond formation (k_{inact}) against inhibitory binding affinity (K_i).

The mechanism of covalent modification, rate of inactivation (k_{inact}) and intrinsic reversibility largely depend on electrophile structure and electronics. Against one nucleophile, certain warheads react irreversibly (*e.g.* enones), whilst others are reversible (*e.g.* 2-cyanoacrylamides).

In this example, reversibility is achieved by tuning the acidity of the acryl α-proton using electron-withdrawing groups (EWGs). For this purpose, the cyano-motif is most common. Irreversible electrophiles include acrylamides, epoxides and acrylates whilst 2-cyanoacrylamides, disulphides and boronic acids represent reversibly covalent warheads (Scheme 2).[32,33]

Advantages & disadvantages of CKIs

A covalent approach offers several advantages relative to non-covalent inhibitors, typically addressing potency, selectivity, toxicity, dosing and target-scope. These are briefly described below, yet for a more in-depth analysis we refer to following excellent ref. 12, 13, 15 and 40–43.

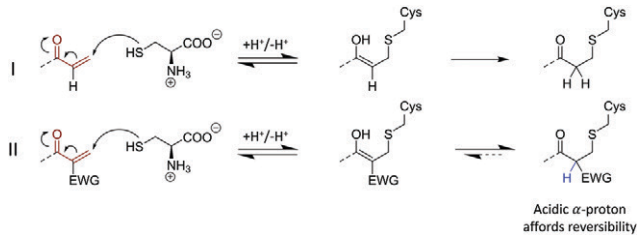

Scheme 2 Reaction schemes of irreversible (I) and reversible (II) covalent interactions of α,β-unsaturated carbonyl electrophiles and nucleophilic cysteines, EWGs: –CN, –F, $–NO_2$.

Advantages

Potency. Drugs aim to achieve strong potency against a therapeutically relevant target. This largely depends on target engagement and binding thermodynamics. Non-covalent molecules rely on intermolecular forces to achieve target recognition and effective binding potency. Increases in molecule size can allow for additional target interactions, however, it may impact pharmacokinetic (PK) parameters (*e.g.* metabolic stability, permeability profiles).

In a covalent inhibitor, the covalent attachment strongly contributes to the overall free-energy of binding (G_B), which can significantly enhance potency whilst maintaining low molecular weight. Non-covalent inhibitors must compete against high concentrations of endogenous substrates (*e.g.* ATP). This is of less concern for covalent therapeutics, which rely upon non-equilibrium binding kinetics,[12] as shown in Fig. 8, comparing potencies of covalent and non-covalent mitogen-activated protein kinase 1 (MAPK1) inhibitors at varying [ATP].[44]

Pharmacodynamics (PD). Where the target is correctly selected, covalent inhibitors can have prolonged duration of action as compared to non-covalent homologs. This effectively decouples pharmacodynamics (PD) from pharmacokinetics (PK) (*i.e.* absorption, distribution, metabolism, excretion), an effect known as PK-PD decoupling. This allows for sustained efficacy beyond metabolic clearance. Several literature examples report compounds with relatively poor PK achieving long lasting therapeutic effects due to extended pharmacodynamics.[45,46] For instance, a single-dose of ibrutinib acting on BTK and other TEC family kinase members maintains >95% target occupancy for 24 h despite a $t_{1/2}$ of 3 h (P.O.) in humans.[46]

Drug dosing. Due to high potency, sustained action and decoupled PK-PD, a clinically relevant advantage of covalent binders is the ability to administer smaller and less-frequent doses.[14]

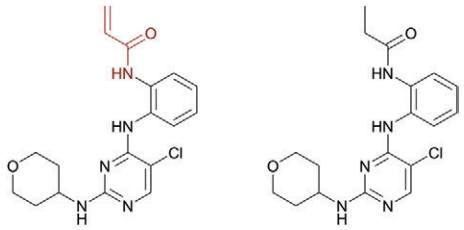

	[ATP] (μM)	IC_{50} (nM)
A	60	8.5
	1000	5.4
B	60	480
	1000	4000

Fig. 8 Biochemical inhibitory concentrations of covalent and non-covalent MAPK1 inhibitors (A and B) comparing the effect of [ATP] on potency.

Although case-specific, these relatively small doses tend to markedly reduce negative side effects due to unpredictable IDTs. This property is in contrast to many non-covalent drugs, which may require frequent and larger doses to maintain therapeutically efficacious plasma concentrations.

Drug resistance. An on-going challenge in drug discovery is acquired mutations, which confer drug resistance, thereby abolishing potency.[47] With regards to non-covalent inhibitors (and to some extent covalent inhibitors), therapy-resistant mutations encourage the development of novel mutant-active structures. In most instances, these mutant-susceptible proteins are present as small clones in cancer patients before therapy. Statistically, the more tumour cells, the more likely resistance might develop due to clonal selection. As such, therapy may fail calling also for improved therapeutics. For instance, despite the overwhelming success of the blockbuster BCR-ABL inhibitor, imatinib, numerous imatinib-resistant mutations (*i.e.* E255K) have been discovered, spawning more potent, mutant-active inhibitors that can be used as arms against CML (*e.g.* nilotinib, dasatinib).[48] Typically, the strongest resistance originates from mutations within the ATP binding site. Recent studies on covalent inhibitors have validated their ability to impede and evade mutation events, and more generally maintain potency against mutant targets.[49] These analyses have suggested, while active-site mutations hinder the initial reversible binding (*i.e.* K_i), subsequent covalent bond formation (*i.e.* k_{inact}) remains possible, assuming the reactive residue has not been altered. Alternatively, it is worth noting the susceptibility of CKIs to mutations of the nucleophilic residue. In such instances, potency can be dramatically lost due to the importance of covalent bond formation for the observed efficacy.

Target scope. CKIs rely heavily on the covalent interaction for potency. Although case-specific, due to a smaller reliance on non-covalent intermolecular interactions, covalent drugs may allow targeting of typically challenging active sites (*i.e.* poorly defined, large and solvent-exposed).[50] For example, inhibition of a protein–protein interaction using a non-covalent inhibitor may require a large and structurally complex compound to achieve effective target occupancy, introducing synthetic or PK challenges. However, in a covalent inhibitor, which may not require extensive binding surface contact, it can allow for high potency while maintaining a small size. Also, target selectivity is an important consideration in any drug discovery program and covalent compounds can be rationally designed to bind poorly conserved target-specific nucleophilic residues.[50] Even if a CKI has a binding affinity for other pockets, these contacts would be transient and will ideally only form an effective long-lived interaction with the target of interest.

Disadvantages

Potency. Very potent and permanent/long-lived target inhibition may not always be beneficial. In situations where transient or partial down-regulation of target activity is required, or if toxicities are associated with prolonged target inhibition, a covalent mechanism of action may not be fitting.[51] As previously mentioned, such issues have been recently explored in the development of reversible covalent inhibitors, with variable potencies and durations of target-interaction.

Safety. Historically, the key deterrent to the development of electrophilic scaffolds relates to concerns of safety and drug-induced IDTs.[41] This is partly linked to the reactive-metabolite theory, which hypothesized that upon metabolism of inert parent compounds, promiscuous reactive electrophiles are generated which may cause immunogenic responses.[52] Notable examples include the commonly used fever medication and analgesic, Acetaminophen. Toxicology studies revealed a primary metabolite, *N*-acetyl-*p*-benzoquinone imine (NAPQI) to be the causative agent.[53] A murine-based study revealed NAPQI indiscriminately modifies >20 liver proteins.[54] Other common examples are the chemical reagent bromobenzene, which upon metabolism forms alkylating epoxides[55] and nitrogen mustards (*e.g.* bis(2-chloroethyl)ethylamine) forming reactive aziridinium motifs as non-specific DNA and protein alkylators (Fig. 9).[56]

In recent literature, highly reactive non-specific electrophiles are typically avoided in covalent lead development. In fact, clinically advanced covalent inhibitors tend to contain stable and moderate or poorly reactive electrophiles (*e.g.* acrylamides). Nonetheless, cytotoxic symptoms can still arise, which are unpredictable, patient-specific and independent of drug pharmacology (*i.e.* IDTs).[57] Extensive unwanted side effect studies into IDTs have shown a correlation between their occurrence and drug dosing, suggesting a daily dose of ≤ 10 mg kg^{-1} essentially eliminates the incidence of IDTs.[57]

Target scope. Targets amenable to covalent inhibition may be limited in certain cases. Recovery of protein activity is a function of target re-synthesis (turn-over rate). Irrespective of how potent or sustained a covalent inhibition profile appears, target activity is re-established upon protein regeneration. Generally, targets chosen for covalent inhibition display slow turn-over rates (*i.e.* 16–24 h), examples include Epidermal Growth Factor Receptors (EGFRs) and Bruton's Tyrosine Kinase (BTK).[40]

Covalent inhibitors generally offer minimal advantage against rapidly synthesized proteins. Preferably, duration of

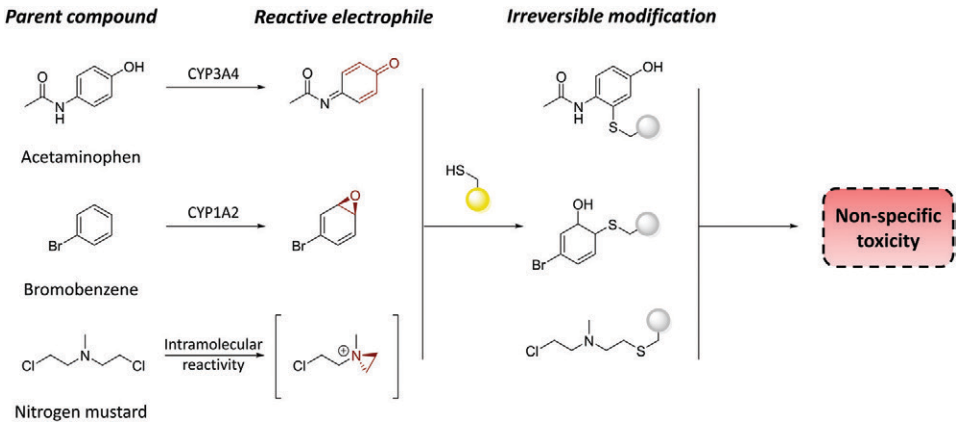

Fig. 9 Examples of cysteine modification using reactive electrophilic metabolites originating from inert parent compounds, resulting in irreversible target inactivation and potentially non-specific toxicities. Adapted from R. A. Bauer,[12] with permission from Elsevier, copyright 2015.

action due to drug binding should exceed the rate of re-synthesis. Nonetheless, while the extent of efficacy is case-specific, it is worth noting that several reports in the literature describe covalent inhibitors against kinases with short half-lives.

For instance, the covalent modification of Interleukin-2-inducible T-cell kinase (ITK) with several CKIs demonstrated a downstream inhibitory effect for 24 h, despite a $t_{1/2}$ of merely 2 h.[58]

Finally, a CKI electrophile requires a complimentary, reactive and accessible nucleophile. If a target lacks this moiety, such an approach would not be suitable. In the context of kinases, extensive mapping of the cysteinome by Leproult *et al.*[59] found 43% of eukaryotic kinases contain at least one cysteine neighbouring the ATP-pocket. While cysteines remain the most pursued residue, other nucleophiles have been targeted (*e.g.* lysine,[60] tyrosine,[61] and serine[62]), which can be applicable to kinases. Hence, despite these limitations, there remains a broad scope of opportunity to pursue a covalent strategy for kinase inhibition.

Approaches towards the discovery of CKIs

Strategies for designing CKIs are in many ways similar to those employed in non-covalent projects, requiring a structural and mechanistic understanding of the target and its role in a disease. There are however unique considerations with regards to target selection and the identification of an appropriate warhead and target residue. These will be addressed below, followed by a brief overview of common approaches for CKI identification.

Selecting an appropriate kinase

Target selection is traditionally decided prior to embarking on a covalent approach, though in some instances it is decided after lead compound identification. The availability of structural and mechanistic knowledge can play an important role in choosing an appropriate kinase target. A well-resolved crystal structure can be highly beneficial in guiding Structure Activity Relationships (SARs) and determining the appropriate trajectory required for covalent bond formation. Mechanistically, the role of the target in disease may provide insight into suitable assays to effectively characterize inhibitor covalency, efficacy and safety profiles.

To date, CKIs generally target kinases implicated in oncology. However, advancements in understanding the safety profiles of covalent therapeutics are likely to expand the applicability of this approach to kinases in other diseases.[43]

Several chemoproteomic approaches have been established to prospectively look for targets amenable to covalent modification. A notable example was reported by the Cravatt group,[63] who employed an Isotopic Tandem Orthogonal Protein Proteolysis – Activity-Based Protein Profiling (isoTOP-ABPP) approach to probe for proteins that could be covalently modified using a series of electrophilic reactive fragments (Fig. 10). This approach employs an alkyne chemical probe that is used to tag amino acids within the proteome. Subsequent enrichment, digestion (using trypsin and Tobacco Etch Virus nuclear-inclusion-a endopeptidase (TEV)) and analysis of probe labelled proteins by quantitative mass spectrometry allows for identification of reactive amino acids and potential new targets. More recently, Browne *et al.*[64] developed a Covalent Inhibitor Target-site Identification (CITe-Id) platform that provides rapid and accurate proteome-wide identification of covalently modified sites using more complex irreversible inhibitors. Using this methodology, Protein Kinase N3 (PKN3), an understudied AGC-type kinase, linked to prostate cancer, was identified as a novel target for covalent modification.

Furthermore, an interesting strategy was recently disclosed by Grey *et al.*,[65] which makes use of a promiscuous covalent inhibitor to identify 23 additional kinases not previously modified. Computational techniques such as Density Functional Theory (DFT) and fingerprint mapping have also been used to predict potential covalent binding sites, aiding in the process of target and residue selection.[66–68]

Considerations in warhead & target–residue selection

It is well established that not all electrophiles can react with every biological nucleophile. Rather, such interactions are quite

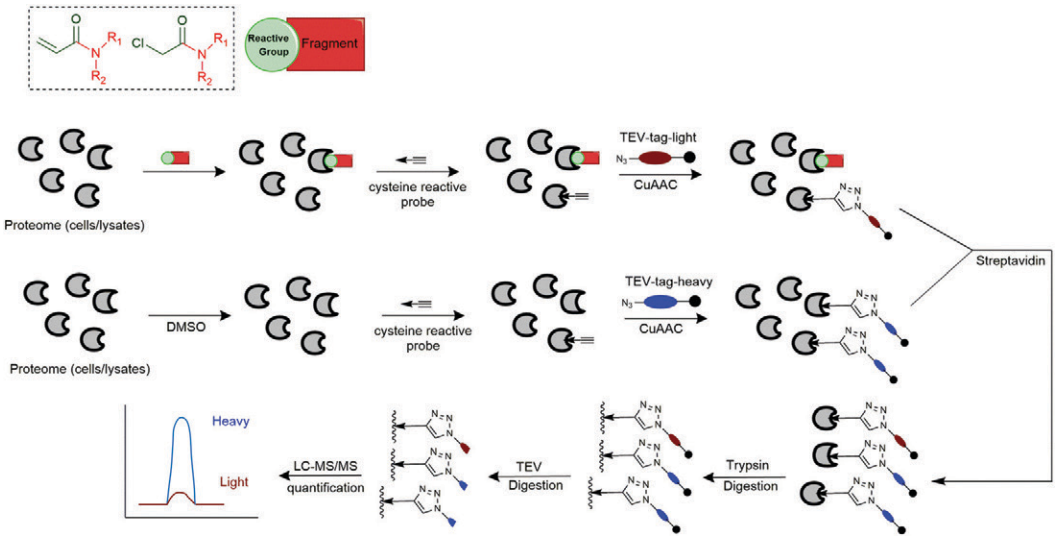

Fig. 10 Schematic for competitive isoTOP-ABPP protocol. (top) Generic structure of an electrophilic fragment, where the electrophilic component is labelled in green and the binding fragment in red, respectively. Adapted and placed in context from ref. 70.

selective and occur along a continuum of relative reactivity, primarily governed by the principal of hard and soft acids and bases (HSAB), as defined by Pearson.[69] This theory categorizes reactive species as relatively ''hard'' or ''soft'', as a function of polarizability, *i.e.* how easily electron density can be delocalized to form covalent bonds. The electron density for ''hard'' species is comparatively immobile and localized near the nucleus (*i.e.* low polarizability). In contrast, ''soft'' substances have delocalized electron clouds, easily distorted, leading to multiple sites of low electron density (*i.e.* high polarizability).[69,70]

For example, the common acrylamide is considered a ''soft'' electrophile due to an extended electron cloud over the conjugated alkenyl and carbonyl moieties. This renders the electron density highly polarizable. Similarly, the anionic cysteine sulfhydryl has a large atomic radius due to the high energy $3sp^3$ orbitals which are far from the nucleus and also polarizable.[71–73] According to HSAB, a nucleophile–electrophile pair of dissimilar hardness will be less reactive due to the presence of a higher potential energy barrier, caused by inadequate orbital overlap. As such, careful consideration of both the warhead and target residue is essential when designing a covalent molecule. While no systematic scale exists to universally quantify hardness and softness across all electrophiles and nucleophiles, several studies have employed computations and quantum mechanical algorithms to derive nucleophilic ($\omega-$) and electrophilic (ω) indices based on the hardness (η) or softness (σ) of various compounds.[71,72,74,75] These indices reflect the propensity of the electrophile to form a covalent adduct with a given biological nucleophile and can serve as a useful tool in deducing an appropriate electrophile–nucleophile pair. This pairing can help reduce undesirable side effects with off-target residues, while increasing the likelihood covalently modifying the kinase of interest.

When considering electrophilic warheads minimally explored in literature, quantifying relative reactivity against several model nucleophiles can be very useful. The $t_{1/2}$ of the parent compound against the abundant cellular nucleophile glutathione (GSH) is a commonly accepted method of comparing the electrophilicity.[76–79] Alternatively, GSH can be substituted for different nucleophilic amino acids to compare relative reactivities towards various residues within the kinome. A recent study by Gilbert *et al.*, characterizes the reactivity of various covalent fragments against serine and cysteine.[80] Furthermore, the ($t_{1/2}$) of several lysine modifying compounds has been reported against *N*-α-acetyl-L-lysine, in addition to the electrophilic reactivities of several pyridinium ylides with various nucleophiles.[81]

Computational techniques that predict GSH/amino acid reactivity using Hammett parameters, quantum mechanical modelling and pK_a predictions are also now available.[82,83] A more detailed discussion of the various chemical reactivity assays can be found in the following reviews.[69,77]

The kinome consists of several nucleophilic residues with varying sites of reactivity. However, in the past decade, CKIs have been largely biased towards cysteine thiols, with a few reports of lysine-targeting inhibitors.

Cysteine

Cysteine represents the most targeted amino acid in the field of CKIs owing to various unique properties. First, relative to the other 19 possible residues it is low in abundance, which represents an attractive feature in the context of kinases where selectivity is challenging. Cysteines also play non-catalytic roles in kinases such as stabilizing protein tertiary structure through intra- and inter-molecular disulphide bonds.[84] They can also be targeted by numerous post-translational modifications (PTMs) including *S*-nitrosylation, *S*-prenylation and oxidation. The most unique feature of cysteine is the high reactivity and chemical plasticity of the anionic thiolate ($Cys\text{-}S^-$).[66]

The susceptibility of cysteine to covalent modification is variable across the kinome. This reactivity, which is largely a

function of pK_a is dependent on location within the desired binding pocket. Surface exposed cysteines tend to be more acidic with a lower pK_a. On average, this improves reactivity relative to their buried counterparts due to the ability of forming H-bond interactions with water and other polar residues. However, the presence of basic residues (*e.g.* lysine, arginine) within the vicinity of buried cysteines can serve to decrease their pK_a, increasing the likelihood of having an available nucleophilic thiol.[85]

While buried cysteines are quite rare, they have been shown to react with a wide range of warheads, particularly Michael acceptors.[77,86] These unique properties have attracted broad interest in this nucleophile resulting in the development of a wide array of cysteine targeting warheads with diverse chemistries.[87]

In 2009, a study by Gray *et al.* revealed that more than 200 kinases (~40% of the kinome) have an accessible cysteine residue that can potentially be targeted by an ATP-competitive CKI.[16] Subsequent analysis by Wu *et al.*[88] lead to the first comprehensive classification of the ''cysteinome''. Despite the possibility of targeting many kinases using this approach, the current landscape of CKIs is heavily biased towards a few major drug targets. These include EGFR, BTK, ITK and JAK3, all of which have an equivalently positioned cysteine within the hinge region of the catalytic ATP binding pocket.

Lysine

Several efforts have been made to target active site lysines in instances where a cysteine is not suitable for modification. Lysines present a potentially attractive nucleophile due to their prevalence in many active sites and at interfaces mediating protein–protein interactions.[89,90] Similar to cysteine, their reactivity is largely governed by the pK_a of the ε-amino nitrogen. Under physiological conditions, most surface exposed lysine residues remain protonated (pK_a ~ 10.4) and not nucleophilic. Conversely, buried lysines can be strikingly acidic due to perturbations in their microenvironment. This in turn results in pK_a values as low as 5.7, improving their nucleophilicity.[81]

Nevertheless, identifying a sufficiently acidic lysine remains a challenge, in addition to finding an appropriate ''hard, yet non-promiscuous electrophile'' (due to the hard-nucleophilic nature of lysines).[43] Model reactions using *N*-α-acetyl lysine (hard nucleophile) have shown reduced reactivity towards soft electrophiles (*i.e.* acrylamides), while exhibiting higher reactivity against certain vinyl sulfone derivatives.[81]

Despite these complications, several accounts in the literature report the covalent modification of lysine residues using various warheads. For example, a sulfonyl fluoride-based probe was recently used to covalently modify Lys514 in Fibroblast Growth Factor Receptor (FGFR; Fig. 11).[91]

Similarly, an activated ester electrophile was recently reported by Dalton *et al.*[92] forming a covalent bond with Lys779 in the P-loop of Phosphoinositide 3-Kinase (PI3Kδ). Furthermore, a comprehensive global profiling of lysine reactivity and ''ligandability'' revealed sulfonyl fluorides and *N*,*N*′-diacylpyrazolecarboamidines as potential amine-reactive electrophiles that can be used to inhibit enzyme activity *via* active site and allosteric mechanisms.[93] Targeting of lysine residues currently remains at the proof-of-concept stage with most of the work largely focused *in vitro*. It remains to be seen what challenges may be encountered when progressing into preclinical studies and whether they can be resolved to design efficacious CKIs.

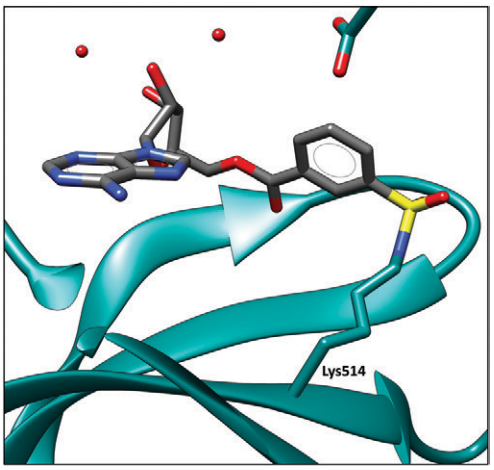

Fig. 11 Covalent modification of Lys514 using a sulfonyl fluoride electrophile, in the active site of EGFR (PDB 5O49).

Other nucleophilic residues

Additional amino acids have the potential to be nucleophilic depending on their microenvironment (*e.g.* Ser, Tyr, His). Covalent modification of such residues relies on careful optimization of the nucleophile–electrophile pair which is primarily governed by the HSAB theory as discussed. Successful targeting of serine and threonine residues has been reported in the context of proteases. However, their lower reactivity and higher abundance makes targeting these residues more challenging, particularly from the perspective of selectivity.[94]

Two inhibitors outlined in this review target residues other than cysteine and lysine. Compound **124** is the first irreversible serine–arginine protein kinase (SRPK1) inhibitor, targeting a tyrosine residue using a sulfonyl fluoride warhead, with kinome-wide profiling demonstrating selectivity for SRPK1/2 (Fig. 12).[95] Moreover, computational studies of EGFR inhibitor **105** suggest a unique covalent interaction of the boronic acid moiety with Asp800 in the kinase hinge region.[96] Given such advancements, there currently exists a considerable interest in targeting amino acids beyond the canonical cysteine and lysine residues to engage additional kinases. Some examples are shown in a recent essay by Jones which addresses recent advancements in chemical probe development beyond the kinase cysteinome.[97]

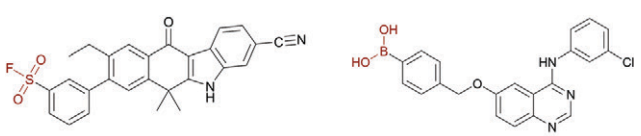

Fig. 12 Chemical structures of compounds **124** and **105**.

Strategies towards covalent lead identification

Most CKIs target the conserved ATP-binding pocket by interacting with non-catalytic nucleophilic residues in the DFG-in/active (type I) or the DFG-out/inactive state (type II). Most of these inhibitors are ATP mimetics, resulting in significant selectivity challenges. Over the years, type II inhibitors have gained traction as they were perceived to be less promiscuous owing to numerous unique DFG-out conformations.[98]

However, a comprehensive analysis of type II inhibitor selectivity by Gray *et al.* revealed >200 kinases can be targeted by this class of molecules, demonstrating that the DFG-out conformation alone may not provide sufficient advantages for inhibitor selectivity.[99]

The cross-reactivity typically observed with type I and II inhibitors is mainly due to the high degree of sequence and structural similarity within the ATP-binding pocket. Despite such challenges, targeting this site provides unique opportunities for CKIs due to the high occurrence of nucleophilic residues within this region, particularly cysteines. A recent examination of potentially druggable cysteines across the kinome revealed 75 kinases amenable to covalent modification with the majority of cysteines located in or around the ATP binding region.[100] However, several inhibitors discussed in this review target cysteines not identified in this analysis. Cross-reactivity may be circumvented by non-ATP binding inhibitors (type III, IV) targeting non-conserved binding regions. However, assays for their reliable identification and characterization remain limited.

Currently, several strategies are available for identifying and designing CKIs including, high-through put screening (HTS), virtual screens and Structure-based Drug Design (SBDD). The majority of which have now been well-established due to advances in bioinformatics and the increasing repository of high-resolution crystal structures. Indeed, much of current covalent kinase drug discovery utilizes rational drug design rather than traditional HTS and phenotypic analysis to identify lead candidates.

The design strategy employed will typically depend on the amount of background knowledge available and accessible chemical entities against a specific target.[101] While a detailed discussion of the various platforms is beyond the scope of this review, given the large contribution of SBDD and selectivity-profiling in CKI development, they are addressed next.

Structure-based drug design (SBDD)

SBDD is a valuable way of utilizing key interactions between an inhibitor-protein pair, allowing medicinal chemists to rationally modify a core scaffold. This can involve several structural biology techniques such as X-ray crystallography and NMR, to gather a sufficient understanding of active site topology with a (covalent) fragment of interest. Iterative derivatization allows for optimal positioning of an electrophilic group towards a targeted nucleophilic residue with the goal of enhancing affinity. In practice, CKIs are designed through the optimization of two components: a warhead (*i.e.* a weak electrophile), to react with a receptor nucleophile and a non-covalent binding motif, essential to guiding the reactive compound to the appropriate target. Key to the success of this approach is selecting a reversible binding component with a suitable selectivity profile whilst moderately inhibiting the desired target. Subsequent modification of this reversible motif allows installation of an electrophile with the correct spatial trajectory. When applicable, it is also vital to consider the region between these components (*i.e.* linker) and optimize structural flexibility for effective covalent bond formation.

SBDD may also elucidate unique target conformations and additional binding sites, providing an effective strategy for designing type II kinase inhibitors and exploiting novel induced pockets.[102,103] Computationally, kinase crystal structures are now also used for virtual HTS campaigns. These methods commonly focus on non-covalent ligand–receptor interactions[104] to achieve complimentary electrophile–nucleophile orientation/distance. However, despite recent advances, such approaches are generally unable to compute explicit rates of covalent bond formation or delineate target-specific warhead reactivity.

Kinase selectivity-profiling

Many inhibitors in this review were derived from previously reported molecules, often originating from screens of archived inhibitors or existing drug core-scaffolds. As such, several CKI discovery programs are initiated using a lead molecule known to target a certain kinase, but later (serendipitously or *via* proteomic analysis) is found to cross-react with various new kinases. Relative to a costly HTS, this technique provides a promising alternative with a high probability of identifying safe, bioavailable, novel and patentable analogues.[105]

Derivatization of these scaffolds has broadened the scope of available ATP mimicking motifs, now including quinazoline, pyrimidines, purines, imidazoles, and quinolines. This selection of structures has expanded the kinase target-pool to include several previously untargeted disease-implicated mutant isoforms.[16] Several platforms are currently available to evaluate the kinome reactivity of small molecules, including KinomeScan from DiscoverX,[106] and Kinativ (a proteomic technology) by ActivX, allowing for quantitative profiling of inhibitors against native kinases in cellular tissue or cell lysate[64,107] Other examples use ABPP platforms, to quantify kinome-wide inhibitor reactivity to characterize the covalently modified proteins within a sample.[105]

Kinase selectivity filters in lead optimization

It is generally accepted that selectivity is important for designing safe CKIs. Optimization often uses subtle features near the ATP binding site to improve selectivity. The nucleophilic residue (*i.e.* Cys) is the first of three selectivity filters, (defined by Shokat *et al.*[108]) commonly exploited in CKI development, along with gatekeeper residues and the hydrophobic pocket.

Nucleophilic residue

Appropriate selection of the target nucleophile can impact CKI potency and selectivity. Ideally, the residue of interest is solvent-accessible, poorly conserved and near a druggable pocket (within 10 Å).[67] To date, the majority of CKIs have been designed to target the nucleophilic thiol of cysteine residues. In kinases, very few conserved cysteines serve key catalytic functions, making them an ideal candidate to develop exceptionally selective inhibitors. This approach limits covalent modification to proteins containing a targetable cysteine. As briefly mentioned, additional nucleophilic residues (*e.g.* lysine, serine, tyrosine) have been explored but their utility remains to be determined, leaving a clear gap in understanding patterns of electrophile reactivity in amino acid selectivity.[109]

Gatekeeper residue

As the first residue of the hinge region connecting the amino/carboxy lobes, gatekeeper residues are able to regulate access (when small, *i.e.* Thr), or blockage (when large, *i.e.* Phe) to a hydrophobic cavity.[110] Thus, they can specifically sensitize many kinases to certain small-molecules. A heterocyclic scaffold orienting bulky groups towards a large gatekeeper residue can cause an undesirable steric clash, whilst maintaining potency against kinases with smaller gatekeepers (*i.e.* more accessible pocket). Recently, this strategy was employed by Zhou *et al.* to generate lead candidate **3**, an EGFR inhibitor which exploits the clinically-important gatekeeper T790M mutation to achieve mutant-selectivity.[111]

A commonly cited example can be seen in Ponatinib which was developed against gatekeeper mutation T315I within ABL kinase.[112] Given that an estimated 20% of the kinome have small gatekeeper residues, this method is ideally combined with additional distinct features of the ATP pocket, to ensure adequate selectivity.[110] Recently, Analog-sensitive (AS) kinase technology has emerged as a chemical genetic technique that utilizes engineered gatekeeper mutations to develop highly specific inhibitors.[113]

The examples above highlight the diverse utility of the gatekeeper residue as an approach to enhance kinase selectivity.

Hydrophobic pocket

This region of the binding cavity is mainly composed of hydrophobic residues and not occupied by the endogenous co-substrate (ATP). The shape and size are primarily controlled by the gatekeeper residue and an additional conserved lysine. The presence of a bulky gatekeeper (*i.e.* Phe in Cyclin-dependent Kinase, CDK2) results in a small cavity, delimited by β-sheets (4,6) and the gatekeeper residue. In the case of a small gatekeeper (*i.e.* Thr, EGFR), a larger cavity is seen, which extends towards β-sheet (5) and the α-C helix (Fig. 13).[30] Characterized by high plasticity due to flexible amino/carboxyl lobe orientations and the added conformational variability of the DFG motif, the hydrophobic pocket is often exploited to engage unique interactions to further enhance selectivity. Tong *et al.* were first to demonstrate the use of this special cavity as a druggable ATP-subsite using the very specific MAPK14 inhibitor, *p*-fluorophenylpyridinylimidazole.[114] The extent to which CKIs are selective remains a contentious issue. Ideally a kinase inhibitor would inhibit a single target, however given the diversity of available kinase and their evident structural similarities within kinase families, this is a formidable task. Many have argued that it may be more useful to simultaneously inhibit several therapeutically relevant kinases, and that it is more important to speak in terms of selectivity profiles as opposes to absolute selectivity.[115] Successful examples for broad range kinase blockers include broad range tyrosine kinase inhibitors developed against EGFR or against ABL oncoproteins.[116,117]

A powerful approach to evaluate proteome-wide selectivity was developed by Cravatt *et al.* who used ABPP coupled with

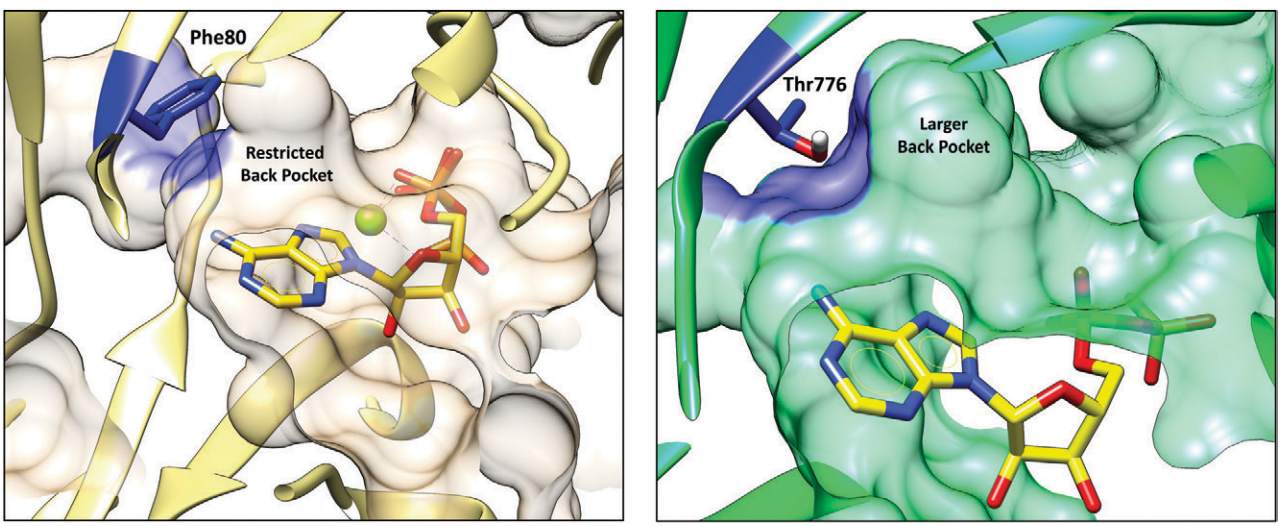

Fig. 13 Comparison of different hydrophobic pocket accessibilities provided by a large (CDK2) and a small (EGFR) gatekeeper residue. (left) In the ATP-CDK2, the large Phe gatekeeper residue limits accessibility to the back pocket (PDB 1B39). (right) A smaller residue as in EGFR, provides greater access to the back pocket (PDB 2GS6).

quantitative mass spectrometry to globally map cellular targets of kinase inhibitors. Interestingly, molecular probes of FDA-approved covalent drugs; ibrutinib (BTK inhibitor) and afatinib (EGFR inhibitor) showed less selectivity for their intended target (1–1000 nM), with certain off-target kinases labelled at pharmacologically relevant concentrations.[118] Despite these observations, both inhibitors remain efficacious *in vivo* and clinically successful, although efforts to further improve their selectivity remain ongoing.

Electrophiles & advances in CKI development

Electrophiles may be cations (*e.g.* NO^+), polar groups (*e.g.* carbonyls), polarizable centres (*e.g.* Cl_2) and certain Lewis acids (*e.g.* BH_3). In the context of drug discovery, the application of electrophilic motifs requires careful assessment of efficacy, selectivity, stability, toxicity, and mechanism-of-action. In the last few decades several recurring electrophiles have been utilized, including α-halo carbonyls, acrylates, vinyl sulfones and acrylamides (Fig. 14).

The earliest methods to measure electrophilicity include the Mayr–Patz equation and the Mayr reactivity scale.[119] Currently, as a first step, electrophile reactivity is routinely measured against cellular nucleophiles such as GSH (~1–10 mM in cell).[120] In recent literature, Flanagan *et al.*[82] characterized the GSH reactivity (*i.e.* $k_{pseudo1st}$) of common electrophiles at physiological conditions (pH 7.4, 37 °C). Weerapana *et al.*[121,122] quantified the reactivity of several carbon-based electrophiles and profiled their proteome-wide cysteine reactivity.

While GSH is not the most reactive cellular nucleophile, it is often used as a high-throughput measure of Phase II metabolic reactivity. Reactivity towards thiol nucleophiles can be modulated using steric and electronic derivatization. As seen in Table 2, introducing electron-withdrawing aryl groups can improve the reactivity of the typically mild acrylamide (structure 4 *vs.* structure 9). Conversely, the use of steric bulk (*e.g.* α-methyl) can attenuate the electrophilicity of the very reactive α-bromoacetamide (structure 14 *vs.* structure 11). Finally, despite the added steric bulk of α,β-dimethyl substituents, the unsaturated ketone, lacking electron-donating heteroatoms (*i.e.* O, N – reduce electrophilicity *via* resonance) is the most reactive.

The kinome, like many protein families, includes a range of nucleophiles (*e.g.* –SH, –OH, $–NH_2$), with varying reactivity to individual warheads, subject to cellular and molecular variables such as, target protein concentration, nucleophile accessibility, cofactors, and surface topography. Therefore, while isolated models are of great value to understand fundamental reactivity, these observed trends may dramatically vary in different microenvironments in a cellular context.

Next, we report recent CKI developments and provide insight into the successes, innovations and challenges associated with certain electrophiles and nucleophilic target enzymes. Compounds were extracted from SciFinder and NCBI databases. Best efforts have been taken to ensure the inclusion of all relevant molecules within the timeframe described. Note, important work on covalent inhibitors/warheads published during the revision process has not been discussed.

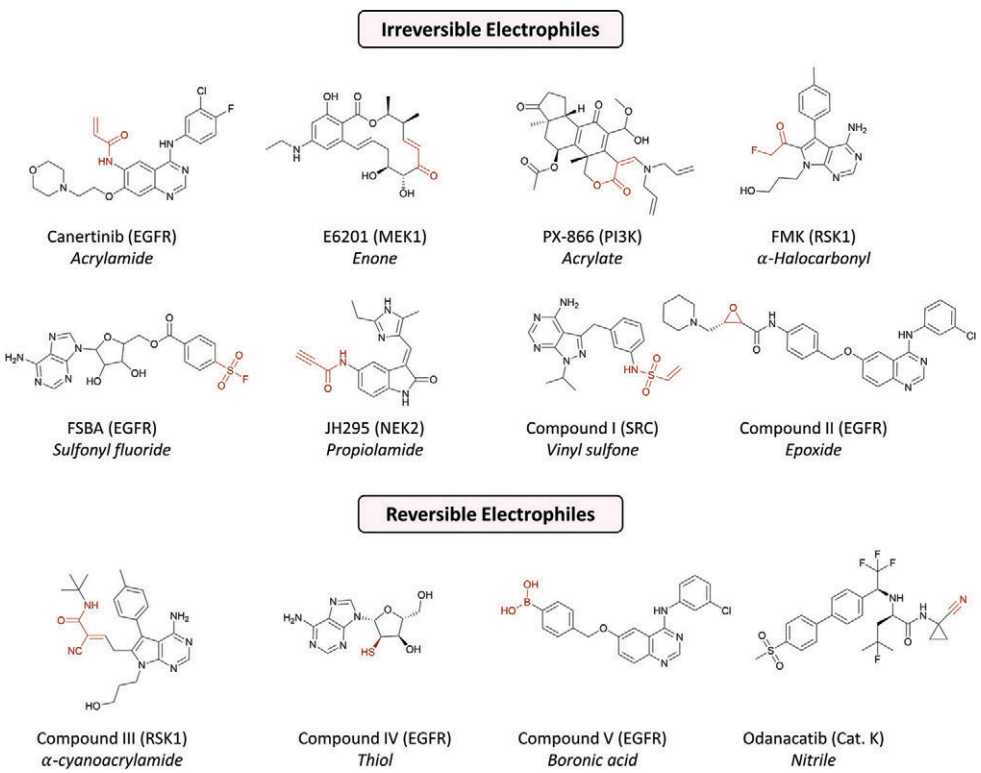

Fig. 14 Chemical structures of small-molecules utilizing irreversible (top) and reversible (bottom) covalent electrophiles.

Table 2 Pseudo-first order kinetics of GSH addition reactions (pH 7.4, 37 °C), in order of increasing reactivity. Data extracted from Flanagan *et al.*[83]

	GSH $k_{pseudo1st}$ (10^{-5}, s^{-1})			
Electrophile reactivity	0.3	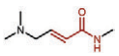	21.6	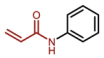
	0.3	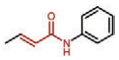	36.7	
	0.3	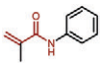	43.3	
	1.2		48.3	
	1.2		120	
	5.0		233	
	6.0		273	
	13.3	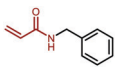	1298	

Acrylamides & α,β unsaturated electrophiles

Conjugation of alkenyl motifs to EWGs (*e.g.* carbonyls) relays carbonyl electrophilicity to the unsaturated β-carbon, forming a Michael acceptor, suitable for attack by soft nucleophiles (Fig. 15).[123] Common examples include acrylates, propiolamides and activated alkenes. Discussed in detail by Mendez and Gazquez using HSAB, nucleophiles can regioselectivity attack at the carbonyl carbon or the β-position (Fig. 16).[124,125]

Nucleophilic addition to acrylamides primarily depends on basicity, where strong bases (*i.e.* hard nucleophiles; organolithiums) undergo 1,2-addition and weak bases (*i.e.* soft nucleophiles; thiols) result in 1,4 or conjugate addition. The softness of cellular nucleophiles has propelled this class of electrophiles to the forefront of CKI development. Due to moderate electrophilicity, ease-of-synthesis and relative metabolic stability, the unsaturated carbonyls represent, by far, the most common electrophile in drug discovery. As of 2018, all FDA-approved covalent kinase inhibitors (Section 4) use this motif, with 5 of the 6 utilizing the versatile acrylamide.

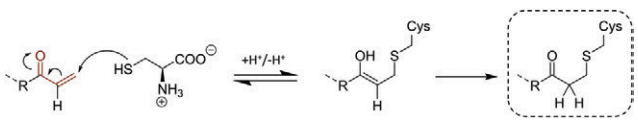

Fig. 15 General mechanism of covalent modification by α,β-unsaturated carbonyls (R = $-CH_2-$, $-NH-$, $-O-$).

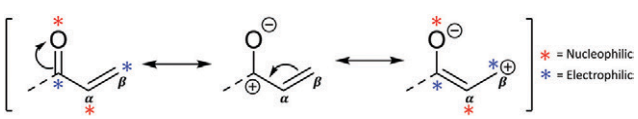

Fig. 16 Electron movement in α,β-unsaturated carbonyls through resonance-mediated tautomerization, highlighting nucleophilic and electrophilic sites.

Acrylamides

Acrylamides are a sub-family of α,β-unsaturated carbonyls characterized by their unique reactivity profile and soft electrophilic nature. The additional nitrogen heteroatom extends conjugation *via* resonance, yielding attenuated reactivity, a desirable feature for covalent inhibitors. Unfunctionalized acrylamides are only minimally reactive towards thiol nucleophiles and virtually non-reactive against amino acids of dissimilar hardness. Thus, acrylamides are the most utilized electrophile in CKI development.[77]

The attractive nature of acrylamides lies largely in their tunability. Rational substitutions at the α or β carbon can modulate their reactivity and reversibility, with efforts to characterize their intrinsic reactivity profiles extensively reported in literature. Recently, researchers at Amgen assessed the GSH reactivity of several aryl-acrylamides with varying ortho, meta and para substituents.[126,127] Acrylamides substituted with *N*-aryl, *N*-alkyl and/or varied substituents at the α or β positions revealed heightened reactivity for *N*-substituted scaffolds relative to carbon substituted counterparts.[79] Taunton *et al.* have pioneered the development of reversible covalent acrylamide derivatives, and demonstrated the advantages of reversibility in the context of ligand residence time.[33]

In the past decade, 66 distinct CKIs have been identified which use an acrylamide warhead. These small molecules are distributed across four main kinases, with 48 of the 66 (~70%) targeting EGFR, BTK, JAK3, and FGFR. The remaining 18 are spread amongst members of the tyrosine protein kinase (TEC) family. These inhibitors and their engagement with the target are reviewed, with a short description of the kinase target, relevant indications, and therapeutic relevance.

EGFR

EGFR is a member of the Receptor tyrosine–protein kinase (ErbB) family of transmembrane tyrosine kinase receptors known to play a pivotal role in regulating cell proliferation, survival, adhesion, migration and differentiation.[128,129] Activating EGFR mutations such as L858R constitutively activate the receptor, independent of ligand stimulation, and hyperactivate downstream signalling pathways that promote pro-proliferative process.[130] As a result, EGFR has emerged as an attractive and clinically validated drug target in cancer therapy with numerous candidates in clinical trials. Despite promising data, efficacy has been limited due to acquired resistance and the rapid development of TKI resistant mutations (*e.g.* T790M), which spawned renewed interest in a third generation of mutant selective CKIs targeting Cys797 (Table 3).

In an attempt to develop a novel series of inhibitors for the treatment of Gefitinib/Erlotinib resistant non-small cell lung cancer (NSCLC), Young Cha *et al.* identified two potent irreversible Her1/2 inhibitors, **1** and **2** (Fig. 17). An SAR focused around the key *N*-acryloyl and 4-aminoquinazoline moieties revealed that a conformationally rigid L-proline at the C_6 position of the quinazoline core was necessary for dual Her1/2 inhibition. In addition, substituting the C_7 position

Table 3 Summary of the *in vitro*, *in cellulo* and kinetic mechanistic profile of EGFR inhibitors **1–11**. Compiled information below is based upon available data reported

			In vitro (nM)		*In cellulo* (nM)						
#	Reversible	Nucleophile	Isoform	IC_{50}	Cell line	IC_{50}	$t_{1/2}$ (h)	K_i (nM)	k_{inact} (ms^{-1})	k_{inact}/K_i (M^{-1} s^{-1})	Stage
1		C797/C805	HER1/2	24	A-431	8	3.2[a]				Discovery
2		C797/C805	HER1/2	11	A-431	7	4.2[a]				Discovery
3		C797	$EGFR^{T790M}$		PC9 GR	14	1.76[a]				Preclinical
4		C797	$EGFR^{T790M}$		PC9	14					Discovery
5		C797	$EGFR^{T790M/L858R}$	0.98	H1975	16					Discovery
6		C797	$EGFR^{T790M/L858R}$	0.93	H1975	14					Discovery
7		C797			H1975	96	0.352[b]				Discovery
8		C797	$EGFR^{T790M/L858R}$		H1975	32		21.5	5.1	2.41×10^5	Preclinical
9		C797	$EGFR^{T790M/L858R}$	1	H1975	11	3.0[a]				Phase II
10	•	C797	$EGFR^{T790M/L858R}$	37							Discovery
11	•	C797	$EGFR^{T790M/L858R}$	83							Discovery

[a] Hepatocytes. [b] Liver microsomes.

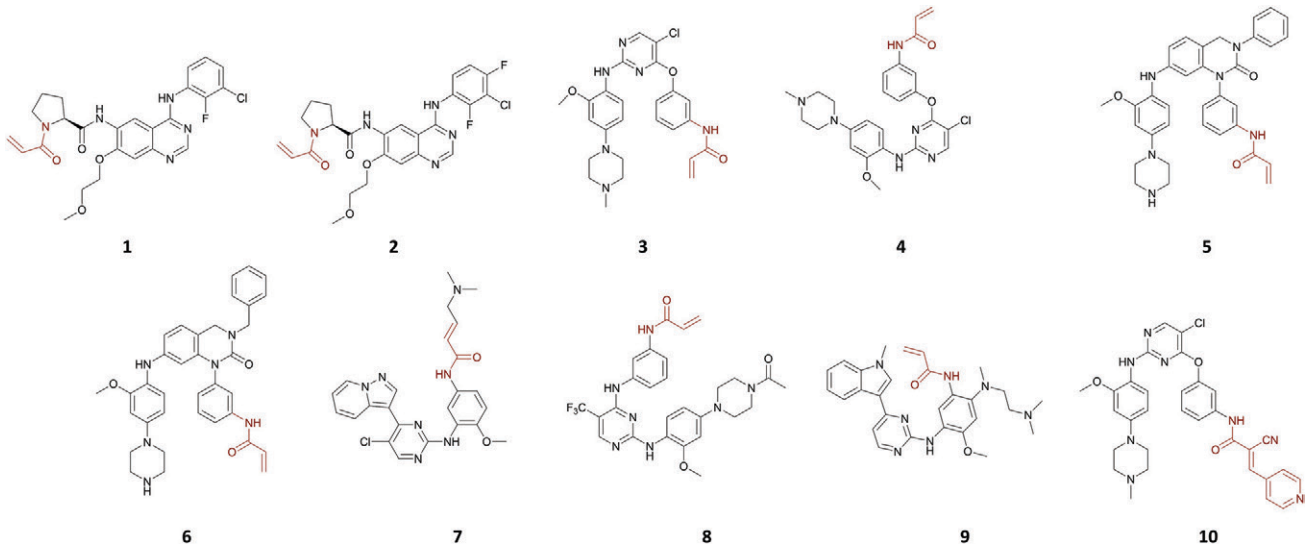

Fig. 17 Chemical structures of EGFR-targeting inhibitors **1–11** with acrylamide warheads reported between 2007–2018.

with a methoxyethyloxy and C_4 with di- or tri-halo-substituted anilines was vital for potency in both *in vitro* enzymatic and cellular assays. Subsequent biological evaluation in a Gefitinib/Erlotinib-resistant NSCLC cell line demonstrated the ability of **1** and **2** to overcome clinically reoccurring drug resistance (**1**, IC_{50} = 24 nM and **2**, IC_{50} = 11 nM), though minimal selectivity for wild-type (WT) over the mutant was observed. In an A431 (Her-1 overexpressing human breast cancer cell line) cell washout experiment (8 h), **1** maintained inhibition of EGFR phosphorylation with only 15% recovery after 8 h, confirming its irreversible nature. Evaluation of both inhibitors *in vivo* in female nude mice (subcutaneous xenograft of A431 cell line) showed significant reduction in tumour size with a high safety margin.[131]

With most EGFR inhibitors possessing a central quinazoline, Zhou *et al.* hypothesized the anilinoquinazoline core may not be optimal against $EGFR^{T790M}$ due to reliance on H-bonding with the Thr gatekeeper ($EGFR^{WT}$). Screening a focused library of common kinase inhibitor scaffolds revealed pyrimidine compound **3**, which showed enhanced inhibition of EGFR phosphorylation in NIH-3T3 cells harbouring different $EGFR^{T790M}$ alleles (relative to clinical inhibitors such as neratinib).[132] Interestingly, when used in $EGFR^{WT}$ HC11 cells, **3** was unable to inhibit $EGFR^{WT}$ phosphorylation at 100 nM, demonstrating mutant selectivity. A crystal structure of **3** in complex with $EGFR^{T790M}$ revealed a crucial hydrophobic contact between the chloro-substituent on the pyrimidine ring and the Met790 gatekeeper and was hypothesized to contribute to the enhanced potency against the mutant protein (Fig. 18).

This result was consistent with *in vivo* evaluation, where no effective inhibition of $EGFR^{WT}$ was observed in tumour mouse modelling. In a 2 week efficacy study, treatment with **3** resulted in significant tumour reduction compared with the vehicle in two T790M containing murine models.[111] Compound **3** has since been used as a model template scaffold for various mutant selective-EGFR covalent inhibitors.

As part of this effort to develop novel core-scaffolds selective for $EGFR^{T790M}$, a small library of common heterocyclic moieties was prepared, and their anti-proliferative effects analysed using PC9 prostate carcinoma cells ($EGFR^{del\ E746\text{-}A750}$) and PC9

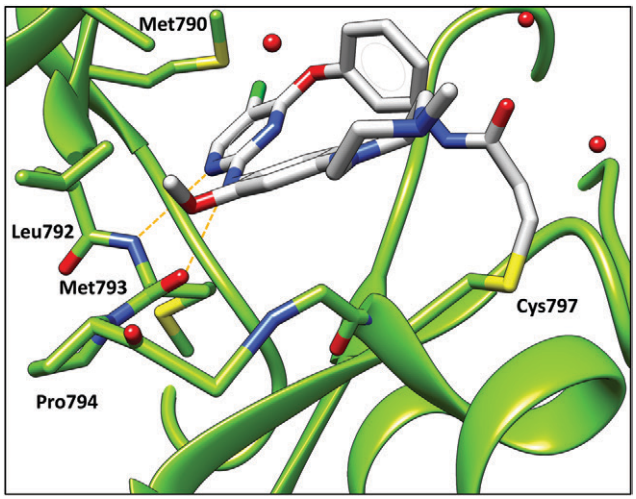

Fig. 18 Crystal structure of **3** bound to EGFR T790M (PDB 3IKA in the active conformation "DFG-in". Note the additional hydrophobic interaction between the chloro-substituent (green) and Met790, which is proposed to contribute to enhanced mutant selectivity.

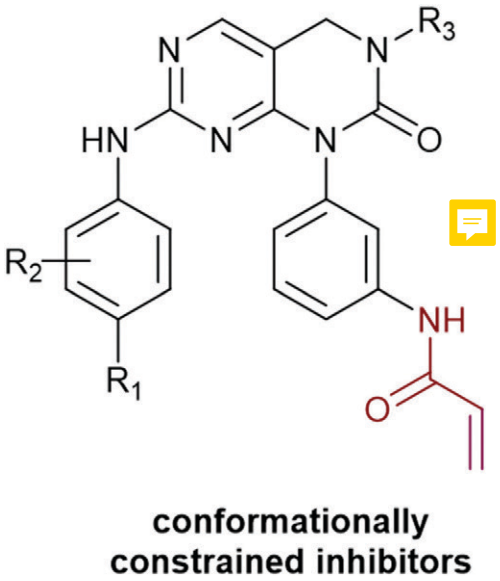

Fig. 19 Design of conformationally restrained derivatives of **3** requiring a large hydrophobic group at the R3 position, as new EGFR inhibitors.

growth-resistance cells ($EGFR^{del\ E746\text{-}A750/T790M}$). Several purine, pyrrolopyrimidine and pyridine containing compounds were identified, which exhibited potency and mutant selectivity. Representative pyrimidine compound **4** blocked proliferation of $EGFR^{T790M}$ PC9 cells with an EC_{50} of 14 nM. To confirm target engagement, and a covalent mode-of-action, $EGFR^{C797S}$ transformed IL-3 independent murine hematopoietic Ba/F3 cell lines, where the reactive cysteine was mutated with a serine (C797S), were treated with **4** and was shown to be not active. When profiled against a panel of 400 kinases, **4** showed strong binding to several other proteins, namely those harbouring an analogous positioned cysteine.

Given the success of the pyrimidine scaffold in mutant-selective EGFR inhibition, many 2-oxo-3,4-dihydropyrimido[4,5-*d*] derivatives were designed from molecule **3**. Further structural modification revealed the necessity for the 1-(4-methylpiperazinyl) group for effective EGFR kinase inhibition in conjunction with a large hydrophobic group at the R_3 position (Fig. 19), leading to the identification of lead molecules **5** and **6**. In both H1975 NSCLC cells bearing $EGFR^{L858R/T790M}$ and HCC827 cells harbouring $EGFR^{del\ E746\text{-}A750}$, **5** and **6** displayed dose-dependent inhibition of EGFR phosphorylation. However, these compounds only moderately affected EGFR activation in A431[24] and A549[25] cells (harbouring overexpressed $EGFR^{WT}$ and the k-Ras mutation). This is characteristic of other reversible and irreversible EGFR inhibitors and proposed to be due to a complex genomic background and the high affinity for ATP.[133] *In vivo* evaluation of **6** in a $EGFR^{L858R/T790M}$ driven human NSCLC xenograft mouse model of H1975 demonstrated its ability to inhibit tumour growth and induce tumour stasis at 30 mg kg^{-1} day^{-1} (P.O.), though no further analysis has been reported since these results.[134]

In an alternative approach, scientists at Merck screened a selection of published reversible and irreversible inhibitors to identify a L858R/T790M double-mutant selective scaffold. Simultaneous optimization of both covalent and non-covalent components using a GSH reactivity assay culminated in the discovery of **7**. When tested in H1975 (double-mutant), PC9 (activating mutant) and Calcu3 (wild-type) cell lines, **7** demonstrated encouraging and selective mutant antiproliferative activity with EC_{50} values of 0.099, 0.14, and 1.78 μM, respectively. Oral dosing (60 mg kg^{-1} day^{-1}) in a H1975 xenograft model showed significant efficacy, with 105% total growth inhibition (TGI) after 7 days relative to the gefitinib standard, which showed minimal TGI (8%) after 7 days at an oral dose of 100 mg kg^{-1} day^{-1}. Relatively poor solubility (1.6 μM) and a 4.2 μM inhibitory concentration against the hERG K^+-ion channel necessitated further scaffold optimization.[76]

Several other derivatives with varying intrinsic reactivities and potencies were also reported in this study. Of interest, compound **VI**, which was postulated to undergo an addition/elimination reaction, substituting the morpholine moiety for glutathione *via* an intramolecular base catalysis mechanism by the α-morpholine (Fig. 20). Though not the lead candidate, this unique mechanism-of-action shows the impact substituents effects can have on electrophilic tunability.[76]

In 2013, Walter *et al.* reported the preclinical development of a covalent mutant selective inhibitor **8**, which was found through mass spectrometry to covalent modify Cys797 in the ATP binding pocket. *In vitro*, **8** is approximately 22-fold more potent against $EGFR^{L858R/T790M}$ [$k_{inact}/K_i = (2.41 \pm 0.30) \times 10^5\ M^{-1}\ s^{-1}$] over $EGFR^{WT}$ [$k_{inact}/K_i = (1.12 \pm 0.14) \times 10^4\ M^{-1}\ s^{-1}$] and is selective against 434 other kinases with only 13 off-targets at 0.1 μM. This selectivity was also apparent *in vivo* in both NSCLC and A431 xenograft models, where minimal TGI was observed against $EGFR^{WT}$ containing A431 models. Inhibitor efficacy was tested in a bis-transgenic $EGFR^{L858R/T790M}$; CCSP-rtTA model, which mimics T790M acquired resistance to erlotinib and gefitinib (50 mg kg^{-1} twice daily) and showed

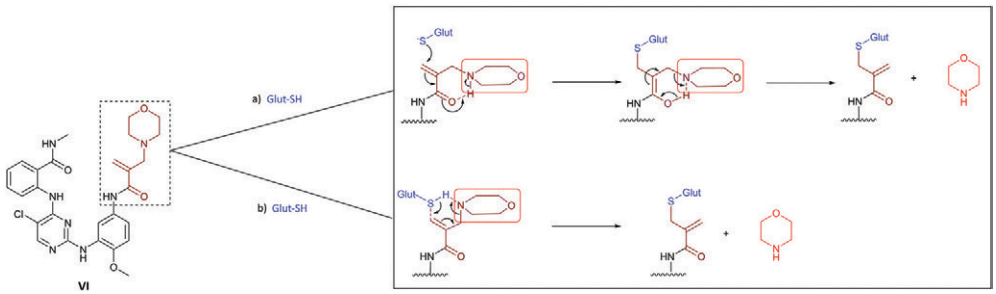

Fig. 20 Proposed mechanism for the nucleophilic substitution of compound **VI** with GSH.[78]

marked reduction in tumour burden and cell proliferation in lung tumour sections.

To address potential acquired resistance, NCI-H1975 (L858R/T790M) cells were exposed to increasing concentrations of **8** over several months, until resistance was developed. All five resistant clones contained the original L858R/T790M mutation and a significant enrichment of genes involved in epithelial–mesenchymal transition (EMT).[135] While **8** entered clinical trials in early 2014, development has since been halted due to poor response rates and lack of efficacy.[136]

A structurally distinct mono-anilino-pyrimidine compound **9** was developed by AstraZeneca in late 2014. Unlike previous pyrimidine scaffolds **3** and **8**, inhibitor **9** possessed an electrophilic substituent on the pyrimidine C_2 substituent, a C-linked heterocyclic pyrimidine at C_4 and no substituent at the pyrimidine 5-position. It was found to be highly potent against various EGFR mutants (*i.e.* $EGFR^{T790M}$), and exhibited a large selectivity window, specifically against kinases outside the EGFR family (where activity was observed against 3 of 9 kinases with an analogous Cys). Metabolite-identification (MetID) studies revealed that the active circulating metabolite AZ5104 can target both HER2/4 kinases. Antitumor activity was observed in xenograft and transgenic mutant $EGFR^{T790M}$ disease models as well as in a proof-of-principal clinical study in two patients with EGFR mutant-positive NSCLC (with minimal side effects). Clinical pharmacokinetic analysis also indicated impressive stability ($t_{1/2}$ = 50 h), significantly higher than would be predicted from initial preclinical data (mouse $t_{1/2}$ = 3 h).[137]

The first covalent-reversible analogues were developed by Basu *et al.* through molecular modelling of core scaffold, **3**. Tuning the spatial and electronic moieties of the olefin warhead lead to identification of **10** and **11**. Amongst the two, **10** was found to be the most potent, with IC_{50} values of 150 and 37 nM for $EGFR^{L858R}$ and $EGFR^{L858R/T790M}$, respectively. The superior inhibitory activity was proposed to be a result of an interaction between the 4-pyridyl moiety and the side chain of Asn800 located at the lip of the ATP binding pocket. **11**, with the less sterically demanding cyclopropyl group, also showed significant potency against the $EGFR^{WT}$ though both compounds were less potent than the original lead scaffold, **3**. This result illustrated that added substituents at the β-carbon of the 2-cyanoacrylamide may negatively affect potency. An attempt to confirm the reversible mechanism of action in a $c\text{-}Src^{T338M/S345C}$ model using MS was unsuccessful, potentially due to unspecific labelling of cysteines.[138]

Subset screening and SBDD of aminopyrazine hinge-binding derivatives culminated in the discovery of lead molecule **12** (Fig. 21). This was found to be a very potent inhibitor of $EGFR^{L858R/T790M}$ and it effectively inhibited autophosphorylation in NCI-H1975 cells. A crystal structure of **12** bound to JAK3 (used as a surrogate due to a Met-gatekeeper residue) established binding of the aminopyrazine motif to the hinge region, the pyrazolopiperidine in the solvent channel and a covalent bond

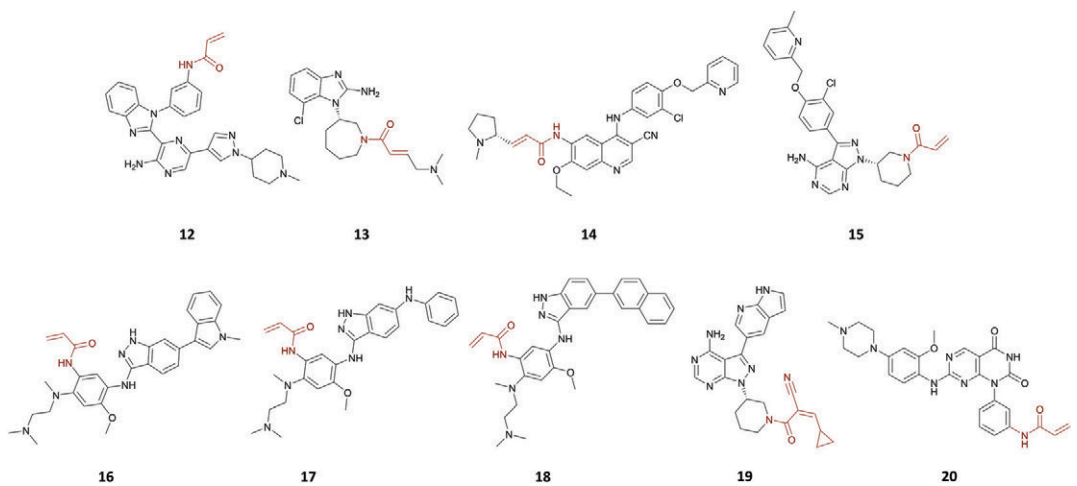

Fig. 21 Chemical structures of EGFR targeting inhibitors **12–20** with acrylamide warheads reported between 2007–2018.

Table 4 Biochemical and cellular characterization data for inhibitors **12–20**

			In vitro (nM)		*In cellulo* (nM)						
#	Reversible	Nucleophile	Isoform	IC_{50}	Cell line	IC_{50}	$t_{1/2}$ (h)	K_i (nM)	k_{inact} (ms^{-1})	k_{inact}/K_i (M^{-1} s^{-1})	Stage
12		C797	$EGFR^{T790M/L858R}$	<1	H1975	14					Discovery
13		C797			H1975	4.18					Phase II
14		C797	EGFR/HER2	13	SHR1258	5.1					Phase II
15		C797	$EGFR^{T790M}$	19	H1975	<0.3	0.8[a]				Discovery
16		C797	$EGFR^{T790M/L858R}$	4.8	H1975	417		149	6.17	4.14×10^4	Discovery
17		C797	$EGFR^{T790M/L858R}$	<1	H1975	191		7.4	2.83	3.83×10^5	Discovery
18		C797	$EGFR^{T790M/L858R}$	1.1	H1975	960		28	8.3	2.98×10^5	Discovery
19	•	C797	$EGFR^{T790M/L858R}$	20				51	2.83	5.55×10^4	Discovery
20		C797	$EGFR^{T790M/L858R}$	0.3	H1975	44	85.4[b]				Discovery

[a] Hepatocytes. [b] Human (*in vivo*).

between the acrylamide functionality and Cys909. Despite encouraging *in vitro* data, prospects of this compound for further clinical progression were minimal due to poor physical properties (*i.e.* solubility) and metabolic instability (human liver microsomes CL_{int} = 120 μL min^{-1} mg^{-1}). In spite of these limitations, *in vivo* experiments in immunocompromised mice bearing PC9 and NCI-H1975 xenografts, showed significant TGI (>117%) (Table 4).[139]

Using HTS, a reversible mutant-selective hit against EGFR was utilized to develop clinical candidate **13**. Incubation with both wildtype and mutant EGFR constructs resulted in a single main product per protein construct, with an added mass of 495 Da. Subsequent LC-MS/MS enzymatic digestion identified adducts localized to Cys797 as the major site of reactivity. Minor GSH adducts (<5%) were found upon incubation for 1 h with 10 mM GSH, suggesting a low risk of non-specific covalent binding. This is impressive considering the high rate of GSH adduct formation (~60%) observed for afatinib. Currently, **13** is in numerous clinical trials and has demonstrated an overall response rate of 60% in NSCLC patients with $EGFR^{T790M}$ mutations.[140]

A novel irreversible EGFR/HER2 dual tyrosine kinase inhibitor **14**, is being developed for the treatment of HER2-positive breast cancer. Excellent *in vitro* activities and good dose–response linearity were observed in all animals at the preclinical stage, in addition to drug-like physicochemical properties ($\log D_{7.4}$ = 2.68, solubility 13.2 μM in fasted state stimulated intestinal fluid, FaSSIF, pH = 6.5). The primary route of metabolism was found to be *via* CYP3A4 and to a lesser degree CYP1B1, CY2C8, CYP2C19, CYP2D6, and CYP3A5 enzymes. This necessitates the monitoring of drug-drug interactions (DDIs) when co-administered with CYP inhibitors. Currently under clinical investigations, **14** has shown anti-tumour effects in several patients with HER2 positive advanced breast cancer, in six phase I and one phase I/II trials currently in progress.[141]

Given the discovery that BTK CKI ibrutinib is moderately active against $EGFR^{T790M}$,[142] Hu *et al.* rationally designed **15**, observing improved activity against the T790M isoform (typically drug-resistant) whilst maintaining good selectivity over $EGFR^{WT}$. In a panel of cell lines expressing wild-type and mutant EGFR, **15** potently inhibited $EGFR^{L858R,del\ 119,T790M}$ and $EGFR^{L858R/T790M}$ (GI_{50} = 0.3–1.3 nM) maintaining >500-fold selectivity over $EGFR^{WT}$ (GI_{50} = 5400 nM). Using C797S mutant proteins, a significant loss in potency (50–10 000-fold) was observed, suggesting an irreversible mechanism of action. This was further supported by synthesis of a non-covalent saturated propionamide analogue, which showed minimal activity against the EGFR mutants. A crystal structure of **15** in complex with $EGFR^{T790M}$ revealed a distinct binding mode where the kinase adopts a DFG-in-c-Helix-out conformation, a feature rarely observed for covalent EGFR inhibitors. Although significant TGI was observed in H1975 xenograft models (60%) at 100 mg kg^{-1} day^{-1}, relatively higher dosages were required to achieve anti-tumour efficacy relative to other inhibitors used in clinic. This may be attributed to the poor PK of **15** and a short *in vivo* $t_{1/2}$ of 0.8 h.[143]

A structure-guided re-design of indazole-based derivatives led to a series of conformationally rigid compounds which potently inhibited $EGFR^{T790M}$. The indazole scaffold was proposed to occupy the space between the hinge region and EGFR gatekeeper residue, while not interacting with Met790. Model compounds, **16**, **17**, and **18** were the most promising of the series with remarkably fast rates of covalent bond formation against $EGFR^{L858R/T790M}$ (0.37, 0.17 and 0.50 min^{-1}, respectively). Inhibitor incubation with $EGFR^{T790M}$ resulted in a mass increase corresponding to a single covalent modification. Lead inhibitors showed high microsomal stability and low clearance in mouse plasma. Selectivity profiling of **17** at a higher concentration, 1 μM, revealed several off-target kinase hits, all of which possessed an equivalently positioned cysteine.[144]

A second reversibly covalent EGFR inhibitor **19**, was designed using crystal structures of covalent pyrazolo[3,2-*d*]-pyrimidines scaffolds, which had previously shown excellent inhibition profiles against $EGFR^{T790M}$. Compound **19** possessed favourable selectivity for $EGFR^{L858R/T790M}$ (IC_{50} = 20 ± 13 nM) as compared to $EGFR^{WT}$ (IC_{50} = 96 ± 26). In the SelectScreen profiling assay, **19** inhibited almost all kinases possessing a homologous cysteine (>50% at 1 μM). Covalent reversibility was verified using MS, where incubation of **19** with $EGFR^{L858R/T790M}$ formed a single covalent adduct which was displaced by introducing irreversible scaffolds VII-I (Fig. 22). Further investigations are required to develop more drug-like compounds with improved PK and PD.[145]

In a more recent study, superposition of two previously reported irreversible covalent inhibitors followed by an extensive SAR led

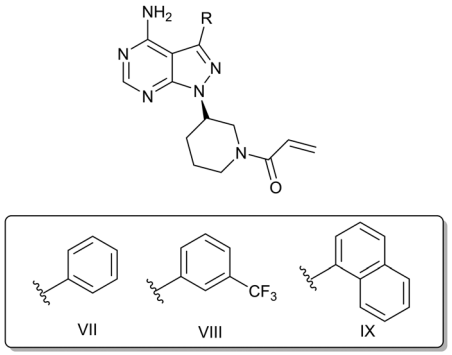

Fig. 22 Structures of the irreversible derivatives of **19** utilized in the mass spectrometry experiments.

to the identification of **20**. The resultant CKI was 263-fold more potent against $EGFR^{L858R/T790M}$ as compared to $EGFR^{WT}$, which was proposed to be a result of improved occupation of the S2 pocket. Washout experiments in H1975 cells illustrated sustained inhibition of double mutant EGFR and a downstream signalling partner kinase ERK for >12 h. Preliminary *in vivo* pharmacokinetic properties (I.V. and P.O.) were found to be favourable, with a $t_{1/2}$ of 1.1 h and modest oral bioavailability, F = 35%. *In vivo* evaluation demonstrated significant TGI (73%) in H1975 xenograft mouse models, with 37% TGI observed in the A431 mouse model.[146]

BTK

Briefly, BTK is a member of the TEC subfamily of kinases, which functions as a critical component in the BCR signalling pathway.[147,148] Loss of function mutations in BTK have been associated with the depletion of B-cells and circulating immunoglobulins, revealing an essential function of BTK for B-lymphopoiesis. Moreover, BTK activity downstream of BCR signalling is crucial for development of acute B-cell leukaemia and B-cell lymphomas.[149,150] As a result, BTK is an attractive therapeutic target for oncological and autoimmune disorders. The clinical success of the first generation BTK inhibitor ibrutinib, has catalysed widespread interest in covalent approaches to BTK inhibition, with numerous inhibitors reported in the literature and in clinical development. In such endeavours, nucleophilic active-site residue Cys481 has been of primary interest for CKI development (Fig. 23 and Table 5).

In 2011, Kim *et al.* developed a series of small covalent inhibitors of BTK based on the imidazo[1,5-*a*]quinoxaline scaffold. Modelling and SAR studies showed that enhanced selectivity was achieved with a methylated C_8 amide, an aryl group at C_4 and an oxygen heteroatom linking the core to the C_4 ring. Lead compound **21** showed >120-fold selectivity for BTK over homologous kinases (tyrosine protein kinase LYN, lymphocyte specific protein tyrosine kinase LCK, SRC), while lower selectivity was observed against EGFR. In Ramos cells, BTK phosphorylation was potently inhibited with an IC_{50} of 48 nM. Murine PK parameters were assessed by I.V. and P.O. (2 mg kg^{-1} and 10 mg kg^{-1} respectively) and shown to be favourable (I.V. $t_{1/2}$ = 1.5 h, P.O. AUC = 876 ng mL^{-1}, P.O. F = 34%). *In vivo* studies in a collagen-induced arthritis (CIA) mouse model, revealed significant inhibition of disease progression relative to the vehicle at 10 and 30 mg kg^{-1}.[151]

Inspired by a previously developed inhibitor of cytoplasmic BMX kinase, compound **59**, Gray *et al.*, using kinome-wide screening and SBDD, developed tricyclic quinoline **22** as a covalent BTK inhibitor. For a given molecule, the selectivity score $S(x)$, where x signifies the activity threshold, offers a measure to assess compound selectivity against a large fraction of the kinome. The S score can be obtained by dividing the number of inhibited protein kinases having a value greater than x, by the total number of tested kinases:

$$s(x) = \frac{\text{number of values} \geq x}{\text{total number of values}} \quad (4)$$

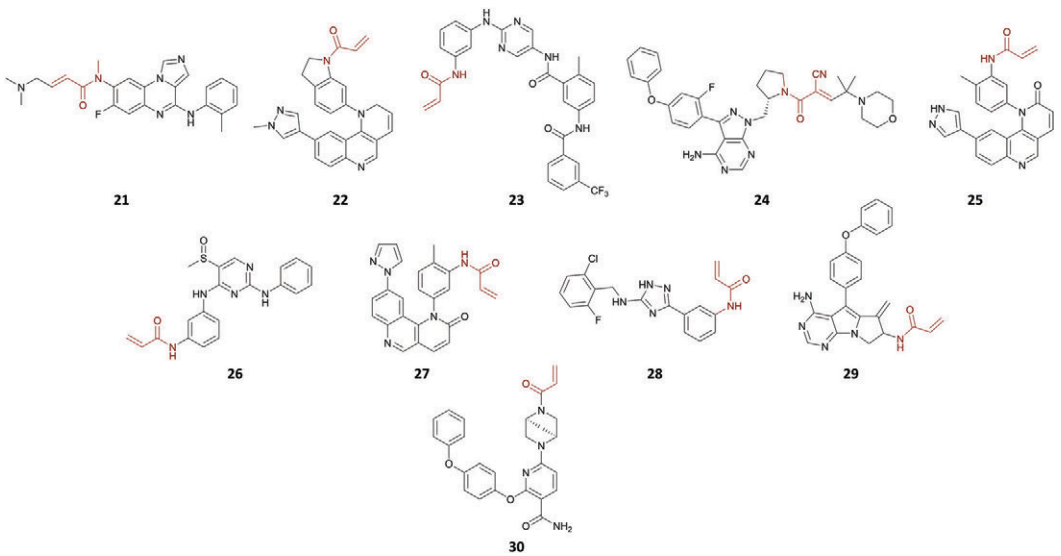

Fig. 23 Chemical structures of BTK targeting inhibitors **21–30** with acrylamide warheads reported between 2007–2018.

Table 5 Biochemical and cellular characterization data for inhibitors **21–30**

#	Reversible	Nucleophile	*In vitro* (nM)		*In cellulo* (nM)						Stage
			Isoform	IC_{50}	Cell line	IC_{50}	$t_{1/2}$ (h)	K_i (nM)	k_{inact} (ms^{-1})	k_{inact}/K_i (M^{-1} s^{-1})	
21		C481	BTK	1.93	1E5 B	3.41				5.32×10^4	Discovery
22		C481	BTK	6.59	Ramos	370					Discovery
23		C481	BTK	5	DoHH2	73	2.8[a]				Discovery
24		C481	BTK	3.3	Ramos	11		11	4.70	4.27×10^5	Discovery
25		C481	BTK	9.4	TMD8	0.31					Discovery
26		C481	BTK	3.76		5.85	1.3[b]				Discovery
27		C481	BTK	26.42							Discovery
28		C481	BTK	1.91							Discovery
29		C481	BTK	0.4	TMD8	16	0.57[a]				Discovery
30		C481	BTK	0.7			72[a]				Discovery

[a] Hepatocytes. [b] Mouse (*in vivo*).

Exquisite CKI selectivity was obtained ($S(35)$ = 0.01),which is a significant improvement over ibrutinib. Against the C481S mutant, a 300-fold loss of potency was observed, demonstrating the strong reliance of inhibitor affinity on covalent bond formation. A target-engagement assay using a biotinylated analogue of **22** revealed 50% labelling of BTK at 100 nM after 4 h. Interestingly, in addition to inhibiting kinase activity, this CKI induces BTK degradation at concentrations 3–5 times lower than the GI_{50}, providing an alternative mechanism to antagonize non-kinase dependent BTK function. While poor metabolic stability rendered it unsuitable for further *in vivo* studies, it remains a promising scaffold for further lead development.[152]

Li *et al.* sought to develop the first series of dual-action type II BTK inhibitors by targeting both kinase activation and catalytic function using a class of 2,5-diaminopyridimine-containing derivatives. Optimization of the initial non-covalent fragment revealed a preference for a phenyl group in the tail region, as it forms π–π stacking interactions with Tyr476. Extensive studies exploring various electrophiles with differing reactivities revealed compound **23** utilizing an acrylamide warhead. No reaction was observed between **23** (100 μM) and GSH (5 mM) in phosphate-buffered saline (PBS) buffer, suggesting minimal indiscriminate thiol reactivity. Kinase selectivity was similar to ibrutinib, where ABL, HER4, LCK, P38α and Vascular endothelial growth factor receptor (VEGFR) proteins were inhibited at 0.5 μM. Covalent bond formation was confirmed through MS, while washout experiments further supported this notion, as a sustained inhibitory effect was observed after 2 h exposure. Successive *in vivo* pharmacokinetic evaluation revealed moderate stability ($t_{1/2}$ = 2.8 h) and additional preclinical studies on mouse xenograft models inoculated with human lymphoma DoHH2 cells, showed a 66% reduction in tumour size when administered with 20 mg kg^{-1} of **23**.[153]

Taunton *et al.* were the first to explore the possibility of engaging BTK Cys481 using reversible covalent inhibitors. By inverting the orientation of a cysteine-reactive 2-cyanoacrylamide relative to the kinase active site, they identified potent and selective BTK inhibitors demonstrating biochemical residence times (τ) spanning a few minutes to several days. This new orientation provided opportunities for modulating inhibitor residence time by manipulating the steric and electronic properties of the electrophilic β-carbon.

Exploration of inhibitors containing polar and branched-alkyl capping substituents resulted in the discovery of **24** (τ = 167 ± 21 h), which was confirmed to be reversible with the quantitative recovery of compound following trypsin digest experiments. It also displayed extended kinase inhibition, with only 25% recovery of BTK function after 72 h of dialysis (as expected for an inhibitor with a slow off-rate). To assess whether sustained residence time translated into a prolonged pharmacodynamic effect in rodents, PP-BODIPY was used to determine levels of BTK engagement in rat peripheral blood mononuclear cells (PBMCs) after P.O. dosing of 40 mg kg^{-1}. While plasma levels peaked at 1 h (104 ± 66 ng mL^{-1}) and were shown to be significantly reduced at 14 h (3 ± 3 ng mL^{-1}), PD assessment of BTK occupancy showed prolonged and high % of target engagement, despite metabolic clearance from the systemic circulation. This result is proposed to reflect the slow dissociation event of **24** from BTK *in vivo*.[33]

Compound **25**, initially designed as a dual covalent inhibitor, targeting both BTK and MAPK interacting protein kinases (MNK), with the underlying hypothesis that inhibition may generate greater efficacy in cell lines only moderately sensitive to BTK inhibitors. A reversible analogue of **25** containing the inert propionamide lost all inhibitory activity, supporting a covalent binding mechanism was responsible for efficacy. Interestingly, against MNK1/2, only a 2-fold loss in potency was observed. Cellular washout experiments showed rapid recovery of eIF4E phosphorylation (MNK substrate), consistent with a reversible interaction of **25** with MNK kinase. In a panel of Chronic lymphocytic leukaemia (CLL) and Acute myeloid leukaemia (AML) patient cells, **25** showed greater potency over single agents ibrutinib and potent dual MNK/JAK inhibitor cercosporamide. While this may be attributed to the synergistic effect of dual inhibition, it is noted that in some cell lines (*e.g.* TMD8) this strategy did not confer any advantages. While sub-optimal PK properties limited *in vivo* application, this dual CKI inhibitor class provided an excellent proof of principal.[154]

Compound **26** was developed from the clinical candidate and irreversible BTK inhibitor, Spebrutinib. The authors proposed conformationally constraining this scaffold, specifically restricting the C–N bond rotation between aryl groups, to improve the orientation of the electrophilic warhead in the BTK active site. A cyclization-focused SAR to increase rigidity did not result in

observable improvements relative to acyclic analogues. The most promising compound developed, **26**, utilized an acyclic diaminopyrimidine scaffold to achieve enhanced potency. Unlike the cyclic derivatives, **26** observed high plasma stability across various species (86.7%, 94.3% and 90.7% remaining in humans, dogs and rats, respectively). The poorer stability of the cyclic analogues was hypothesized to be due to improved accessibility of the acrylamide to cellular nucleophiles in this conformation.[155]

Using SBDD, highly selective BTK inhibitor **27** was recently reported in literature. In a Ramos B cell line, it potently blocked phosphorylation of BTK Tyr223 (EC_{50} <100 nM) and inhibited downstream phosphorylation of Tyr1217 in PLCγ2 (IC_{50} <300 nM). The dependence on an irreversible interaction for the observed potency was confirmed by the testing of a non-covalent propionamide analogue as well as using site-directed mutagenesis studies of BTK^{C481S} mutants. In both cases, the inhibitor was virtually inactive (EC_{50} > 3000 nM). In a human MH74 cell line, **27** had no apparent effects on the anti-proliferation action of the cells demonstrating it acted by directly affecting the modulation of BTK signalling and not by degradation of B-cells or synovial cells. In a KinomeScan binding assay, **27** exhibited an enhanced selectivity profile, avoiding many of the off-targets typically inhibited by ibrutinib ($S(10)$ = 0.01 at 1 μM). In an adjuvant-induced arthritis rat model (an inflammation *in vivo* model for rheumatoid arthritis (RA)), **27** showed better efficacy than ibrutinib with half the dosage used (12.5 mg kg^{-1} day^{-1}). This superior activity was also shown in the arthritis index assessment (alternative indicator of RA) where it performed better relative to other common BTK inhibitors.[156]

A virtual screen identified lead compound **28**, exhibiting an impressive BTK/TEC selectivity ratio of 160-fold (BTK IC_{50} = 1.91 ± 0.02 nM; TEC IC_{50} = 306 ± 75 nM), relative to 17-fold observed in ibrutinib (BTK IC_{50}, 0.11 ± 0.01 nM; TEC IC_{50}, 1.86 ± 0.01 nM). Co-crystallization of **28** with BTK, revealed a covalent bond with Cys481 and three critical H-bonding interactions within the hinge binding region to the Thr474 gatekeeper and backbone residues, Glu475 and Met477. The irreversible interaction was confirmed by LC-MS/MS. Similar to **27**, **28** inhibited the autophosphorylation of BTK and downstream target PLCγ2 with varying potencies in Ramos cells (0.05–10 μM).[157]

An alternative medicinal chemistry approach was initiated by A. Zhang *et al.* to design new core structures for improved BTK inhibition. Replacing the pyrazolo[3,4-*d*]pyrimidine of ibrutinib with a tricyclic structure and modulating the electrophilic warhead led to the identification of **29** as a highly potent BTK inhibitor (IC_{50} = 0.4 nM). Compound **29** exhibited superior efficacy *in vitro* and *in vivo* relative to ibrutinib and had marginally improved $t_{1/2}$ of 0.57 h (ibrutinib $t_{1/2}$ = 0.42 h) and an overall enhanced PK profile in rats. In female CB-17 SCID nude mice bearing human TMD8 tumour cells, treatment with **29** (at 15 mg kg^{-1}) resulted in relative tumour volumes (RTV) of 6.6, whilst ibrutinib required higher doses (25 mg kg^{-1}), suggesting improved antitumor efficacy *in vivo*. MetID revealed two major metabolites, *p*-oxidation of the phenyl group in the diphenyl ether component leading to *p*-hydroxylated structures as well as significant dihydroxylation of the vinyl moieties (Fig. 24).[158]

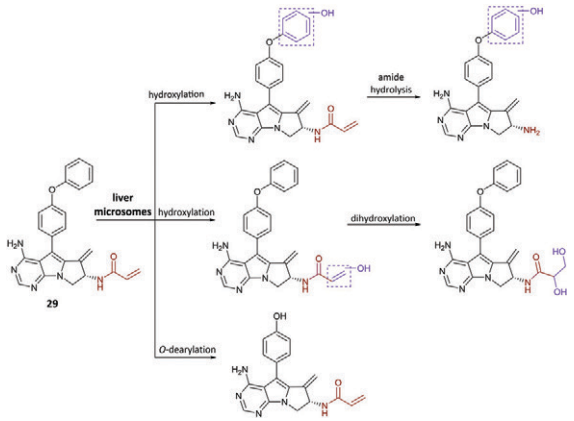

Fig. 24 MetID of lead compound **29** illustrating the two proposed oxidation pathways.

Starting with an initial fragment hit, Sherer *et al.* discovered a novel irreversible BTK inhibitor with an enhanced selectivity profile relative to ibrutinib. As seen in Fig. 25A, by overlaying their hit fragment X with the co-crystal structure of ibrutinib, they hypothesized that substituting the phenoxy-phenyl group, which occupies the hydrophobic pocket of BTK, with a pyridine carboxamide moiety could improve potency. Subsequent structural optimization led to the identification of **30** (BTK IC_{50} = 0.7 nM). Resolving the X-ray structure of this inhibitor bound to BTK confirmed covalent bond formation to Cys481 with a unique H-bonding interaction between methylene group proton and a neighbouring H_2O molecule (Fig. 25B). In addition to good cellular potency and PK profile, **30** inhibited only 3 other kinases (>50%) at 1 μM, which contrasts with ibrutinib which inhibits more than 35 off-targets at this concentration.[159]

JAK3

Janus kinases (JAKs) are a family of four non-receptor tyrosine kinases (JAK 1, 2, 3, and TYK2).[160] Upon cytokine-stimulation, these enzymes activate downstream STAT transcription factors which ultimately regulate gene expression mechanisms governing cell proliferation and survival. Genetic deletion studies have illustrated clear preferences for JAK gene products coupling/dimerizing with diverse receptors.[161–164] All four family members have been implicated in numerous diseases, including autoimmune disorders, inflammatory diseases. The JAK–STAT pathway represents a core cancer pathway in general for virtually all tumours linked with cytokine, growth factor and hormone signalling with rapid chromatin remodelling capacity, making them relevant therapeutic targets.[165–168] In the context of a covalent approach to kinase inhibition, it is currently limited to JAK3 as it contains a poorly conserved isoform-specific cysteine (Cys909) in the active site. However, JAK3 possesses a relatively short re-synthesis time ($t_{1/2}$ ~ 3 h), making it a problematic covalent target.

The first reversible covalent JAK3 inhibitor, was reported by London *et al.* who used a novel computational method

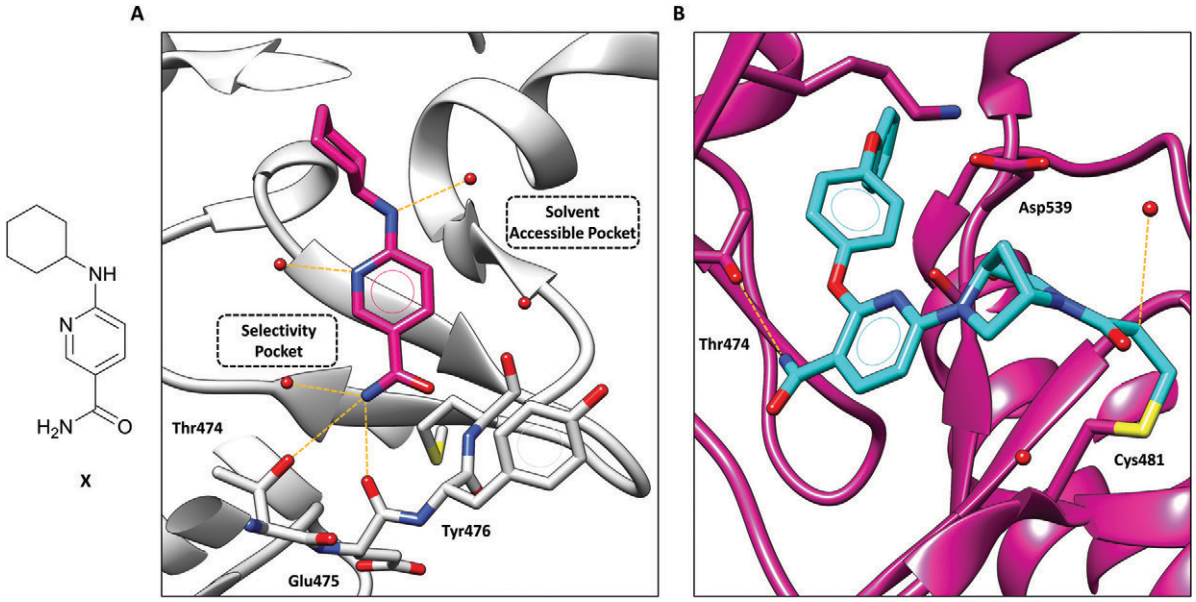

Fig. 25 (A) Overlay of fragment hit **X** in the binding pocket of BTK (PDB 6DI0). Authors proposed extension of the non-covalent scaffold into the hydrophobic selectivity pocket could serve to enhance potency.[153] (B) X-ray crystal structure of 30 bound to BTK (PDB 6DI5) illustrating the unique H-bonding interaction between the methylene group proton and the H_2O molecule.

(DOCKovalent) to screen a large library of electrophilic small molecules. An initial preliminary screen of a virtual 2-cyanoacrylamide library suggested larger fragments may be required to covalently modify Cys909. Subsequent derivatization of hit fragment screening identified two potent compounds, **31** and **32**, which inhibited JAK3 with IC_{50} values of 49 nM and 93 nM, respectively (Fig. 26). At concentrations up to 10 μM, no other JAK isoform was targeted, likely due to the absence of an analogous active site cysteine. However, against 9 different kinases containing a homologous cysteine, **31** was found to potently inhibit BLK (IC_{50} = 22 nM), HER4 (IC_{50} = 44 nM) and ITK (IC_{50} = 221 nM) but **31** showed 30-fold selectivity for JAK3 over the other six kinases. Jump dilution experiments were utilized to confirm their covalent reversibility.[104]

Based on available crystal structures of JAK kinases and previous work on tricyclic JAK inhibitors,[169–171] Goedken *et al.* designed several covalent tricyclic scaffolds. The most promising analogue was the acrylamide-containing compound, **33**. In a Time-resolved Fluorescence Resonance Energy Transfer (TR-FRET) kinetics binding assay, **33** showed displacement of the binding probe at all concentrations up to 0.64 nM (sub-stoichiometric to JAK3) and the derived k_{inact}/K_i value of 1.0×10^7 M^{-1} min^{-1} revealed a 200-fold improvement compared to previous tricyclic inhibitors.[171] Jump dilution experiments showed no recovery of JAK3 activity relative to control analogues. MS experiments identified an epitope containing Cys909 was specifically modified by **33**, suggesting an irreversible binding mechanism (Table 6). Against the remaining JAK isoforms, **33** exhibited a strong selectivity profile and showed >100-fold selectivity for JAK3 over ITK, BTK and EFGR (all containing equivalent cysteines).

In a cytokine-dependent cellular assay (IL-2 stimulation requiring JAK3 and JAK1), **33** had an EC_{50} of 19 nM, but showed no activity in JAK2-dependent assays that is more myeloid cytokine specific highlighting its utility as a JAK3-specific CKI.[172] Starting from previously described EGFR inhibitor **3**, replacement of the ether moiety with an aminomethylene linker (–$NHCH_2$–)

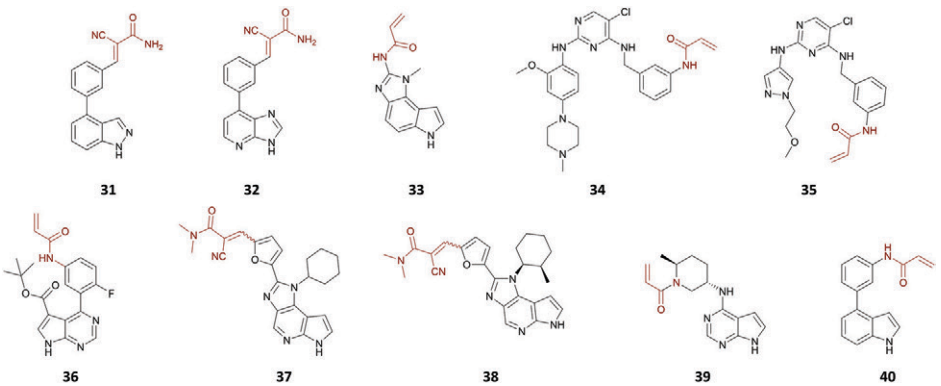

Fig. 26 Chemical structures of JAK3 targeting inhibitors **31–40** with acrylamide warheads reported between 2007–2018.

Table 6 Biochemical and cellular characterization data of inhibitors **31–40**

			In vitro (nM)		*In cellulo* (nM)						
#	Reversible	Nucleophile	Isoform	IC_{50}	Cell line[a]	EC_{50}	$t_{1/2}$ (h)	K_i (nM)	k_{inact} (ms^{-1})	k_{inact}/K_i (M^{-1} s^{-1})	Stage
31	•	C909	JAK3	41							Discovery
32	•	C909	JAK3	93							Discovery
33		C909	JAK3	7	IL-2 T-blasts	19				1.6×10^4	Discovery
34		C909	JAK3	4.8	TEL-JAK3	69	0.078[b]				Discovery
35		C909	JAK3	<0.5	TEL-JAK3	19	0.055[b]				Discovery
36		C909	JAK3	0.43							Discovery
37	•	C909	JAK3	9			3[b]				Discovery
38	•	C909	JAK3	17							Discovery
39		C909	JAK3	0.35			2[b]	6310	2.32	3.6×10^5	Preclinical
40		C909	JAK3	0.14							Discovery

[a] Given the complexity of the JAK signalling pathways, few IC_{50}s have been reported in indication specific cell lines. Several publications report EC_{50} for Ba/F3 transfected cells activated by certain cytokines or stimulating factors which are illustrated in the table above. [b] Human (*in vivo*).

generated the highly potent JAK3 inhibitor, **34**. This compound selectively inhibited proliferation of JAK3-dependent Ba/F3 cells (IC_{50} = 69 nM) while no anti-proliferative effects were observed in non JAK3-dependent cell lines up to 3 μM. An X-ray co-crystal structure confirmed covalent bond formation between the acrylamide warhead and Cys909 with the phenyl group of **34** interacting with Leu956 in the floor of the ATP-binding cleft. This feature is distinctly different from how **3** binds EGFR and is likely a function of the extended linker length. Unfortunately, such a promising *in vitro* profile did not translate *in vivo* with no effect on tumour size observed in $KrasG^{12D}$, $Lkb1^{L/L}$ driven lung adenocarcinoma mouse models.

Further SARs identified CKI **35** as the most potent and selective compound in the series. It observed >70-fold selectivity for JAK3 over remaining isoforms (biochemical) and 390-fold selectivity window in JAK-transformed Ba/F3 cells. Unfortunately, hepatic stability in mouse liver microsomes (MLM) was poor ($t_{1/2}$ = 3.30 min) and thus *in vivo* evaluation was not persued.[173]

To dissect the role of JAK3 in γ_C – receptor signalling, the JAK3-selective chemical probe **36** was identified from a series of acrylamide containing a pyrrolopyrimidine core reported in a previous patent application.[174] **36** was highly JAK3-selective in biochemical assays with >3000-fold selectivity for JAK3 over the remaining JAK kinases. Against a panel of kinases with an equivalently positioned cysteine, selectivity was maintained at 50-fold. Using this molecular probe, the authors document a second wave of IL-2 mediated signalling, which is much more sensitive to inhibitor **36** and is sufficient to block cellular entry into S-phase, consequently inducing apoptosis. While not designed as an inhibitor with therapeutic applications, this study demonstrated the utility of CKIs as probes to interrogate kinase biology.[175]

To develop a highly selective JAK3 chemical probe, Forester *et al.* discovered that using the reversibly covalent 2-cyanoacrylamide motif dramatically improved the potency of early hit compounds, yielding, **37** and **38** as promising lead compounds. Studies into the binding kinetics of **37** revealed longer ligand residence times with JAK3 relative to TYK2 (τ = 50 min and 1.40 min, respectively). Subsequent washout experiments revealed recovery of the bioluminescence resonance energy transfer (BRET) ratio after 1 h which agrees with a reversible mechanism of action. While only a non-covalent interaction was observed in the co-crystal structure of **37** with JAK3, **38** was found to form both non-covalent and covalent adducts, which underlines the reversible character of the covalent interaction (Fig. 27). These binding modes were further verified by MS. In subsequent studies, **37** was found to have a favourable MLM stability with 58% of compound remaining after 3 h.[176] A more comprehensive SAR around this scaffold was detailed in a following publication.[177]

Pre-clinical candidate **39**, was reported by Pfizer as an isoform-selective JAK3 inhibitor. In a TR-FRET competition assay and further verified *via* an X-ray co-crystal structure, **39** was shown to irreversibly inhibit the kinase. Functional assessment in T-cell differentiation assays showed treatment with **39** suppressed JAK3-dependent signalling in Th1 (IL-2 stimulated) and Th17 (IL-21 stimulated) cells as measured by IFNγ, while sparing JAK1-dependent signalling cascades. Compound **39** exhibited impressive PK profiles and was orally administered in preclinical models of inflammation. Predicted human PK provided an approximate blood clearance of 5.6 mL min^{-1} kg^{-1}, a steady state volume distribution of 1.3 L kg^{-1}, P.O. F = 90%, and a systemic $t_{1/2}$ of 2 h. In two rodent models (arthritis and encephalomyelitis), **39** significantly reduced disease severity at 30–100 mg kg^{-1}.[178] A later publication by the same group describes the SAR and approaches utilized to optimize electrophilic reactivity, which ultimately led to the discovery of this CKI.[179]

Using Tofacitinib (an FDA approved pan-JAK inhibitor), Linhong He *et al.* designed a series of 7*H*-pyrrolo[2,3-*d*]pyrimidine scaffolds as JAK3 inhibitors. An investigation around various electrophilic warheads identified the following order of potency: acrylamide ≈ α-haloketone > methyl acrylamide > 2-chloropropanamide > (*E*)-but-2-enamide/3-methylbut-2-enamide, which led to acrylamide inhibitor **40** (IC_{50} = 0.14 nM). When profiled against 9 kinases with analogous cysteines, this CKI observed >1700-fold selectivity for JAK3 and was inactive towards the remaining structures (IC_{50} > 1 μM). Computational covalent docking studies revealed **40** extended into the kinase hydrophobic pocket, potentially forming hydrogen bonding interactions with Ala853, Met902, Leu905, Val884 and Leu828. Pre-incubation with JAK3 followed by a jump dilution analysis showed complete JAK3 inactivation, relative

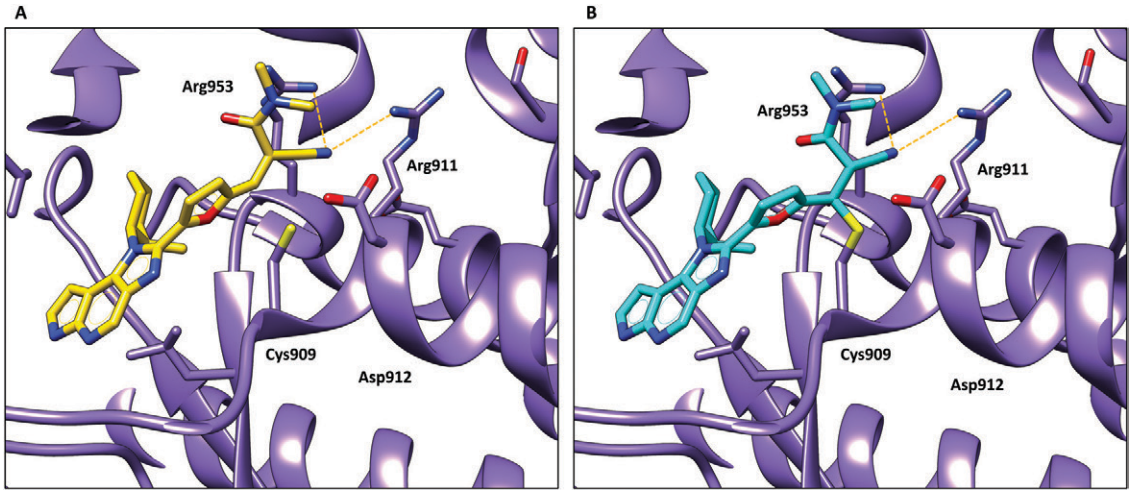

Fig. 27 (A) **37** non-covalently bound to JAK3 active site (PDB 5IWM), (B) crystal structure of covalently bound **38** (PDB 5LWN).

to the control confirming irreversibility. To evaluate the anti-inflammatory efficacy of this inhibitor, the inflammatory response was assessed in a carrageenan-induced paw edema test where **40** showed a 23.78% paw size increase.[180]

FGFR

The FGFR family is comprised of four functional receptor members FGFR1–4 and many growth factor ligands, each containing a conserved extracellular ligand-binding domain, a single transmembrane region and a cytosolic domain.[181] Activation of downstream pathways is responsible for cell growth, metabolism, proliferation and differentiation. Sequencing of solid tumours has identified aberrant signalling of FGFR kinases in 7% of cancers, implicating it as a potential point of therapeutic intervention.[182] It has since been heavily investigated with many non-covalent inhibitors reported in the clinic and literature.[183–185] However, *in vivo* efficacy of such derivatives is limited by their rapid clearance prompting the search for irreversible CKI with improved pharmacokinetics. Efforts to develop covalent inhibitors were made feasible due to the presence of two conserved cysteine residues in the ATP binding pocket, which are amenable to modification.

Gray *et al.* reported one of the first covalent pan-FGFR inhibitors that can overcome kinase inhibitor resistance. Their initial lead, **41**, was a potent and selective inhibitor with biochemical IC_{50} values of 9.2, 6.2, 11.9, and 189 nM against FGFR1, 2, 3, and 4, respectively (Fig. 28). Compound **41** blocked activation of FGFR and associated downstream signalling partners by covalent modification of Cys486 (validated using a biotin-labelled probe). Yet this inhibitor was weakly potent against the $FGFR^{V561M}$ gatekeeper mutation. The authors propose that this is due to a steric clash between the bulky dichloro-dimethoxyphenyl substituent on **41** and the Met residue.[186]

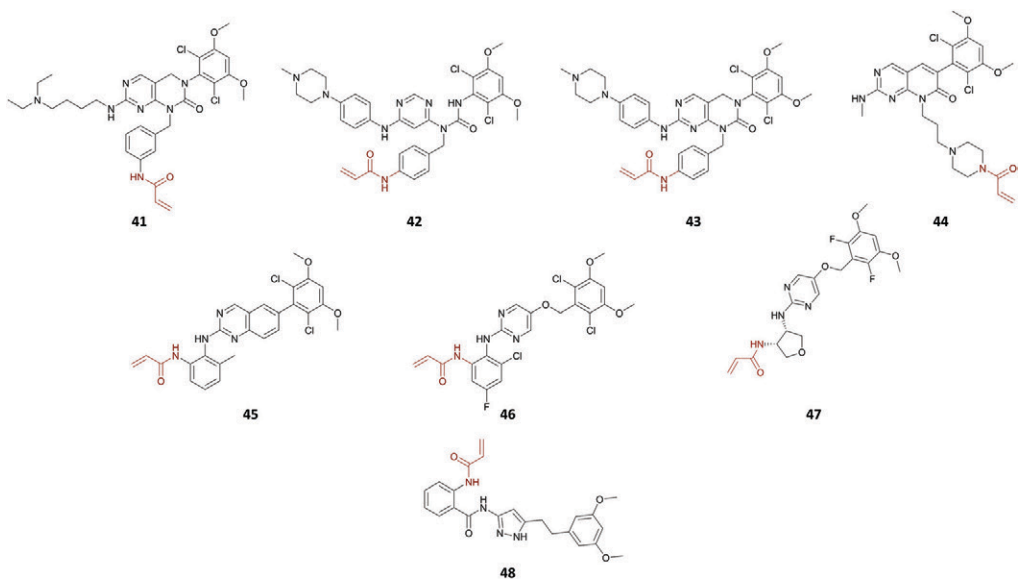

Fig. 28 Chemical structures of FGFR targeting inhibitors **41–48** with acrylamide warheads reported between 2007–2018.

Table 7 Biochemical and cellular characterization data for inhibitors **41–48**

			In vitro (nM)		*In cellulo* (nM)						
#	Reversible	Nucleophile	Isoform	IC_{50}	Cell line	IC_{50}	$t_{1/2}$ (h)	K_i (nM)	k_{inact} (ms^{-1})	k_{inact}/K_i (M^{-1} s^{-1})	Stage
41		C486	FGFR1	9.2							Discovery
42		C486	FGFR	1–93	H2077	3.9					Discovery
43		C486	FGFR	1–64	H2077	5.3					Discovery
44	•	C486	FGFR1	0.6	SNU16	2.6	3.8[a]	1.6	1.9	1.2×10^6	Phase I
45		C552	FGFR4	3	Hep 3B	70	2.3[a]	27	2.0	6.0×10^4	Discovery
46		C552	FGFR4	2.6	MDA-MB-453	380					Discovery
47		C552	FGFR4	13							Discovery
48		C477/C552	FGFR4	1.5						5.1×10^6	Discovery

[a] Hepatocytes.

Several analogues of **41** were explored to overcome $FGFR^{V561M}$, culminating in the discovery of compounds **42** and **43**. Both compounds potently inhibited Ba/F3 cells (dependent on $FGFR^{WT}$ and mutant $FGFR2^{V564M}$) with EC_{50} values between 1–93 nM (Table 7).

Against a panel of 456 kinases, **42** and **43** displayed strong binding to FGFR1-4, with an $S(1)$ selectivity score of 10 and 15, respectively at 1 μM. These compounds also inhibited $FGFR2^{V564M}$ in Ba/F3 cells with a higher potency than original scaffold, **41**. An alanine mutation of the reactive cysteine within FGFR2 resulted in a complete loss of potency, proving the importance of covalency for the observed activity. A co-crystal structure of **42** bound to the FGFR4 kinase domain revealed covalent bond formation between Cys477 in the kinase P-loop and a ''π–π stacking sandwich'' interaction between the 3,5-dimethoxyphenylgroup and the 4-acrylamidobenzyl group, which stabilizes the DFG-out conformation (a unique feature not previously reported in FGFR crystal structures).[49] Despite this heightened potency, these did not prove to be ideal drug candidates due to mild/severe phenotypic changes observed *in vivo* with embryonic zebrafish animal model testing. Further efforts were conducted to identify a suitable preclinical leads, resulting in more advanced inhibitors.[187]

In 2017, Principia Biopharma published the design and discovery of a series of irreversible covalent FGFR1-4 inhibitors which culminated in the discovery of clinical candidate, **44**. The authors reasoned that a pan-FGFR inhibitor would provide the widest therapeutic utility owing to the heterogeneity of FGFR isoforms and the varied dependence on cancers of several signalling pathways. Compound **44** showed excellent biochemical occupancy and cellular potency (FGFR1 IC_{50} = 0.6 nM, SNU16 IC_{50} = 2.6 nM), prolonged target engagement (96% FGFR1 occupancy at 24 h) and $<30\%$ hERG inhibition at 1 μM. A kinome screen against 251 kinases identified FGFR1–4 and Colony stimulating factor 1 receptor (CSF1R) as the main targets, where further studies confirmed CSF1R binding was non-covalent. In a rat PK study (I.V. 2 mg kg^{-1}), rapid clearance was observed while demonstrating high exposure (AUC = 4348 ng mL^{-1}) with good metabolic stability ($t_{1/2}$ = 3.8 h). Similar studies in higher order mammals (*i.e.* monkeys, dogs) also revealed similar clearance results, though large differences in oral exposure and bioavailability were observed. This was attributed to the varying intestinal and gastric pH levels amongst different species as well as their different rates of metabolism. *In vivo* experiments suggested long-lasting FGFR target inhibition, and efficacy studies using SNU16 gastric cancer xenograft mice (10 mg kg^{-1} P.O.) showed the ability to lower levels of phospho-FGFR2 and reduce tumour growth by ~68%. Currently, this CKI is in phase 1 clinical trials.[188]

FGFR4

The development of FGFR4-specific covalent inhibitors has gained wide spread interest in the past three years due to the specific role played by the FGFR4–FGF19 complex in hepatocellular carcinoma (HCC).[189] To date, many of the FGFR inhibitors developed are either biased towards FGFR1–3 or equipotent against all FGFR family members. As such they suffer from toxicities related to off-target activity which has been characterized in both animals and human patients.[190] Interestingly, FGFR4 possesses a unique cysteine in the hinge region (Cys552) that is not present in any of the other FGFR members. It has since been used as an additional selectivity filter for the design of highly selective FGFR4 targeting CKIs.

Compound **45** was the first selective covalent FGFR4 inhibitor, able to spare all other FGFR analogues (FGFR1–3) by targeting FGFR4-specific Cys552. Expanding on the previously reported clinical candidate **44**, authors hypothesized a 60° dihedral rotation of the aniline phenyl ring would direct the *ortho*-substituted acrylamide towards Cys552, an orientation that would otherwise clash with a tyrosine side chain in FGFR1–3. Compound **45** showed potent inhibition of FGFR4 enzyme activity (IC_{50} = 3 nM) with weak activity amongst the other FGFR isoforms (IC_{50} > 100 nM) in addition to an impressive selectivity profile ($S(1)$ = 0.005, 3 μM). In FGFR-dependent cell lines MDA-MB-453 and Hep 3B, potent and dose-dependent reduction in downstream signalling was observed including FGFR substrate 2 (FRS2), MAPK, and protein kinase B (AKT) with minimal inhibition of fibroblast growth factor 1 (FGF) phosphorylation events. *In vivo* studies using Hep3B xenografts (HCC disease model) and initial pharmacokinetic analysis revealed moderate bioavailability (F = 18%), $t_{1/2}$ (2.3 h) along with dose-dependent tumour inhibition (P.O., 10 mg kg^{-1}).[191]

Given the isoform selectivity and clinical potential of **45**, Ke Ding *et al.* synthesized a series of 2-aminopyrimidine

derivatives starting from the X-ray structure of this CKI bound to FGFR4. Given the lowest energy conformation of *n*-butane is the anti-configuration, where the dihedral angle of the carbon atoms is approximately 180°, it was postulated that it may be possible to mimic the co-planar configuration of C_a, C_b, C_c, C_d, in compound **45**. A subsequent SAR resulted in the identification of lead compound **46**, with an IC_{50} of 2.6 nM against FGFR4. It also exhibited enhanced selectivity (IC_{50} >10 000 nM against FGFR1–3). Note, the α, β saturated propionamide analogue showed significantly reduced potency (FGFR4 IC_{50} >10 000 nM), consistent with a covalent mechanism of action. Target specificity was demonstrated against a panel of 468 kinases with *S*(1) and *S*(35) selectivity scores of 0.007 and 0.01 at 1.0 μM. Against a panel of breast cancer cell lines, **46** inhibited MDA-MB-453 cells with an IC_{50} of 380 nM, similar to that of **45**, but was unable to suppress MCF-7 and MDA-MB-231 growth at 10 μM, further supporting the strong and selective efficacy against FGFR4.[192]

Compound **47** was discovered by structural analysis of non-covalent pan-FGFR inhibitor ASP5878 (Fig. 29). Computational modelling studies suggested ASP5878 bound FGFR4 in a similar manner to **45**, forming two H-bonds with key hinge region residues. Exploration of the electronic and steric effects of a phenylacrylamide scaffold led to identification of **47** (FGFR4 IC_{50} = 13 nM), which was 300-fold more potent than its opposite enantiomer. Compound **47** showed greater plasma stability (96% remaining after 2 h), improved solubility, and was found to have minimal activity against the major CYP p450 cytochrome detoxifying liver enzymes. Less than 20% inhibition was seen when **47** was tested against a panel of 7 kinases at 10 μM. The promising *in vitro* profile prompted an *in vivo* PK study. Unfortunately, I.V. dosing at 1 mg kg^{-1} in mice failed to deliver any quantifiable exposure, likely resulting from first pass elimination due to microsomal instability. Efforts to address this issue are currently underway.[193]

Compound **48** was identified *via* introduction of an acrylamide warhead into known pan-FGFR inhibitor, AZD4547 (Fig. 29). Addition of the acrylamide to the *ortho* position of the phenyl benzamide moiety was proposed to bring the acrylamide proximal to either Cys552 or Cys477. Specifically, the conformer which oriented the warhead towards Cys477 was expected to more stable due to an intramolecular H-bond between the acrylamide and benzamide carbonyl groups. Studies on a $FGFR4^{C477A}$ mutant strongly supported this hypothesis, with a 400-fold loss in activity observed (FGFR4 IC_{50} = 0.8 nM, $FGFR4^{C477A}$ IC_{50} = 443 nM) in addition to a 1000-fold improved interaction with $FGFR4^{WT}$ (k_{inact}/K_i = 5.1 × 10^6 M^{-1} s^{-1}) compared to the C477A variant (k_{inact}/K_i of 5.1 × 10^2 M^{-1} s^{-1}). In terms of Cys552, only a 5-fold loss in potency was observed against $FGFR4^{C552A}$ suggesting a weaker dependence on this covalent interaction, despite MS studies confirming covalent modification of both sites. A co-crystal structure of **48** bound to the FGFR4 kinase domain confirmed the covalent bond with P-loop Cys477, conserving the key hinge and back-pocket interactions made by AZD4547. To our knowledge this is the only FGFR4 CKI to target Cys477.[194]

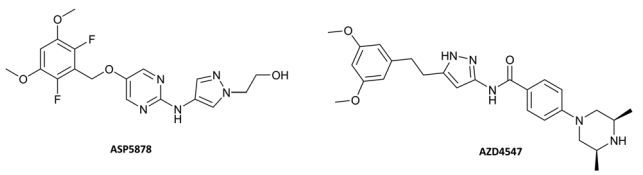

Fig. 29 Structures of non-covalent pan-FGFR inhibitors ASP5878 and AZD4547.

Other kinases

ITK. Similar to BTK, ITK is a member of the TEC family. Primarily localized to immune cells, it is thought to play an important role in the development and function of T-cells, particularly Th_2 cells.[195] Th_2 deficiencies have been observed to be implicated in asthma and other autoimmune deficiencies, highlighting the potential therapeutic utility of ITK inhibitors. More specifically, $ITK^{-/-}$ mice show greatly attenuated symptoms in disease models of asthma, prompting interest amongst the scientific community to develop such small molecules, though no drugs have yet succeeded to be used in asthmatic patients.[196]

The first covalent ITK drug discovery program was initiated by researchers at Pfizer in 2012. Interestingly, a traditional pulse-chase experiment suggested a $t_{1/2}$ of ~2 h, typically not ideal for a covalent-based approach. However, despite such fast protein turn-over, incubation of cells with a covalent inhibitor seemingly stabilized ITK kinase, drastically increasing the $t_{1/2}$ to ~22 h, and therefore justifying the use of a CKI. Given target validation, a corporate compound repository was then screened against ITK for potential covalent leads. Upon identifying a hit, subsequent structural optimization led to lead candidate, **49** (Fig. 30 and Table 8). This small molecule was found to be highly potent in enzymatic and cell-based assays with IC_{50} values of 31 and 48 nM (in IP1 and hWB cell lines, respectively), maintaining potency even with high [ATP] (K_m ATP for ITK = 5 μM). Insight into the binding kinetics of the inhibitor validated the irreversible covalent interaction, however high sequence homology with BTK (~70%), and reduced nucleophilicity of Cys442 (pK_a ~ 8.5 due to Asp445 at *i* + 3) rendered selectivity a major hurdle for this class of molecules.[58]

Highly potent ITK inhibitor **50** was identified from structure-based optimization of a non-covalent binding scaffold. In a LanthaScreen™ kinetic binding assay, it was observed to evoke a two-step, time-dependent inhibition profile with an initial rapid (<1 min) binding event, followed by a slower onset of inhibitory action, which is consistent with an irreversible mechanism. Selectivity profiling demonstrated a clear preference for ITK over other kinases such as BTK and EGFR. *In vitro* biological evaluation in PBMCs showed potent cellular activity at 2 h post washout relative to the non-covalent control which lost all potency. Interestingly, a pulse-chase experiment revealed a longer $t_{1/2}$ in the absence of inhibitor (>24 h), in contrast to what was previously reported. It also revealed an increase in rates of protein re-synthesis (*i.e.* shorter $t_{1/2}$) when incubated with the CKI **50**. Impressively, this compound

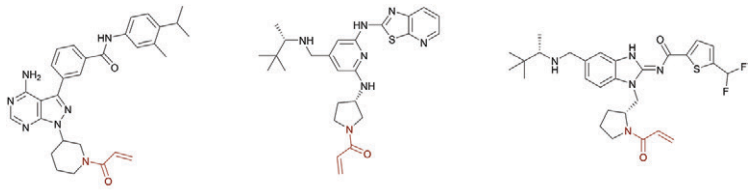

Fig. 30 Chemical structures of ITK targeting inhibitors **49–51** with acrylamide warheads reported between 2007–2018.

Table 8 Biochemical and cellular characterization data for inhibitors **49–51**

			In vitro (nM)		*In cellulo* (nM)						
#	Reversible	Nucleophile	Isoform	IC_{50}	Cell line	IC_{50}	$t_{1/2}$ (h)	K_i (nM)	k_{inact} (ms^{-1})	k_{inact}/K_i (M^{-1} s^{-1})	Stage
49		C442	ITK	2			0.12[a]			1.61×10^4	Discovery
50		C442	ITK	5						520×10^3	Discovery
51		C350/442	ITK/RLK	1.4/0.3						$4.6/47 \times 10^5$	Preclinical

[a] Hepatocytes.

inhibited T-cell activation following 18 h of stimulation with anti-CD3, *in vivo*.[197]

Dual ITK/RLK (resting lymphocyte kinase) inhibitor **51** was discovered using SBDD. *In vitro* kinase assays revealed a small number of off-targets with only three non-TEC family kinases inhibited by >90% at a concentration of 1 μM. Selectivity was further validated in Jurkat T-cells possessing mutant ITK or overexpressing RLK apart from reported STAT3/5 missense mutations. Additional kinetic analysis in a microfluidic kinase assay revealed time-dependent inhibition, consistent with a covalent mechanism-of-action. Furthermore, **51** was also observed to block T-cell receptor (TCR) or Fc receptor (FcR)-induced cellular and molecular activation, blocking TCR-induced calcium flux and NFAT action in CD4 and CD8 T-cells. Moreover, inhibition of naiive primary TCR-induced proliferation was observed without direct toxicity, making it a good candidate drug for Peripheral T-cell Leukaemia and Lymphoma. Examination of the PK and PD profile in mice revealed target occupancy of 54% as long as 14 h post-incubation, where the concentration of **51** in the blood plasma was 10-fold lower than the IC_{50}. This demonstrates sustained pharmacodynamic effects despite inhibitor clearance.[198]

RSK2/MSK1. Ribosomal S6 kinase 2 (RSK2) and Mitogen and stress activated protein kinase 1 (MSK1) are a pair of related kinases implicated in a variety of inflammatory and oncogenic process. The CTD of RSK2 and MSK1 contains a poorly conserved, non-catalytic cysteine, which is uniquely found in ~2% of the human kinome. However, unlike RSK2, MSK1 has methionine gatekeeper.[199,200] Despite their similarity, kinase selectivity remains challenging, with 2 of 3 inhibitors presented below expressing dual inhibition. It is interesting to note that all covalent RSK2 and MSK1 acrylamide-based inhibitors operate *via* a reversible covalent mechanism, largely pioneered in work by Taunton *et al.*

Inhibitor **52** was identified from an extensive screen of various electrophilic pyrrolopyrimidine scaffolds, designed to be analogues of various Michael acceptors (Fig. 31). The unique reversible covalency was validified using several assays. In a kinetic trapping assay, inhibition of the RSK2-CTD was long-lived but fully reversible, with complete dissociation occurring on the timescale of several h. Washout experiments in MDA-MB-231 (breast cancer) cells revealed ligand residence within RSK1/2 was indistinguishable from previously reported irreversible inhibitor FMK, with apo-protein levels detected only after ~48 h (presumed as the rate of re-synthesis) (Table 9). Further inspection of the UV spectrum revealed the 2-cyanoacrylamide absorption peak following unfolding of the RSK2-**52** complex, further validating the reversibility.[201]

Initially guided by X-ray crystal structures, an indazole fragment was structurally derivatized to afford dual RSK2/MSK1 inhibitor **53**. Selectivity screens against a panel of 26 kinases showed only Never in mitosis related kinase 2 (Nek2) and serine/threonine-protein kinase 1 (Plk1) as significantly off-targets at 1 μM (77% and 84%, respectively). A co-crystal structure of CKI **53** with RSK2 revealed packing of the indazole against the Met493 gatekeeper and nestling of the trimethoxyphenyl motif between the side chains of Ile428, Met496, and Lys451 (Fig. 32). Inhibition of CTD-mediated autophosphorylation of full-length RSK2 and MSK1 was observed in cells at an IC_{50} of ~100 nM. Further *in cellulo* work with the cAMP-response element binding transcription factor (CREB), indicated that MSK1/2 play a critical role in promoting CREB phosphorylation by the kinase N-terminal domain.[202]

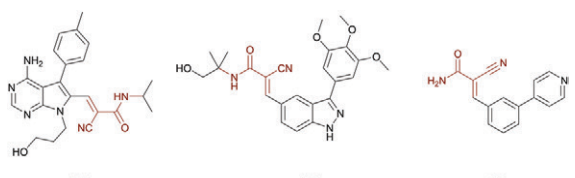

Fig. 31 Chemical structures of RSK2/MSK1 targeting inhibitors **52–54** with acrylamide warheads reported between 2007–2018.

Table 9 Biochemical and cellular characterization data for inhibitors **52–54**

#	Reversible	Nucleophile	*In vitro* (nM) Isoform	IC_{50}	*In cellulo* (nM) Cell line	IC_{50}	$t_{1/2}$ (h)	K_i (nM)	k_{inact} (ms^{-1})	k_{inact}/K_i (M^{-1} s^{-1})	Stage
52	•	C436/C458	RSK2	4							Discovery
53	•	C436/C458	MSK1/RSK	12							Discovery
54	•	C436/C458	RSK2/MSK1	42							Discovery

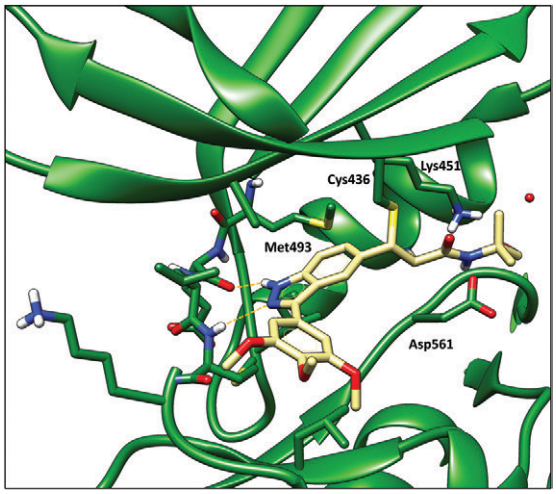

Fig. 32 Crystal structure of **53** bound RSK2 T493M (PDB 4JG8).

Using the DOCKovalent platform,[104] London *et al.* converted 12 000 aldehyde fragments from the ZINC database into electrophilic 2-cyanoacrylamide fragments to generate a virtual covalent library. Computational docking of this set of ligands against Cys436 of RSK2 and subsequent compound synthesis culminated in the discovery of **54**. In the presence of 0.1 mM ATP and 10 mM GSH, **54** inhibited $RSK2^{WT}$ and $RSK2^{T493M}$ with impressive sub-micromolar potency (IC_{50} = 430 nM). In mammalian cells stimulated with phorbol myristate acetate (PMA), which activated upstream signalling cascades of RSK2 and MSK1, CKI **54** successfully inhibited the auto-phosphorylation of wild-type MSK1 with similar potencies (EC_{50} < 1 μM).[104]

CDK. CDKs are a class of serine–threonine kinases known for their role in regulating the cell cycle, transcription, mRNA processing and nerve cell differentiation. Association of these kinases with regulatory protein cyclin results in an active cyclic-CDK complex which subsequently phosphorylates protein substrates involved in cell cycle progression.[203] To date, 20 CDK family members have been reported in the human kinome, each modifying differing substrates. Due to such roles, great effort has been invested in developing CDK inhibitors as anti-cancer agents.[204] Specific interest in covalent inhibitors has recently emerged following the identification of uniquely distributed cysteines amongst the CDK family.

The first covalent CDK inhibitor was reported by Gray *et al.* in 2014. The phenylaminopyrimidine scaffold containing an acrylamide warhead **55** potently inhibited CDK7 (IC_{50} = 3.7 nM) (Fig. 33). Incubation of a biotinylated derivative with recombinant CDK7-cyclin-H-MAT1 (*i.e.* active CDK7 complex), in addition to MS experiments confirmed covalent modification at Cys312, located outside the kinase domain. This CKI was able to inhibit CDK7 substrate, RNA polymerase II (RNAPII) CTD phosphorylation at Ser5 and Ser7 at 250 nM in Jurkat cells (Table 10). It also induced sustained downregulation of RNAPII CTD phosphorylation in washout experiments, confirming the irreversible mode of action. Sequence alignment of CDK1-20 revealed the targeted Cys312 was unique to CDK7, however CDK12 and CDK13 also contained accessible cysteines. In a bioluminescent xenograft mouse model of human T-ALL cells, reduced proliferation was demonstrated at a well-tolerated dose of 10 mg kg^{-1}.[205] CDK12 and CDK13 have been proposed to play an important role in gene expression through phosphorylation of Ser2 of RNAPII.

To further address the functional consequences of their inhibition, CKI **56** was designed from the previously reported covalent CDK7 scaffold, **55**. Changing the benzamide moiety to a piperidine improved selectivity for CDK12/13 relative to CDK7/9. Co-crystallization with CDK12 revealed covalent modification at Cys1039, also found outside the ATP binding site (similar to Cys312 in CDK7). In Jurkat cells, **56** blocked elongation and hyperphosphorylation of RNAPII, consequently causing a loss of gene expression and the induction of cell death. Specifically, it was found to decrease expression of DNA damage response genes and certain super-enhancer-associated transcription factor genes. This study highlights the potential use of CDK12/13 inhibitors for certain therapeutic applications in addition to their utility as chemical probes to interrogate CDK function.[206]

JNK. c-Jun N-terminal kinases (JNK) are a subfamily of MAP kinases involved in regulating a range of biological processes in response to cellular stress (*i.e.* cytokine activity, UV irradiation, heat shock, cancer cell attachment, *etc.*). For instance, these stress kinases bind and phosphorylate Ser63 within the transcriptional activation domain of c-Jun protein substrates and are also involved in STAT1/3 serine phosphorylations.[207] In addition, JNKs play a central role in inflammatory signalling pathways, which has implicated aberrant function in various human pathologies including cancer, immune diseases and neurodegenerative disorders.[208,209] These findings have stimulated research efforts into small-molecule JNK inhibitors for applications in chemical biology and drug discovery.

All JNK isoforms share a homologous reactive cysteine, which was exploited for the design of selective JNK inhibitor, **57**. Notably, the flag methyl group optimally occupies a small hydrophobic pocket (a feature also seen in Imatinib) which is thought to strongly contribute to the observed selectivity ($S(10)$ = 0.025 at 1 μM). Regarding efficacy, **57** was capable of

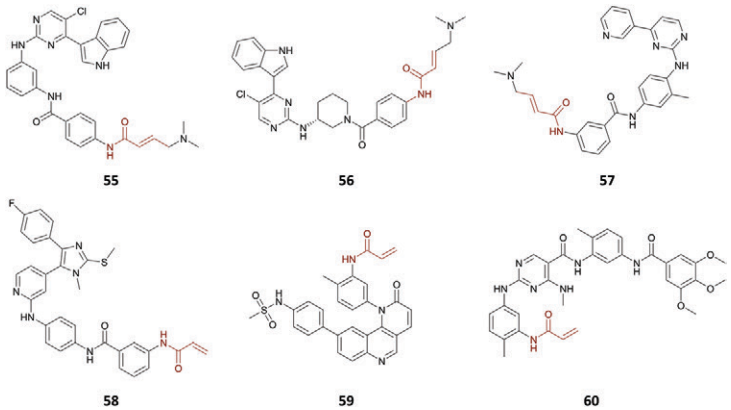

Fig. 33 Chemical structures of CDK, JNK, BMX targeting inhibitors **55–60** with acrylamide warheads reported between 2007–2018.

Table 10 Biochemical and cellular characterization data for inhibitors **55–60**

			In vitro (nM)		*In cellulo* (nM)						
#	Reversible	Nucleophile	Isoform	IC_{50}	Cell line	IC_{50}	$t_{1/2}$ (h)	K_i (nM)	k_{inact} (ms^{-1})	k_{inact}/K_i (M^{-1} s^{-1})	Stage
55		C312	CDK7	3.2	Jurkat	55					Discovery
56		C1039	CDK12	158							Discovery
57		C154	JNK3	0.98							Discovery
58		C154	JNK3	0.3							Discovery
59		C496	BMX	8	RV-1	2540					Discovery
60		C496	BMX	11	RV-1	3450	0.8[a]				Discovery

[a] Hepatocytes.

selectively inhibiting c-Jun phosphorylation without affecting off-target proteins. This effect was sustained for several h following inhibitor wash-out, which in addition to the 100-fold loss of potency against serine JNK mutants (lacking the cysteine nucleophile), validates an irreversible binding mechanism. At this stage, the extensive biochemical and selectivity profiling of **57** as a JNK-specific inhibitor, suggests promising utility as a pharmacological probe for JNK-dependent signal transduction.[210]

As efforts continue to enhance selectivity and potency of JNK targeting small-molecules, Muth *et al.* developed an isoform-selective JNK3 inhibitor. The tissue distribution of JNK3 differs from JNK1 and JNK2, with expression predominantly localized to the heart, testis and brain. Several siRNA-mediated genetic knockdown experiments have identified JNK3 as a promising therapeutic target for the treatment of various neurodegenerative disorders such as Huntington's, Parkinson's and Alzheimer's disease. The most promising candidate, **58** is a 2 nM JNK3 inhibitor with an $S(50)$ score of 0.037, inhibiting 15 other kinases at 0.5 μM. Selectivity was mainly attributed to the methylation of the imidazole at N_1 and key intermolecular interactions within hydrophobic region I. While limited selectivity was seen within the JNK family, **58** showed good metabolic stability in male human liver microsomes (HLMs) with only 13% degradation observed over a 3 h period.[211]

BMX. BMX is a member of the TEC family (which also includes ITK, TEC, BTK, and TXK). Similar to the remaining TEC kinases, BMX consists of a Pleckstrin Homology (PH) domain, which facilitates membrane association, a Tec Homology (TH) domain constituting a proline-rich region, along with an SH3, SH2 and a carboxyl terminus kinase domain.[212] While its role in disease progression remains under study, numerous lines of biological evidence have suggested implications in tumorigenicity, cell motility, adhesion, angiogenesis, proliferation and differentiation.[213–216] More specifically, BMX action and high expression were observed in several prostate cancer cell lines making it an attractive target for small molecule interrogation.

To assess the pharmacological consequences of inhibiting BMX activity in prostate cancer, a KinomeScan approach was carried out to identify lead pharmacophores against this kinase with modest binding affinity. As a result, a class of tricyclic quinolines with modest potency were discovered and these were subsequently optimized to generate **59**, which targets Cys496 to inhibit recombinant BMX kinase activity with an IC_{50} of 8.0 nM. Compound **59** exhibited a selectivity score of 0.01, with activity against BTK (IC_{50} = 10.4 nM). *In vitro* assays against both BMX^{WT} and mutant BMX^{C496S} confirmed it to be inactive against the non-nucleophilic cysteine mutant at concentrations below 10 μM. Despite these potent nM half-maximal inhibitory concentrations, in cells, **59** was only able to inhibit prostate cancer cell proliferation with micromolar potency. The cellular effects of **59** on proteins levels was assessed in RV-1 transfected cells, which showed a significant and sustained reduction in protein concentration for 72 h relative to the non-covalent propyl amide control compound.[217]

To improve kinase selectivity, the design of a type II inhibitor (where it binds to the DFG-out conformation) was carried out by Liang *et al.* Extensive SAR exploration resulted in the

discovery of CKI **60** with an $S(1)$ score of 0.01 against a comprehensive panel of 468 kinases at 1 μM. Interestingly, while **60** showed strong binding with Discoidin domain receptor 1 (DDR1), p38α and ABL kinases, it exhibited minimal affinity towards the pursued target, BMX.

The authors hypothesized that the assay conditions might disfavour the preferred DFG-out conformation. To validate this, K_d values of **60** were determined using microscale thermophoresis technology against both the active (DFG-in) and inactive (DFG-out) BMX kinase. The experiments confirmed the hypothesis, with an observed 120-fold selectivity for DFG-out. *In silico* covalent docking studies, with modification of Cys496, validated a docking pose favouring occupation of the key hydrophobic pocket with the bulky 3,4,5-trimethoxybenzene motif in the more accessible in DFG-out conformation. An 80-fold loss in *in vitro* potency was observed against BMX^{C496S} relative to BMX^{WT}. Further optimizations are necessary due to a limited PK profile (I.V., $t_{1/2}$ = 0.80 ± 0.34 h, P.O., not bioavailable).[218]

ERK1/2. The extracellular signal-regulated kinases (ERK) 1/2 are a family of related enzymes involved in RAS, RAF, MEK, ERK signalling. As with many kinases, constitutive activation of this pathway is highly-associated with multiple human cancers involving the phosphorylation of AP-1 family members such as Jun and Fos proteins as well as the phosphorylation of multiple STAT family members.[219] In response, pharmaceutical agents have been developed to target ERK proteins, which have successfully reduced tumour growth in xenograft mouse models. These studies validated the clinical utility of targeting ERK kinases, particularly in overcoming acquired resistance to RAF and MEK inhibitors.[220]

To develop potent and selective covalent inhibitors of ERK1/2, a biochemical assay for ERK2 was employed to yield initial lead compound, **61** (IC_{50} = 8.5 nM, [ATP] at K_m), which targeted Cys166 (Fig. 34). This inhibitor was relatively stable against GSH ($t_{1/2}$ = 2.53 h) compared to a previous series, utilizing alkenyl sulphonamide electrophiles ($t_{1/2}$ = 0.26 h) (Table 11). Structural derivatization generated CKI **62** containing a pyridyl nitrogen, (IC_{50} = 3.1 nM, [ATP] at K_m) possessing moderate stability against GSH ($t_{1/2}$ = 0.70 h). Washout experiments with **62** showed direct inhibition of ERK2 substrate phosphorylation for a duration of 48 h (consistent with the reported $t_{1/2}$ of ERK2; 54 h). While considered a highly potent compound, moderate *in vitro* stability and poor intrinsic clearance data (rat hepatocytes, >250 μL min^{-1} mg^{-1}) limited the scope of *in vivo* experiments. This prompted the synthesis of trifluoromethyl variant **63**, which despite failing to improve clearance rates, was able to attain 7–9-fold free plasma coverage above the observed cellular IC_{50} when co-administered with the irreversible CYP inhibitor 1-aminobenzotriazole. This strategy markedly improves the feasibility of *in vivo* exploration.[44]

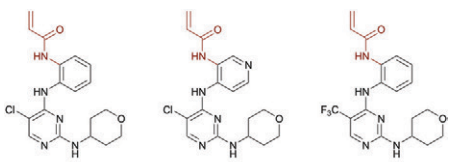

Fig. 34 Chemical structures of ERK1/2 targeting inhibitors **61–63** with acrylamide warheads reported between 2007–2018.

FAK. Focal adhesion kinase (FAK) is a ubiquitously expressed non-receptor tyrosine kinase involved in integrin-mediated signal transduction. FAK signalling also promotes RHO/RAC GTPase activation and downstream PAK kinase activation regulating antagonistically STAT3/5 and the locus repressor BCL6 oncoproteins. FAK is a scaffold protein kinase frequently overexpressed in hematopoietic cancers, localized in epithelial cell layers within focal adhesions. Its overexpression and/or hyperactivation has been implicated in a variety of cancers due to roles in cell migration and angiogenesis.[221] Numerous small-molecule agents are now in clinical trials as FAK inhibitors, none of them utilize a covalent mechanism.

To assess the viability of covalent FAK inhibitors, Yen-Pon Expédite *et al.*, utilized kinome-wide sequence analysis and the structure of the ATP binding site to identify a targetable residue, Cys427 in the glycine-rich loop. Optimal positioning of a reactive acrylamide into a 2,4-dianilinopyrimidine scaffold (known to tightly bind FAK) generated lead candidate, **64** (Fig. 35 and Table 12). A co-crystal structure confirmed covalent modification and showed the carbonyl of Ile428 H-bonding with the squaramide (–NH–), which is thought to be critical for appropriately orienting the warhead. This CKI blocked FAK autophosphorylation in squamous cell carcinoma (SCC) lines. Also, relative to the non-covalent control, **64** did not lose potency after washout, which suggests irreversible/long-lived target engagement. *In vitro* kinase profiling against a small panel of 10 kinases showed only 20% inhibition on the IR (insulin receptor) kinase at 1 μM), proving **64** to be more selective relative to known non-covalent FAK inhibitor TAE226 which exhibits high potency towards IR (IC_{50} = 26 nM) (Fig. 36).[222] The unwanted impact on Insulin receptor signalling could also

Table 11 Biochemical and cellular characterization data for inhibitors **61–63**

			In vitro (nM)		*In cellulo* (nM)						
#	Reversible	Nucleophile	Isoform	IC_{50}	Cell line	IC_{50}	$t_{1/2}$ (h)	K_i (nM)	k_{inact} (ms^{-1})	k_{inact}/K_i (M^{-1} s^{-1})	Stage
61		C166	ERK2	85	A375	57	2.5[a]				Discovery
62		C166	ERK2	31	A375	41	0.73[a]				Discovery
63		C166	ERK2	69	A375	53					Discovery

[a] Liver microsomes.

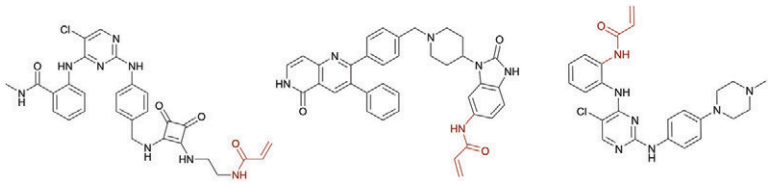

64 FAK 65 AKT 66 TAK

Fig. 35 Chemical structures of FAK, TAK, AKT targeting inhibitors **64–66** with acrylamide warheads reported between 2007–2018.

Table 12 Biochemical and cellular characterization data for inhibitors **64–66**

			In vitro (nM)		*In cellulo* (nM)						
#	Reversible	Nucleophile	Isoform	IC_{50}	Cell line	IC_{50}	$t_{1/2}$ (h)	K_i (nM)	k_{inact} (ms^{-1})	k_{inact}/K_i (M^{-1} s^{-1})	Stage
64		C427	FAK	0.6	SCC	1730					Discovery
65		C296/310	AKT	0.2				497	1.2	2.34×10^3	Discovery
66		C174	TAK1	50			0.1[a]			6.87×10^3	Discovery

[a] Human (*in vivo*).

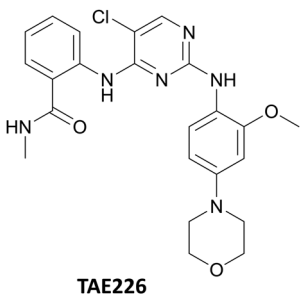

TAE226

Fig. 36 Structure of non-covalent FAK inhibitor TAE226.

negatively influence IGFR signalling due to receptor heterodimerisation, altering many cellular processes, most importantly glucose metabolism and cellular growth.

AKT. AKTs/PKB have been heavily investigated as therapeutic targets in oncology due to their role in the regulation of various signalling pathways including cell proliferation, metabolism, growth and angiogenesis.[223] Structurally, AKT features a regulatory PH domain and a canonical ATP binding site. PH domains have been typically exploited as an allosteric pocket for drug design to overcome selectivity issues seen with traditional ATP-mimetic scaffolds.[224] PH allosteric inhibitors stabilize the inactive (PH-in) conformation, thereby introducing an additional selectivity filter.

In an effort to combine the selectivity of allosteric PH domain inhibitors with the pharmacological and therapeutic benefits of CKIs, Weisner *et al.* designed compound **65**. This inhibitor was structurally derived from a previously described 1,6-naphthyridinone scaffold and the allosteric non-covalent clinical candidate, MK-2206. Tryptic digests and ESI-MS/MS analysis confirmed Cys296 and Cys310 as the nucleophilic sites of covalent modification, but neither was preferentially targeted over the other. Selectivity profiling of **65** against 100 kinases – which included members of the AGC kinase family and other kinases containing a PH domain – impressively revealed AKT isoforms 1–3 as the only targets (>80% inhibition at 1 μM). In cellular studies, using breast, prostate and gastrointestinal cancer cell lines, **65** induced a dose-dependent decrease of phospho-Akt at both Thr308 and Ser473, which correlated well with a reduction in phosphorylated downstream Akt substrate Glycogen Synthase Kinase 3 Beta (GSK3β).[225]

TAK1. Transforming Growth Factor-β-Activated Kinase 1 (TAK1) plays a major role in regulating cell transcription and apoptosis through a variety of signal transduction pathways including those stimulated by pro-inflammatory cytokines such as Toll-like Receptor (TLP) ligands, IL-1 and Tumour Necrosis Factor Alpha (TNFα).[226] Due to such widespread control of key cellular processes, dysregulation of TAK activity has been implicated in several diseases, spurring interest in the development selective TAK1 inhibitors in recent years.[227–229]

While several non-covalent small molecule inhibitors of TAK1 have been reported, compound **66** is to our knowledge the only covalent inhibitor reported in literature within the last 10 years. As a potent CKI (IC_{50} = 50 nM), it was derived from a similar analogue of the previously described EGFR inhibitor, **3**. The acrylamide electrophile was repositioned from *meta* to the *ortho* position. Additional efforts revealed an added benefit of the C_5 chloro-substituent which facilitated key interactions between the electrophile and the kinase gatekeeper residue. SAR studies also revealed that an amine linkage imparted enhanced stability over the previously employed ether linker in MLM. A KinomeScan against a large panel of 468 kinases revealed a score of $S(1)$ = 0.10 at 1 μM, with 10 other kinases inhibited which all possessed an equivalently positioned cysteine. Finally, consistent with a covalent mechanism of action, **66** was found to exhibit a time-dependent improvement in potency with increasing incubation in biochemical assays.[230]

α,β unsaturated electrophiles

Originally isolated from the herb Artemisia sciatia (commonly used for ulcerogenic and inflammatory aliments), natural product

sesquiterpene lactone **67** (artemisolide), was reported as an irreversible inhibitor of nuclear factor kappa-B kinase beta (IKK-β) (Fig. 37). More specifically, in using a moderately electrophilic acrylate, this CKI irreversibly modifies Cys179 within the dynamic kinase A-loop. This interaction was shown to effectively inhibit lipopolysaccharide (LPS) induced NF-κB activation in cellular macrophages. This result was relevant as genomic studies found IKK-β to play important roles in NF-κB induced inflammatory responses.[231] Compound **67** showed moderate dose-dependent inhibition in both biochemical and cellular assays (IC_{50} = 8 and 10 μM, respectively). Same studies performed with the C179A mutant abrogated all potency, confirming covalent mode-of-action.[232]

Pyranonapthoquinone **68** (lactoquinomycin) was recently validated as a cysteine targeting CKI of AGC family, Protein Kinase B (AKT/PKB) through modification of T-loop cysteines (Cys296, Cys310) (Table 13). This was found to occur *via* a novel allosteric mechanism using the strongly electrophilic enone (α,β-unsaturated ketone) warhead. Structural homology within kinase active sites introduces challenges in achieving selectivity. In this example, targeting poorly conserved residues and allostery was utilized as a double-pronged strategy to circumvent such issues.

Derived from the Wyeth Natural Product library, kinetic studies on this potent scaffold (IC_{50} = 149 nM) revealed a non-competitive binding mechanism, suggesting allostery. Covalent irreversibility was confirmed by a time-dependent inhibitory profile and the loss of potency against C296A/C310A double competitive binding mechanism, suggesting allostery. Covalent irreversibility was confirmed by a time-dependent inhibitory profile and the loss of potency against C296A/C310A double mutants. In addition, achieving selectivity was achieved as **68** showed no activity (up to 200 μM) against several homologous kinases (*e.g.* PKA).[233] While potent and selective, the reactive quinone core-scaffold of **68** has been associated with non-specific toxicity, redox reactivity and non-specific alkylation.

Quinozaline-based benzoquinone **69** is a proposed irreversible inhibitor of VEGFR, targeting Cys1045 in the catalytic domain.

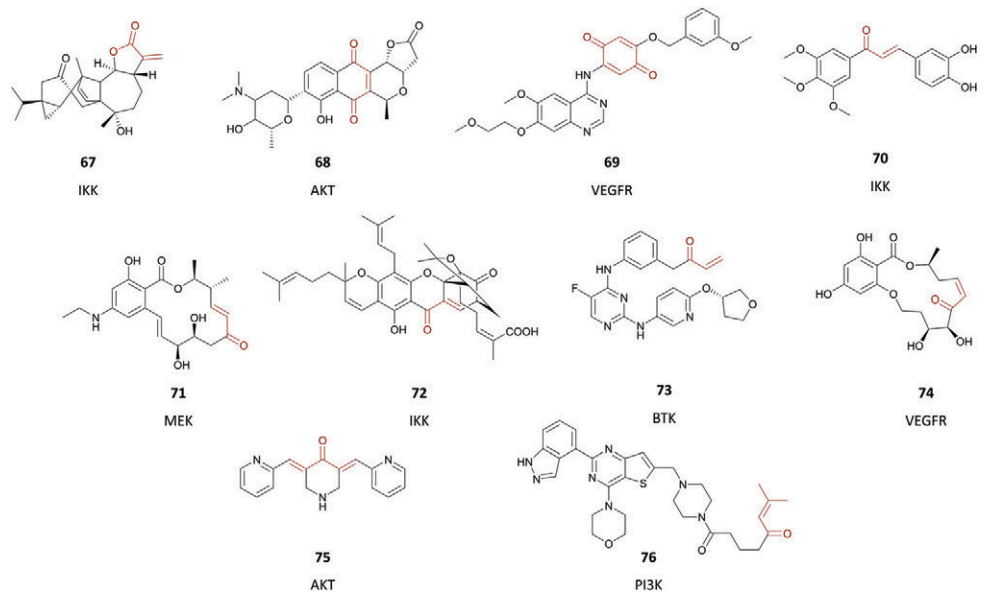

Fig. 37 Chemical structures of inhibitors **67–76** with α,β-unsaturated electrophiles reported between 2007–2018.

Table 13 Biochemical and cellular characterization data for inhibitors **67–76**

			In vitro (nM)		*In cellulo* (nM)						
#	Reversible	Nucleophile	Isoform	IC_{50}	Cell line	IC_{50}	$t_{1/2}$ (h)	K_i (nM)	k_{inact} (ms^{-1})	k_{inact}/K_i (M^{-1} s^{-1})	Stage
67		C179	IKK-β	>5000	RAW 264.7	>5000					Discovery
68		C296/C310	AKT-1	149	HEK293	125					Discovery
69		C1045	VEGFR-2	50							Discovery
70		C179	IKK-β	1900	H2009	2600					Preclinical
71		C297	MEK-1	52	THP-1–33	50	4.2[a]				Phase II
72		C179	IKK-β	300	RAW 264.7	500	0.26[b]				Preclinical
73		C481	BTK	10	CTLL-2	100					Discovery
74		C1045	VEGFR-2	30	RENCA	150	1.0[c]				Preclinical
75	•	C311	AKT-2	20	MDA-MB-435	1000					Discovery
76		C862	PI3K-α	6.8	SKOV3	77.6	2.4[c]				Preclinical

[a] Human (*in vivo*). [b] Mouse (*in vivo*). [c] Hepatocytes.

Interestingly, the authors proposed an initial redox interaction between the quinone electrophile and cysteine thiol forming a semiquinone-sulfhydryl radical pair. This produced in combination an irreversible adduct through reductive addition. To support a covalent mechanism, a relatively small loss in potency (5-fold) was observed upon increasing ATP concentration (1000-fold), a hallmark of irreversible covalent inhibitors. Computational docking studies positioned the electrophilic β-carbon of the electrophilic quinone ~4.2 from the cysteine of interest and thereby amenable to covalent modification.[234] Nonetheless, further studies are needed to unequivocally validate irreversible binding such as site-directed mutagenesis, covalent-adduct characterization and time-dependent inhibition. As discussed above with **68**, the benzoquinone core may be problematic to clinical progression.

The privileged chalcone scaffold (1,3-diaryl-2-propen-1-one), has been historically utilized in various medicinal applications (typically against inflammation and cancer).[235] Chalcone-derivative, **70**, was reported as covalent inhibitor of IKK-β. Similar to **67**, this molecule targets NF-κB signalling by engaging Cys179 with a relatively weak half-maximal inhibitory concentration (IC_{50} = 1.90 μM). An extensive SAR of EDGs (*e.g.* –OH, $–OCH_3$) and varied methylation patterns were utilized to tune warhead reactivity and IKK-β inhibition. While moderate potency was observed in lung cancer cell lines (H2009, A549, IC_{50} = 1.1, 2.6 μM respectively), **70** was efficacious in preclinical murine studies (~57% reduction of *in vivo* xenografts in H2009 lung tumours). While this compound uses a highly reactive, irreversibly covalent enone moiety, a respectable safety profile was demonstrated *in vivo*. Further toxicity studies revealed insignificant toxicities, minimal weight fluctuations and no observable pathological abnormalities over a six-day period with I.P. administration of 1 mg per mouse per day.[236]

Originally derived from the natural product (F152A1), macrocycle **71** (E6201) has been identified as a more metabolically stable covalent MEK1 inhibitor targeting Cys297 using an electrophilic enone (Fig. 38). This compound exhibited promising anti-inflammatory and anti-hyperproliferative properties, which translated into good efficacy in a psoriasis model. Relatively high potency was observed in both biochemical and cellular assays (IC_{50} = 5.2, 50 nM respectively) as well as against human keratinocyte proliferation (IC_{50} = 160 nM). Topical application in varied dermatitis mouse models showed efficacy and good *in vivo* PK. The authors suggest this to be largely due to the macrocyclic scaffold, which avoids efflux by *p*-glycoproteins, P-gp. Promisingly, both I.P. and P.O. administrations in murine models showed relatively good bioavailability (F = 0.95, 0.35, respectively).[237] Since these results were reported, this compound has progressed into phase I and into phase II clinical studies for chronic plaque psoriasis (Clinical trial identifier: NCT00539929).

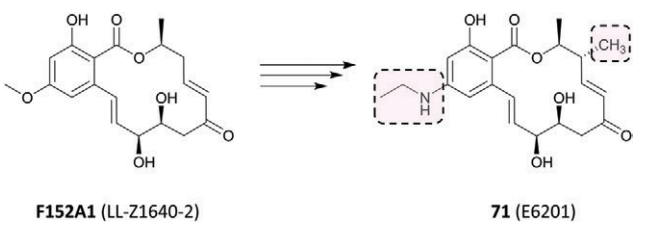

Fig. 38 Chemical structure of MEK1 inhibitor **71**, structurally derived from parent resorcylic acid F1521A1 (LL-Z1640-2).

Prenylated xanthone **72** (Gambogic acid), typically found in the resin of Garcinia plants was recently observed to have general antitumor activity. Mechanistic studies reported this scaffold as a covalent inhibitor of IKK-β also targeting Cys179 *via* an enone warhead (similar to **67** and **70**). Irreversible binding was initially explored using proteomic pull-down assays, followed by disruption of target-engagement upon incubation with excess dithiothreitol (DTT). Additional mass spectrometry studies further validated this mechanism of action. Potency was also dose-dependently attenuated with increasing [GSH] (deactivates electrophilic enone) and an almost complete loss of inhibitor potency was observed upon saturating the reactive enone (loss of electrophilicity). Additionally, no potency was seen against C179A IKK-β mutants. Good potency was observed in both biochemical and cellular assays (IC_{50} = 300, 500 nM, respectively) and promising PK data revealed rapid tissue distribution (T_{max} = 5 min) and clearance ($t_{1/2}$ = 0.26 h) upon I.V. administration of a 4 mg kg^{-1} per rat dose.[238]

Small molecule **73**, utilizing a central pyrimidine scaffold and an enone electrophile, was reported as an irreversible BTK inhibitor targeting the commonly pursued Cys481. This inhibitor displays an IC_{50} of <10 nM in biochemical studies while cellular data suggest an IC_{50} of 100 nM in relevant cell lines. Whilst data surrounding this compound is scarce, target engagement and covalent adduct formation with BTK was confirmed *via* mass spectrometry. However, in addition to being potent against BTK, activity was also observed against ITK and EGFR family member kinases (IC_{50} = 10–100 nM). Interestingly, by using the aliphatic α,β unsaturated system (rather than an aryl scaffold) and introducing the benzylic methylene spacer, the authors have further attenuated the electrophilicity of the highly reactive enone. Modulating conjugation patterns is another method commonly used to tune warhead reactivity.[239]

Resorcylic acid (RAL) derivative **74**, containing a *cis*-enone was reported as an irreversible VEGFR inhibitor, targeting Cys1045 with good biochemical and cellular potency (IC_{50} = 30, 150 nM, respectively). RALs have been validated as ATP-competitive inhibitors through initial studies on 5*Z*-7-oxozeaenol and hypothemycin.[240] Structural insights into the binding pose of these scaffolds allowed for the rational insertion of an electrophilic warhead with optimal distance and orientation, thereby achieving covalent modification. While this derivative exhibited low to moderate stability (DTT half- = 0.56 h, mouse blood plasma $t_{1/2}$ = 1 h), it was equipotent relative to clinical standard, sunitinib, in abrogating tumour growth, metastasis and angiogenic responses in an orthotopic mouse model of renal carcinomas. Given the stability data and relatively short half-lives, the *in vivo* results demonstrate the power of covalent inhibitors and the advantages of decoupled PK-PD. CKIs are not governed by the typical binding equilibria of their non-covalent counterparts, hence

rapid target inactivation (PD) allows poor to moderate PK to be tolerated without substantial loss in efficacy.[241]

Similar to chalcones, the curcumin scaffold is historically known to have various medicinal attributes (*i.e.* anti-inflammatory, anti-cancer, anti-angiogenic).[242] Therefore, structural derivatization of this core structure to generate structures with improved solubility, PK and target potency is thought to be of great pharmacologic utility. Recently, monocarbonyl curcumin derivative **75** was reported as a covalent AKT2 inhibitor (IC_{50} = 20 nM). Authors propose this potency to be a result of covalent modification of Cys311. Note, while no X-ray, mutagenesis or spectrometric data was reported to validate this hypothesis, curcumin-analogues have been previously shown to form covalent reversible bonds with thiol–nucleophiles (*i.e.* GSH).[243] Modelling studies suggested binding within a region proximal to Cys311. Binding kinetics revealed a mixed inhibition model with a dominating competitive binding mode.[244]

Class I PI3Ks (α, β, γ, δ) play critical roles in cell proliferation and hyperactive PI3K mutations are frequently found in cancers, such as breast or prostate carcinomas and serve as disease driving oncogenes.[245] While many reversible PI3K inhibitors are in development,[246] toxicities associated with pan-inhibition have been reported, and further the case for developing isoform-selective small molecules. Compound **76** was designed as a selective covalent PI3Kα inhibitor targeting Cys862, which is unique to PI3Kα, and a potential driver of selectivity. Derived from PI3Kγ inhibitor, GDC-0941, **76** exhibited strong biochemical and cellular potencies (IC_{50} = 6.80, 77.6 nM, respectively). The compound is 23-fold, 34-fold and 500-fold selective for the α isoform relative to β, γ and δ, respectively. Covalent modification was validated through time-dependent inhibition and spectrometry data whereby a covalent adduct was observed only with PI3Kα (Table 14).

Finally, **76** showed good metabolic stability in murine *in vivo* studies ($t_{1/2}$ = 2.4 h) and potent *in vivo* activity on PI3Kα signaling (by immunoblotting murine spleen lysates for PI3Kα biomarker P-Akt^{Ser473}), and represents the first validated PI3Kα selective inhibitor (Fig. 39).[247]

While most kinase inhibitors are designed to target the ATP binding pocket, this strategy is inherently challenging due to competing intracellular ATP and selectivity issues arising from structural homology and the presence of >1000 ATP-dependent non-kinase enzymes.[248,249] Recent alternate approaches to mitigate these challenges involve the use of substrate-competitive inhibitors (rather than ATP-competitive) as kinases also recognize substrate specific polypeptides. Although these epitopes are typically not considered drug-like, phenylalanine-mimetic **77** was reported as an irreversible AKT1 inhibitor by incorporation into known kinase binding sequences. Compound **77** is shown to modify activation loop Cys310 of ATK1. As a proof-of-concept study, promising potency was observed (IC_{50} = 0.58 μM) and irreversible binding was confirmed *via* time-dependent inhibition and covalent adduct formation using mass spectrometry studies (Fig. 40).[250]

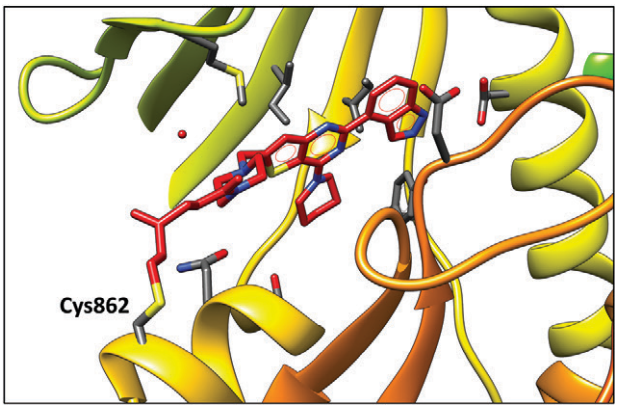

Fig. 39 Crystal structure of PI3Kα selective **76** highlighting the covalent modification of Cys862 (PDB 3ZIM).

The identification of reversible covalent inhibitors targeting poorly conserved non-catalytic cysteines remains a challenging task. Nonetheless, this approach has been regarded as a potential strategy to circumvent off-target toxicities of irreversible binders. The covalent activated-acroylnitrile warhead is known to reversibly react with thiols.[35]

This motif was recently incorporated into a pyrrolopyrimidine scaffold to form heteroaryl-acroylnitriles **78** and **79**, both reported as reversible covalent RSK2 inhibitors targeting Cys436. Compounds **78** and **79** were found to be highly potent

Table 14 Biochemical and cellular characterization for inhibitors **77–88**

			In vitro (nM)		*In cellulo* (nM)						
#	Reversible	Nucleophile	Isoform	IC_{50}	Cell line	IC_{50}	$t_{1/2}$ (h)	K_i (nM)	k_{inact} (ms^{-1})	k_{inact}/K_i (M^{-1} s^{-1})	Stage
77		C310	AKT-1	580	HCT116	>5000					Discovery
78		C436	RSK-2	12	MDA-MB-231	5					Discovery
79		C436	RSK-2	47	MDA-MB-231	14					Discovery
80		C46	IKK-α/β	400	RAW 264.7	2000		30.25	129	4.26×10^6	Preclinical
81		K2187	mTOR	1500	CEM	1760					Preclinical
82		C715	IRE-1α	>5000	HeLa	>5000					Discovery
83		C481					0.013[a]			2.87	Preclinical
84		C199	GSK-3β	530	T67	900					Discovery
85		C38	MEK6	4500							Discovery
86		C424	PK-M2	6	K562	3900		50	0.517	1.03×10^4	Preclinical
87		C452	JAK-2	1500	MDA-MB-231	3000					Preclinical
88		C46	IKK-β	400	RAW 264.7	1670			0.65		Discovery

[a] Hepatocytes.

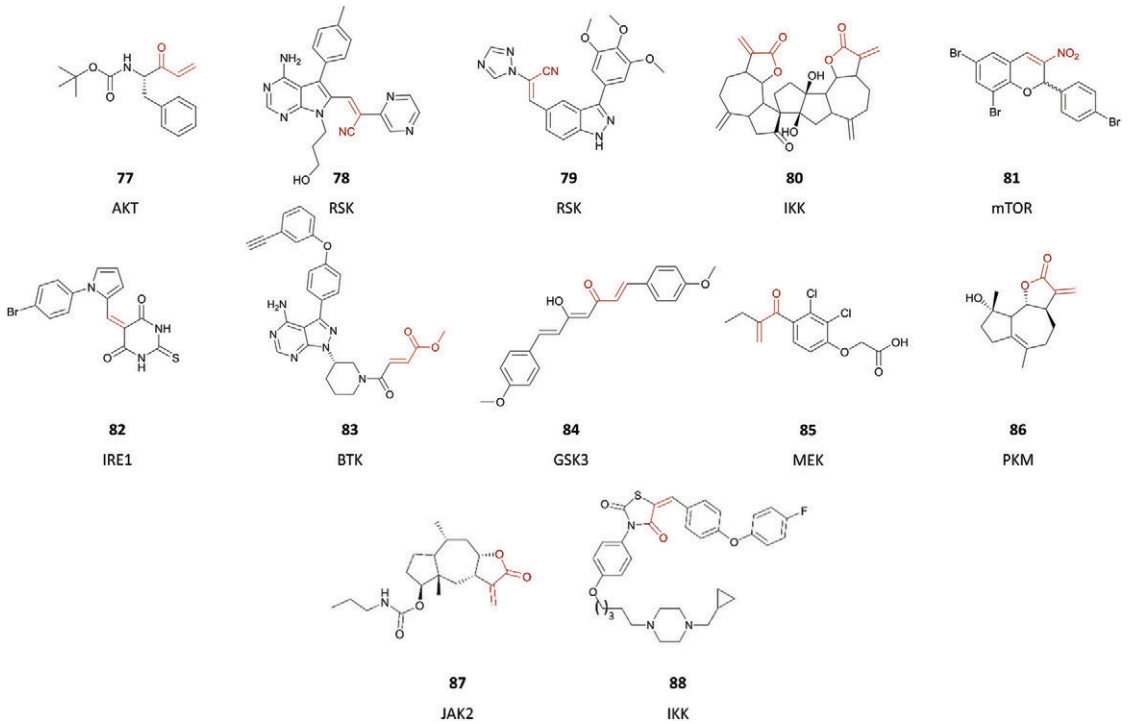

Fig. 40 Chemical structures of inhibitors **77–88** with α,β-unsaturated electrophiles reported between 2007–2018.

in biochemical assays (IC_{50} = 12 and 47 nM, respectively). Reversibility was validated *via* guanidine-mediated protein unfolding and inhibitor recovery (91.7%). The mechanism of reversible covalent modification of acroylnitriles can be seen in Fig. 41. Compound **79** showed good selectivity (200-fold) for RSK2 relative to Nek2, a non-related kinase with a homologous cysteine. Close analysis of the co-crystal structure suggested a steric clash between the 1,2,4-triazole and Nek2 F148, while RSK2 residue L546 escapes this detrimental interaction. In addition to these CKIs, the authors also report a kinetic study of acroylnitrile reactivity against thiols (generating β-elimination rates) where they hypothesize electrophile reversibility should increase with α-carbon proton acidity. To study this, DFT was utilized to calculate proton affinities of covalent adduct conjugate bases. The data analyzed was in agreement with the "acidity" hypothesis and showed a good positive correlation with experimentally derived elimination rates (R^2 = 0.96).[251]

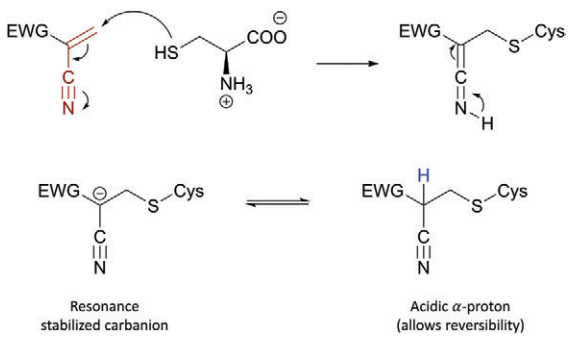

Fig. 41 Mechanism of reversible covalent modification of activated-acroylnitrile electrophiles against thiols.

The IKK complex is composed of IKKα and IKKβ catalytic subunits. Two distinct pathways are typically described for NF-κB activation; one considered non-canonical, dependent on IKKα and a canonical one, dependent on IKKβ.[252] Structurally unique natural product sesquiterpene lactone dimer **80** (Ainsliadimer A) was reported as an irreversible inhibitor of both IKKα/β (targeting both pathways), modifying Cys46. Target engagement with IKKα/β was initially confirmed *via* pull-down assays, with no binding observed against the IKKγ isoform. Incubation with excess DTT and saturation of the electrophilic β position resulted in the loss of potency (suggesting an irreversible mechanism), while binding kinetics revealed a time-dependent inhibition profile. After progressing into preclinical studies on human gastric adenocarcinoma xenografts, 30 mg kg^{-1} daily dosing (I.V.) decreased tumour size by ~50% over a 16 day period with minimal observed toxicity.[253]

As previously mentioned, dysregulation of PI3K/mTOR signalling is a hallmark of various human cancers.[245] Chromene **81**, derived from PI3K inhibitor (S14161) is reported to irreversibly modify mTOR kinase at Lys2187. Cytotoxicity studies against mTOR-addicted T-cells revealed promising potency (IC_{50} = 1.70 μM). Cancers of the breast epithelial cells are known to be heavily reliant on PI3K/mTOR signalling. In this regard, the use of mTOR inhibitor **81** was found to be efficacious across several breast cancer cell lines (*e.g.* Her2+, Her2−), with half-maximal inhibitory concentrations ranging between 1.0–6.0 μM. A remarkable selectivity profile was seen against 243 kinases, where at 1.0 μM, only mTOR was inhibited >80%. Computational

docking studies, suggested a covalent interaction with Lys2187, which showed proximal positioning of the electrophile. Wash-out experiments as well as reducing and boiling conditions were all unable to demonstrate inhibitor recovery, suggesting an irreversible mechanism of binding. In preclinical studies, doses of 10 mg kg^{-1} successfully reduced tumour growth in an orthotopic human MDA-MB-231 triple negative breast cancer (TNBC) mouse model. This molecule was also able to prevent lung metastasis in NSG (NOD/SCID/γc) mice.[254]

Unfolded Protein Response (UPR), a cellular protective mechanism in response to endoplasmic reticulum (ER) stress is controlled by transmembrane kinase inositol-requiring enzyme 1 (IRE1), which has been implicated in many cancers.[255] Medicinal chemistry efforts to inhibit IRE1-α function revealed small molecule pyrimidinedione **82** (UPRM8) as an allosteric and irreversible covalent inhibitor. This compound targets Cys715 (DFG + 2 position) of the kinase A-loop, distal from the conserved ATP binding pocket. The electrophilic reactive centre is reported as the alkenyl moiety Michael acceptor, between the pyrrole and pyrimidine heterocycles. While not exceptionally active, the molecule displayed relatively weak potency against IRE1 kinase in biochemical assays (IC_{50} = 8.40 μM). Thiol reactivity was confirmed using mass spectrometry and site-directed mutagenesis on an IRE1 yeast variant (containing a homologous Cys832). Both C832A and C832S mutants exhibited attenuated potency. While human IRE1 experiments were not reported, it is likely the observed trends are reproducible considering the high homology between both IRE1 isoforms.[103]

Covalent inhibitors are generally characterized by rapid target inactivation. Subsequently, prolonged residence in systemic circulation and sustained plasma concentrations can lead to undesirable proteome-wide and time-dependent off-target effects (*i.e.* toxicity).[118] A novel strategy to evade this challenge is to use metabolically-labile electrophiles to impart kinetic selectivity.[256] In this model, electrophiles achieve rapid target engagement and post covalent modification the remaining free drug is rapidly metabolized, minimizing off-targets. As proof-of-principle, ibrutinib-analogue **83**, was developed with a labile fumarate-ester electrophile targeting Cys481. When incubated with carboxylesterase (CES) enzyme, almost complete loss of proteome cross-reactivity was observed in a concentration and time-dependent manner, relative to the more promiscuous ibrutinib. Furthermore, this result was validated *in vivo* using mice (which have heightened CES activity) treated with 20 mg kg^{-1} of **83** and visualizing inhibitor reactivity *via* ABPP. In essence, by introducing metabolic lability, this strategy generates rapidly acting irreversible inhibitors, with minimal off-target reactivity due to CES-mediated degradation.[256]

Small-molecule targeting of Alzheimer's disease (AD) is a challenging endeavour, partly due to the complex networks of dysregulated pathways feeding into this pathology.[257] Hyper-phosphorylation of Tau-protein causing unfolding and brain deposition as amyloid plaques is a hallmark of AD.[258] Glycogen synthase kinase (GSK3β) is a Ser/Thr kinase, commonly found in the central nervous system (CNS), and is known to regulate Tau phosphorylation, amongst many other processes. Similar to the design of **75**, curcumin-β-keto-enol **84** was reported as an irreversible GSK3β inhibitor (IC_{50} = 580 nM) targeting Cys199. Reactivity against the aminothiol cysteamine, confirmed the ability to form a Michael addition adduct. Note, blood–brain-barrier (BBB) permeability is critical for drugs targeting the CNS. In a permeability assay, the compound observed a borderline profile ($P_e = 2.8 \times 10^{-6}$ cm s^{-1}), which suggested minimal penetrance into the CNS and the brain.[243]

Over the years, several hit-identification methods (*e.g.* HTS, phenotypic, *in silico*) have been explored to elucidate novel molecules that modulate protein activity. DNA-encoded molecule libraries have lately gained traction as an efficient tool for this purpose, due to a combinatorial approach that is rapidly amplifiable.[259,260] Interaction determination using unpurified protein (IDUP) is a recently reported solution-phase *in vitro* protocol to identify protein binders (*i.e.* hits) from DNA-encoded libraries and unpurified protein in one pot.[259,261] Using IDUP (750 ligands/289 kinases), the authors reported the approved diuretic drug, Ethacrynic acid, **85** as an irreversible MEK inhibitor targeting allosteric, poorly conserved Cys38 (IC_{50} = 4.50 μM). A covalent adduct was observed using mass spectrometry along with a 30-fold loss in activity upon enone saturation to confirm the presence of some irreversible binding. Surprisingly, potency was only reduced by ~3-fold against MEK C38A mutants, which suggests **85** may target other nucleophilic residues and/or potency is not solely driven by cysteine targeting and covalent modification.[262]

Aerobic glycolysis provides critical resources for the growth of rapidly dividing cancer cells. Oncogenic metabolic reprogramming is regulated by pyruvate kinases (PKs), namely PKM2 (monomers, dimers and tetramers).[263] Dimeric PKM2 can translocate into the nucleus as a transcription regulator to activate oncogenes as well as to drive glycolytic flux towards increased biomass, thereby supplying oncogenesis. PKM2 modulators are known to reduce nuclear translocation by inducing tetramer formation.[264] An interesting study on natural product-derived **86** (micheliolide), reported this molecule as an irreversible allosteric PKM2 activator. The compound tightly binds PKM2 (K_i = 50 nM) and specifically modifies Cys424. Immunoblotting on treated C424S mutants showed no reactivity and removal of the electrophilic acrylate abrogated activity. To improve bioavailability, authors pursued a pro-drug approach *via* a dimethylamino-variant (DMA-86), allowing the slow release of active compound under physiological conditions, as seen in Fig. 42. This approach successfully improved stability and the overall therapeutic window. Further *in vivo* studies on zebrafish xenografts (1–10 μg mL^{-1} of DMA-**86**) saw significant size reduction of human HL60 leukemic tumours (transplanted 2 days post fertilization).[265]

The JAK/STAT cascade is a core cancer pathway that can drive other core cancer pathways such as angiogenesis, survival, cell cycle progression, immune modulatory activity or metabolism among other things. JAK–STAT activity is a master regulatory circuit for chromatin shape and gene transcription. Cellular proliferation is translated into metabolism and cellular survival is tightly regulated by this signalling cascade. Hence, it has been widely implicated in numerous pathologies within the fields of immunology, chronic inflammatory disease,

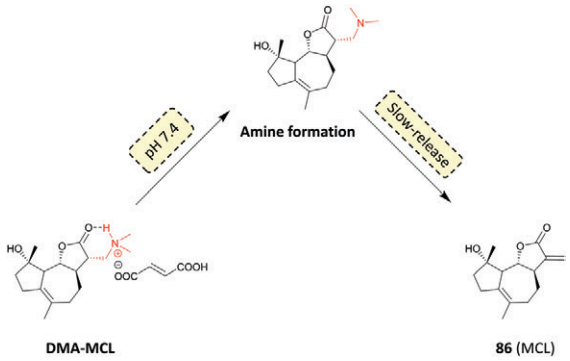

Fig. 42 Mechanism of **86** (MCL) release under physiological conditions *in vivo* using a DMA-MCL parent scaffold.

autoimmunity, infectious disease or cancer initiation as well as progression.[266]

In an effort to disrupt this pathway, sesquiterpene lactone **87** was reported as a covalent JAK2 inhibitor, targeting non-catalytic SH2 domain Cys452 (IC_{50} = 1.50 μM). Validation of an irreversible interaction involved evaluating *in vitro* potency after incubation with thiol nucleophiles (DTT/GSH). These thiols successfully deactivated the compound and no activity was observed. A similar effect was seen upon saturating the reactive enone (a common sequence of experiments to probe a potential covalent binding mechanism). Further confirmation was achieved using mass spectrometry, where a covalent adduct with the appropriate mass was detected. Cellular studies indicate this compound inhibits both IL-6 and constitutively active STAT3. I.V. administration (25 mg kg^{-1}) to human colon adenocarcinomas in nude mice, reduced tumour size by ~50% (over 18 days), with minimal toxicity.[267]

Thiazolidinedione **88** was reported from a series of 24-hit derived structures as a sub-micromolar irreversible inhibitor of IKKβ (IC_{50} = 400 nM), targeting Cys46 with a therapeutic goal of modulating NF-κB activation (similar to **77**). Hit-to-lead optimization was achieved by varying both the electronic and steric bulk whilst considering the effects on electrophile reactivity. This approach achieved a ~250-fold rise in potency. Binding assays revealed a time dependent IKKβ kinase inhibition likely owing to a covalent interaction. In regards to cellular activity, moderate cytotoxicity (assessed by macrophage viability) was observed (IC_{50} = 1670 nM).[268]

α-Halo-substituted carbonyls

One of the earliest successes towards site-specific covalent modification involved the use of α-halo-substituted carbonyl moieties, with early reports from Schoellmann and Shaw (1963) targeting serine proteases.[269] The electron-withdrawing carbonyl enhances C–X bond polarity (where X = I, Br, Cl, F), forming a highly electron deficient, electrophilic α-carbon. Interestingly, their precise mechanism of nucleophilic attack remains contentious. Against thiol nucleophiles, two mechanistic scenarios have been suggested, seen in Fig. 43. Mechanism I, involves a nucleophilic substitution (S_N2) at the α-carbon. Mechanism II proceeds *via* nucleophilic addition at the carbonyl, forming a hemithioketal intermediate and a strained sulfonium, which subsequently rearranges to furnish the desired thioether.[62]

Alternative mechanisms beyond S_N2, stem from early reports by Pearson *et al.*[270] who described the isolation of electrophilic epoxides after treatment with sodium methoxide (mechanism II). Nonetheless, mechanism I is generally accepted. Notably, nucleophilic addition is reversible, whilst substitution at the α-carbon is irreversible, enhancing the chances of isolating the S_N2 product. However, it is worth noting, in certain cases (*e.g.* hydroxyl nucleophiles), tetrahedral intermediate adducts (mechanism II) have been observed.[271,272] In either case, reactivity is largely governed by the leaving group. As a general rule, weak bases are better leaving groups. Considering electronegativity, size and bond strength, in isolated conditions, the following trend is seen; I > Br > Cl > F.

Altogether, the heightened reactivity, ease-of-installation, and breadth of knowledge surrounding this class of electrophiles has made α-halo-carbonyls very useful building blocks in drug discovery as potential covalent therapeutics as well as in chemical biology as affinity probes in proteomic analyses (*e.g.* iodoacetamide).[122]

Downstream signalling of Ser/Thr specific p90 RSKs involves cross-talk between C- and N-terminal catalytic domains (CTD, NTD, respectively).[273] CTD-mediated autophosphorylation is suggested to facilitate NTD activation and enzyme function. Previously reported adenine-derived fluoromethyl ketone FMK,[274] was the first irreversible CTD-selective RSK1/RSK2 inhibitor, targeting Cys436 (HEK293 cells EC_{50} = 150 nM). Note, within the α-halocarbonyl series, fluoromethyl-electrophiles are least reactive and represent mild alkylating agents.

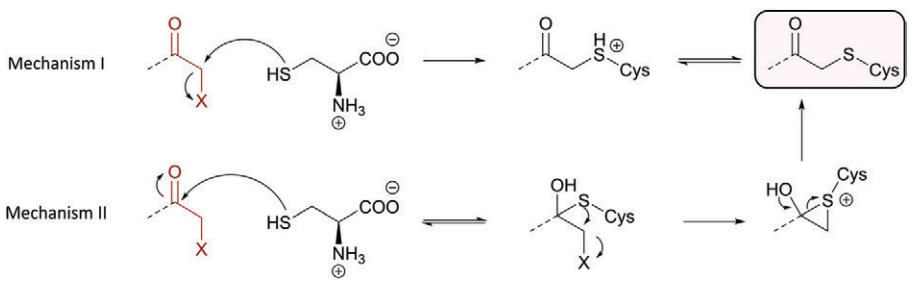

Fig. 43 General proposed mechanisms of covalent adduct formation for α-halo-substituted carbonyls (X = F, Cl, Br, I).

Selectivity for the CTD was achieved by exploiting a selectivity filter (Thr gatekeeper residue tolerating FMK binding) and a CTD-specific covalent interaction. Recently, a propargylamine variant **89**, was reported as a 2nd generation RSK1/RSK2 inhibitor, equipotent to FMK *in vitro*, yet this substance has 5-fold improved cellular potency (IC_{50} = 30 nM). Structurally, this compound serves a dual-purpose, as an inhibitor and a molecular probe (Fig. 44).[275]

Thienylchloromethylketone **90**, was reported as the first irreversible inhibitors of Alzheimer's Disease (AD)-implicated GSK3β activation and proposed to target Cys199. Through extensive lead optimization and SARs to achieve optimal reactivity, this compound was the most potent (IC_{50} = 500 nM) and displayed a non-competitive binding mode. Authors suggest the protonated Lys85 residue neighbouring the kinase active site promotes covalent interaction with Cys199 by stabilizing the anionic leaving group. This hypothesis was supported *in vitro*, where reactivity with thiol–nucleophiles (*e.g.* DTT) was catalysed in a more basic environment. Note, this may also improve cysteine nucleophilicity. An irreversible interaction with GSK3β was confirmed using wash-out experiments and quantifying inhibitor recovery.[276] After validating kinase modification, the authors expanded their design strategy and reported bromomethylketone derivatives, **91** and **92**, containing maleimide and benzimidazole core-scaffolds, respectively. While **92** was equipotent to **90**; CKI **91** gained 100-fold *in vitro* potency (IC_{50} = 5.0 nM). Derivatives lacking the halide leaving group exhibited a dramatic loss in potency (~150-fold), confirming the importance of the Cys199 interaction for inhibition. The potency of **91** and **92** can be attributed to a more optimized structure, improving the binding interaction, coupled with a more reactive bromomethyl-electrophile. Mass spectrometry data confirmed covalent adduct formation, whilst the methylketone derivative (negative control) showed no modification (Table 15).[277]

A proof-of-principle study utilizing a chemogenetic approach, based on covalent complementarity to achieve selectivity, reported **93** as an irreversible Src inhibitor targeting a gatekeeper Cys338 mutant residue. Generally, gatekeeper mutants have diminished kinase activity, however enzyme kinetics studies confirmed Src T338C mimics almost identically WT-activity and the authors argued that T338C preserves site geometry.

Therefore, **93** represents a mutant-selective (>15-fold) and highly potent fluoromethylketone inhibitor, (Src^{T338C} IC_{50} = 317 nM, Src^{WT} IC_{50} > 5000 nM). Interestingly, α-chloroacetamide derivatives were either inactive or 3-fold less potent. This demonstrates the attenuated reactivity of the amide backbone relative to the ketone series within α-halocarbonyl warheads. Wash-out experiments confirmed an irreversible interaction with mutant but not WT-Src. Also, with regards to kinome-wide selectivity, minimal off-targets were observed against a panel of 307 kinases using 1 μM of inhibitor.[278]

The activity of homo-dimeric Ser/Thr kinase Nek2, thought to play a role in early mitosis bipolar spindle assembly has been widely implicated in oncogenesis (*i.e.* overexpression seen in breast tumours, testicular seminoma and diffuse large B-cell lymphomas).[279,280] SBDD, guided by a co-crystal structure with an oxindole fragment (PDB 2JAV) targeting a poorly conserved non-catalytic P-loop Cys22, yielded several promising CKIs. In this library, oxindole-derived chloromethylketone **94** was reported as a potent and irreversible Nek2 inhibitor (IC_{50} = 6.0 nM). While a focused SAR of common electrophiles (*e.g.* acrylamides, vinyl sulfones, *etc.*) was performed, the highly

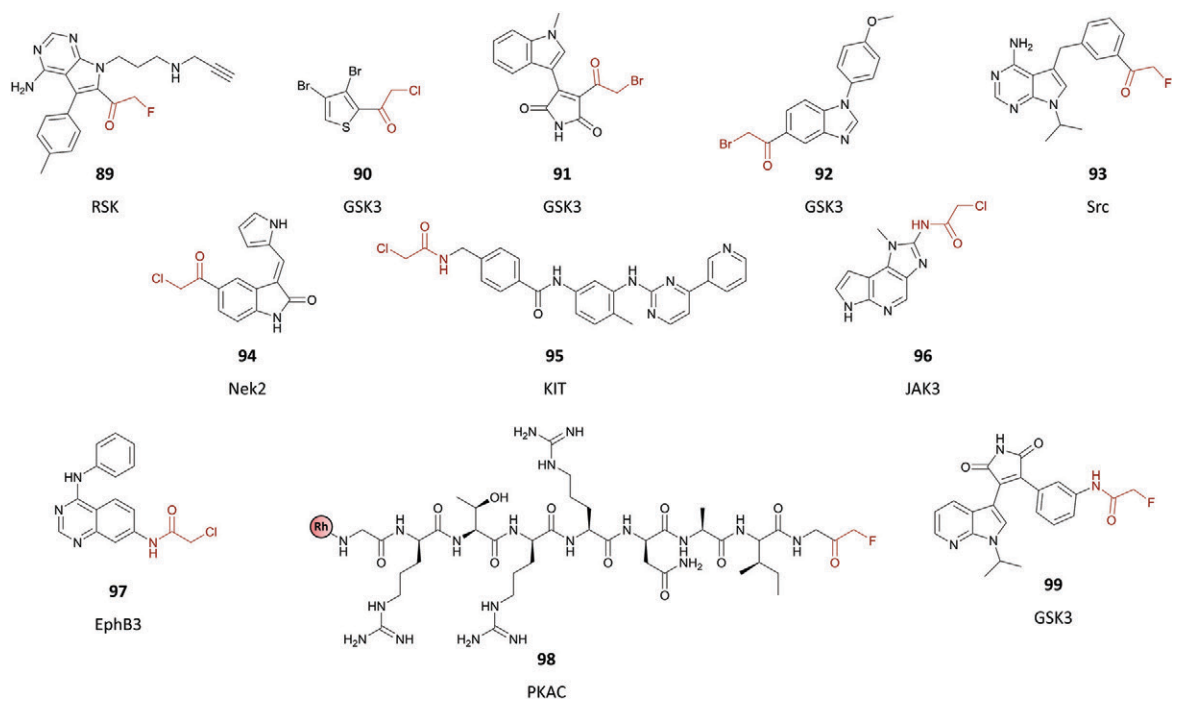

Fig. 44 Chemical structures of inhibitors **89–99** with α-halo-substituted electrophiles reported between 2007–2018.

Table 15 Biochemical and cellular characterization data for inhibitors **89–99**

#	Reversible	Nucleophile	*In vitro* (nM) Isoform	IC_{50}	*In cellulo* (nM) Cell line	IC_{50}	$t_{1/2}$ (h)	K_i (nM)	k_{inact} (ms^{-1})	k_{inact}/K_i (M^{-1} s^{-1})	Stage
89		C436	RSK-1/2	20	HEK293	30					Discovery
90		C199	GSK-3β	500	GCNs	5000	24[b]				Discovery
91		C199	GSK-3β	5	GCNs	51	18[b]				Discovery
92		C199	GSK-3β	580							Discovery
93		C338	SRC^{T338C}	19	NIH-3T3	3000					Discovery
94		C22	Nek-2	6							Discovery
95		C788	KIT	788							Discovery
96		C909	JAK-3	0.6	IL-2 T-blasts[a]	1260				3.50×10^3	Discovery
97		C717	EphB-3	55	HEK293	170					Discovery
98		C199	PKACα	12				459	28.3	6.17×10^3	Discovery
99		C199	GSK-3β	17	RS4;11	900	10[b]				Discovery

[a] Given the complexity of the JAK signalling pathways, few IC_{50}s have been reported in indication specific cell lines. Several publications report EC_{50} for Ba/F3 transfected cells activated by certain cytokines or stimulating factors which are illustrated in the table above. [b] Liver microsomes.

reactive α-chloromethylketone remained the most potent, a trend also observed in isolated thiol-reactivity studies. The irreversible interaction with Nek2 was confirmed by mass spectrometry and surprisingly a >2000-fold drop in potency was seen against Nek2 C022V mutants.[281]

Structural homology represents a recurring challenge in developing selective kinase inhibitors. This is typically addressed by exploiting various selectivity handles, such as allosteric sites, gate keeper or poorly conserved, non-catalytic residues whether reversibly or *via* the use of covalent binders.[282] Imatinib-derived α-chloroacetamide **95** represents a highly selective approach to kinase targeting. This inhibitor employs two filters; a covalent interaction (targeting Cys788) and an additional structural bias, with preference for the DFG-out (inactive) kinase conformation of KIT kinase (IC_{50} = 788 nM). Through SBDD, **95** was generated based on an imatinib-KIT co-crystal structure (PDB 1T46). The success of this highly biased approach was validated by a superior kinome selectivity profile. This is partly because only a very small subset of kinases tolerates the imatinib-scaffold, with an ideally positioned cysteine in their inactive conformation. The use of kinase conformation bias represents a novel strategy to obtain isoform selectivity.[59]

Tricyclic chloroacetamide **96** was reported as a potent, irreversible and selective JAK3 inhibitor, designed to target JAK3-specifc Cys909, reporting an impressive IC_{50} of 3.0 pM after a 2 h preincubation. Kinetic studies into the binding of this compound revealed an ATP-competitive mechanism. Irreversible JAK3 modification was confirmed *via* mass spectrometry and wash out experiments. As for gene product selectivity, against the remaining three JAK family kinases (JAK1, JAK2 and TYK2) this compound displayed an astonishing $>10^6$-fold preference for JAK3 *in vitro*. While very impressive, altogether, the compound was found to display moderate cellular potency in the relevant cell lines (IC_{50} = 1.26 μM).[172] Nevertheless, given the *in vitro* potency and remarkable selectivity, with appropriate structural derivatization, **96** has potential to generate analogs with cellular activity.

As with most kinases, aberrant activity of erythropoietin-producing human hepatocellular (Eph) kinases (EphA4, EphB1, EphB3, EphB4) is implicated in anti-apoptotic events and oncogenesis.[283] Using structural bioinformatics, a series of electrophilic quinazolines (including chloroacetamide **97**) were reported as the first irreversible EphB3-selective inhibitors (Fig. 45). This kinase contains a unique hinge-region Cys717, which are only found in two other enzymes, LKB1 and PINK1, providing a powerful selectivity filter. Interestingly, in the context of EphB3, only the α-halocarbonyls were potent, reporting a biochemical IC_{50} of 55 nM. Acrylamides and vinylsulfonamides showed minimal activity and no significant activity was seen against C717S mutants. A kinase selectivity screen (98 kinases) revealed EGFR as the major off-target (75% inhibition at 200 nM). This is explained by the high affinity of this kinase for the quinazoline scaffold (common in EGFR inhibitors). While this inhibitor had very good potency *in cellulo* (IC_{50} = 170 nM), more recent optimizations yielded a 2nd generation chlorohydroxyl anilino-derivative with a ~56-fold gain in cellular potency (IC_{50} = 3 nM) and no significant EGFR inhibition.[284]

Similar to **77**, an alternative strategy to design kinase-specific inhibitors involves selectively targeting the substrate-binding pocket. In this manner, fluoromethylketone polypeptide **98** (PKI 14–22) was reported as an irreversible, substrate-competitive inhibitor of cAMP-dependent Protein Kinase A Catalytic Subunit

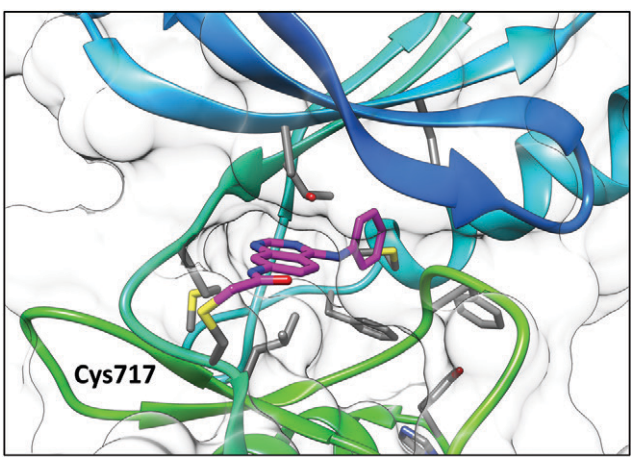

Fig. 45 Crystal structure of EphB3 kinase with quinazoline **97** bound at Cys717 (PDB 5L6P).

Alpha (PKACα) targeting non-catalytic Cys199 (biochemical IC_{50} = 11 nM). Removal of the electrophilic centre caused a ~5-fold drop in activity. Structurally, the compound includes a Rhodamine B tag (Rh), allowing fluorescent-based validation of covalent modification, which was confirmed *via* mass spectrometry and mutagenesis studies (using C199A). This compound represents the first irreversible substrate-competitive inhibitor of PKACα.[285]

In an extensive structural derivatization effort to develop selective GSK3β inhibitors, (aza)indolyl maleimide **99**, containing a mildly reactive fluoroacetamide electrophile, was reported as an irreversible and selective inhibitor targeting Cys199 (similar to **90–92**) with a biochemical IC_{50} of 17 nM. Rational scaffold design was aided by initial covalent docking studies, which situated the electrophile proximal to Cys199. Mass spectrometry studies confirmed the irreversible interaction, while pharmacokinetic studies showed no interaction with P-gp, a $t_{1/2}$ of 0.34 h in liver microsomes and relatively good blood–brain barrier (BBB) penetrance. TAK1 kinase shares a homologous cysteine, whilst CDK2 exhibits high sequence homology to GSK3β. In a focused study, **99** showed relatively minimal potency against either TAK1 (IC_{50} = 2753 nM) or CDK2 (IC_{50} = 639 nM), confirming GSK3β selectivity.[286]

Miscellaneous electrophiles

In the past century, pivotal developments in the chemical modification of proteins, along with rapid progress in organic chemistry, crystallography, molecular and structural biology have all catalysed the advancement of covalent inhibitors. By probing protein function *via* characterizing surface topologies and the role of key structural domains, additional nucleophiles (Ser, Tyr, His) have become targetable.[287,288] These findings, coupled with the recent promise of tuning warhead reactivity, have facilitated the development of many novel electrophilic structures beyond the common α,β-unsaturated systems or halo-substituted carbonyls.

From planar maleimides, reactive epoxides, reversible (weakly covalent) boronic acids to serine-targeting sulfonyl fluorides, these diverse scaffolds possess varying electrophilicity, size, nucleophile-specificity and chemistries (Fig. 46). Modulation of these properties using steric and inductive effects, as well as optimizing for binding pocket size, nucleophile reactivity and covalent bonding mechanism, can generate a broad spectrum of electrophiles tailored to specific applications in chemical biology or drug discovery.

Dietary isothiocyanates (ITCs), a class of electrophile-bearing natural chemopreventives naturally found in plants have been observed to possess anti-cancer activity.[289] To delineate the mechanism behind this efficacy, a very simple ITC, phenethyl isothiocyanate (PE-ITC) **100** was reported as an irreversible Mitogen-activated Protein Kinase 1 (MEKK1) inhibitor (Fig. 48).

MEKK1 is an upstream modulator of signalling pathways controlling cellular stress-response, with key roles in survival and anti-apoptosis. This compound was suggested to target Cys1238 within the ATP binding pocket, reacting at the

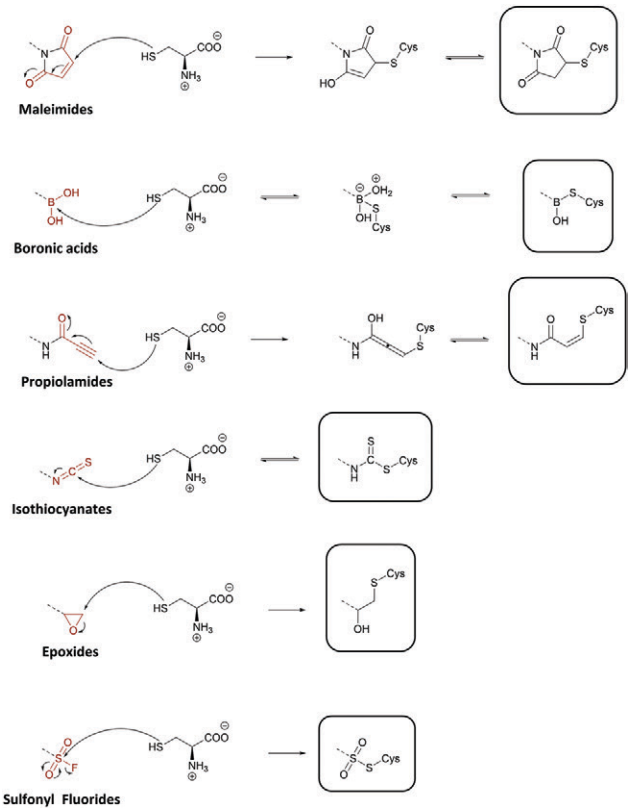

Fig. 46 General mechanisms detailing the covalent modification of miscellaneous electrophiles by cysteine thiol nucleophiles.

electrophilic isothiocyanate carbon (biochemical IC_{50} = 12.5 μM). This relatively weak potency may be attributed to the inherent mild reactivity of ITC motifs as well as the simple, non-optimized structure of the inhibitor. While binding assays against MEKK1 revealed an ATP-competitive mechanism, no activity was seen against C1238V mutants, indicating the importance of Cys1238 towards the observed potency.[290]

6-Ethynyl thieno[3,2-*d*]pyrimidine **101**, is a potent and irreversible EGFR inhibitor targeting Cys797 (biochemical IC_{50} = 7.0 nM). The design was inspired by a previously reported acetylene-containing ErbB4 (HER4) inhibitor shown to inactivate the analogous Cys803. Initially, adduct formation to the terminal alkyne was unexpected, given the lack of an obvious electrophile. However, aided by MS and an X-ray crystal structure, a covalent interaction at the alkyne was in fact validated. In a period of 3 h, **101** was found to alkylate 83% of EGFR, with complete inhibition after 20 h, translating into good cellular efficacy (IC_{50} = 100 nM). In a BT474 breast cancer *in vivo* xenograft mouse model, tumour regression was visible at 100 mg kg^{-1} (note, inhibition was evident even at 30 mg kg^{-1}).[291] The proposed mechanism for terminal alkyne reactivity with Cys797 can be seen in Fig. 47.

Electrophilic di-epoxide diterpenoid **102** (17-hydroxyjolkinolide B) was found to be a potent inhibitor of IL-6 induced and constitutively active STAT3 by inactivating JAK kinases (biochemical IC_{50} = 4.0 nM). The authors demonstrate the observed potency to be caused by the covalent cross-linking of JAK1/2 and TYK2 monomers. While no specific reactive

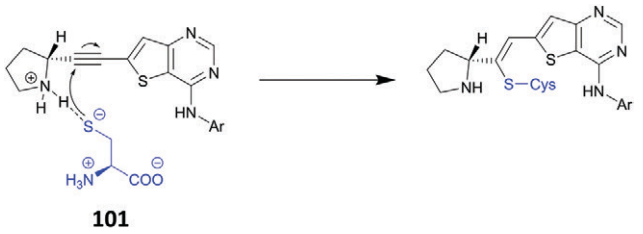

Fig. 47 Proposed mechanism of alkyne electrophilicity with Cys797 in the active site of HER4 kinase.

nucleophile was confirmed, incubation studies with thiol-containing GSH markedly mitigated STAT3 activation and signalling, indicating cysteine sulfhydryls as a potential target nucleophile (Table 16).[292]

Mass spectrometry revealed a covalent adduct, with an inhibitor : protein ratio of 1 : 2. Selectivity screens on several proteins revealed this cross-linking process to be JAK specific. No dimerization events were observed with Bovine Serum Albumin (BSA), Platelet Derived Growth Factor (PDGFR), Green Fluorescent Protein (GFP) or EGFR. Kinase-specific selectivity studies (at 50 μM) against 50 kinases showed minimal inhibition of all enzymes except one, IKKβ. This compound was also moderately potent against various cancer tumor cells (IC_{50} < 10 μM). While the use of cross-linking agents to alter protein function or activity has been known for many years, the application of such a covalent strategy in the context of CKIs represents a novel approach to kinase inhibition.[293]

p38 MAP kinases (p38α) are Ser/Thr kinases and key regulators of inflammatory cytokine production. Consequently, aberrant p38α activity has been implicated in various cytokine-sensitive diseases (*e.g.* osteoarthritis, rheumatoid arthritis, *etc.*).[294] As a result, pharmacological intervention with covalent small molecules has been pursued as a therapeutic strategy. In one example, dialkynylimidazole, **103**, was reported as a selective, irreversible inhibitor of p38α, reacting similar to **101** at the alkyne warhead (IC_{50} = 200 nM, 100% kinase inhibition observed at 10 μM). Against 53 other kinases, only one enzyme, MAPK4, was inhibited >90% at 20 μM.

While previous studies report pyridinylimidazoles to confer hepatotoxicity due to the inhibition of CYP450 cytochrome detoxifying enzymes, this compound showed only 4% inhibition of CYP2D6 at 10 μM. Note, while shown to be irreversible, authors have not reported a precise nucleophilic site or exact mechanism-of-action.[295]

Dysregulated p21-activated kinase 1 (Pak1) activity, a cytoplasmic Ser/Thr kinase, has been linked to oncogenesis.[296] Disulfide **104** (IPA-3) was reported as an allosteric and reversible covalent Pak1 inhibitor, binding the kinase regulatory domain (RD; $K_{d(app)}$ = 100 nM). However, the true mechanism of action and reactive nucleophile remains unknown. While Pak1 does contain surface cysteine residues, previous work by the authors

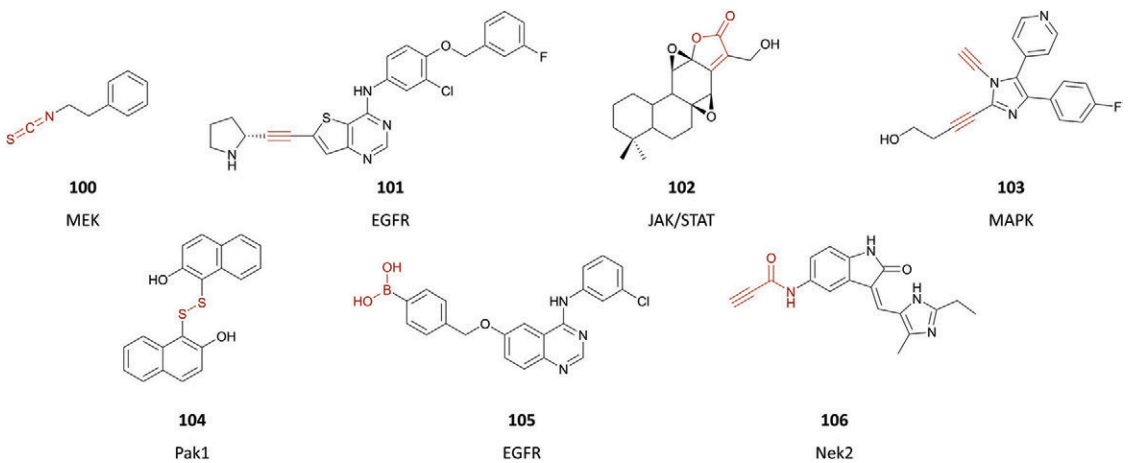

Fig. 48 Chemical structures of inhibitors **100–106** with miscellaneous electrophiles reported between 2007–2018.

Table 16 Biochemical and cellular characterization data for inhibitors **100–106**

			In vitro (nM)		*In cellulo* (nM)						
#	Reversible	Nucleophile	Isoform	IC_{50}	Cell line	IC_{50}	$t_{1/2}$ (h)	K_i (nM)	k_{inact} (ms^{-1})	k_{inact}/K_i (M^{-1} s^{-1})	Stage
100		C1238	MEKK1	>5000							Discovery
101		C797	EGFR	7	HN5	94		100	0.167	1.67×10^3	Preclinical
102		Cxxx	JAK1/2	4	HepG2	>5000					Discovery
103			MAPKα	200							Discovery
104	•		Pak1	2500	HEK293	5000		1920			Discovery
105	•	C797/D800	EGFR	850	A431	1820					Discovery
106		C22	Nek2	770	A549	1300	1.0[a]				Discovery

[a] Liver microsomes.

demonstrated a lack of any reactive cysteine. Nonetheless, kinetic assays revealed a slow binding profile, with electrophilic warhead reversibility validated by a dose-dependent decrease in target occupancy with increasing [DTT].[297] Note, the reactivity with DTT does elude to a propensity to be targeted by thiols.

Besides Lewis acid behaviour, vacant Boron p-orbitals permit interconversion between sp^2 (neutral) and sp^3 (anionic) hybridizations. Near a nucleophile, this allows for weak covalent interactions (B–O σ-bond energy = 18 kcal mol^{-1}).[298]

A crystal structure of cancer therapeutic bortezomib with 20S proteasome elegantly demonstrates this concept (PDB 2F16, Thr–OH adduct forming a stable borate). In a similar manner, boronic acid conjugated 4-anilinoquinazoline **105** was reported as a covalent EGFR inhibitor (55% modification at 1.0 μM).

The structural optimization of linker length was critical in positioning $B(OH)_2$ within an appropriate distance of either Cys797 or Asp800 donors. Time-dependent inhibition and wash out experiments confirmed the extended efficacy and covalent interaction. While direct target engagement experiments were not reported, both docking and quantum mechanical-generated poses placed the electrophilic boron within reach of either Cys787/Asp800 residues.[299]

Similar to **94**, oxindole propiolamide **106** (JH295) was reported as a selective covalent Nek2 inhibitor, also targeting Cys22 (IC_{50} = 770 nM). This compound is ~130-fold less active than **94**, highlighting the impressive reactivity of α-halo carbonyls. Mass spectrometry confirmed a covalent adduct against the wild-type kinase and not the C022V mutant. Oxindole scaffolds are known to inhibit Cdk1 function,[300] which can block mitotic entry, and prevent the study of Nek2 in mitosis. Thus, during optimization, Nek2:Cdk1 selectivity was an important consideration for the authors. SBDD revealed that the 2-imidazole position was critical, and structural optimization generated a ~26-fold Nek2 selective compound. Relative to halocarbonyl **94**, the propiolamide is 20-fold more stable against cellular thiols, (BME $t_{1/2}$ = 60 minutes), which was proposed to explain the superior cellular activity of this warhead.[281] Interestingly, the related butynamide derivative was >25-fold lower in activity, possibly due to a steric clash in the active site. These data demonstrate the sensitivity of certain nucleophile–electrophile pairs and their intolerance to subtle structural variability.

Thiadiazolidindione **107** (Tideglusib) is a validated inhibitor of GSK3β, currently in phase IIa/IIb trials for AD.[301] Although this scaffold is known to engage the kinase *via* a non-ATP-competitive binding mode, recent studies into the mechanism of action elucidated a covalent interaction, targeting Cys199 (IC_{50} = 105 nM). Minimal recovery of kinase activity upon wash-out and time-dependent inhibition (1 h pre-incubation IC_{50} = 5 nM) specifically suggested an irreversible mechanism. While studies on the C199A mutant showed a 70-fold loss in potency, 1 h preincubation against these GSK mutants still achieved impressive potency (IC_{50} = 60 nM). Further binding kinetic analyses against C199A revealed the compound can attain a prolonged residence time (>2 h). Therefore, the authors suggest, while the Cys199 interaction contributes to potency, it is not essential (Fig. 49).[302]

In screening 300 000 ligands to determine novel Pyruvate Kinase (PK) inhibitors, saccharin-type structures were identified as potential lead compounds. Further synthetic derivatization furnished **108** (DBS) as an ATP competitive, covalent PK inhibitor (IC_{50} PK-R, PK-M2 = 8 and 16.3 μM, respectively) targeting Lys335. Time-dependent inhibition and the loss of activity against K335R mutants suggested an irreversible binding mechanism. Impressively, a focused screen of two non-kinase enzymes (lactate dehydrogenase and luciferase) with analogous lysine residues showed no potency (Table 17). As for the mechanism of action, aided by modelling studies and X-ray structures, the authors propose that PK inhibition involves an irreversible nucleophilic attack (Lys335) at the C_3 carbon of the saccharin moiety, releasing 4-mercaptobenzoic acid as a leaving a group.[303]

eEFK2 (atypical kinase sub-family) plays a role in regulating protein synthesis and is implicated in promoting tumour survival and proliferation.[304] Carbonitrile **109** was reported as a reversible covalent inhibitor of eEFK2, exhibiting time-dependent

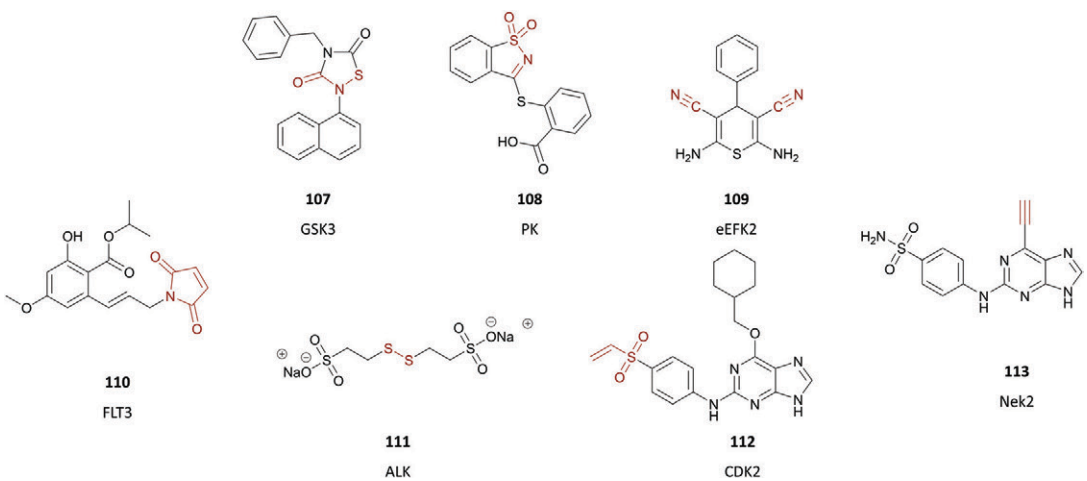

Fig. 49 Chemical structures of inhibitors **107–113** with miscellaneous electrophiles reported between 2007–2018.

Table 17 Biochemical and cellular characterization data for inhibitors **107–113**

#	Reversible	Nucleophile	*In vitro* (nM)		*In cellulo* (nM)		$t_{1/2}$ (h)	K_i (nM)	k_{inact} (ms^{-1})	k_{inact}/K_i (M^{-1} s^{-1})	Stage
			Isoform	IC_{50}	Cell line	IC_{50}					
107		C199	GSK-3β	105	HepG2	60	41[a]	500	0.58	1.16×10^3	Phase II
108		K335				>5000					Discovery
109	•	C146	eEFK-2	>5000				>5000	1.70	12.14	Discovery
110		C179	FLT-3	540	MV-4-11	1730					Discovery
111	•	C1156/C1235		>5000			1.47[b]				Phase III
112		K89						1310	6.55	5.00×10^3	Discovery
113		C22									Discovery

[a] Hepatocytes. [b] Human (*in vivo*).

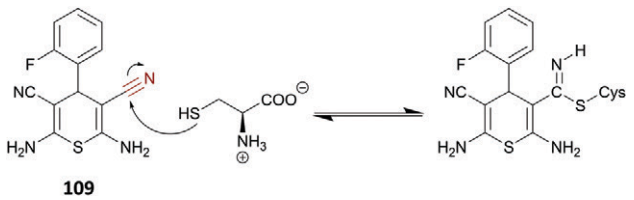

Fig. 50 Proposed covalent modification mechanism of carbonitriles using cysteine nucleophiles, forming reversible thioimidate complexes.

inhibition by seemingly targeting the poorly conserved active site Cys146 and forming a thioimidate complex, with low potency (IC_{50} = 60 μM). Kinetic studies revealed a two-step binding mechanism; a fast-initial step before a slower inactivation step, with slow reversibility ($\tau \sim 19$ min). This is interesting, as typical covalent mechanisms generally report slow binding, followed by rapid covalent bond formation (Fig. 50). The predicted binding pose of this inhibitor roughly positions the nitrile moiety within 4.5 of Cys146. Site-directed mutagenesis revealed a ~14-fold loss in potency against C146A mutants, suggesting this reversible covalent interaction contributes to binding. Also, the authors were able to demonstrate that all available thiols are not susceptible to this scaffold, as incubation with excess GSH showed no observed reaction.[305] Note, given the relatively high IC_{50}, it is difficult to ascertain whether the observed inhibition is a result of target engagement or non-specific interactions.

FLT3 is a cytokine receptor kinase with implications in hematologic pathologies (*i.e.* AML), with numerous inhibitors currently in clinical development.[306] Maleimide **110** containing a more synthetically feasible ring-opened resorcylic acid core was reported as a covalent FLT3 inhibitor, targeting Cys179 (IC_{50} = 0.54 μM). Within this study, a focused electrophile SAR probing the potency of Michael acceptors, acrylamides and vinylsulfones proved the maleimide warhead to be the most potent. Computational docking studies of a structural variant predicted the Cys179 to be ~3.8 from the maleimide olefin. To confirm thiol-reactivity, NMR studies used cysteamine and GSH as model systems, and as predicted, the rapid disappearance of alkenyl protons was observed. Kinetic studies into inhibitor k_{off} showed no kinase dissociation, suggesting an irreversible interaction.[307]

In separate randomized phase II/III clinical trials for NSCLC, the use of non-toxic, water-soluble disulphide **111** (BNP7787, Tavocept) in combination with standard-of-care therapies showed significant improvements in overall survival.[308] Studies into this mechanism reported the disulphide scaffold as a cysteine-specific reversible covalent inhibitor of Anaplastic Lymphoma Kinase (ALK). The covalent modification of ALK, forming what are known as mercapto-ethanesulfonate (MESNA) adducts occurs *via* mixed disulphides at Cys1156/1235 (IC_{50} = 9.16 mM). As a comparably weak, reversible electrophile, the disulphide moieties were proposed to drastically disrupt P-loop and A-loop conformations within the ALK kinase domain. While alone this compound is not an effective inhibitor, the disruption of kinase domains was proposed to explain the signification potentiation (10–30%) observed when **111** was co-administered with the highly potent ATP-competitive ALK inhibitor, crizotinib.[309]

Adenine derived sulfonamide **112** (NU6300) with a vinyl sulfone warhead has been reported as the first irreversible ATP-competitive inhibitor of CDK2 (K_d = 1.31 μM). A SBDD approach, in addition to mutation studies on nucleophiles proximal to the ATP-site, revealed the poorly conserved Lys89 as the site of covalent modification (a result later validated by X-ray crystallography and mass spectrometry). In a selectivity screen against a panel of 131 kinases, only three proteins exhibited >50% inhibition (with 4 h pre-incubation, 1 μM of inhibitor). In addition, **112** was also found to be potent in cells by studying the inhibition of CDK2-dependent downstream targets (*e.g.* Rb tumour-suppressor protein).[310]

A common method to probe protein function utilizes siRNA. Despite being a gold-standard, this technique can be limited by issues of selectivity, specialized protocols and cell/organism viability.[311] In certain cases, small-molecules have surpassed siRNA as alternative pharmacological tools to modulate cellular components and study biochemistry. Using chemo-genetics to introduce a V022C mutation to confer molecule sensitivity, **113** was reported as a covalent inhibitor of Plasmodium falciparum, pfNek2, (IC_{50} = 501 nM). Although a non-human orthologue, high sequence identity between both proteins allows this compound to be a valuable tool to interrogate Nek2 biology. Covalent adduct formation was confirmed by mass spectrometry, whilst wash-out studies, coupled with minimal recovery in the kinase assay, validated the irreversible nature of this interaction.[312]

Plk1 plays important regulatory roles in mitosis (*e.g.* mitotic entry, spindle assembly) and pharmacological inhibition results in mitotic arrest and subsequent cell death in various human cancers.[313] Identified from a library of ~20 000 small

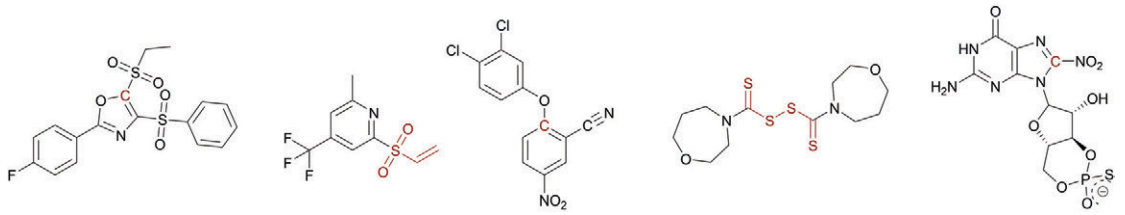

Fig. 51 Chemical structures of inhibitors **114–118** with miscellaneous electrophiles reported between 2007–2018.

Table 18 Biochemical and cellular characterization data for inhibitors **114–118**

			In vitro (nM)		*In cellulo* (nM)						
#	Reversible	Nucleophile	Isoform	IC_{50}	Cell line	IC_{50}	$t_{1/2}$ (h)	K_i (nM)	k_{inact} (ms^{-1})	k_{inact}/K_i (M^{-1} s^{-1})	Stage
114		K209/K388/K574	Plk-1	1220	A549	2500					Preclinical
115		K540									Discovery
116		C646									Preclinical
117	•	C240	PDK-1	26	A549	225		109	0.547	5.14×10^3	Preclinical
118		C42/C195	PKG	>5000				>5000	4.50	2.00×10^2	Discovery

molecules, oxazole **114** (T521), was reported as a lysine-targeting non-competitive covalent Plk1 inhibitor (IC_{50} = 1.22 μM), binding to the polo-box domain (PDB) (Fig. 51). Impressively, **114** is highly selective and is ~410-fold less active against tumour-suppressors PLK2 and PLK3. Mass spectrometry studies confirmed covalent modification with a 3 : 1 ratio of inhibitor : protein (Lys209, Lys388, Lys574, respectively) (Table 18).

The proposed mechanism of action involves nucleophilic substitution at the (δ+) ethylsulfonyl oxazole carbon. While the compound successfully induced mitotic arrest, apoptosis and cell-cycle delay, indiscriminate cytotoxicity was observed. Nonetheless, *in vivo* murine tumour model studies using A549 xenografts showed a marked decrease in size and volume.[314] Conversely, another strategy recently reported the first cell-based screening tool for PLK inhibition, which found vinyl sulfone **115** as a covalent alkylator of Plk1. A focused screen for nucleophile reactivity showed rapid reactions with lysine and cysteine but not histidine residues. This structure is proposed to specifically bind the PDB of Plk1 (reporting His538 and Lys540 as potential sites).[315] Note, it has been suggested that the simple scaffold coupled with electrophilic reactivity may cause non-specific modification and the characteristics associated with a pan-assay interference compounds (PAINS).

116 is a broad-spectrum antiviral compound, discovered in 1982 to inhibit early viral replication resulting in promising activity against Poliovirus (PV) (anti-PV EC_{50} = 6.80 μM).[316] Recent studies into the cellular target of this molecule reported **116** as an allosteric and covalent inhibitor of PI4Kβ kinase. The current understanding about the role of PI4K in viral infections suggests that viral proteins activate the kinase to produce phosphatidylinositol-4-phosphate (PI4P), which indirectly promotes the formation of the virus replication complex.[317] Irreversibile modification was first suggested as the mechanism-of-action, given time-dependent antiviral activity (7-fold rise after a 24 h pre-incubation). This was confirmed by mass spectrometry studies, which in addition to proteomics and site-directed mutagenesis revealed Cys464 as the site of covalent modification. Considering the positioning of EWGs relative to the halo-substituted phenoxy-motif, it was proposed that the mechanism of action proceeded through a nucleophilic aromatic substitution (S_NAr) releasing 3,4-dichlorophenol (Fig. 52).[318]

Dependence on aerobic glycolysis, with amplified conversion of glucose to lactate at normal oxygen levels is a hallmark of cancer, known as the Warburg effect.[319] Pyruvate dehydrogenase kinase (PDK) modulates mitochondrial respiration and aerobic glycolysis, implicating dysregulated activity in disease. Specifically, PDK1 is linked to the metabolic re-programming of

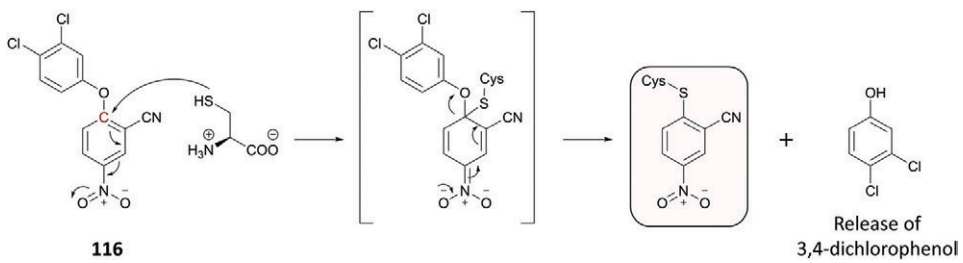

Fig. 52 Proposed S_NAr mechanism of covalent modification between **116** and cysteine nucleophiles.

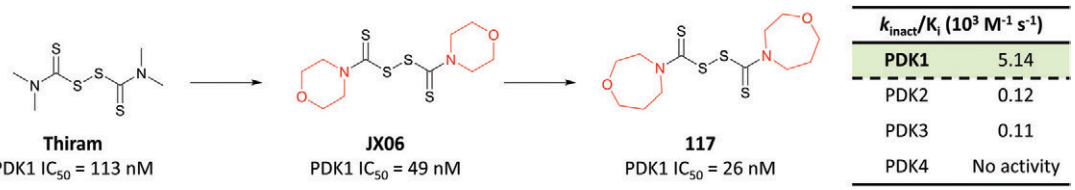

Fig. 53 Generational development of potent and highly selective PDK1 inhibitor **117** from parent thiuram disulphide Thiram.

cancer cells.[320] An initial screen of ~600 compounds revealed the simple thiuram disulphide (Thiram) as a potent PDK1 inhibitor (IC_{50} = 113 nM). Morpholinyl derivative JX06 was found to be a more active/selective variant (PDK1-4 IC_{50} = 49, 101, 313, >10 000 nM). JX06 represented the first covalent PDK1 inhibitor, targeting conserved Cys240 *via* reversible mixed disulfides.[321] Further optimization through ring expansion yielded **117** with improved potency, selectivity, and *in vivo* efficacy (IC_{50} = 26 nM) (Fig. 53).

As with JX06, GSH attenuates inhibitor potency, re-affirming the importance of the disulphide. Successful regression of tumour growth in A459 murine xenografts (over 21 days, 80 mg kg^{-1}) was observed with no apparent toxicity. This supports the therapeutic utility of reversible covalent disulphides as efficacious anticancer agents.[322]

cGMP-dependent Protein Kinase G (PKG) regulates numerous cellular processes including vascular smooth muscle relaxation and neuronal synaptic plasticity.[323] The design of small-molecule PKG modulators represents a common strategy for studying the biology of these Ser/Thr kinases. Recent evidence suggests inhibition of dysregulated PKG activity to have therapeutic utility in bacterial and cancer diseases. 8-nitroguanosine **118** was reported as an irreversible covalent activator of PKG1α, functioning *via* an *S*-guanylation like-reaction (at the guanosine nitro-carbon) targeting Cys42/Cys195 (IC_{50} = 22.0 μM). This proposed mechanism of action was supported by immunohistochemistry, utilizing an anti-*S*-guanylation antibody. Electrophilic thiol-reactivity was validated *via* mass spectrometry and incubation with free cysteine. This compound also successfully inhibited acetylcholine-induced vascular relaxation of mouse aorta vessels (a phenotypic response linked to PKG function).[324]

In an attempt to identify novel hits with therapeutic utility against FGFR4-driven disease, a selectivity-focused approach, targeting poorly conserved Cys552, yielded dipyridylamine **119**[325] and 2-formylquinoline **120**[326] as potent covalent inhibitors (IC_{50} = 53 and 57 nM, respectively) (Fig. 54). The designed inclusion of *ortho*-pyridyl and *para*-nitro motifs in **119** allows for an irreversible S_NAr mechanism, whilst the in **120** reacts *via* a reversible hemi-thioacetal adduct (confirmed by X-ray crystallography). While these represent simple scaffolds, by targeting Cys552, the authors were able to show impressive selectivity, with no inhibition of FGFR1–3, up to 10 μM. FGFR4 C552A mutants were unreactive, validating the site of covalent modification. In a follow-up study, the 2-formylquinoline (**120**) scaffold was further optimized to probe the utility of aldehydes as putative reversible covalent inhibitors. Consequently, through expansive derivatization, tetrahydronapthyridine urea (THNU) **121** was identified as a more potent FGFR4 inhibitor, with an 8-fold increase in potency (K_d = 5 nM, IC_{50} = 6.8 nM) along with an extended residence time (τ = 235 min) and promising cellular activity (IC_{50} = 108 nM) (Table 19).[326]

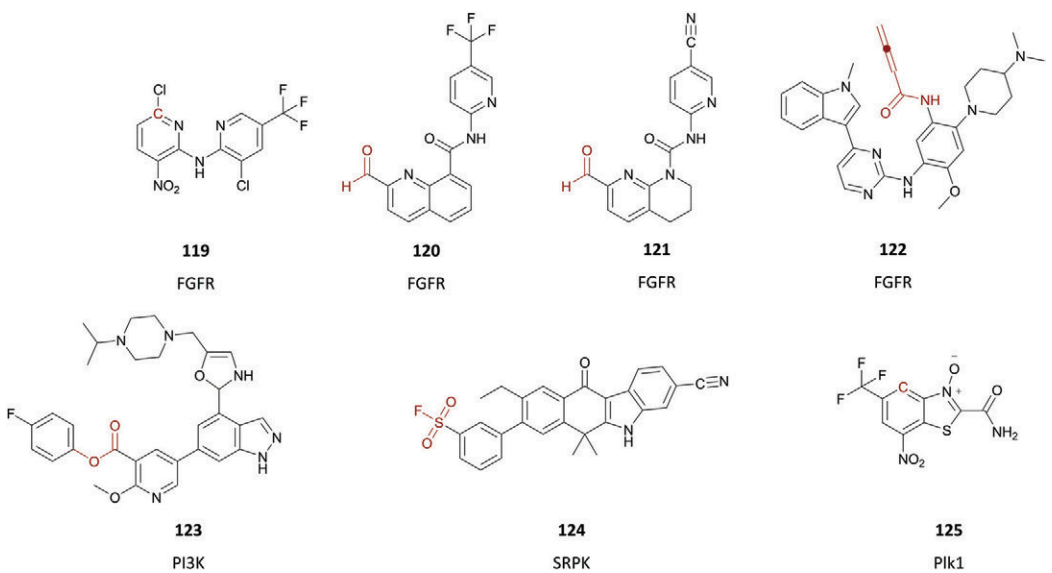

Fig. 54 Chemical structures of inhibitors **119–125** with miscellaneous electrophiles reported between 2007–2018.

Table 19 Biochemical and cellular characterization data for inhibitors **119–125**

#	Reversible	Nucleophile	*In vitro* (nM)		*In cellulo* (nM)		$t_{1/2}$ (h)	K_i (nM)	k_{inact} (ms^{-1})	k_{inact}/K_i (M^{-1} s^{-1})	Stage
			Isoform	IC_{50}	Cell line	IC_{50}					
119		C552	FGFR-4	53						3.00×10^4	Discovery
120	•	C552	FGFR-4	57							Discovery
121	•	C552	FGFR-4	6.8	Ba/F3	108		5.0			Discovery
122		C797	EGFR	6.3	NCI-H1975	33			5.04		Discovery
123		K779	PI3K-δ	7.9			1.32	260	5.50	2.10×10^4	Discovery
124		Y227	SRPK-1/2	35.6	HeLa	1087					Discovery
125	•	C67	Plk1	2470							Discovery

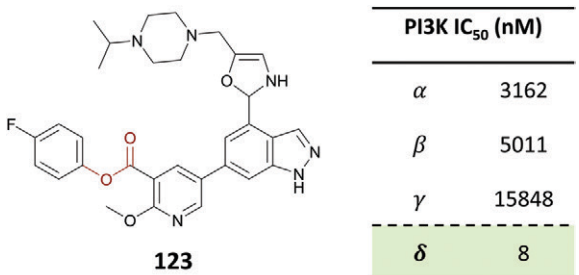

Fig. 55 Selectivity profile of lysine targeting PI3Kδ inhibitor **123**.

Inhibitor **123**, containing an electrophilic phenolic ester was reported as the first covalent and selective PI3Kδ inhibitor (Fig. 55). While targeting cysteine nucleophiles is successful in kinase inhibition, the pursuit of alternative residues remains of great utility. This is due to the fact that less than half the human kinome contains a nucleophilic thiol near the ATP binding site.[327] With this in mind, **123** was designed to target catalytic Lys779 (forming an amide-adduct) with a sustained duration of action (>48 h). While a correlation was observed between potency and ester-bound EWG strength, suggesting carbonyl electrophilicity to be important for activity, kinetic studies revealed a stronger correlation with K_i rather than k_{inact}. This implies the potency of **123** is largely governed by the initial non-covalent binding prior to enzyme inactivation. Note, this compound does not react with *N*-Boc-lysine (pH 7.4, 37 °C), yet readily reacts with Lys779. This demonstrates the important role of the binding site microenvironment in facilitating nucleophilic attack. Most impressively, *in vitro* and proteomic analysis in cells revealed strong PI3Kδ-selectivity relative to the other homologous PI3K isoforms.[328]

Alternative splicing of pre-mRNA (a key process for cell homeostasis) is in part controlled by protein co-factors, which are in turn regulated by SR protein kinases (SRPKs 1–3).[329] Deregulated SRPK1 activity is shown to cause aberrant splicing, with implications in various pathologies.[330] Using SBDD, and known ALK inhibitor Alecitinib as a core-scaffold, sulfonyl fluoride **124** (SRPKIN-1) was reported as an irreversible SRPK1/2 inhibitor (IC_{50} = 35 and 98 nM, respectively). This represents the first tyrosine-targeting covalent inhibitor (SRPK1 Tyr227, neighbouring the ATP site).

As electrophiles, sulfonyl fluorides (SFs) are uniquely diverse in their target nucleophile reactivity, with reports of modifying activated Ser residues and in certain cases Thr, Lys, His and Cys residues. This can be of great use for developing covalent therapies or probing important cellular proteins.[331] For example, tyrosine targeting allowed for an impressive selectivity profile. Also, potent antiangiogenic effects were seen in an age-dependent macular degradation (AMD) mouse model.[95]

Lastly, benzothiazole *N*-oxide **125** was reported as an ATP-competitive, covalent inhibitor of Plk1 with a novel reversible mechanism-of-action (IC_{50} = 2.47 μM). Compound **125** selectively targets Cys67 *via* an S_NAr mechanism, going through a reversible Meisenheimer complex (MC). This structure was further supported by NMR and UV-Vis experiments. This report represents the first example of utilizing the MC intermediate in the context of covalent kinase inhibitors. Plk1 C67S mutants observed no activity (up to 100 μM), validating the importance of Cys67 as the site of modification. The authors suggest that the absence of a leaving group upon forming the MC allows for mechanistic reversibility, preventing irreversible adduct formation. However, the formation of this reversible complex is very context specific. This approach, utilizing a mechanistic filter represents a novel approach to achieve kinase selectivity, avoiding indiscriminate off-target modifications.[332]

FDA-approved covalent kinase inhibitors

Advancing a discovery program towards a drug candidate is a significant challenge (Fig. 56). Recent estimates predict a time-frame of 10–15 years, 1–2 billion USD and a 5–15% success rate.[333] These statistics do vary by therapeutic indication, while ~3.4% of lead molecules in oncology programs will be approved, this value rises to ~33.4% for anti-infective drugs.[334] In the last 10 years, studies have determined lack of efficacy and/or safety as the major causes for clinical failure.[335–339] Often drugs do not target the proposed target. A recent paper proposes CRISPR-cas9 genetic targeting validation as an important step in target and lead validation.[340] A recent review by Hwang *et al.*[336] of 640 agents in phase III revealed that of the 54% small molecules which failed to progress, more than half (57%) did not meet efficacy endpoints, whilst 17% were halted for safety reasons.

Poor outcomes are attributed to incorrect dosing, poor study design (*i.e.* sample size, target population, study end-points) and a poor understanding of target function or disease biology.

The benefits of covalent inhibitors include superior efficacy and improved selectivity (if optimized correctly) with the

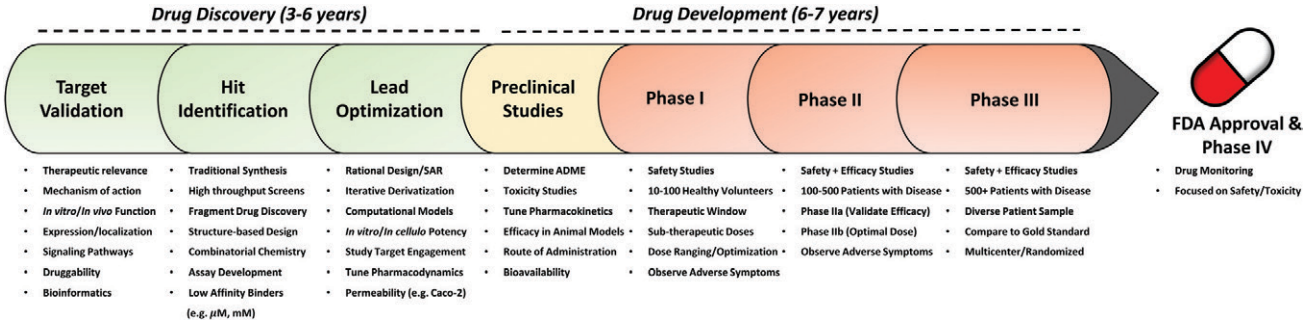

Fig. 56 General stages of drug discovery and development. Common experiments and approaches involved in each stage are listed.

potential for sustained potency using smaller doses. These properties, coupled with recent advances in the rational tuning of warhead reactivity, have solidified CKIs position in drug pipelines as a promising strategy to circumvent the above clinical challenges. The following sections detail the clinical landscape of kinase-targeting covalent inhibitors by highlighting the 6 FDA-approved small molecules (as of October 1st, 2018). These drugs target BTK and EGFR kinases using acrylamide (5) and 2-butynamide (1) electrophiles.

Epidermal growth factor receptors (EGFRs)

Cellular homeostasis largely depends on effective signal transduction. In a series of controlled events, the action of extracellular stimuli (*i.e.* physical or chemical) on cellular receptors modulates intracellular signalling cascades to elicit a biological response. One of the earliest studied class of signalling molecules are growth factors (*e.g.* NGF, IL-6), pioneered by Rita Levi-Montalcini and Stanley Cohen in the 1950s.[341–343] These molecules have broad regulatory roles in cell growth, differentiation and embryonic development, acting on growth factor receptors.[343] Characterizing the epidermal growth factor,[344] a mitogenic-polypeptide was a key milestone as it led to the discovery of the EGF receptor (EGFR), a 170 kDa transmembrane glycoprotein with extracellular ligand binding abilities as well as intracellular kinase activity, which was a novel finding.

EGFR (also known as HER1, ErbB1) as the archetype RTK is part of the HER/ErbB family, which also consists of HER2 (ErbB2), HER3 (ErbB3) and HER4 (ErbB4).[345] EGFR is a single-chain modular glycoprotein, with a ligand binding ectodomain, a hydrophobic transmembrane, a short juxta-membrane region and an intracellular catalytic kinase domain. Extracellular ligand-binding promotes homo/hetero-dimerization of receptor monomers, activating kinase activity and the autophosphorylation of C-terminal tyrosines. These residues subsequently bind SH2 and/or pTyr binding domains of intracellular proteins, activating several downstream signalling pathways (*e.g.* JAK/STAT, RAS-RAF-MAPK, PI3K-AKT-mTOR, PKC, *etc.*).[345,346] To date, 11 ErbB protein-specific growth factor proteins have been characterized.[347]

HER2 remains an orphan RTK with no known endogenous ligand and also represents the preferred dimerization partner in ErbB signalling. HER3 lacks intrinsic kinase activity and only functions upon binding HER1, HER2, and HER4. For a more detailed review of ErbB biology, see ref. 345 and 347–349.

Aberrant activity of EGFRs is implicated in human pathology. Historically, studies into this class of kinases revealed the first association between receptor expression and tumorigenesis.[350] Since then, EGFR overexpression has been observed in 40–80%, 65% and 84% in NSCLC, epithelial, and squamous tumour tissue, respectively. EGFR hyperactivity is known to stimulate uncontrolled cell division and angiogenesis whilst evading apoptosis,[349] whereas deficiencies in signalling are implicated in neurodegenerative ailments such as Alzheimers.[351] Aided by the of significant data surrounding EGFR ligands, their role in disease and advances in structural characterization, these kinase have become a key target for pharmacological modulation, whether in therapy or as a tool to improve our understanding of cell or cancer biology.

Various strategies to inhibit EGFR function have been explored in recent years.[352] These have included ectodomain-targeting antibodies (*e.g.* cetuximab),[353] bifunctional scaffolds to recruit immune effector cells (*e.g.* MDX-447)[354] and antibody-toxin conjugates (*e.g.* scFv-14e1-ETA).[355] Kinase activity is typically interrogated by ATP-competitive inhibitors (*i.e.* erlotinib).[356] Other approaches aim to target endogenous ligand activity with EGF vaccines (*e.g.* CIMAvax-EGF)[357] eliciting immune responses producing anti-EGF antibodies. Antisense oligodeoxynucleotides (*i.e.* inactivates mRNA) have also been used to block EGFR synthesis (*e.g.* AS-21).[358] While each approach provides specific benefits, the use of small molecules remains the most common. Quinazoline ZD1839 (gefitinib, Iressa) was the first EGFR inhibitor approved in 2003 as a third-line therapy for NSCLC[359] and quickly followed by structural variant erlotinib (Tarceva). Since this 1st generation, 2nd (*e.g.* afatinib, dacomitinib, neratinib), 3rd (*e.g.* osimertinib)[360] and more recently 4th generation (*e.g.* EAI045) compounds have been reported.[361] Typically, such generational development aims to improve drug pharmacology, while exploring novel or alternative inhibitory mechanisms to sustain potency against recurring resistance.

Loss of efficacy due to drug resistance is a common theme in drug discovery. Whether through intrinsic or acquired mechanisms (acting alone or in concert), this remains a major hurdle to sustained clinical success.[362] Genomic modifications (*e.g.* point mutations) within or nearby the kinase ATP binding site can rapidly abolish the

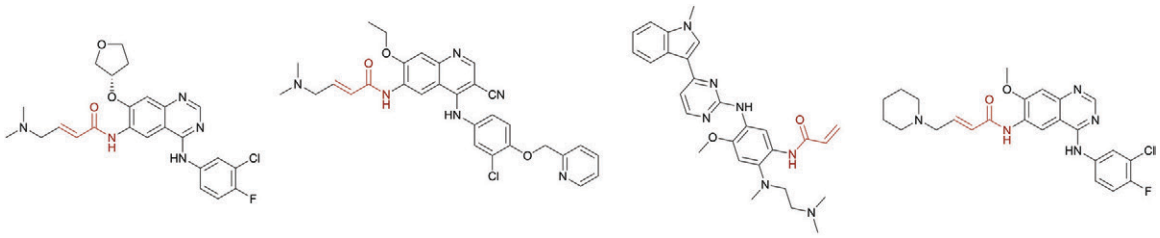

Fig. 57 Chemical structure of FDA-approved EGFR targeting CKIs. Electrophilic warheads are highlighted.

Table 20 Biochemical, cellular and pharmacokinetic parameters of FDA-approved EGFR targeting CKIs

TCI	Nucleophile	$EGFR^{L858R/T790M}$ IC_{50} (nM)	$t_{1/2}$ (h)	K_i (nM)	k_{inact} (ms^{-1})	k_{inact}/K_i (μM^{-1} s^{-1})	Dose (mg)	T_{max} (h)	Route	F (%)
Afatinib	C797	7.3	37	0.16	2.4	15	40	4–6	P.O.	92
Neratinib	C797	9.4	14	0.14	1.1	7.86	40	2–8	P.O.	95
Osimertinib	C797	15.0	48	1.46	5.5	3.77	40–80	6	P.O.	97
Dacomitinib	C797	6.0	70	0.63	1.8	2.86	15–45	6	P.O.	80

potency of ATP-competitive molecules. This was evident with 1st generation EGFR inhibitors gefitinib and erlotinib. While these approved therapies successfully mitigated cancer progression, this response can be greatly diminished within 6–8 months of treatment as a number of patients develop resistance and cancer recurrence (acquired T790M mutation).[363] In response to this data, Kwak[364] and Kobayashi[365] initially suggested irreversible small molecules to possibly serve as an effective strategy to sustain potency and overcome gefitinib/erlotinib-resistant EGFR mutants.

Afatinib

BIBW2992 (Afatinib), was approved in 2013 for late-stage $EGFR^{L858R+}$/$EGFR^{19del+}$ NSCLC (Fig. 57 and Table 20). In addition to the anilinoquinazoline core scaffold, it contains an acrylamide warhead and functions as an ATP-competitive inhibitor targeting Cys797, Cys805, and Cys803 of EGFR, HER2, and HER4, respectively (*via* a Michael addition mechanism). Relative to 1st generation inhibitors, whilst afatinib is equipotent against both $EGFR^{WT}$ and $EGFR^{L858R}$ (IC_{50} ~ 0.5 nM), the unique binding mechanism and electrophilicity of this CKI allows for sustained potency against the typically resistant $EGFR^{L858R/T790M}$ (IC_{50} = 10 nM). It is worth noting, *in vitro* binding assays revealed impressive affinities (K_d = 0.2–1.0 nM) against several other recurring mutants as well (*e.g.* L861Q, A750P, P753S), which elegantly demonstrates the tolerance of covalent ligands towards commonly detrimental point mutations.[366]

In a large-scale screening initiative against a panel of 440 human kinases (~82% of the kinome), afatinib exhibited an IC_{50} < 10 nM against only 3 proteins (EGFR, HER2, and HER4). This remarkable selectivity was further validated in cellular and *in vivo* antitumor studies and in all cases, afatinib was several-fold more active than clinical standards (*e.g.* gefitinib).[366]

Slow EGFR protein re-synthesis ($t_{1/2}$ = 8–24 h) coupled with the prolonged and selective potency of afatinib allowed for comparably small doses in preclinical models (20 mg kg^{-1}, P.O.), translating into a daily dose of 40–50 mg in a phase I trial. Note, the non-covalent gefitinib typically requires a much higher dose (250 mg) to achieve similar efficacy.[367]

In phase III trials (LUX-lung 3 and LUX-lung 6) on patients with $EGFR^{+}$ advanced lung adenocarcinomas and NSCLC, afatinib nearly doubled progression-free survival (PFS) compared to standard chemotherapy (*i.e.* cis-platin, pemetrexed/gemcitabine) with an acceptable safety profile.[368] In a more recent head-to-head clinical trial (LUX-lung 7) against gefitinib, afatinib was unable to improve overall survival (OS) while it achieved slightly improved PFS.[369] Nonetheless, this compound clearly demonstrated the clinical utility of CKIs and remains a milestone in kinase-targeting covalent therapies.

Neratinib

Expanding on the afatinib discovery program, a second EGFR inhibitor, HKI-272 (Neratinib) was approved in 2017 as an adjuvant therapy for early-stage $HER2^{+}$ breast cancer.[370] First reported by Rabindran *et al.*[371] in 2004 as a pan-ErbB inhibitor, it represents one of the earliest kinase-targeting covalent scaffolds with preclinical efficacy. It was rationally designed as a 3-cyanoanilinoquinoline with an optimally positioned acrylamide warhead targeting HER2 Cys805 (structurally derived from previous EGFR inhibitor EKB-569). The lipophilic 2-pyridynylmethyl motif was proposed to occupy a HER2-specific hydrophobic channel, driving potency and selectivity. Another important structural motif is the positioning of a substituted basic amine (*e.g.* dimethylamine, piperidine, *etc.*) neighbouring the electrophilic warhead. This is commonly seen in 2nd generation EGFR inhibitors (*e.g.* afatinib). While steric bulk at the β-carbon may hinder nucleophiles, early binding models and acrylamide reactivity studies have suggested the addition of a basic group at this position can accelerate enzyme inactivation (k_{inact}), facilitating thiolate formation and improving cysteine reactivity.[371] As a polar group, the amine can also play a pharmacokinetic role by enhancing aqueous solubility. Relative to afatinib, albeit a less potent inhibitor, neratinib

displayed good *in vitro* activity against HER2 (IC_{50} = 59 nM) as well as in $HER2^+$ breast cancer cell lines and xenografts tumour models. While it is inactive in cells with low HER2 expression (*e.g.* MCF-7), this inhibitor is generally more promiscuous in the context of the human kinome. A recently published 5 year follow up of a phase III trial (ExteNET) confirmed the clinical efficacy of neratinib.[372] Neratinib treatments consistently resulted in improved outcomes in invasive disease free survival (iDFS) compared to placebo. More recent studies have suggested ErbB inhibitors able to pass through the BBB can be very useful in mitigating CNS-metastasis in $HER2^+$ breast cancer (typically seen in 30–50% of patients).[373]

While afatinib and neratinib remain efficacious therapy options, clinical challenges and acquired resistance mechanisms have recently been reported. Examples include the identification of a neratinib-resistant HER2 gatekeeper mutation (T798I)[374] and the failure of afatinib to overcome $EGFR^{T790M+}$ NSCLC at clinically relevant dosages due to dose-limiting toxicities.

Osimertinib

Partly in response to these reports, a 3rd generation of EGFR inhibitors began development (*e.g.* avitinib, naquotinib). The first approval was achieved by AZD-9291 (Osimertinib) in 2017, for advanced $EGFR^{T790M+}$ NSCLC.[370] This compound has selectivity for the T790M EGFR mutant and weak activity against $EGFR^{WT}$. Osimertinib is particularly special, as it elegantly shows how an adaptive and collaborative approach in industry can accelerate drug discovery. After identifying the need for $EGFR^{T790M}$ selective therapeutics, in only 36 months, a drug candidate with clinical efficacy was generated.[375] Relative to previous scaffolds, as a monoanilinopyrimidine, osimertinib retains the reactive acrylamide and the neighbouring basic amine. Computational modelling of afatinib against $EGFR^{T790M}$ revealed an unfavourable steric clash between M790 and the bulky 3-chloro-4-fluoroaniline moiety, suggesting a possible explanation for the observed loss in potency. Osimertinib effectively escapes this unwanted interaction, achieving complete receptor occupancy with undiminished potency.[360] In addition to the steric hypothesis, studies by Yun *et al.* propose that T790M confers resistance by improving the binding affinity of kinase to ATP.[376]

Osimertinib is $\sim$200-fold more active against $EGFR^{T790M}$ relative to $EGFR^{WT}$. This selectivity in addition to cellular potency, acceptable pharmacokinetics (P.O. $t_{1/2}$ $\sim$3 h) and extended efficacy in preclinical models of $EGFR^{T790M}$ tumours allowed rapidly progression into clinical trials.[377] Although FDA-approved, it remains actively enrolled in $>$10 trials (phase I, II, III) whether as a mono/co- or adjuvant therapeutic for variations of $EGFR^+$ NSCLC. In a recently reported phase III trial (AURA3), using a daily dose of 80 mgs, osimertinib was found to be significantly superior against advanced NSCLC, extending PFS by $\sim$6 months with minimal adverse side-effects relative to clinical standards (platinum/pemetrexed).[378]

While considered a clinical success, the powerful selective pressure applied by osimertinib on genetically unstable oncogenes makes acquired resistance inevitable. Several resistance mechanisms have already been characterized (as early as during phase I), with examples including resistant point mutations (*e.g.* C797S, L718Q) and amplification of HER2/cMET signaling.[379] The C797S mutation is particularly detrimental, considering the importance of Cys797 for the mechanistic functioning of all covalent EGFR inhibitors. The less nucleophilic Ser797 residue is unable to irreversibly bind osimertinib at physiological conditions. Extensive medicinal chemistry efforts are currently ongoing to develop 4th generation inhibitors, which overcome osimertinib resistance. Thiazole EAI045 was recently published as the first non-covalent, non-ATP competitive, allosteric EGFR inhibitor, which retains activity against the $EGFR^{L858R/T790M/C797S}$ triple-mutant protein in the monomer state.[361] Günther *et al.* has also reported reversible trisubstituted pyridynylimidazoles as novel C797S active inhibitors.[380]

Dacomitinib

The most recent approval was given in 2018 to 2nd generation EGFR inhibitor, PF-00299804 (Dacomitinib) from Pfizer as an oral first-line therapeutic for $EGFR^{L858R+}$/$EGFR^{19del+}$ metastatic NSCLC,[381] similar to afatinib. Although structurally related, dacomitinib does contain a unique piperidine moiety. It is an irreversible cysteine targeting pan-EGFR inhibitor, with *in vitro* IC_{50} values of 6.0, 45.7 and 73.7 nM against EGFR, HER2 and HER4, respectively.[382] While more efficacious CKIs have since been reported (*e.g.* osimertinib), during development, dacomitinib (at 45 mg kg^{-1}) was the first covalent inhibitor to show a significant improvement in both PFS (14.7 *vs.* 9.2 months) and OS (31.4 *vs.* 28.0 months) against 1st generation EGFR inhibitors (*e.g.* gefitinib, 250 mg kg^{-1}) in therapy naïve patients (ARCHER 1050 trial).[383] However, while most EGFR inhibitors in the clinic report a degree of toxicity, dacomitinib is especially linked to high-grade adverse effects (typically gastrointestinal) and the need for dose-reductions was observed in higher-than average frequencies. This has been suggested to be partly due to the irreversible non-selective inhibition of several ErbB isoforms. Other limitations of dacomitinib involve the lack of data surrounding CNS potency and BBB penetrance, which are relevant parameters in metastatic breast cancer and NSCLC.[384]

Bruton's tyrosine kinase (BTK)

B-cell receptor signalling regulates multiple cellular processes crucial for normal B-cell growth and survival. Notably, clinical evidence has implicated this pathway in the pathogenesis of several B-cell malignancies, including Diffuse Large B-cell Lymphoma (DLBCL), Mantle-cell Lymphoma (MCL) and B-cell Chronic Lymphocytic Leukaemia (CLL). This has generated a significant interest in designing inhibitors targeting kinases within this signalling cascade, particularly the upstream target BTK.[385] Bruton's agammaglobulinemia tyrosine kinase (BTK) is a non-receptor cytoplasmic tyrosine kinase belonging to the TEC family of kinases. It is comprised of five domains including the PH, TH, SH1, SH2, SH3 domains, each of which has the potential to interact with various proteins involved in signal transduction. BTK expression is mainly localized to

B-cell lineage lymphoid cells where it signals downstream of BCR and regulates a myriad of processes such as survival, activation, proliferation, differentiation and maturation of B-cells. BTK activation after engagement of BCR is a multi-step process which begins with the generation of phosphatidylinositol (3,4,5)-triphosphate (PIP_3) on the inner leaflet of the membrane by PI3K, providing a docking site for the PH domain of BTK.[386] Subsequent translocation of BTK to the membrane results in the phosphorylation of Tyr551 by Syk and Lyn kinases in addition to autophosphorylation of Tyr223 resulting in the induction of multiple critical signalling pathways including STAT5, PI3K/Akt/mTOR, PLCγ2 and NF-κB.[387–389]

Dysregulation of these pathways has implicated BTK activity in a variety of B-cell malignancies and autoimmune disorders. In humans, mutations of the BTK gene results in X-linked agammaglobulinemia (XLA), a disease characterized by low counts of B lymphocytes and immunoglobulins as well as recurring infections.[390] This primary phenotypic defect demonstrates the exclusive role of BTK in B-cell development and immunoglobin production, suggesting it may be a useful therapeutic target in treating immunological disorders.[391] Additionally, several studies have suggested a direct relationship between BTK activity and the development of malignancy. Inhibition of BTK in CLL prevents NFκB DNA binding, which induces apoptosis, reduces cell proliferation and diminishes cellular responses to tissue chemokines (*e.g.* CXCL12, CXCL13, CCL19).[392–395] In MCL cells, siRNA mediated knockdown of BTK significantly decreases pYSTAT3 levels thereby inhibiting the NFκB pathway, both of which are essential for MCL growth and cellular migration.[396]

In 1999, the first BTK small molecule inhibitor (LFM-A13) displayed anti-leukemic activity *in vitro* (IC_{50} = 17 μM) (Fig. 58).[397] More selective inhibitors have since been developed with an extensive focus on irreversible covalent inhibitors, due to the presence of a poorly conserved Cys481 in the ATP binding site. This covalent strategy has led to the development of the first FDA approved BTK inhibitor, ibrutinib. More recently, a 2nd generation inhibitor acalabrutinib, was approved in 2017 for the treatment of CLL (Fig. 59). Interest in a BTK inhibition remains high, with 6 other BTK CKIs actively in varying stages of clinical trials for several therapeutic indications.

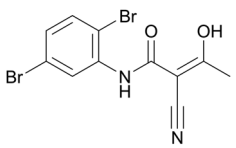

LFM-A13

Fig. 58 Structure of first BTK small molecule inhibitor LFM-A13.

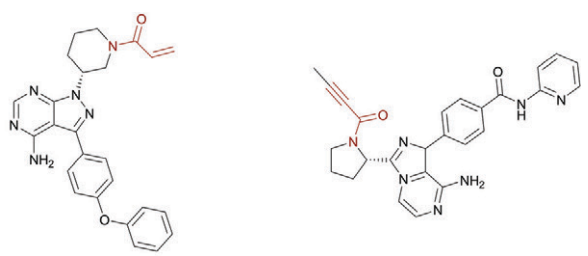

Ibrutinib (Imbruvica®)
Celera/Pharmacyclics/Johnson & Johnson

Acalabrutinib (Calquence®)
Acerta/AstraZeneca

Fig. 59 Chemical structure of FDA-approved BTK inhibitors. Electrophilic warheads are highlighted.

Ibrutinib

PCI-32765 (ibrutinib) was first approved for the treatment of MCL in 2013, becoming the first BTK inhibitor to receive FDA approval (Table 21). Initially developed by Pharmacyclics, it is a potent (IC_{50} = 0.5 nM) orally bioavailable CKI which irreversibly modifies Cys481 in the active site of BTK with the use of an acrylamide electrophile.[398] Despite BTK potency, ibrutinib does have significant activity (IC_{50} < 100 nM) against 19 other kinases, 7 of which contain an equivalently positioned cysteine reactive (BMX, BLK, ITK, TEC, EGFR, HER2, and JAK3). Nevertheless, in the DOHH2 B-cell lymphoma cell line, a fluorescently tagged derivative of ibrutinib bound exclusively to BTK, requiring only 10 nM to achieve complete target occupancy. *In vitro* studies demonstrated its ability to block BTK phosphorylation to inhibit signalling downstream of BCR. Subsequent preclinical *in vivo* studies inhibited disease progression in a collagen-induced arthritis model, which induced objective clinical responses in canines with spontaneous non-Hodgkin lymphoma (NHL).[399]

In the initial phase I trials, an objective response rate (ORR) of 60% was achieved in 50 patients with refractory Follicular lymphoma (FL), CLL, MCL, Marginal Zone Lymphoma (MZL), DLBCL and Waldenström Macroglobulinemia (WM) at relatively small doses of 1.5–12.5 mg kg^{-1}.[400] Compared to clinical standards, ibrutinib demonstrated superior responses in PFS with minimal toxicities in phase II and III trials.[401] Specifically, in the RESONATE-17 phase II trial, heavily pre-treated patients (n = 144) with CLL demonstrated high OS and PFS rates with ibrutinib after a median follow-up of 27.6 months.[402] Consistent with this data, a comparative phase III trial between the FDA approved mono-clonal antibody ofatumumab and ibrutinib established the superiority of the CKI with respect to ORR and OS. In particular, greatest response was observed amongst patients with relapsed CLL, including those who poorly responded to previous treatment regiments.[403] The efficacy of ibrutinib as a single therapeutic agent has led to exploration of

Table 21 Biochemical, cellular and pharmacokinetic parameters of FDA-approved BTK inhibitors

TCI	Nucleophile	BTK IC_{50} (nM)	$t_{1/2}$ (h)	K_i (nM)	k_{inact} (ms^{-1})	k_{inact}/K_i (μM^{-1} s^{-1})	Dose (mg)	T_{max} (h)	Route	F (%)
Ibrutinib	C481	0.5	4–6	54.2	2.7	0.050	140	0.5	P.O.	4–20
Acalabrutinib	C481	5.1	5.5	181	5.6	0.031	100	0.75	P.O.	25

synergistic combinations, particularly as a combination therapy in refractory CNS lymphoma.[404] To date it has been approved for 5 other indications (other than MCL), which include CLL, WM, small lymphocytic lymphoma (SLL), MZL and chronic graft *versus* host disease.

Overall, the clinical data validates BTK as an excellent target for B-cell lymphomas, and ibrutinib treatment as an efficacious therapeutic strategy for CLL. Despite this, toxicities (albeit limited), are higher than standard treatments such ofatumumab or chlorambucil, with ~5% of clinical patients experiencing bleeding and atrial fibrillation.

These symptoms have been associated with non-specific covalent modification of other homologous cysteine-containing kinases and non-covalent binding to off-target proteins (*e.g.* modifying Src Tyr418 and its subsequent implication in bleeding).[405] Irreversible binding to EGFR, TEC, ITK, and T-cell X Chromosome Kinase (TXK) may also be related to adverse toxicities such as rash, diarrhoea and arthralgias.[401,403,406] In addition, several resistance mechanisms have emerged including the C481S mutation which blocks covalent binding resulting in significant loss of potency (>1000 nM) and acquired resistance in MCL and CLL patients.[407] Such reports along with the undesired effect of off-targets have prompted the development of a 2nd generation of inhibitors which are more selective towards BTK to circumvent these clinical challenges.

Acalabrutinib

ACP-196 (Acalabrutinib) is a second generation irreversible BTK inhibitor which was recently granted accelerated approval in 2017 for MCL in pre-treated patients. Compared to first-in-class ibrutinib, acalabrutinib exhibits improved pharmacological features including enhanced plasma exposure, rapid oral absorption, and better selectivity with reduced off-target effects. It possesses a unique, relatively inert 2-butynamide electrophile, which is proposed to be activated by the relative positioning to the electron-withdrawing imidazopyrazine core.

In a GSH assay, acalabrutinib demonstrated reduced reactivity relative to the acrylamide in ibrutinib and spebrutinib (currently in clinical trials). This tempered electrophilicity is hypothesized to play a key role in reducing the inhibition of cysteine containing off-target kinases and subsequent toxicities. A more extensive comparative study between the two approved BTK CKIs carried out by Patel *et al.* demonstrated similar biological and molecular consequences in primary CLL cells, but different effects in T-lymphocytes. This was proposed to be due to inhibition of LCK and SRC phosphorylation by ibrutinib, an effect not observed with acalabrutinib at clinically relevant doses.[408]

In healthy humans, complete BTK occupancy was observed as early as 3 and as late as 12 h following a single 100 mg dose. Such saturating concentrations result in near complete inhibition of BCR-induced functional responses (as measured by CD69 expression).[409] A later study in patients with relapsed CLL (n = 60), including those with del(17p) achieved an impressive ORR of 95%. Moreover, the report demonstrated toxicities typically associated with ibrutinib (*e.g.* atrial fibrillation, bleeding) were not observed in patients with relapsed/refractory CLL when treated with acalabrutinib, even after a 14 month follow-up.[406]

Both BTK inhibitors discussed thus far have been approved for the treatment of non-immunological disorders. There are, however, several inhibitors currently being assessed in both oncological and autoimmune diseases including HM71224 (olmutinib), spebrutinib, evobrutinib, PRN1008, BMS-986195, and BIIB068, all of which are reversibly covalent or irreversible inhibitors of BTK (Fig. 60).[410–415] Aside from BMS-986195, these molecules utilize an acrylamide warhead, with most exhibiting equivalent potency to ibrutinib with enhanced selectivity.

The widespread clinical success of covalent BTK and EGFR inhibitors has strongly catalysed the in-depth exploration of covalent inhibitors in recent years as viable therapeutic strategies against additional kinase targets. Generally, with the rapid advancements in chemical biology, target identification, small-molecule design and the ever-evolving understanding of electrophilic reactivity, recent endeavours have been typically focused around the rational tuning of warhead reactivity whilst maintaining adequate potency and overarching efficacy.

General perspective & trend analysis

A detailed analysis of the molecules presented within this review has revealed various trends in the recent development of electrophilic warheads and CKIs (Fig. 61).

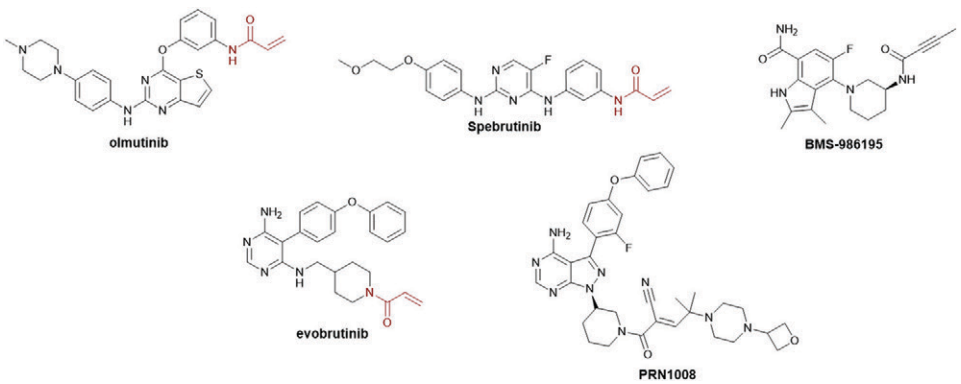

Fig. 60 Structures of current BTK inhibitors in clinical trials. The structure of BIIB068 has been omitted as it has not been disclosed.

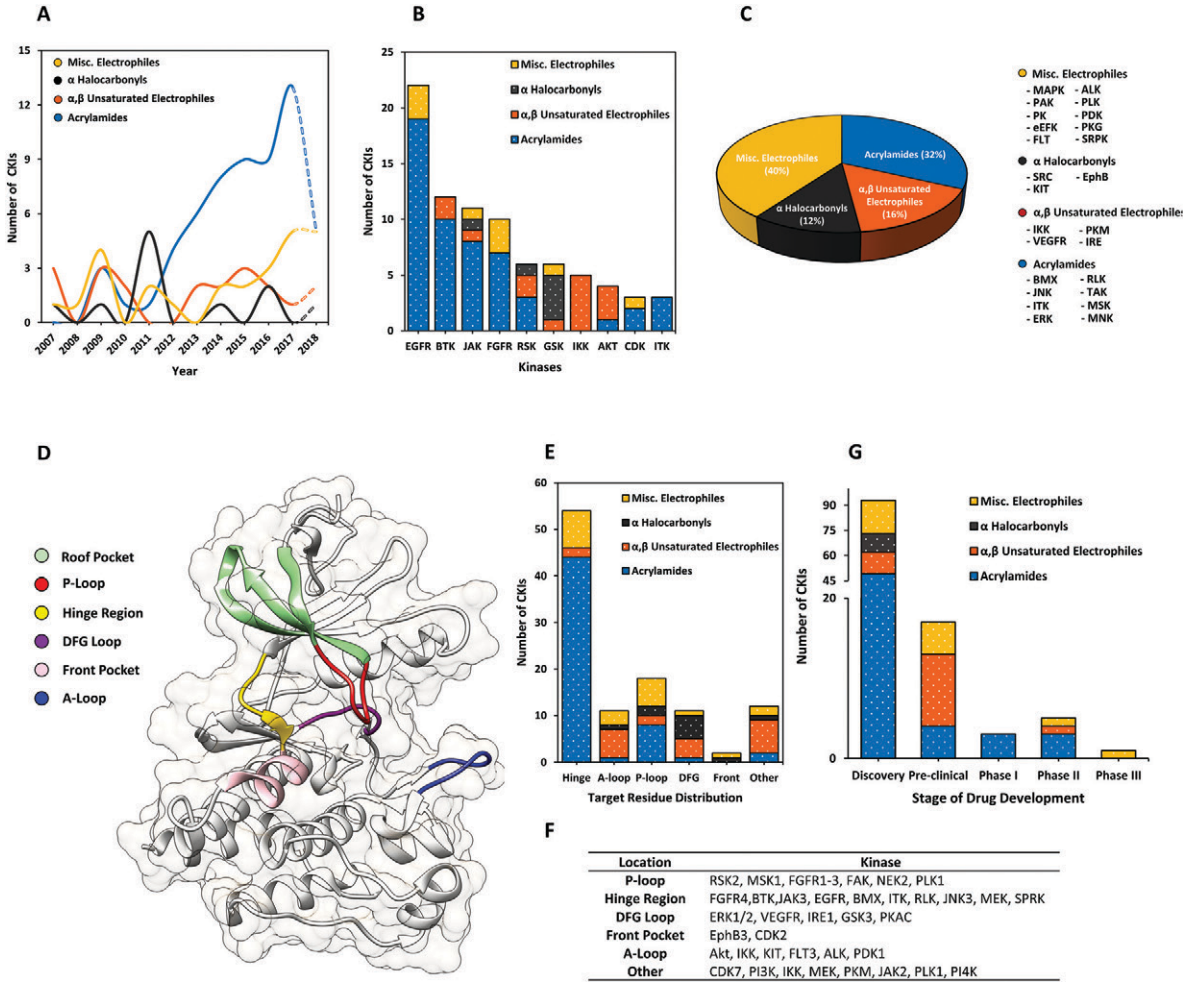

Fig. 61 (A) Variance in electrophilic warheads reported in literature within CKIs between 2007–2018. (B) The top 10 kinases targeted by CKIs while listing the types of warheads utilized to drug them. (C) Pie-chart displaying the kinases reported in literature targeted by only one type of electrophile family. (D) Ribbon diagram describing the main regions in and around the ATP binding site of a prototypical kinase. (E) Number of CKIs modifying residues within different regions of a kinase ATP binding site. (F) List of kinases and the corresponding location in which the targeted nucleophilic residue resides. Kinases mentioned twice are targeted at >1 residue in different locations. (G) Number of CKIs in literature and current stage of development (compiled as of late 2018).

First, to gain an understanding of the physicochemical landscape of CKIs in the last 10 years, seven structural parameters (molecular weight, LogP, H-bond donors, H-bond acceptors, rotatable bonds, polar surface area and stereocenters) were computed for 117 CKIs listed within this review. The mean physicochemical properties can be seen in Table 22 below. Values were also computed for the 6 FDA-approved CKIs for comparative purposes.

Table 22 Mean physicochemical properties of reported CKIs (N = 117) and FDA-approved CKIs (N = 6)

Physicochemical properties	Reported CKIs	FDA-approved CKIs
Molecular weight (g mol^{-1})	432.17	486.43
$A\log P$	3.58	4.04
Hydrogen bond donors	1.85	1.83
Hydrogen bond acceptors	4.39	4.83
Rotatable bonds	6.04	7.5
Polar surface area (Å^2)	99.88	97.68
Chiral centers	0.80	0.5

In terms of the first four properties, the inhibitors appear on average, to abide by the commonly pursued Lipinski Rule-of-5 for orally bioavailable therapies, though several exceptions exist.[247] The compounds also exhibit a relatively high degree of structural flexibility (~6.04 rotatable bonds). While this may affect stability, membrane permeability and raise the entropic penalty upon binding, it can also improve tolerance (relative to rigid scaffolds) against sterically clashing point mutations and subsequent resistance.

Moreover, the compounds have good polar surface area (PSA), given recommended values for BBB and cell permeability are PSAs less than 90 and 140 Å^2, respectively.[416,417] Several CKI discovery programs have demonstrated the benefit of chiral centres in the appropriate positioning of electrophiles,[418] notably seen in afatinib, ibrutinib and acalabrutinib, with the average CKIs in literature possessing ~1 chiral centre. Comparatively, while the properties of FDA-approved scaffolds were quite similar, they remain slightly heavier, with a small increase in hydrophobicity ($A\log P$ = 4.0) and more degrees of freedom (~7.5 rotatable bonds).

Note, when designing covalent leads and considering key structural characteristics (*i.e.* central-core, functional groups, *etc.*) it is important to consider PAINs scaffolds. For example, curcumins (compounds **75**, **84**) and thiazolidinediones (compound **88**) have been widely characterized as PAINs molecules by Baell *et al.*[419,420] If neglected, these false-positives may lead to unpredictable pharmacology in a complex cellular environment, hampering the chances of developing a successful clinical lead.

To analyse the landscape of electrophiles within CKIs in recent literature, Fig. 61A displays the variance in the number of warheads reported between 2007–2018 from the following categories: acrylamides, α-halocarbonyls, α,β-unsaturated structures and miscellaneous electrophiles. From this data, the adoption of acrylamide starts in 2011, where the more reactive α-halocarbonyl derivatives were the more common electrophile of choice. Over the past few years, there has been an increased use of alternative miscellaneous electrophiles (*e.g.* propynamides, vinyl sulfones). This recent surge is possibly due to pursuits of novelty, targeting non-cysteine nucleophiles or other less reactive residues requiring more electrophilic warheads relative to the tempered acrylamide. While α,β-unsaturated structures and α-halocarbonyls were commonly used, the recent scarcity of these scaffolds is likely due to their greater electrophilicity. Regardless of the general trend observed above, the choice of an optimal electrophile (*i.e.* size, reactivity, nucleophile specificity, *etc.*) is highly dependent on the choice of target and specific goals of the research program.

Next, Fig. 61B describes the number of reported CKIs per kinase class (displaying the top 10 entries). From this analysis, it is seen that irrespective of isoform specificity, EGFR is the most frequently targeted enzyme, followed by BTK, JAK and FGFR kinases. This is not unsurprising considering the extensive interest in EGFR kinases by academia and industry as well as the amount of available data (*e.g.* structural, biological, cellular). Also, EGFR inhibitors have been already validated as viable medicinal agents for many years since the initial success of afatinib. As for covalent warheads, the versatility and broad applicability of the acrylamide electrophile is very evident; of the top 10 kinases which have been heavily targeted, $>60\%$ utilize this motif.

Conversely, as seen in Fig. 61C certain kinases have been solely targeted by one class of warhead. For instance, of the 25 structures shown, SRC, KIT and EphB kinases have only been successfully modified by α-halocarbonyls, while IKK, PKM, IRE and VEGFRs only *via* α,β-unsaturated electrophiles.

More detailed studies would be needed to explain such patterns (whether in terms of electrophile reactivity, target residue nucleophilicity or accessibility, *etc.*).

To assess the spatial distribution of targeted nucleophilic residues, we segmented the active conformation of the kinase catalytic domain into several known regions in or around the ATP binding site: the hinge region, front pocket, A-loop, P-loop and DFG-loop (Fig. 61D–F). Remote residues in allosteric regions or outside of the ATP binding pocket were grouped separately as ''other''. More than 50% of all covalent inhibitors discussed and detailed mechanistically in this review target a residue located within the kinase hinge region, potentially due to greater conformational flexibility and improved residue accessibility within this sub-pocket. Modification of the hinge region residues is dominated by inhibitors targeting EGFR, ITK, BTK, JAK3, along with several members of an 11-kinase subfamily. Interestingly, all these members share an equivalently positioned cysteine residue. Thus, while this region appears highly druggable, selectivity may prove challenging given the conserved nature of hinge cysteines, especially if single isoform selectivity is desired. While targeting poorly conserved residues outside of the hinge region is scarce, it has proven advantageous in providing an added selectivity filter. For example, CDK7 inhibitor **55** (with an acrylamide warhead) utilizes a remote non-catalytic cysteine to confer a high degree of selectivity amongst structurally homologous kinases.[205] Several FDA approved EGFR inhibitors enhance the target cysteine nucleophilicity by substituting the acrylamide with proximal basic amines (*e.g.* dimethylamino, piperidine, morpholine, *etc.*),[360,371] reducing the pK_a of thiol nucleophiles, enhancing reactivity and accelerating covalent bond formation.

To visualize the clinical scope of CKIs in relation to the type of electrophile, the listed compounds were categorized within the various stages of drug development (as of late 2018, described in Fig. 61G). Firstly, the large number of CKIs in the discovery phase nicely depicts the recent resurgence of this class of inhibitors and the broad interest in the covalent approach. Second, the presence of compounds in all three phases of clinical trials demonstrates the ongoing and increasing interest in exploring the clinical potential of CKIs.

It is evident, the acrylamides remain the 'workhorse' clinical electrophile and, to the best of our knowledge, all α-halocarbonyl-containing compounds remain investigational, with no reported preclinical studies, likely due to the reactivity of these electrophiles and the potential for IDTs.

The prevalence of acrylamides is largely attributed to a good balance between electrophilicity, target nucleophile selectivity and metabolic stability.[83] Relative to other warheads, acrylamides are inherently less reactive and more cysteine selective (although known to react with histidine and lysine),[421] which is thought to reduce off-targets. They react less readily with cellular nucleophiles (*e.g.* GSH), improving drug plasma concentrations and sustaining efficacy. Acrylamides are one of the most widely studied electrophiles, with a surplus of knowledge regarding their mechanism of action and activity in varying environments (*in vitro*, *in cellulo*, and *in vivo*). On the other hand, challenges with this motif generally involve achieving structural novelty and selective targeting of non-cysteine nucleophiles.

When considering the entire human kinome, 38 different enzymes have been covalently targeted ($\sim$6.1%, assuming a total value of 625 kinases), as illustrated in Fig. 62. Interestingly, the reported CKIs span a broad range of enzymes across the phylogenetic tree. Tyrosine kinases (TKs) are the most heavily targeted, with at least one member in each family reported to undergo covalent modification except for CK1s, GYCs and CAMKs.

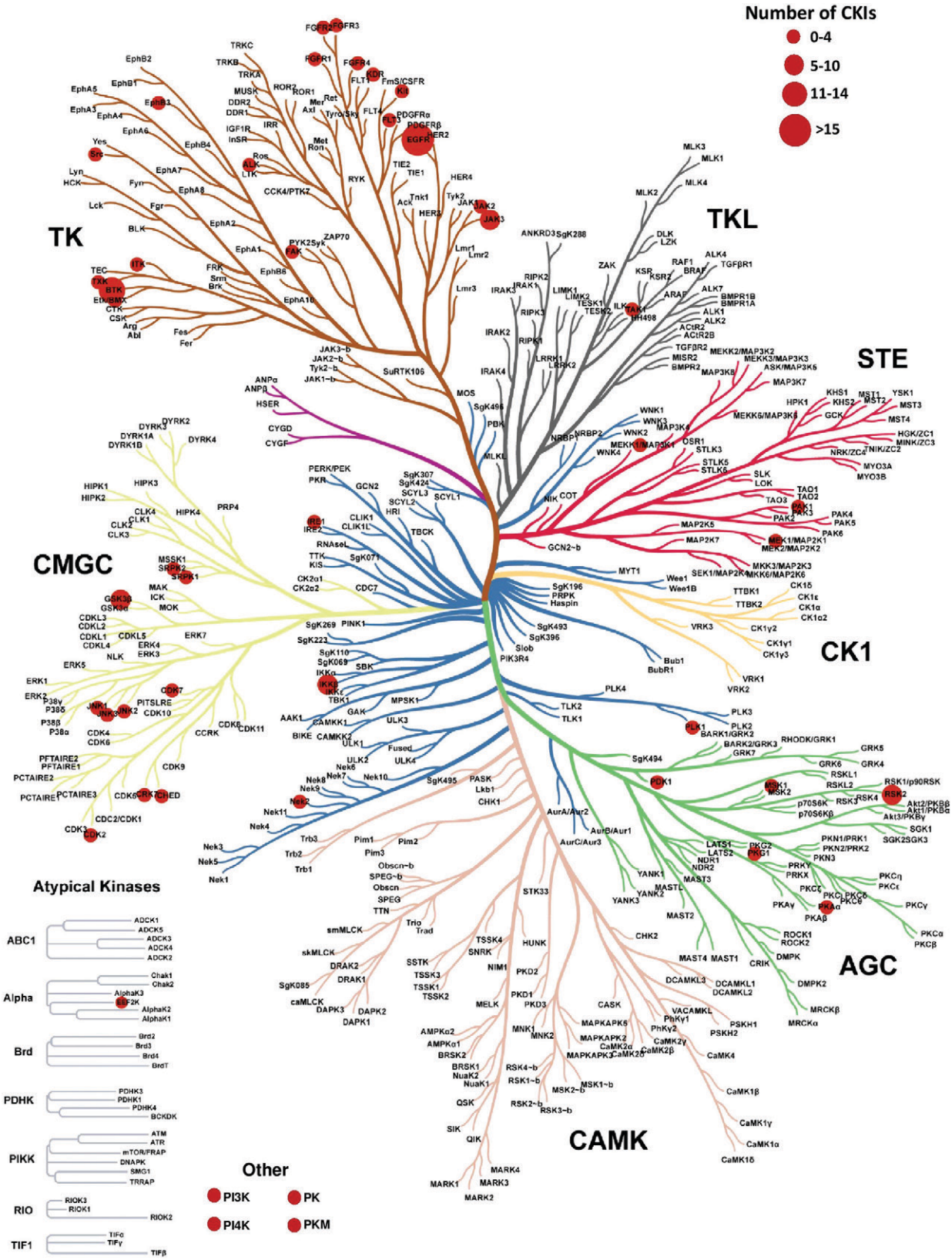

Fig. 62 Phylogenetic tree of the human kinome displaying the distribution of kinases covalently targeted between 2007–2018.

Also, while certain isoforms have recently garnered more interest as therapeutic targets, there continues to exist many potentially druggable kinases, which remain understudied and minimally explored by small molecule covalent modulation.

Covalent inhibitors are characterized by having superior potency, extended, or irreversible target inactivation, and high isoform selectivity. Beyond their clinical value, these qualities can be useful in the broader context of chemical biology. Briefly, covalent-based molecular probes can have various applications such as the study of cell or molecular biology following target inactivation (similar to methods such as; siRNA knockdown or PROTAC approaches that rely on proteolytic degradation targeting usually *via* E3 ubiquitin ligase linker probes). Recently, work by Nijmeijer *et al.* utilized vinylic pyrimidine probes (Michael acceptor electrophiles) as reversibly covalent agonists to study the function of GPCR proteins (specifically the Histamine H4 receptor).[422]

Other uses involve the versatile technique of ABPP (*e.g.* fluorophosphonates, iodoacematide), which has seen innumerable applications since the initial pioneering work by Lui *et al.* and the Cravatt group on profiling the cellular activity of serine hydrolases.[423] While certain probes are rationally designed, others are commonly derived from lead molecules which fail as drug candidates due to poor AMDET or clinical efficacy. For a more detailed discussion on the recent advances and benefits of covalent molecular probes, please see the following ref. 424–426.

In general, *in vitro* analysis of covalently binding ligands requires special considerations given the time-dependent and irreversible or long-lived nature of their target engagement. While any individual technique may be misleading, an appropriate combination of several biophysical and mechanistic studies can accurately identify pharmacologically relevant covalent scaffolds. As seen in Table 23 various methods have been used to characterize CKIs with varying degrees of throughput. For example, the IC_{50} biochemical assay provides evidence of ligand ability to inhibit enzyme activity in a high-throughput manner.[427] Proteomic approaches such as ABPP have emerged as a powerful tool to evaluate covalent interactions and interrogate target engagement more directly.[118,428] Additionally, site-directed mutagenesis studies on target nucleophiles (*e.g.* cysteine to alanine) and the use of non-electrophilic derivatives can provide further insight into the covalent mechanism of action. However, such techniques are low-throughput and they are typically reserved for later stage candidates. Ideally, strategies are coupled with MS studies to confirm the formation of covalent adducts inhibition (whether reversible or irreversible).

In a recent analysis by Abbvie, the merits and pitfalls associated with the various modes of CKI validation are discussed in the context of BTK inhibitors.[429] It can be concluded from such reports that a combination of approaches is necessary to address the time-dependent, covalent nature of CKIs in a manner suitable for the accurate and reliable generation of useful covalent scaffolds.

Despite obvious limitations, the biochemical and cellular IC_{50} assay continues to be one of the most common tools to characterize CKI potency. However, thermodynamic principles governing IC_{50} render this assay highly dependent on enzyme concentration, with the lowest possible measurable IC_{50} being half the total target protein concentration.

As such, reliance on single-time point IC_{50} values does not consider the time-dependent nature of covalent interactions that arises from varying reactivities of the electrophilic warheads. Hence it may lead to certain scaffolds being overlooked in SAR studies.[12] More recently, medicinal chemists have introduced the notion of time-dependent IC_{50} to circumvent this issue, where several data points are measured at different pre-incubation times with a progressive increase in potency (lower IC_{50}) observed for irreversible binders. Note, it is critical that pre-incubation times and target concentration be carefully controlled if direct comparisons are to be made between structurally distinct scaffolds. Furthermore, the ability to distinguish the most potent molecules may be lost if the assay time is too long as theoretically the IC_{50} of all irreversible inhibitors will approach half the total enzyme concentration if incubated long enough. Nevertheless, the robustness and versatility of this technique allows effective ranking of various molecules with largely differing activities to deduce relative potency trends.[430]

What has received less attention in the last decade is characterization of the kinetics of covalent bond formation. As previously discussed, covalent inhibitors exhibit a two-step binding mechanism that involves an initial non-covalent event (defined by K_i) and a second observed rate of inactivation (k_{inact}). Together, the overall potency of a covalent interaction is defined by the ratio of (k_{inact}/K_i), a second order rate constant.[430] This ratio accounts for both the non-covalent binding component and rate of covalent bond formation. In this way, two covalent inhibitors may have drastically different k_{inact}/K_i ratios while binding the target with equal affinity (similar K_i) if they exhibit varied rates of inactivation

Table 23 Common methods for the characterization of covalent inhibitors. Extended from data within Harris *et al.*[429] with permission from SAGE Journals, copyright 2018

Experiment	Measured parameter	Throughput
Enzymatic activity	IC_{50} Time dependent IC_{50}	High to very high
Substrate competition	Substrate dependence on IC_{50}	High
In vitro drug washout	Reversibility of inhibition	Low
In cellulo drug washout	Reversibility of occupancy Recovery of enzyme activity over time	Low
Mass spectrometry	Stoichiometry and site of modification	Low
Activity progress curve analysis	k_{inact}, K_i (or k_{inact}/K_i)	Low
Enzymatic activity of nucleophilic residue mutant	IC_{50}	Low
Non-reactive inhibitor analog	IC_{50}	High

(different k_{inact}). It is common that more selective inhibitors demonstrate much larger k_{inact}/K_i ratios than non-selective counterparts. Therefore, it is critical that both parameters be carefully quantified and optimized in biochemical or binding assays to adequately evaluate the individual contributions of K_i to the observed potency. Limited examples exist in the literature that utilize k_{inact}/K_i values to drive CKI SARs, which may be largely due to the low-throughput of measuring these values as this tends to be more time-consuming, specialized, and costly. Of the 125 inhibitors addressed in this review only 27 compounds reported k_{inact}/K_i values. Recently, there have been numerous reports of more high-throughput alternatives to measure this ratio, which represent significant improvements over traditional IC_{50} measurements. These approaches typically involve measuring IC_{50} as a function of time, allowing an estimate of $k_{obs}/[I]$ or *via* competitive-binding assays using irreversible molecular probes.[431–434]

To evaluate the individual contributions of k_{inact} and K_i, all available data was compiled to generate the quadrant plot in Fig. 63. While all these inhibitors showed remarkably potent IC_{50} values, the CKIs ($n = 27$) spanned a wide range of K_i values (0.1 to 800 nM), and thus their k_{inact}/K_i ratios were also quite varied. Interestingly, while all the approved EGFR inhibitors occupied (Quadrant III), with potent K_i values (<10 nM) and moderate k_{inact} (<0.005 s^{-1}), the approved BTK compounds had weaker K_i profiles. In such instances, the rapid rate of covalent inactivation may serve as a compensatory for the less potent non-covalent binding component. On the other hand, it may also suggest that EGFR inhibitors require a more potent K_i for adequate drug potency relative to BTK which is consistent with current literature describing the importance of non-covalent binding interactions for EGFR inhibition.[435]

Upon further examination of the FDA approved drugs described in Section 4, it is clear the small molecules share specific structural and mechanistic properties, which have likely contributed to their clinical success. All six compounds are highly potent irreversible inhibitors (K_i = 0.1–100 nM), with weak-to-moderate rates of inactivation (k_{inact} = 0.001–0.005 s^{-1}). All compounds undergo covalent bond formation *via* 1,4-Michael addition reactions and all have relatively acceptable selectivity profiles. Also, they generally inhibit well-studied, slow turn-over kinases (*e.g.* EGFR, BTK), targeting relatively acidic hinge region cysteines (EGFR C797, pK_a = 5.5 and BTK C481, pK_a = 7.7, typical thiol pK_a = 8.3–8.5) using acrylamide electrophiles (except for acalabrutinib, which evokes a butynamide motif). In summary, these orally bioavailable cancer therapies require dosages of 20–140 mg kg^{-1} with adequate therapeutic windows, displaying impressive pharmacodynamics and sufficient pharmacokinetics as prerequisites for clinical success.

The BTK inhibitor acalabrutinib, was the first non-acrylamide containing CKI to receive FDA approval. As such, it has become an excellent example of how rational tuning of an electrophilic warhead *via* structural derivatization and steric bulk can serve to modulate protein family member/kinase selectivity. While structurally similar to ibrutinib, the removal of the terminal acrylamide and inclusion of a more hindered 2-butynamide electrophile reduces covalent reactivity (primarily reducing k_{inact}). This in turn mitigates the off-target reactivity and subsequent toxicity concerns commonly seen with ibrutinib, while sustaining the necessary clinical efficacy against BTK-driven MCL survival protein expression.

In surveying the literature (beyond just kinases), 34 unique electrophiles were identified, each of which was used to modify a distinct set of nucleophilic residues. The results can be seen in Fig. 64. What is evident, while the acrylamide remains the most commonly used electrophile in CKI development, it has only been used to target Cys, Ser and Lys nucleophiles. *N*-Hydroxysuccinimide esters (NHS-esters) appear to be the most widely applicable warhead, reacting with Cys, Lys, Ser, Tyr, Thr and Arg residues. From the context of the residues, all the available nucleophiles have been modified besides Glu. Finally, it is very clear that the common Cys is the most successfully targeted residue.

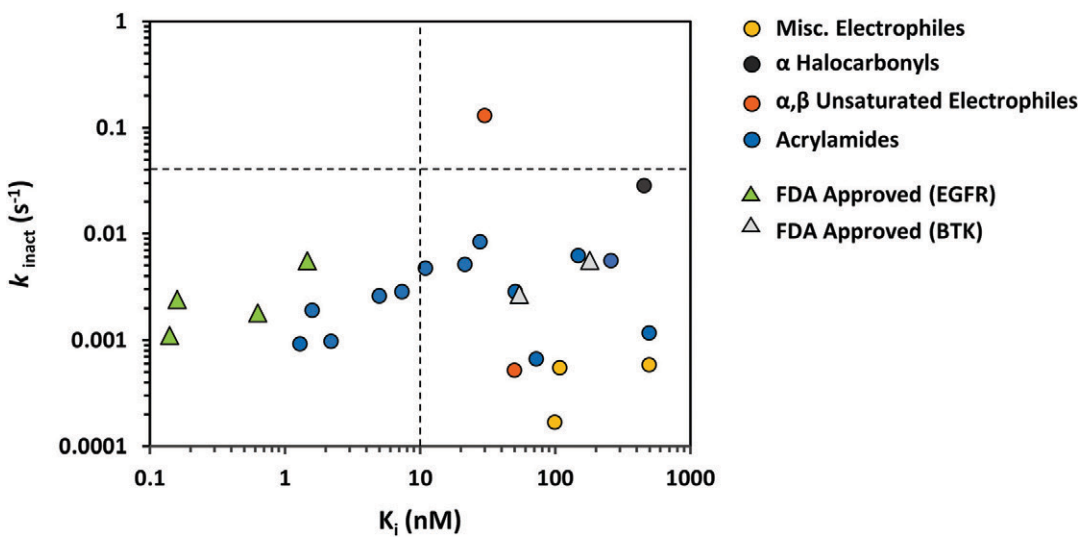

Fig. 63 Quadrant plot depicting all available K_i and k_{inact} values for the various warheads including FDA approved CKIs.

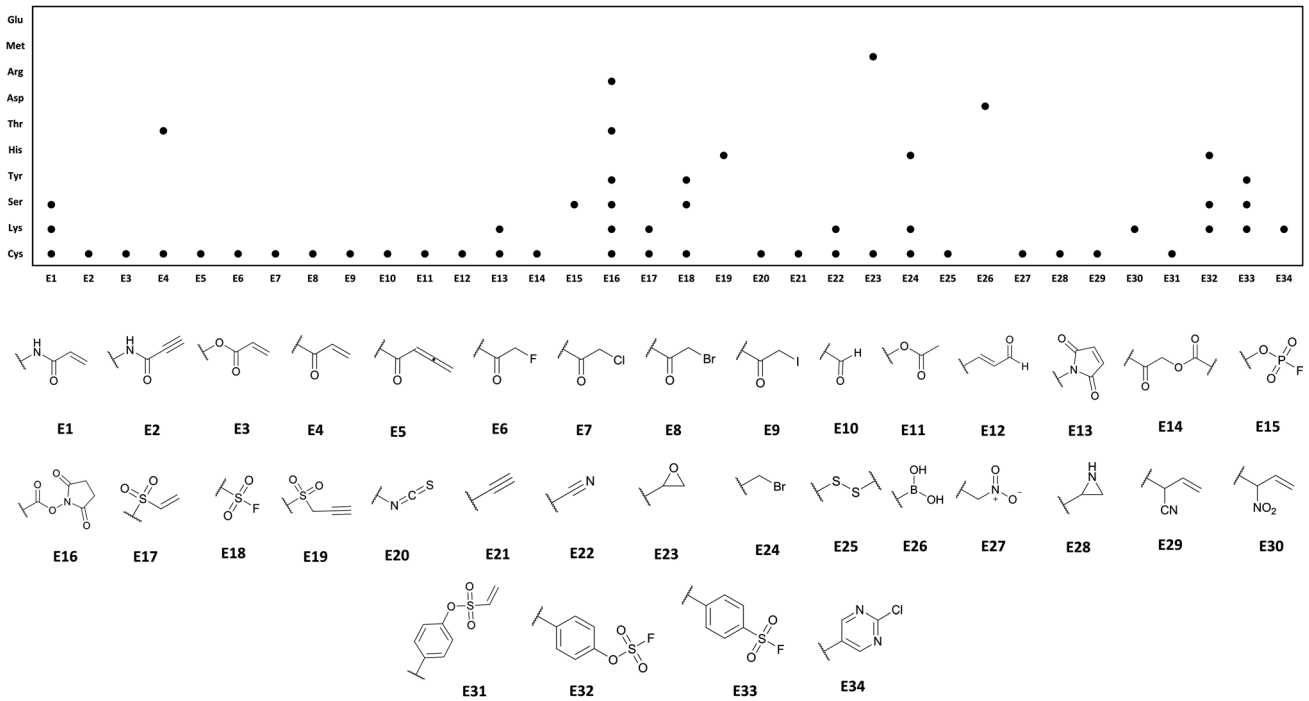

Fig. 64 Survey of reported warheads used within CKIs between 2007–2018 and the nucleophilic residues covalently modified.

A common approach to improve the $\Delta G_{\text{Binding}}$ in drug design, involves scaffold rigidification to lower the entropic penalty of binding. In certain cases, rigidifying molecules can improve membrane permeability and metabolic stability.[436] Competitive kinase inhibitors, such as ATP mimetics, commonly contain an inherently rigid central poly-aryl scaffold (*e.g.* adenines, quinolines, quinazolines, pyrimidines *etc.*). While advantageous and critical to achieving potency along with kinome selectivity, such rigidity can contribute to the poor tolerance against detrimental point mutations. Concurrently, acquired resistance is a complex process with several contributing mechanisms in addition to active site point-mutations (*e.g.* elevated efflux pump expression, metabolic reprogramming, epigenetics). Therefore, while scaffold flexibility or covalent targeting may improve potency against mutant drivers, they are insufficient to fully address this phenomenon. Proposed strategies to combat resistance generally discuss concepts of combinatorial/sequential therapies, personalized medicine or tumour biopsies followed by mutant-selective therapeutics and optimized dosing protocols.[437–439]

Despite their ability to harness a unique interface between irreversible and reversible modes of inhibition, reversible covalent inhibitors remain relatively scarce in the field of CKI drug discovery. This may be due to the notion that irreversible binding is required to fully reap the benefits of covalent modification (*i.e.* extended efficacy, PK-PD decoupling, infrequent dosing, *etc.*). Alternatively, it may result from a limited understanding – until very recently – of how to modulate irreversibility and ligand residence time (τ).

The ability to tune residence time through manipulation of the electronic and steric environment of a warhead was introduced by Taunton and colleagues, who rationally designed novel and tuneable electrophiles that can broadly vary their residence times to affect potency.[440] This approach appears very promising and can be useful in therapeutic settings requiring sustained non-permanent target engagement, but also in applications where rapid detachment is preferred. This provides an additional handle for selectivity not available in conventional irreversible covalent modifiers. Now licensed to Principia Biopharma Inc., the first cyano-acrylamide based inhibitor **24** has now entered clinical trials for Immune Thrombocytopenic Purpura with great interest surrounding its efficacy and performance in the clinic.[413]

Modifying reversibility, ligand residence time (and potency) is often performed to alleviate toxicity and unwanted off-target effects. Often the electrophile of interest may be hyper-reactive or completely unreactive with a specific residue. Therefore, the use of various steric or electronic substituents (*i.e.* EDGs, EWGs) could serve to achieve the desired reactivity. Most of the recent literature on modulating warhead reactivity focus on acrylamides. However, several groups have now reported on the substituent effects of newer warheads including aryl halides and fluorobenzenes.[441–444]

While these warheads have not been applied to CKIs, they represent a unique opportunity to expand the chemical space of electrophiles and they help to develop new covalent modifiers that could potentially be more stable and selective.

Reversible covalent modification also presents a unique opportunity to tackle unexplored kinases and venture into novel chemical space, given that current covalent inhibitor IP is largely saturated with acrylamide bearing heterocyclic scaffolds. The use of reversibility may also extend beyond the

canonical olefin warhead, with the prospect to explore the benefits of new substituted motifs, which could broaden the applicability of CKIs towards many kinases yet to be explored *via* a covalent strategy.

Labour intensive and low throughput GSH reactivity assays continue to be the most commonly utilized tool to evaluate relative reactivities for different warheads. Various computational methods have been developed to predict GSH reactivities using Hammett parameters, quantum mechanical modelling and pK_a predictions.[82,83] These strategies can aid in deducing trends associated with varying substituents and help prioritize compounds for synthesis and further testing. One such computational method, which has yet to be heavily explored in the context of CKIs is known as Matched Molecular Pairs Analysis (MMPA). This technique considers the effect of varying electrophilic warheads on a certain scaffold by analysing structure–activity relationships.[445] This enables the calculation of a warhead correction factor (between compounds containing a similar non-covalent binding component but a different warhead), which can be used to estimate changes in specific parameters (*e.g.* GSH reactivity). However, differing electrophiles may exhibit suboptimal positioning and geometry, which may hinder the identification of more potent and stable compounds. Irrespective of how warhead reactivity is characterized, understanding the electronic and steric role of substituents has repeatedly been shown to be imperative in enablement of covalent inhibitors. In addition, most computational methods do not consider the 3D shape a molecule adopts in an aqueous environment, and the potential steric hinderances which might affect GSH nucleophilic attack at the electrophilic site.

Over the past 10 years, covalent Inhibitors have been rationally designed to encompass several enzyme classes beyond kinases. Serine and cysteine proteases reside at the forefront of such endeavours with several different warheads (outside acrylamides) being utilized. While yet to be explored in the context of kinases, these electrophilic components may serve as a toolbox with the potential to be incorporated into kinase inhibitors to diversify the scope of current CKIs. Additionally, they present unique opportunities to engage nucleophilic residues that are incompatible with traditional warheads (*i.e.* acrylamides). Tuning of their electronic and steric properties may aid in reducing unwanted off-target and cytotoxic effects, thus allowing for rational incorporation into pharmacologically relevant lead compounds.

Conclusions

As master regulators of cell signalling, the aberrant activity of protein kinases has been widely implicated in human disease. An increasing understanding of kinase biology coupled with coinciding developments in structural biology, organic synthesis and drug design have propelled these enzymes to the forefront of therapeutically attractive targets with widespread interest from industry and academia. Since the remarkable success with the initial approval of the anti-leukaemia drug and ABL oncokinase family inhibitor imatinib (Gleevec or STI571), small molecules have been repeatedly validated as a viable strategy to modulate kinase activity *in vivo*. While relatively successful, challenges typically concern themes of kinase selectivity and acquired drug resistance.

Although inhibitors generally engage their targets reversibly, scaffolds which bind covalently forming permanent (irreversible) or long-lived (reversible covalent) adducts offer several unique benefits (*i.e.* prolonged inhibition, sub-nanomolar potencies, PK-PD decoupling and smaller/infrequent doses). These attributes along with advances in protein modification, lead optimization and tuning electrophilic reactivity have catalysed a resurgence of CKIs in the last 10 years, with >120 inhibitors in literature, 6 FDA-approvals and many inhibitors in clinical development.

In reviewing this field, several trends became evident; acrylamides (and structural variants) are the most commonly utilized electrophile, largely due to an optimal balance of reactivity, stability and tunability. Nevertheless, in recent times, novel warheads are rapidly emerging as viable alternatives (*i.e.* 2-butynamide, seen in acalabrutinib), typically to access isoform-specific active sites or nucleophiles that also achieve structural novelty. Such new developments are necessary to escape the tight intellectual property surrounding acrylamides. Future pre-clinical testing in models might see more genetic testing to exclude off-target toxicity as the mode-of-action. Currently, EGFR, BTK, JAK3 and/or FGFR kinases remain as the most targeted enzymes in the human kinome. The hinge-region is the most commonly modified sub-pocket and cysteine thiols are by far the most pursued nucleophiles. Over the reviewed period, several kinases were successfully modified for the first time (*i.e.* SRPK, ITK, CDK, *etc.*) with many yet to be explored in a covalent context (*i.e.* TYK2, HER3, Nek1, *etc.*). Furthermore, several reports demonstrated the covalent modification of residues other than Cys (*i.e.* Tyr, Asp), while Glu remains the only nucleophile yet to be modified.

Although IC_{50} remains a gold standard and it is heavily cited in recent literature, it is highly limited in the context of CKIs. As discussed above the 2nd order rate constant [k_{inact}/K_i (M^{-1} s^{-1})] represents a more accurate and relevant tool to assess covalent inhibition of enzymes *in vitro*. While a complete paradigm shift away from IC_{50} measurements is unlikely, it is important to highlight the uniqueness of covalent binding molecules in terms of target engagement in assay design. Also, it is worth noting the value of k_{inact} and K_i values in delineating relative contributions of electrophilic and reversible binding motifs to the apparent potency. This is becoming more evident in literature as several reports cited the use of k_{inact}/K_i (M^{-1} s^{-1}) in SAR studies to optimize covalent bonding (k_{inact}) or target recognition (K_i).

Partly in response to concerns of toxicity due to the permanent modification of cellular proteins, reversible covalent inhibitors have emerged as a highly versatile alternate approach with broad applicability in drug design. Their ability to span a wide spectrum of reversibility through the rational steric and electronic control allows this special class of molecules to interrogate the kinome

covalently and safely, with the potential of achieving tuneable isoform-selective reactivities whilst limiting undesirable off-targets.

As research into these reversibly covalent structures develops, it will be important to observe how such molecules perform in a clinical setting relative to their irreversible counterparts in terms of efficacy, safety and tolerance towards the recurring TKI challenge of acquired drug resistance. Future medicinal chemistry efforts in this field must aim to fully de-risk covalent modifiers whilst sustaining their characteristic potencies. In addition, it would be of great value to fully characterize the reactivity, stability and metabolic profile of relevant electrophilic species *in vivo* as well as to use this approach to explore challenging targets, which are not amenable to traditional small molecule inhibitors.

Abbreviations

ABL	Abelson murine leukaemia
ABPP	Activity-based protein profiling
AD	Alzheimer disease
AKT	Protein kinase B
ALK	Anaplastic lymphoma kinase
AMD	Age-dependent macular degradation
AML	Acute myeloid leukaemia
AS	Analog-sensitive
ASA	Acetyl salicylic acid
ATP	Adenosine triphosphate
AUC	Area-under curve
BBB	Blood brain barrier
BCR	Breakpoint cluster region
BRET	Bioluminescence resonance energy transfer
BSA	Bovine serum albumin
BTK	Bruton's tyrosine kinase
CDK	Cyclin-dependent kinase
CES	Carboxylesterase
CIA	Collagen-induced arthritis
CITe-Id	Covalent inhibitor target-site identification
CKI	Covalent kinase inhibitor
CLL	Chronic lymphocytic leukaemia
CML	Chronic myelogenous leukaemia
CNS	Central nervous system
COX	Cyclooxygenase
CREB	cAMP-response element binding transcription factor
CSF1R	Colony stimulating factor 1 receptor
CYP	Cytochrome P450
DDI	Drug–drug interaction
DDR	Discoidin domain receptor
DFT	Density functional theory
DLBCL	Diffuse large B-cell lymphoma
DPP	Dipeptidyl exopeptidase
DTT	Dithiothreitol
EDG	Electron donating group
EGFR	Epidermal growth factor receptor
EMT	Epithelial–mesenchymal transition
Eph	Erythropoietin-producing human hepatocellular
ER	Endoplasmic reticulum
ETC	Electron transport chain
ERK	Extracellular signal-regulated kinase
EWG	Electron withdrawing group
FAK	Focal adhesion kinase
FaSSIF	Fasted-state stimulated intestinal fluid
FcR	Fc receptor
FGFR	Fibroblast growth factor receptor
FL	Follicular lymphoma
FRET	Fluorescence resonance energy transfer
FRS2	FGFR substrate 2
GFR	Green fluorescent protein
GSH	Glutathione
GSK	Glycogen synthase kinase
HCC	Hepatocellular carcinoma
HSAB	Hard–soft acid–base
HTS	High-throughput screening
iDFS	Invasive-disease free survival
IDT	Idiosyncratic toxicity
IDUP	Interaction determination using unpurified protein
IRE	Inositol-requiring enzyme
IsoTOP	Isotopic tandem orthogonal protein proteolysis
ITK	Inducible T-cell kinase
JAK	Janus kinase
JNK	c-Jun N-terminal kinases
LPS	Lipopolysaccharide
MAPK	Mitogen-activated protein kinase
MCL	Mantle-cell lymphoma
MESNA	Mercapto-ethane sulphonate
MetID	Metabolite identification
MLM	Mouse liver microsomes
MMPA	Matched molecular pairs analysis
MNK	MAPK interacting protein kinases
MSK	Mitogen and stress activated protein kinase
MZL	Marginal zone lymphoma
NAPQI	*N*-Acetyl-*p*-benzoquinone
Nek	Never-in-mitosis related kinase
NSCLC	Non-small cell lung cancer
ORR	Objective response rate
OS	Overall survival
PAINS	Pan-assay interference compounds
Pak	p21-activated kinase
PBMC	Peripheral blood mononuclear cells
PBS	Phosphate-buffered saline
PDGFR	Platelet derived growth factor receptor
PDK	Pyruvate dehydrogenase kinase
PFS	Progression-free survival
P-gp	P-glycoproteins
PH	Pleckstrin homology
Ph^+	Philadelphia chromosome positive
PI3K	Phosphoinositide-3-kinase

PI4P	Phosphatidylinositol-4-phosphate
PIP_3	Phosphatidylinositol (3,4,5)-triphosphate
PKG	cGMP-dependent protein kinase G
PKN3	Protein kinase N3
PSA	Polar surface area
PTM	Post-translational modification
RA	Rheumatoid arthritis
RAL	Resorcylic acid
RLK	Resting lymphocyte kinase
RNAPII	RNA polymerase II
RSK	Ribosomal S6 kinase
SAR	Structure–activity relationship
SBDD	Structure-based drug design
SCC	Squamous cell carcinoma
SH	Src homology
SLL	Small lymphocytic lymphoma
SRPK	Serine–arginine protein kinase
STAT	Signal transducer and activator of transcription
TAK	Transforming growth factor-β-activated kinase
TCR	T-cell receptor
TEV	Tobacco etch virus nuclear-inclusion-a endopeptidase
TGI	Total growth inhibition
TH	Tec homology
TLP	Toll-like receptor
TNBC	Triple-negative breast cancer
TNF	Tumour necrosis factor
TR	Time-resolved
TXK	T-cell X chromosome kinase
UPR	Unfolded protein response
VEGFR	Vascular endothelial growth factor receptor
WM	Waldenström Macroglobulinemia
WT	Wild type
XLA	X-linked agammaglobulinemia

Conflicts of interest

There are no conflicts of interest to declare.

Acknowledgements

P. T. G is supported by research grants from the Natural Sciences and Engineering Research Council of Canada, Canadian Institutes of Health Research (as well as under the frame of ERA PerMed), a Canada Research Chair, and infrastructure grants from the Canadian Foundation for Innovation and the Ontario Research Fund. Y. S. R is supported by a fellowship for research in Duchenne Muscular Dystrophy. Funding to S. N. C is acknowledged from Ludwig Institute for Cancer Research, Fondation contre le cancer, Salus Sanguinis, projects Action de recherché concertée (ARC) 16/21-073 and WelBio F 44/8/5 - MCF/UIG – 10955 and Foundation ''Les avions de Sébastein''. R. M. is kindly supported by the Austrian Science Fund (FWF) [SFB-F04707, SFB-F06105, and under the frame of ERA-NET (I 4157-B)] as well as by a private donation from Liechtenstein.

References

1 M. J. R. Desborough and D. M. Keeling, *Br. J. Haematol.*, 2017, **177**, 674–683.
2 J. R. Vane and R. M. Botting, *Thromb. Res.*, 2003, **110**, 255–258.
3 M. J. Thun, M. M. Namboodiri and C. W. Heath, *N. Engl. J. Med.*, 1991, **325**, 1593–1596.
4 Z.-M. Chen, *Lancet*, 1997, **349**, 1641–1649.
5 P. M. Ridker, N. R. Cook, I.-M. Lee, D. Gordon, J. M. Gaziano, J. E. Manson, C. H. Hennekens and J. E. Buring, *N. Engl. J. Med.*, 2005, **352**, 1293–1304.
6 P. Erhlich, *Lancet*, 1913, 445–451.
7 J. N. Langley, *J. Physiol.*, 1901, **27**, 224–236.
8 J. N. Langley, *J. Physiol.*, 1905, **33**, 374–413.
9 R. P. Ahlquist, *Am. J. Physiol.*, 1948, **153**, 586–600.
10 R. J. Lefkowitz, J. Roth, W. Pricer and I. Pastan, *Proc. Natl. Acad. Sci. U. S. A.*, 1970, **65**, 745–752.
11 L. E. Limbird, *Mol. Interventions*, 2004, **4**, 326.
12 R. A. Bauer, *Drug Discovery Today*, 2015, **20**, 1061–1073.
13 M. H. Potashman and M. E. Duggan, *J. Med. Chem.*, 2009, **52**, 1231–1246.
14 A. J. T. Smith, X. Zhang, A. G. Leach and K. N. Houk, *J. Med. Chem.*, 2009, **52**, 225–233.
15 J. Singh, R. C. Petter, T. A. Baillie and A. Whitty, *Nat. Rev. Drug Discovery*, 2011, **10**, 307–317.
16 J. Zhang, P. L. Yang and N. S. Gray, *Nat. Rev. Cancer*, 2009, **9**, 28–39.
17 H. Zhang, A. Photiou, A. Grothey, J. Stebbing and G. Giamas, *Cell. Signalling*, 2012, **24**, 1173–1184.
18 J. Moscat and M. T. Diaz-Meco, *EMBO Rep.*, 2000, **1**, 399–403.
19 P. Cohen, *Nat. Cell Biol.*, 2002, **4**, E127–E130.
20 T. Hunter and B. M. Sefton, *Proc. Natl. Acad. Sci. U. S. A.*, 1980, 77, 1311–1315.
21 P. Lahiry, A. Torkamani, N. J. Schork and R. A. Hegele, *Nat. Rev. Genet.*, 2010, **11**, 60–74.
22 D. Torti and L. Trusolino, *EMBO Mol. Med.*, 2011, **3**, 623–636.
23 E. Buchdunger, J. Zimmermann, H. Mett, T. Meyer, M. Müller, B. J. Druker and N. B. Lydon, *Cancer Res.*, 1996, **56**, 100–104.
24 P. le Coutre, L. Mologni, L. Cleris, E. Marchesi, E. Buchdunger, R. Giardini, F. Formelli and C. Gambacorti-Passerini, *J. Natl. Cancer Inst.*, 1999, **91**, 163–168.
25 R. Capdeville, E. Buchdunger, J. Zimmermann and A. Matter, *Nat. Rev. Drug Discovery*, 2002, **1**, 493–502.
26 P. Wu, T. E. Nielsen and M. H. Clausen, *Drug Discovery Today*, 2016, **21**, 5–10.
27 M. E. M. Noble, J. A. Endicott and L. N. Johnson, *Science*, 2004, **303**, 1800–1805.
28 A. C. Dar and K. M. Shokat, *Annu. Rev. Biochem.*, 2011, **80**, 769–795.
29 L. K. Gavrin and E. Saiah, *Med. Chem. Commun.*, 2012, **4**, 41–51.

30 F. Zuccotto, E. Ardini, E. Casale and M. Angiolini, *J. Med. Chem.*, 2010, **53**, 2681–2694.
31 V. Lamba and I. Ghosh, New Directions in Targeting Protein Kinases, http://www.eurekaselect.com/98477/article, accessed January 22, 2019.
32 A. Bandyopadhyay and J. Gao, *Curr. Opin. Chem. Biol.*, 2016, **34**, 110–116.
33 J. M. Bradshaw, J. M. McFarland, V. O. Paavilainen, A. Bisconte, D. Tam, V. T. Phan, S. Romanov, D. Finkle, J. Shu, V. Patel, T. Ton, X. Li, D. G. Loughhead, P. A. Nunn, D. E. Karr, M. E. Gerritsen, J. O. Funk, T. D. Owens, E. Verner, K. A. Brameld, R. J. Hill, D. M. Goldstein and J. Taunton, *Nat. Chem. Biol.*, 2015, **11**, 525–531.
34 C.-U. Lee and T. N. Grossmann, *Angew. Chem., Int. Ed.*, 2012, **51**, 8699–8700.
35 I. M. Serafimova, M. A. Pufall, S. Krishnan, K. Duda, M. S. Cohen, R. L. Maglathlin, J. M. McFarland, R. M. Miller, M. Frödin and J. Taunton, *Nat. Chem. Biol.*, 2012, **8**, 471–476.
36 R. B. Pritchard, C. E. Lough, D. J. Currie and H. L. Holmes, *Can. J. Chem.*, 1968, **46**, 775–781.
37 P. J. Tummino and R. A. Copeland, *Biochemistry*, 2008, **47**, 5481–5492.
38 R. E. Pratley and A. Salsali, *Curr. Med. Res. Opin.*, 2007, **23**, 919–931.
39 I. Brandt, J. Joossens, X. Chen, M.-B. Maes, S. Scharpé, I. D. Meester and A.-M. Lambeir, *Biochem. Pharmacol.*, 2005, **70**, 134–143.
40 T. A. Baillie, *Angew. Chem., Int. Ed.*, 2016, **55**, 13408–13421.
41 D. S. Johnson, E. Weerapana and B. F. Cravatt, *Future Med. Chem.*, 2010, **2**, 949–964.
42 Z. Zhao and P. E. Bourne, *Drug Discovery Today*, 2018, **23**, 727–735.
43 R. Lonsdale and R. A. Ward, *Chem. Soc. Rev.*, 2018, **47**, 3816–3830.
44 R. A. Ward, N. Colclough, M. Challinor, J. E. Debreczeni, K. Eckersley, G. Fairley, L. Feron, V. Flemington, M. A. Graham, R. Greenwood, P. Hopcroft, T. D. Howard, M. James, C. D. Jones, C. R. Jones, J. Renshaw, K. Roberts, L. Snow, M. Tonge and K. Yeung, *J. Med. Chem.*, 2015, **58**, 4790–4801.
45 M. W. Jann, *Pharmacotherapy*, 2000, **20**, 1–12.
46 M. S. Davids and J. R. Brown, *Future Oncol.*, 2014, **10**, 957–967.
47 C. Holohan, S. Van Schaeybroeck, D. B. Longley and P. G. Johnston, *Nat. Rev. Cancer*, 2013, **13**, 714–726.
48 N. P. Shah, J. M. Nicoll, B. Nagar, M. E. Gorre, R. L. Paquette, J. Kuriyan and C. L. Sawyers, *Cancer Cell*, 2002, **2**, 117–125.
49 L. Tan, J. Wang, J. Tanizaki, Z. Huang, A. R. Aref, M. Rusan, S.-J. Zhu, Y. Zhang, D. Ercan, R. G. Liao, M. Capelletti, W. Zhou, W. Hur, N. Kim, T. Sim, S. Gaudet, D. A. Barbie, J.-R. J. Yeh, C.-H. Yun, P. S. Hammerman, M. Mohammadi, P. A. Jänne and N. S. Gray, *Proc. Natl. Acad. Sci. U. S. A.*, 2014, **111**, E4869–E4877.
50 R. Lagoutte, R. Patouret and N. Winssinger, *Curr. Opin. Chem. Biol.*, 2017, **39**, 54–63.
51 S. Ohlson, *Drug Discovery Today*, 2008, **13**, 433–439.
52 J. A. Miller, *Drug Metab. Rev.*, 1998, **30**, 645–674.
53 D. J. Jollow, J. R. Mitchell, W. Z. Potter, D. C. Davis, J. R. Gillette and B. B. Brodie, *J. Pharmacol. Exp. Ther.*, 1973, **187**, 195–202.
54 Y. Qiu, L. Z. Benet and A. L. Burlingame, *J. Biol. Chem.*, 1998, **273**, 17940–17953.
55 Y. M. Koen and R. P. Hanzlik, *Chem. Res. Toxicol.*, 2002, **15**, 699–706.
56 V. R. Thompson and A. P. DeCaprio, *Chem. Res. Toxicol.*, 2013, **26**, 1263–1271.
57 S. Nakayama, R. Atsumi, H. Takakusa, Y. Kobayashi, A. Kurihara, Y. Nagai, D. Nakai and O. Okazaki, *Drug Metab. Dispos.*, 2009, **37**, 1970–1977.
58 C. W. Zapf, B. S. Gerstenberger, L. Xing, D. C. Limburg, D. R. Anderson, N. Caspers, S. Han, A. Aulabaugh, R. Kurumbail, S. Shakya, X. Li, V. Spaulding, R. M. Czerwinski, N. Seth and Q. G. Medley, *J. Med. Chem.*, 2012, **55**, 10047–10063.
59 E. Leproult, S. Barluenga, D. Moras, J.-M. Wurtz and N. Winssinger, *J. Med. Chem.*, 2011, **54**, 1347–1355.
60 J. Pettinger, K. Jones and M. D. Cheeseman, *Angew. Chem., Int. Ed.*, 2017, **56**, 15200–15209.
61 K. V. Ruddraraju and Z.-Y. Zhang, *Mol. BioSyst.*, 2017, **13**, 1257–1279.
62 J. C. Powers, J. L. Asgian, Ö. D. Ekici and K. E. James, *Chem. Rev.*, 2002, **102**, 4639–4750.
63 K. M. Backus, B. E. Correia, K. M. Lum, S. Forli, B. D. Horning, G. E. González-Páez, S. Chatterjee, B. R. Lanning, J. R. Teijaro, A. J. Olson, D. W. Wolan and B. F. Cravatt, *Nature*, 2016, **534**, 570–574.
64 C. M. Browne, B. Jiang, S. B. Ficarro, Z. M. Doctor, J. L. Johnson, J. D. Card, S. C. Sivakumaren, W. M. Alexander, T. M. Yaron, C. J. Murphy, N. P. Kwiatkowski, T. Zhang, L. C. Cantley, N. S. Gray and J. A. Marto, *J. Am. Chem. Soc.*, 2019, **141**, 191–203.
65 S. Rao, D. Gurbani, G. Du, R. A. Everley, C. M. Browne, A. Chaikuad, L. Tan, M. Schröder, S. Gondi, S. B. Ficarro, T. Sim, N. D. Kim, M. J. Berberich, S. Knapp, J. A. Marto, K. D. Westover, P. K. Sorger and N. S. Gray, *Cell Chem. Biol.*, 2019, **26**, 818–829.
66 S. M. Marino and V. N. Gladyshev, *J. Biol. Chem.*, 2012, **287**, 4419–4425.
67 A. Chaikuad, P. Koch, S. A. Laufer and S. Knapp, *Angew. Chem., Int. Ed.*, 2018, **57**, 4372–4385.
68 E. Awoonor-Williams and C. N. Rowley, *J. Chem. Inf. Model.*, 2018, **58**, 1935–1946.
69 J. A. H. Schwöbel, Y. K. Koleva, S. J. Enoch, F. Bajot, M. Hewitt, J. C. Madden, D. W. Roberts, T. W. Schultz and M. T. D. Cronin, *Chem. Rev.*, 2011, **111**, 2562–2596.
70 R. G. Pearson, *Coord. Chem. Rev.*, 1990, **100**, 403–425.
71 R. M. LoPachin, D. S. Barber and T. Gavin, *Toxicol. Sci*, 2008, **104**, 235–249.
72 T. W. Schultz, R. E. Carlson, M. T. D. Cronin, J. L. M. Hermens, R. Johnson, P. J. O'Brien, D. W. Roberts, A. Siraki, K. B. Wallace and G. D. Veith, *SAR QSAR Environ. Res.*, 2006, **17**, 413–428.

73 M. Gehringer and S. A. Laufer, *J. Med. Chem.*, 2019, **62**(12), 5673–5724.
74 P. K. Chattaraj, U. Sarkar and D. R. Roy, *Chem. Rev.*, 2006, **106**, 2065–2091.
75 R. M. LoPachin, T. Gavin, A. DeCaprio and D. S. Barber, *Chem. Res. Toxicol.*, 2012, **25**, 239–251.
76 R. A. Ward, M. J. Anderton, S. Ashton, P. A. Bethel, M. Box, S. Butterworth, N. Colclough, C. G. Chorley, C. Chuaqui, D. A. E. Cross, L. A. Dakin, J. É. Debreczeni, C. Eberlein, M. R. V. Finlay, G. B. Hill, M. Grist, T. C. M. Klinowska, C. Lane, S. Martin, J. P. Orme, P. Smith, F. Wang and M. J. Waring, *J. Med. Chem.*, 2013, **56**, 7025–7048.
77 P. A. Jackson, J. C. Widen, D. A. Harki and K. M. Brummond, *J. Med. Chem.*, 2017, **60**, 839–885.
78 S. G. Kathman, Z. Xu and A. V. Statsyuk, *J. Med. Chem.*, 2014, **57**, 4969–4974.
79 V. J. Cee, L. P. Volak, Y. Chen, M. D. Bartberger, C. Tegley, T. Arvedson, J. McCarter, A. S. Tasker and C. Fotsch, *J. Med. Chem.*, 2015, **58**, 9171–9178.
80 J. S. Martin, C. J. MacKenzie, D. Fletcher and I. H. Gilbert, *Bioorg. Med. Chem.*, 2019, **27**, 2066–2074.
81 U. P. Dahal, A. M. Gilbert, R. S. Obach, M. E. Flanagan, J. M. Chen, C. Garcia-Irizarry, J. T. Starr, B. Schuff, D. P. Uccello and J. A. Young, *MedChemComm*, 2016, **7**, 864–872.
82 M. E. Flanagan, J. A. Abramite, D. P. Anderson, A. Aulabaugh, U. P. Dahal, A. M. Gilbert, C. Li, J. Montgomery, S. R. Oppenheimer, T. Ryder, B. P. Schuff, D. P. Uccello, G. S. Walker, Y. Wu, M. F. Brown, J. M. Chen, M. M. Hayward, M. C. Noe, R. S. Obach, L. Philippe, V. Shanmugasundaram, M. J. Shapiro, J. Starr, J. Stroh and Y. Che, *J. Med. Chem.*, 2014, **57**, 10072–10079.
83 R. Lonsdale, J. Burgess, N. Colclough, N. L. Davies, E. M. Lenz, A. L. Orton and R. A. Ward, *J. Chem. Inf. Model.*, 2017, **57**, 3124–3137.
84 D. Liu and D. Cowburn, *Biophys. Rep.*, 2016, **2**, 33–43.
85 S. M. Marino and V. N. Gladyshev, *J. Mol. Biol.*, 2010, **404**, 902–916.
86 S. De Cesco, J. Kurian, C. Dufresne, A. K. Mittermaier and N. Moitessier, *Eur. J. Med. Chem.*, 2017, **138**, 96–114.
87 P. Ábrányi-Balogh, L. Petri, T. Imre, P. Szijj, A. Scarpino, M. Hrast, A. Mitrović, U. P. Fonovič, K. Németh, H. Barreteau, D. I. Roper, K. Horváti, G. G. Ferenczy, J. Kos, J. Ilaš, S. Gobec and G. M. Keserű, *Eur. J. Med. Chem.*, 2018, **160**, 94–107.
88 S. Wu, H. Luo (Howard), H. Wang, W. Zhao, Q. Hu and Y. Yang, *Biochem. Biophys. Res. Commun.*, 2016, **478**, 1268–1273.
89 A. C. Eliot and J. F. Kirsch, *Annu. Rev. Biochem.*, 2004, **73**, 383–415.
90 G. Akçay, M. A. Belmonte, B. Aquila, C. Chuaqui, A. W. Hird, M. L. Lamb, P. B. Rawlins, N. Su, S. Tentarelli, N. P. Grimster and Q. Su, *Nat. Chem. Biol.*, 2016, **12**, 931–936.
91 H. Mukherjee, J. Debreczeni, J. Breed, S. Tentarelli, B. Aquila, J. E. Dowling, A. Whitty and N. P. Grimster, *Org. Biomol. Chem.*, 2017, **15**, 9685–9695.
92 S. E. Dalton, L. Dittus, D. A. Thomas, M. A. Convery, J. Nunes, J. T. Bush, J. P. Evans, T. Werner, M. Bantscheff, J. A. Murphy and S. Campos, *J. Am. Chem. Soc.*, 2018, **140**, 932–939.
93 S. M. Hacker, K. M. Backus, M. R. Lazear, S. Forli, B. E. Correia and B. F. Cravatt, *Nat. Chem.*, 2017, **9**, 1181–1190.
94 J. C. Powers, J. L. Asgian, Ö. D. Ekici and K. E. James, *Chem. Rev.*, 2002, **102**, 4639–4750.
95 J. M. Hatcher, G. Wu, C. Zeng, J. Zhu, F. Meng, S. Patel, W. Wang, S. B. Ficarro, A. L. Leggett, C. E. Powell, J. A. Marto, K. Zhang, J. C. K. Ngo, X.-D. Fu, T. Zhang and N. S. Gray, *Cell Chem. Biol.*, 2018, **25**, 460–470.
96 H. S. Ban, T. Usui, W. Nabeyama, H. Morita, K. Fukuzawa and H. Nakamura, *Org. Biomol. Chem.*, 2009, **7**, 4415.
97 L. H. Jones, *Angew. Chem., Int. Ed.*, 2018, **57**, 9220–9223.
98 J. Blanc, R. Geney and C. Menet, *Anticancer Agents Med. Chem.*, 2013, **13**, 731–747.
99 Z. Zhao, H. Wu, L. Wang, Y. Liu, S. Knapp, Q. Liu and N. S. Gray, *ACS Chem. Biol.*, 2014, **9**, 1230–1241.
100 Z. Zhao, Q. Liu, S. Bliven, L. Xie and P. E. Bourne, *J. Med. Chem.*, 2017, **60**, 2879–2889.
101 Q. Liu, Y. Sabnis, Z. Zhao, T. Zhang, S. J. Buhrlage, L. H. Jones and N. S. Gray, *Chem. Biol.*, 2013, **20**, 146–159.
102 L. T. Alexander, H. Möbitz, P. Drueckes, P. Savitsky, O. Fedorov, J. M. Elkins, C. M. Deane, S. W. Cowan-Jacob and S. Knapp, *ACS Chem. Biol.*, 2015, **10**, 2116–2125.
103 D. D. Waller, G. Jansen, M. Golizeh, C. Martel-Lorion, K. Dejgaard, T. C. Shiao, J. Mancuso, Y. S. Tsantrizos, R. Roy, M. Sebag, L. Sleno and D. Y. Thomas, *ChemBioChem*, 2016, **17**, 843–851.
104 N. London, R. M. Miller, S. Krishnan, K. Uchida, J. J. Irwin, O. Eidam, L. Gibold, P. Cimermančič, R. Bonnet, B. K. Shoichet and J. Taunton, *Nat. Chem. Biol.*, 2014, **10**, 1066–1072.
105 C. M. Pichler, J. Krysiak and R. Breinbauer, *Bioorg. Med. Chem.*, 2016, **24**, 3291–3303.
106 DiscoverX KINOMEscan Kinase Screening & Profiling Services, https://www.discoverx.com/services/drug-discovery-development-services/kinase-profiling/kinomescan, accessed January 8, 2019.
107 T. K. Nomanbhoy, G. Sharma, H. Brown, J. Wu, A. Aban, S. Vogeti, S. Alemayehu, M. Sykes, J. S. Rosenblum and J. W. Kozarich, *Biochemistry*, 2016, **55**, 5434–5441.
108 M. S. Cohen, C. Zhang, K. M. Shokat and J. Taunton, *Science*, 2005, **308**, 1318–1321.
109 D. A. Shannon and E. Weerapana, *Curr. Opin. Chem. Biol.*, 2015, **24**, 18–26.
110 D. Huang, T. Zhou, K. Lafleur, C. Nevado and A. Caflisch, *Bioinformatics*, 2010, **26**, 198–204.
111 W. Zhou, D. Ercan, L. Chen, C.-H. Yun, D. Li, M. Capelletti, A. B. Cortot, L. Chirieac, R. E. Iacob, R. Padera, J. R. Engen, K.-K. Wong, M. J. Eck, N. S. Gray and P. A. Jänne, *Nature*, 2009, **462**, 1070–1074.
112 F. H. Tan, T. L. Putoczki, S. S. Stylli and R. B. Luwor, *OncoTargets Ther.*, 2019, **12**, 635–645.
113 J. Blethrow, C. Zhang, K. M. Shokat and E. L. Weiss, *Current Protocols in Molecular Biology*, 2004, Chapter 18, Unit 18.11.

114 L. Tong, S. Pav, D. M. White, S. Rogers, K. M. Crane, C. L. Cywin, M. L. Brown and C. A. Pargellis, *Nat. Struct. Mol. Biol.*, 1997, **4**, 311–316.

115 H. Weinmann and R. Metternich, *ChemBioChem*, 2005, **6**, 455–459.

116 K. Yonesaka, K. Kudo, S. Nishida, T. Takahama, T. Iwasa, T. Yoshida, K. Tanaka, M. Takeda, H. Kaneda, I. Okamoto, K. Nishio and K. Nakagawa, *Oncotarget*, 2015, **6**, 33602–33611.

117 H. Udagawa, S. Hasako, A. Ohashi, R. Fujioka, Y. Hakozaki, M. Shibuya, N. Abe, T. Komori, T. Haruma, M. Terasaka, R. Fujita, A. Hashimoto, K. Funabashi, H. Yasuda, K. Miyadera, K. Goto, D. B. Costa and S. S. Kobayashi, *Mol. Cancer Res.*, 2019, molcanres.0419.2019.

118 B. R. Lanning, L. R. Whitby, M. M. Dix, J. Douhan, A. M. Gilbert, E. C. Hett, T. O. Johnson, C. Joslyn, J. C. Kath, S. Niessen, L. R. Roberts, M. E. Schnute, C. Wang, J. J. Hulce, B. Wei, L. O. Whiteley, M. M. Hayward and B. F. Cravatt, *Nat. Chem. Biol.*, 2014, **10**, 760–767.

119 H. Mayr and M. Patz, *Angew. Chem., Int. Ed. Engl.*, 1994, **33**, 938–957.

120 A. Meister, *Science*, 1983, **220**, 472–477.

121 E. Weerapana, G. M. Simon and B. F. Cravatt, *Nat. Chem. Biol.*, 2008, **4**, 405–407.

122 E. Weerapana, C. Wang, G. M. Simon, F. Richter, S. Khare, M. B. D. Dillon, D. A. Bachovchin, K. Mowen, D. Baker and B. F. Cravatt, *Nature*, 2010, **468**, 790–795.

123 G. Casiraghi, F. Zanardi, G. Appendino and G. Rassu, *Chem. Rev.*, 2000, **100**, 1929–1972.

124 F. Mendez and J. L. Gazquez, *J. Am. Chem. Soc.*, 1994, **116**, 9298–9301.

125 R. S. Drago and R. A. Kabler, *Inorg. Chem.*, 1972, **11**, 3144–3145.

126 A. Wissner, E. Overbeek, M. F. Reich, M. B. Floyd, B. D. Johnson, N. Mamuya, E. C. Rosfjord, C. Discafani, R. Davis, X. Shi, S. K. Rabindran, B. C. Gruber, F. Ye, W. A. Hallett, R. Nilakantan, R. Shen, Y.-F. Wang, L. M. Greenberger and H.-R. Tsou, *J. Med. Chem.*, 2003, **46**, 49–63.

127 H.-R. Tsou, N. Mamuya, B. D. Johnson, M. F. Reich, B. C. Gruber, F. Ye, R. Nilakantan, R. Shen, C. Discafani, R. DeBlanc, R. Davis, F. E. Koehn, L. M. Greenberger, Y.-F. Wang and A. Wissner, *J. Med. Chem.*, 2001, **44**, 2719–2734.

128 N. Normanno, A. De Luca, C. Bianco, L. Strizzi, M. Mancino, M. R. Maiello, A. Carotenuto, G. De Feo, F. Caponigro and D. S. Salomon, *Gene*, 2006, **366**, 2–16.

129 S. Sigismund, D. Avanzato and L. Lanzetti, *Mol. Oncol.*, 2018, **12**, 3–20.

130 S. V. Sharma, D. W. Bell, J. Settleman and D. A. Haber, *Nat. Rev. Cancer*, 2007, **7**, 169–181.

131 M. Y. Cha, K.-O. Lee, J. W. Kim, C. G. Lee, J. Y. Song, Y. H. Kim, G. S. Lee, S. B. Park and M. S. Kim, *J. Med. Chem.*, 2009, **52**, 6880–6888.

132 Y. Ito, M. Suenaga, K. Hatake, S. Takahashi, M. Yokoyama, Y. Onozawa, K. Yamazaki, S. Hironaka, K. Hashigami, H. Hasegawa, N. Takenaka and N. Boku, *Jpn. J. Clin. Oncol.*, 2012, **42**, 278–286.

133 K. D. Carey, A. J. Garton, M. S. Romero, J. Kahler, S. Thomson, S. Ross, F. Park, J. D. Haley, N. Gibson and M. X. Sliwkowski, *Cancer Res.*, 2006, **66**, 8163–8171.

134 S. Chang, L. Zhang, S. Xu, J. Luo, X. Lu, Z. Zhang, T. Xu, Y. Liu, Z. Tu, Y. Xu, X. Ren, M. Geng, J. Ding, D. Pei and K. Ding, *J. Med. Chem.*, 2012, **55**, 2711–2723.

135 A. O. Walter, R. T. T. Sjin, H. J. Haringsma, K. Ohashi, J. Sun, K. Lee, A. Dubrovskiy, M. Labenski, Z. Zhu, Z. Wang, M. Sheets, T. S. Martin, R. Karp, D. van Kalken, P. Chaturvedi, D. Niu, M. Nacht, R. C. Petter, W. Westlin, K. Lin, S. Jaw-Tsai, M. Raponi, T. V. Dyke, J. Etter, Z. Weaver, W. Pao, J. Singh, A. D. Simmons, T. C. Harding and A. Allen, *Cancer Discovery*, 2013, **3**, 1404–1415.

136 N. Van Der Steen, C. Caparello, C. Rolfo, P. Pauwels, G. J. Peters and E. Giovannetti, *OncoTargets Ther.*, 2016, **9**, 6065–6074.

137 D. A. E. Cross, S. E. Ashton, S. Ghiorghiu, C. Eberlein, C. A. Nebhan, P. J. Spitzler, J. P. Orme, M. R. V. Finlay, R. A. Ward, M. J. Mellor, G. Hughes, A. Rahi, V. N. Jacobs, M. R. Brewer, E. Ichihara, J. Sun, H. Jin, P. Ballard, K. Al-Kadhimi, R. Rowlinson, T. Klinowska, G. H. P. Richmond, M. Cantarini, D.-W. Kim, M. R. Ranson and W. Pao, *Cancer Discovery*, 2014, **4**, 1046–1061.

138 D. Basu, A. Richters and D. Rauh, *Bioorg. Med. Chem.*, 2015, **23**, 2767–2780.

139 E. J. Hennessy, C. Chuaqui, S. Ashton, N. Colclough, D. A. E. Cross, J. É. Debreczeni, C. Eberlein, L. Gingipalli, T. C. M. Klinowska, J. P. Orme, L. Sha and X. Wu, *ACS Med. Chem. Lett.*, 2016, **7**, 514–519.

140 G. Lelais, R. Epple, T. H. Marsilje, Y. O. Long, M. McNeill, B. Chen, W. Lu, J. Anumolu, S. Badiger, B. Bursulaya, M. DiDonato, R. Fong, J. Juarez, J. Li, M. Manuia, D. E. Mason, P. Gordon, T. Groessl, K. Johnson, Y. Jia, S. Kasibhatla, C. Li, J. Isbell, G. Spraggon, S. Bender and P.-Y. Michellys, *J. Med. Chem.*, 2016, **59**, 6671–6689.

141 X. Li, C. Yang, H. Wan, G. Zhang, J. Feng, L. Zhang, X. Chen, D. Zhong, L. Lou, W. Tao and L. Zhang, *Eur. J. Pharm. Sci.*, 2017, **110**, 51–61.

142 H. Wu, A. Wang, W. Zhang, B. Wang, C. Chen, W. Wang, C. Hu, Z. Ye, Z. Zhao, L. Wang, X. Li, K. Yu, J. Liu, J. Wu, X.-E. Yan, P. Zhao, J. Wang, C. Wang, E. L. Weisberg, N. S. Gray, C.-H. Yun, J. Liu, L. Chen and Q. Liu, *Oncotarget*, 2015, **6**, 31313–31322.

143 C. Hu, A. Wang, H. Wu, Z. Qi, X. Li, X.-E. Yan, C. Chen, K. Yu, F. Zou, W. Wang, W. Wang, J. Wu, J. Liu, B. Wang, L. Wang, T. Ren, S. Zhang, C.-H. Yun, J. Liu and Q. Liu, *Oncotarget*, 2017, **8**, 18359–18372.

144 S. Tomassi, J. Lategahn, J. Engel, M. Keul, H. L. Tumbrink, J. Ketzer, T. Mühlenberg, M. Baumann, C. Schultz-Fademrecht, S. Bauer and D. Rauh, *J. Med. Chem.*, 2017, **60**, 2361–2372.

145 S. Smith, M. Keul, J. Engel, D. Basu, S. Eppmann and D. Rauh, *ACS Omega*, 2017, **2**, 1563–1575.

146 Y. Hao, J. Lyu, R. Qu, Y. Tong, D. Sun, F. Feng, L. Tong, T. Yang, Z. Zhao, L. Zhu, J. Ding, Y. Xu, H. Xie and H. Li, *J. Med. Chem.*, 2018, **61**, 5609–5622.

147 H. Zhang, A. Photiou, A. Grothey, J. Stebbing and G. Giamas, *Cell. Signalling*, 2012, **24**, 1173–1184.
148 R. Kersseboom, V. B. T. Ta, A. J. E. Zijlstra, S. Middendorp, H. Jumaa, P. F. van Loo and R. W. Hendriks, *J. Immunol.*, 2006, **176**, 4543–4552.
149 S. Tsukada, D. J. Rawlings and O. N. Witte, *Curr. Opin. Immunol.*, 1994, **6**, 623–630.
150 M. Cinar, F. Hamedani, Z. Mo, B. Cinar, H. M. Amin and S. Alkan, *Leuk. Res.*, 2013, **37**, 1271–1277.
151 K.-H. Kim, A. Maderna, M. E. Schnute, M. Hegen, S. Mohan, J. Miyashiro, L. Lin, E. Li, S. Keegan, J. Lussier, C. Wrocklage, C. L. Nickerson-Nutter, A. J. Wittwer, H. Soutter, N. Caspers, S. Han, R. Kurumbail, K. Dunussi-Joannopoulos, J. Douhan and A. Wissner, *Bioorg. Med. Chem. Lett.*, 2011, **21**, 6258–6263.
152 H. Wu, W. Wang, F. Liu, E. L. Weisberg, B. Tian, Y. Chen, B. Li, A. Wang, B. Wang, Z. Zhao, D. W. McMillin, C. Hu, H. Li, J. Wang, Y. Liang, S. J. Buhrlage, J. Liang, J. Liu, G. Yang, J. R. Brown, S. P. Treon, C. S. Mitsiades, J. D. Griffin, Q. Liu and N. S. Gray, *ACS Chem. Biol.*, 2014, **9**, 1086–1091.
153 X. Li, Y. Zuo, G. Tang, Y. Wang, Y. Zhou, X. Wang, T. Guo, M. Xia, N. Ding and Z. Pan, *J. Med. Chem.*, 2014, **57**, 5112–5128.
154 H. Wu, C. Hu, A. Wang, E. L. Weisberg, Y. Chen, C.-H. Yun, W. Wang, Y. Liu, X. Liu, B. Tian, J. Wang, Z. Zhao, Y. Liang, B. Li, L. Wang, B. Wang, C. Chen, S. J. Buhrlage, Z. Qi, F. Zou, A. Nonami, Y. Li, S. M. Fernandes, S. Adamia, R. M. Stone, I. A. Galinsky, X. Wang, G. Yang, J. D. Griffin, J. R. Brown, M. J. Eck, J. Liu, N. S. Gray and Q. Liu, *Leukemia*, 2016, **30**, 173–181.
155 Z. Huang, Q. Zhang, L. Yan, G. Zhong, L. Zhang, X. Tan and Y. Wang, *Bioorg. Med. Chem. Lett.*, 2016, **26**, 1954–1957.
156 H. Wu, Q. Huang, Z. Qi, Y. Chen, A. Wang, C. Chen, Q. Liang, J. Wang, W. Chen, J. Dong, K. Yu, C. Hu, W. Wang, X. Liu, Y. Deng, L. Wang, B. Wang, X. Li, N. S. Gray, J. Liu, W. Wei and Q. Liu, *Sci. Rep.*, 2017, **7**, 466.
157 Y. Wang, Y. Sun, R. Cao, D. Liu, Y. Xie, L. Li, X. Qi and N. Huang, *J. Med. Chem.*, 2017, **60**, 8552–8564.
158 Y. Xue, P. Song, Z. Song, A. Wang, L. Tong, M. Geng, J. Ding, Q. Liu, L. Sun, H. Xie and A. Zhang, *J. Med. Chem.*, 2018, **61**, 4608–4627.
159 H. Qiu, L. Liu-Bujalski, R. D. Caldwell, A. V. Follis, A. Gardberg, A. Goutopoulos, R. Grenningloh, J. Head, T. Johnson, R. Jones, I. Mochalkin, F. Morandi, C. Neagu and B. Sherer, *Bioorg. Med. Chem. Lett.*, 2018, **28**, 2939–2944.
160 A. Laurence, M. Pesu, O. Silvennoinen and J. O'Shea, *Open Rheumatol. J.*, 2012, **6**, 232–244.
161 G. Barbieri, L. Velazquez, M. Scrobogna, M. Fellous and S. Pellegrini, *Eur. J. Biochem.*, 1994, **223**, 427–435.
162 M. Müller, J. Briscoe, C. Laxton, D. Guschin, A. Ziemiecki, O. Silvennoinen, A. G. Harpur, G. Barbieri, B. A. Witthuhn and C. Schindler, *Nature*, 1993, **366**, 129–135.
163 S. O. Park, H. L. Wamsley, K. Bae, Z. Hu, X. Li, S. Choe, W. B. Slayton, S. P. Oh, K.-U. Wagner and P. P. Sayeski, *PLoS One*, 2013, **8**, e59675.
164 X. Cao, E. W. Shores, J. Hu-Li, M. R. Anver, B. L. Kelsall, S. M. Russell, J. Drago, M. Noguchi, A. Grinberg and E. T. Bloom, *Immunity*, 1995, **2**, 223–238.
165 J. D. Clark, M. E. Flanagan and J.-B. Telliez, *J. Med. Chem.*, 2014, **57**, 5023–5038.
166 S. J. Thomas, J. A. Snowden, M. P. Zeidler and S. J. Danson, *Br. J. Cancer*, 2015, **113**, 365.
167 A. Verma, S. Kambhampati, S. Parmar and L. C. Platanias, *Cancer Metastasis Rev.*, 2003, **22**, 423–434.
168 M. Buchert, C. J. Burns and M. Ernst, *Oncogene*, 2016, **35**, 939–951.
169 M. Gehringer, E. Pfaffenrot, S. Bauer and S. A. Laufer, *ChemMedChem*, 2014, **9**, 277–281.
170 J. J. Kulagowski, W. Blair, R. J. Bull, C. Chang, G. Deshmukh, H. J. Dyke, C. Eigenbrot, N. Ghilardi, P. Gibbons, T. K. Harrison, P. R. Hewitt, M. Liimatta, C. A. Hurley, A. Johnson, T. Johnson, J. R. Kenny, P. Bir Kohli, R. J. Maxey, R. Mendonca, K. Mortara, J. Murray, R. Narukulla, S. Shia, M. Steffek, S. Ubhayakar, M. Ultsch, A. van Abbema, S. I. Ward, B. Waszkowycz and M. Zak, *J. Med. Chem.*, 2012, **55**, 5901–5921.
171 S. E. Van, B. Fiamengo, J. Edmunds, A. Ericsson, K. Frank, M. Friedman, D. George, J. George, E. Goedken, B. Kotecki, G. Martinez, P. Merta, M. Morytko, S. Shekhar, B. Skinner, K. Stewart, J. Voss, G. Wallace, L. Wang, L. Wang and N. Wishart, *Bioorg. Med. Chem. Lett.*, 2013, **23**, 693–698.
172 E. R. Goedken, M. A. Argiriadi, D. L. Banach, B. A. Fiamengo, S. E. Foley, K. E. Frank, J. S. George, C. M. Harris, A. D. Hobson, D. C. Ihle, D. Marcotte, P. J. Merta, M. E. Michalak, S. E. Murdock, M. J. Tomlinson and J. W. Voss, *J. Biol. Chem.*, 2015, **290**, 4573–4589.
173 L. Tan, K. Akahane, R. McNally, K. M. S. E. Reyskens, S. B. Ficarro, S. Liu, G. S. Herter-Sprie, S. Koyama, M. J. Pattison, K. Labella, L. Johannessen, E. A. Akbay, K.-K. Wong, D. A. Frank, J. A. Marto, T. A. Look, J. S. C. Arthur, M. J. Eck and N. S. Gray, *J. Med. Chem.*, 2015, **58**, 6589–6606.
174 World Intellectual Property Organization, WO2013085802A1, 2013.
175 G. A. Smith, K. Uchida, A. Weiss and J. Taunton, *Nat. Chem. Biol.*, 2016, **12**, 373–379.
176 M. Forster, A. Chaikuad, S. M. Bauer, J. Holstein, M. B. Robers, C. R. Corona, M. Gehringer, E. Pfaffenrot, K. Ghoreschi, S. Knapp and S. A. Laufer, *Cell Chem. Biol.*, 2016, **23**, 1335–1340.
177 M. Forster, A. Chaikuad, T. Dimitrov, E. Döring, J. Holstein, B.-T. Berger, M. Gehringer, K. Ghoreschi, S. Müller, S. Knapp and S. A. Laufer, *J. Med. Chem.*, 2018, **61**, 5350–5366.
178 J.-B. Telliez, M. E. Dowty, L. Wang, J. Jussif, T. Lin, L. Li, E. Moy, P. Balbo, W. Li, Y. Zhao, K. Crouse, C. Dickinson, P. Symanowicz, M. Hegen, M. E. Banker, F. Vincent, R. Unwalla, S. Liang, A. M. Gilbert, M. F. Brown, M. Hayward, J. Montgomery, X. Yang, J. Bauman, J. I. Trujillo, A. Casimiro-Garcia, F. F. Vajdos, L. Leung, K. F. Geoghegan, A. Quazi, D. Xuan, L. Jones, E. Hett, K. Wright, J. D. Clark and A. Thorarensen, *ACS Chem. Biol.*, 2016, **11**, 3442–3451.
179 A. Thorarensen, M. E. Dowty, M. E. Banker, B. Juba, J. Jussif, T. Lin, F. Vincent, R. M. Czerwinski, A. Casimiro-Garcia,

R. Unwalla, J. I. Trujillo, S. Liang, P. Balbo, Y. Che, A. M. Gilbert, M. F. Brown, M. Hayward, J. Montgomery, L. Leung, X. Yang, S. Soucy, M. Hegen, J. Coe, J. Langille, F. Vajdos, J. Chrencik and J.-B. Telliez, *J. Med. Chem.*, 2017, **60**, 1971–1993.

180 L. He, M. Shao, T. Wang, T. Lan, C. Zhang and L. Chen, *Mol. Diversity*, 2018, **22**, 343–358.

181 D. M. Ornitz and N. Itoh, *Wiley Interdiscip. Rev.: Dev. Biol.*, 2015, **4**, 215–266.

182 W.-Y. Zhou, H. Zheng, X.-L. Du and J.-L. Yang, *Cancer Biol. Med.*, 2016, **13**, 260–268.

183 M. Mohammadi, S. Froum, J. M. Hamby, M. C. Schroeder, R. L. Panek, G. H. Lu, A. V. Eliseenkova, D. Green, J. Schlessinger and S. R. Hubbard, *EMBO J.*, 1998, **17**, 5896–5904.

184 N. Kammasud, C. Boonyarat, S. Tsunoda, H. Sakurai, I. Saiki, D. S. Grierson and O. Vajragupta, *Bioorg. Med. Chem. Lett.*, 2007, **17**, 4812–4818.

185 S. Trudel, Z. H. Li, E. Wei, M. Wiesmann, H. Chang, C. Chen, D. Reece, C. Heise and A. K. Stewart, *Blood*, 2005, **105**, 2941–2948.

186 W. Zhou, W. Hur, U. McDermott, A. Dutt, W. Xian, S. B. Picarro, J. Zhang, S. V. Sharma, J. Brugge, M. Meyerson, J. Settleman and N. S. Gray, *Chem. Biol.*, 2010, **17**, 285–295.

187 W. S. Brown, L. Tan, A. Smith, N. S. Gray and M. K. Wendt, *Mol. Cancer Ther.*, 2016, **15**, 2096–2106.

188 K. A. Brameld, T. D. Owens, E. Verner, E. Venetsanakos, J. M. Bradshaw, V. T. Phan, D. Tam, K. Leung, J. Shu, J. LaStant, D. G. Loughhead, T. Ton, D. E. Karr, M. E. Gerritsen, D. M. Goldstein and J. O. Funk, *J. Med. Chem.*, 2017, **60**, 6516–6527.

189 L. Gao, X. Wang, Y. Tang, S. Huang, C.-A. A. Hu and Y. Teng, *J. Exp. Clin. Cancer Res.*, 2017, **36**, 8.

190 M. V. Dieci, M. Arnedos, F. Andre and J. C. Soria, *Cancer Discovery*, 2013, **3**, 264–279.

191 M. Hagel, C. Miduturu, M. Sheets, N. Rubin, W. Weng, N. Stransky, N. Bifulco, J. L. Kim, B. Hodous, N. Brooijmans, A. Shutes, C. Winter, C. Lengauer, N. E. Kohl and T. Guzi, *Cancer Discovery*, 2015, **5**, 424–437.

192 C. Mo, Z. Zhang, C. P. Guise, X. Li, J. Luo, Z. Tu, Y. Xu, A. V. Patterson, J. B. Smaill, X. Ren, X. Lu and K. Ding, *ACS Med. Chem. Lett.*, 2017, **8**, 543–548.

193 Y. Wang, Z. Chen, M. Dai, P. Sun, C. Wang, Y. Gao, H. Zhao, W. Zeng, L. Shen, W. Mao, T. Wang, G. Hu, J. Li, S. Chen, C. Long, X. Chen, J. Liu and Y. Zhang, *Bioorg. Med. Chem. Lett.*, 2017, **27**, 2420–2423.

194 R. A. Fairhurst, T. Knoepfel, C. Leblanc, N. Buschmann, C. Gaul, J. Blank, I. Galuba, J. Trappe, C. Zou, J. Voshol, C. Genick, P. Brunet-Lefeuvre, F. Bitsch, D. Graus-Porta and P. Furet, *Med. Chem. Commun.*, 2017, **8**, 1604–1613.

195 S. Ghosh, K. Bienemann, K. Boztug and A. Borkhardt, *J. Clin. Immunol.*, 2014, **34**, 892–899.

196 Y. Zhong, A. J. Johnson, J. C. Byrd and J. A. Dubovsky, *Postdoc. J.*, 2014, **2**, 1–11.

197 J. D. Harling, A. M. Deakin, S. Campos, R. Grimley, L. Chaudry, C. Nye, O. Polyakova, C. M. Bessant, N. Barton, D. Somers, J. Barrett, R. H. Graves, L. Hanns, W. J. Kerr and R. Solari, *J. Biol. Chem.*, 2013, **288**, 28195–28206.

198 Y. Zhong, S. Dong, K. Thornton, A. Mishra, P. Porcu, M. Bradshaw, A. Bisconte, T. Owens, E. Verner, K. Brameld, J. O. Funk, R. Hill, A. J. Johnson and J. A. Dubovsky, *Blood*, 2014, **124**, 272.

199 K. M. S. E. Reyskens and J. S. C. Arthur, *Front. Cell Dev. Biol.*, 2016, **4**, 56.

200 A. Narayanasamy and Y.-Y. Cho, *Front. Oncol.*, 2013, **3**, 201.

201 I. M. Serafimova, M. A. Pufall, S. Krishnan, K. Duda, M. S. Cohen, R. L. Maglathlin, J. M. McFarland, R. M. Miller, M. Frödin and J. Taunton, *Nat. Chem. Biol.*, 2012, **8**, 471–476.

202 R. M. Miller, V. O. Paavilainen, S. Krishnan, I. M. Serafimova and J. Taunton, *J. Am. Chem. Soc.*, 2013, **135**, 5298–5301.

203 A. Satyanarayana and P. Kaldis, *Oncogene*, 2009, **28**, 2925–2939.

204 M. E. Law, P. E. Corsino, S. Narayan and B. K. Law, *Mol. Pharmacol.*, 2015, **88**, 846–852.

205 N. Kwiatkowski, T. Zhang, P. B. Rahl, B. J. Abraham, J. Reddy, S. B. Ficarro, A. Dastur, A. Amzallag, S. Ramaswamy, B. Tesar, C. E. Jenkins, N. M. Hannett, D. McMillin, T. Sanda, T. Sim, N. D. Kim, T. Look, C. S. Mitsiades, A. P. Weng, J. R. Brown, C. H. Benes, J. A. Marto, R. A. Young and N. S. Gray, *Nature*, 2014, **511**, 616–620.

206 T. Zhang, N. Kwiatkowski, C. M. Olson, S. E. Dixon-Clarke, B. J. Abraham, A. K. Greifenberg, S. B. Ficarro, J. M. Elkins, Y. Liang, N. M. Hannett, T. Manz, M. Hao, B. Bartkowiak, A. L. Greenleaf, J. A. Marto, M. Geyer, A. N. Bullock, R. A. Young and N. S. Gray, *Nat. Chem. Biol.*, 2016, **12**, 876–884.

207 M. A. Siddiqui and P. A. Reddy, *J. Med. Chem.*, 2010, **53**, 3005–3012.

208 K. Sabapathy, *Prog. Mol. Biol. Transl. Sci.*, 2012, **106**, 145–169.

209 J. Cui, M. Zhang, Y.-Q. Zhang and Z.-H. Xu, *Acta Pharmacol. Sin.*, 2007, **28**, 601–608.

210 T. Zhang, F. Inesta-Vaquera, M. Niepel, J. Zhang, S. B. Ficarro, T. Machleidt, T. Xie, J. A. Marto, N. Kim, T. Sim, J. D. Laughlin, H. Park, P. V. LoGrasso, M. Patricelli, T. K. Nomanbhoy, P. K. Sorger, D. R. Alessi and N. S. Gray, *Chem. Biol.*, 2012, **19**, 140–154.

211 F. Muth, A. El-Gokha, F. Ansideri, M. Eitel, E. Döring, A. Sievers-Engler, A. Lange, F. M. Boeckler, M. Lämmerhofer, P. Koch and S. A. Laufer, *J. Med. Chem.*, 2017, **60**, 594–607.

212 L. Tamagnone, I. Lahtinen, T. Mustonen, K. Virtaneva, F. Francis, F. Muscatelli, R. Alitalo, C. I. Smith, C. Larsson and K. Alitalo, *Oncogene*, 1994, **9**, 3683–3688.

213 X. Wen, H. H. Lin, H.-M. Shih, H.-J. Kung and D. K. Ann, *J. Biol. Chem.*, 1999, **274**, 38204–38210.

214 Y. Wang, J. Xia, Z. Fang, F. Li, D. Li, Z. Wang, Y. Feng, J. Zhang, H. Chen, H. Ji and H. Liu, *Oncotarget*, 2017, **8**, 33405–33415.

215 P. Saharinen, N. Ekman, K. Sarvas, P. Parker, K. Alitalo and O. Silvennoinen, *Blood*, 1997, **90**, 4341–4353.

216 L. Qiu, F. Wang, S. Liu and X.-L. Chen, *Burns Trauma*, 2014, **2**, 121–124.

217 F. Liu, X. Zhang, E. Weisberg, S. Chen, W. Hur, H. Wu, Z. Zhao, W. Wang, M. Mao, C. Cai, N. I. Simon, T. Sanda, J. Wang, A. T. Look, J. D. Griffin, S. P. Balk, Q. Liu and N. S. Gray, *ACS Chem. Biol.*, 2013, **8**, 1423–1428.

218 X. Liang, F. Lv, B. Wang, K. Yu, H. Wu, Z. Qi, Z. Jiang, C. Chen, A. Wang, W. Miao, W. Wang, Z. Hu, J. Liu, X. Liu, Z. Zhao, L. Wang, S. Zhang, Z. Ye, C. Wang, T. Ren, Y. Wang, Q. Liu and J. Liu, *J. Med. Chem.*, 2017, **60**, 1793–1816.

219 R. Roskoski, *Pharmacol. Res.*, 2012, **66**, 105–143.

220 R. J. Sullivan, J. R. Infante, F. Janku, D. J. L. Wong, J. A. Sosman, V. Keedy, M. R. Patel, G. I. Shapiro, J. W. Mier, A. W. Tolcher, A. Wang-Gillam, M. Sznol, K. Flaherty, E. Buchbinder, R. D. Carvajal, A. M. Varghese, M. E. Lacouture, A. Ribas, S. P. Patel, G. A. DeCrescenzo, C. M. Emery, A. L. Groover, S. Saha, M. Varterasian, D. J. Welsch, D. M. Hyman and B. T. Li, *Cancer Discovery*, 2018, **8**, 184–195.

221 X. Zhao and J. L. Guan, *Adv. Drug Delivery Rev.*, 2011, **63**, 610–615.

222 E. Yen-Pon, B. Li, M. Acebrón-Garcia-de-Eulate, C. Tomkiewicz-Raulet, J. Dawson, D. Lietha, M. C. Frame, X. Coumoul, C. Garbay, M. Etheve-Quelquejeu and H. Chen, *ACS Chem. Biol.*, 2018, **13**, 2067–2073.

223 G. M. Nitulescu, D. Margina, P. Juzenas, Q. Peng, O. T. Olaru, E. Saloustros, C. Fenga, D. A. Spandidos, M. Libra and A. M. Tsatsakis, *Int. J. Oncol.*, 2016, **48**, 869–885.

224 C. Cherrin, K. Haskell, B. Howell, R. Jones, K. Leander, R. Robinson, A. Watkins, M. Bilodeau, J. Hoffman, P. Sanderson, G. Hartman, E. Mahan, T. Prueksaritanont, G. Jiang, Q.-B. She, N. Rosen, L. Sepp-Lorenzino, D. Defeo-Jones and H. E. Huber, *Cancer Biol. Ther.*, 2010, **9**, 493–503.

225 J. Weisner, R. Gontla, L. van der Westhuizen, S. Oeck, J. Ketzer, P. Janning, A. Richters, T. Mühlenberg, Z. Fang, A. Taher, V. Jendrossek, S. C. Pelly, S. Bauer, W. A. L. van Otterlo and D. Rauh, *Angew. Chem., Int. Ed.*, 2015, **54**, 10313–10316.

226 P. Broglie, K. Matsumoto, S. Akira, D. L. Brautigan and J. Ninomiya-Tsuji, *J. Biol. Chem.*, 2010, **285**, 2333–2339.

227 Y. S. Roh, J. Song and E. Seki, *J. Gastroenterol.*, 2014, **49**, 185–194.

228 J. Totzke, D. Gurbani, R. Raphemot, P. F. Hughes, K. Bodoor, D. A. Carlson, D. R. Loiselle, A. K. Bera, L. S. Eibschutz, M. M. Perkins, A. L. Eubanks, P. L. Campbell, D. A. Fox, K. D. Westover, T. A. J. Haystead and E. R. Derbyshire, *Cell Chem. Biol.*, 2017, **24**, 1029–1039.

229 J. Li, C. Liang, Z.-K. Zhang, X. Pan, S. Peng, W.-S. Lee, A. Lu, Z. Lin, G. Zhang, W.-N. Leung and B.-T. Zhang, *Cell Discovery*, 2017, **3**, 17023.

230 L. Tan, D. Gurbani, E. L. Weisberg, J. C. Hunter, L. Li, D. S. Jones, S. B. Ficarro, S. Mowafy, C.-P. Tam, S. Rao, G. Du, J. D. Griffin, P. K. Sorger, J. A. Marto, K. D. Westover and N. S. Gray, *Bioorg. Med. Chem.*, 2017, **25**, 838–846.

231 Z.-W. Li, W. Chu, Y. Hu, M. Delhase, T. Deerinck, M. Ellisman, R. Johnson and M. Karin, *J. Exp. Med.*, 1999, **189**, 1839–1845.

232 B. H. Kim, J.-Y. Lee, J. H. Seo, H. Y. Lee, S. Y. Ryu, B. W. Ahn, C.-K. Lee, B. Y. Hwang, S.-B. Han and Y. Kim, *Biochem. Biophys. Res. Commun.*, 2007, **361**, 593–598.

233 L. Toral-Barza, W.-G. Zhang, X. Huang, L. A. McDonald, E. J. Salaski, L. R. Barbieri, W.-D. Ding, G. Krishnamurthy, Y. B. Hu, J. Lucas, V. S. Bernan, P. Cai, J. I. Levin, T. S. Mansour, J. J. Gibbons, R. T. Abraham and K. Yu, *Mol. Cancer Ther.*, 2007, **6**, 3028–3038.

234 A. Wissner, H. L. Fraser, C. L. Ingalls, R. G. Dushin, M. B. Floyd, K. Cheung, T. Nittoli, M. R. Ravi, X. Tan and F. Loganzo, *Bioorg. Med. Chem.*, 2007, **15**, 3635–3648.

235 L. W. Wattenberg, J. B. Coccia and A. R. Galbraith, *Cancer Lett.*, 1994, **83**, 165–169.

236 B. Srinivasan, T. E. Johnson, R. Lad and C. Xing, *J. Med. Chem.*, 2009, **52**, 7228–7235.

237 M. Goto, J. Chow, K. Muramoto, K. Chiba, S. Yamamoto, M. Fujita, H. Obaishi, K. Tai, Y. Mizui, I. Tanaka, D. Young, H. Yang, Y. J. Wang, H. Shirota and F. Gusovsky, *J. Pharmacol. Exp. Ther.*, 2009, **331**, 485–495.

238 U. D. Palempalli, U. Gandhi, P. Kalantari, H. Vunta, R. J. Arner, V. Narayan, A. Ravindran and K. S. Prabhu, *Biochem. J.*, 2009, **419**, 401–409.

239 J. Singh, R. Petter, R. W. Tester, A. F. Kluge, H. Mazdiyasni, W. F. Westlin III, D. Niu and L. Qiao, *US Pat.*, US20100249092A1, 2010.

240 A. Schirmer, J. Kennedy, S. Murli, R. Reid and D. V. Santi, *Proc. Natl. Acad. Sci. U. S. A.*, 2006, **103**, 4234–4239.

241 S. Barluenga, R. Jogireddy, G. K. Koripelly and N. Winssinger, *ChemBioChem*, 2010, **11**, 1692–1699.

242 M.-C. Perry, M. Demeule, A. Régina, R. Moumdjian and R. Béliveau, *Mol. Nutr. Food Res.*, 2010, **54**, 1192–1201.

243 R. M. C. Di Martino, A. De Simone, V. Andrisano, P. Bisignano, A. Bisi, S. Gobbi, A. Rampa, R. Fato, C. Bergamini, D. I. Perez, A. Martinez, G. Bottegoni, A. Cavalli and F. Belluti, *J. Med. Chem.*, 2016, **59**, 531–544.

244 A. Brown, Q. Shi, T. W. Moore, Y. Yoon, A. Prussia, C. Maddox, D. C. Liotta, H. Shim and J. P. Snyder, *J. Med. Chem.*, 2013, **56**, 3456–3466.

245 J. A. Engelman, *Nat. Rev. Cancer*, 2009, **9**, 550–562.

246 S. J. Shuttleworth, F. A. Silva, A. R. L. Cecil, C. D. Tomassi, T. J. Hill, F. I. Raynaud, P. A. Clarke and P. Workman, *Curr. Med. Chem.*, 2011, **18**, 2686–2714.

247 M. Nacht, L. Qiao, M. P. Sheets, T. Martin, M. Labenski, H. Mazdiyasni, R. Karp, Z. Zhu, P. Chaturvedi, D. Bhavsar, D. Niu, W. Westlin, R. C. Petter, A. P. Medikonda and J. Singh, *J. Med. Chem.*, 2013, **56**, 712–721.

248 P. M. Fischer, *Curr. Med. Chem.*, 2004, **11**, 1563–1583.

249 K. A. Denessiouk and M. S. Johnson, *Proteins*, 2000, **38**, 310–326.

250 T. Nguyen, R. A. Coover, J. Verghese, R. G. Moran and K. C. Ellis, *ACS Med. Chem. Lett.*, 2014, **5**, 462–467.

251 S. Krishnan, R. M. Miller, B. Tian, R. D. Mullins, M. P. Jacobson and J. Taunton, *J. Am. Chem. Soc.*, 2014, **136**, 12624–12630.

252 H. Häcker and M. Karin, *Sci. STKE*, 2006, re13.

253 T. Dong, C. Li, X. Wang, L. Dian, X. Zhang, L. Li, S. Chen, R. Cao, L. Li, N. Huang, S. He and X. Lei, *Nat. Commun.*, 2015, **6**, 6522.

254 A. Fouqué, O. Delalande, M. Jean, R. Castellano, E. Josselin, M. Malleter, K. F. Shoji, M. D. Hung, H. Rampanarivo, Y. Collette, P. van de Weghe and P. Legembre, *J. Med. Chem.*, 2015, **58**, 6559–6573.

255 J. Hassler, S. S. Cao and R. J. Kaufman, *Dev. Cell*, 2012, **23**, 921–923.

256 B. W. Zaro, L. R. Whitby, K. M. Lum and B. F. Cravatt, *J. Am. Chem. Soc.*, 2016, **138**, 15841–15844.

257 J. Marx, *Science*, 2007, **316**, 1416–1417.

258 M. L. Billingsley and R. L. Kincaid, *Biochem. J.*, 1997, **323**, 577–591.

259 G. Zimmermann and D. Neri, *Drug Discovery Today*, 2016, **21**, 1828–1834.

260 N. Favalli, G. Bassi, J. Scheuermann and D. Neri, *FEBS Lett.*, 2018, **592**, 2168–2180.

261 L. M. McGregor, T. Jain and D. R. Liu, *J. Am. Chem. Soc.*, 2014, **136**, 3264–3270.

262 A. I. Chan, L. M. McGregor, T. Jain and D. R. Liu, *J. Am. Chem. Soc.*, 2017, **139**, 10192–10195.

263 H. R. Christofk, M. G. Vander Heiden, M. H. Harris, A. Ramanathan, R. E. Gerszten, R. Wei, M. D. Fleming, S. L. Schreiber and L. C. Cantley, *Nature*, 2008, **452**, 230–233.

264 D. Anastasiou, Y. Yu, W. J. Israelsen, J.-K. Jiang, M. B. Boxer, B. S. Hong, W. Tempel, S. Dimov, M. Shen, A. Jha, H. Yang, K. R. Mattaini, C. M. Metallo, B. P. Fiske, K. D. Courtney, S. Malstrom, T. M. Khan, C. Kung, A. P. Skoumbourdis, H. Veith, N. Southall, M. J. Walsh, K. R. Brimacombe, W. Leister, S. Y. Lunt, Z. R. Johnson, K. E. Yen, K. Kunii, S. M. Davidson, H. R. Christofk, C. P. Austin, J. Inglese, M. H. Harris, J. M. Asara, G. Stephanopoulos, F. G. Salituro, S. Jin, L. Dang, D. S. Auld, H.-W. Park, L. C. Cantley, C. J. Thomas and M. G. Vander Heiden, *Nat. Chem. Biol.*, 2012, **8**, 839–847.

265 J. Li, S. Li, J. Guo, Q. Li, J. Long, C. Ma, Y. Ding, C. Yan, L. Li, Z. Wu, H. Zhu, K. K. Li, L. Wen, Q. Zhang, Q. Xue, C. Zhao, N. Liu, I. Ivanov, M. Luo, R. Xi, H. Long, P. G. Wang and Y. Chen, *J. Med. Chem.*, 2018, **61**, 4155–4164.

266 A. V. Villarino, Y. Kanno and J. J. O'Shea, *Nat. Immunol.*, 2017, **18**, 374–384.

267 H. Huang, J. Niu, F. Wang, L. Hu and Q. Yu, *Invest. New Drugs*, 2019, **37**, 452–460.

268 A. Elkamhawy, N. Youn Kim, A. H. E. Hassan, J. Park, J.-E. Yang, K.-S. Oh, B. H. Lee, M. Y. Lee, K. J. Shin, K.-T. Lee, W. Hur and E. J. Roh, *Eur. J. Med. Chem.*, 2018, **157**, 691–704.

269 G. Schoellmann and E. Shaw, *Biochemistry*, 1963, **2**, 252–255.

270 R. G. Pearson, S. H. Langer, F. V. Williams and W. J. McGuire, *J. Am. Chem. Soc.*, 1952, **74**, 5130–5132.

271 M. W. Hunkapiller, M. D. Forgac and J. H. Richards, *Biochemistry*, 1976, **15**, 5581–5588.

272 J. P. G. Malthouse, N. E. Mackenzie, A. S. F. Boyd and A. I. Scott, *J. Am. Chem. Soc.*, 1983, **105**, 1685–1686.

273 C. Hauge and M. Frödin, *J. Cell Sci.*, 2006, **119**, 3021–3023.

274 M. S. Cohen, C. Zhang, K. M. Shokat and J. Taunton, *Science*, 2005, **308**, 1318–1321.

275 M. S. Cohen, H. Hadjivassiliou and J. Taunton, *Nat. Chem. Biol.*, 2007, **3**, 156–160.

276 D. I. Perez, S. Conde, C. Pérez, C. Gil, D. Simon, F. Wandosell, F. J. Moreno, J. L. Gelpí, F. J. Luque and A. Martínez, *Bioorg. Med. Chem.*, 2009, **17**, 6914–6925.

277 D. I. Perez, V. Palomo, C. Pérez, C. Gil, P. D. Dans, F. J. Luque, S. Conde and A. Martínez, *J. Med. Chem.*, 2011, **54**, 4042–4056.

278 A. L. Garske, U. Peters, A. T. Cortesi, J. L. Perez and K. M. Shokat, *Proc. Natl. Acad. Sci. U. S. A.*, 2011, **108**, 15046–15052.

279 B. R. Mardin, C. Lange, J. E. Baxter, T. Hardy, S. R. Scholz, A. M. Fry and E. Schiebel, *Nat. Cell Biol.*, 2010, **12**, 1166–1176.

280 D. G. Hayward, R. B. Clarke, A. J. Faragher, M. R. Pillai, I. M. Hagan and A. M. Fry, *Cancer Res.*, 2004, **64**, 7370–7376.

281 J. C. Henise and J. Taunton, *J. Med. Chem.*, 2011, **54**, 4133–4146.

282 C. Harrison, *Nat. Rev. Drug Discovery*, 2012, **11**, 21.

283 K. Kullander and R. Klein, *Nat. Rev. Mol. Cell Biol.*, 2002, **3**, 475–486.

284 A. Kung, Y.-C. Chen, M. Schimpl, F. Ni, J. Zhu, M. Turner, H. Molina, R. Overman and C. Zhang, *J. Am. Chem. Soc.*, 2016, **138**, 10554–10560.

285 R. A. Coover, N. M. Luzi, S. Korwar, M. E. Casile, C. E. Lyons, D. L. Peterson and K. C. Ellis, *Org. Biomol. Chem.*, 2016, **14**, 4576–4581.

286 Z. Yang, H. Liu, B. Pan, F. He and Z. Pan, *Org. Biomol. Chem.*, 2018, **16**, 4127–4140.

287 G. E. Means and R. E. Feeney, *Bioconjugate Chem.*, 1990, **1**, 2–12.

288 O. Boutureira and G. J. L. Bernardes, *Chem. Rev.*, 2015, **115**, 2174–2195.

289 P. J. Thornalley, *Anti-cancer Drugs*, 2002, **13**, 331–338.

290 J. V. Cross, F. W. Foss, J. M. Rady, T. L. Macdonald and D. J. Templeton, *BMC Cancer*, 2007, **7**, 183.

291 E. R. Wood, L. M. Shewchuk, B. Ellis, P. Brignola, R. L. Brashear, T. R. Caferro, S. H. Dickerson, H. D. Dickson, K. H. Donaldson, M. Gaul, R. J. Griffin, A. M. Hassell, B. Keith, R. Mullin, K. G. Petrov, M. J. Reno, D. W. Rusnak, S. M. Tadepalli, J. C. Ulrich, C. D. Wagner, D. E. Vanderwall, A. G. Waterson, J. D. Williams, W. L. White and D. E. Uehling, *Proc. Natl. Acad. Sci. U. S. A.*, 2008, **105**, 2773–2778.

292 H. M. Hammarén, A. T. Virtanen, J. Raivola and O. Silvennoinen, *Cytokine*, 2019, **118**, 48–63.

293 Y. Wang, X. Ma, S. Yan, S. Shen, H. Zhu, Y. Gu, H. Wang, G. Qin and Q. Yu, *Cancer Res.*, 2009, **69**, 7302–7310.

294 X. Guo, R. E. Gerl and J. W. Schrader, *J. Biol. Chem.*, 2003, **278**, 22237–22242.

295 J. Li, T. S. Kaoud, C. Laroche, K. N. Dalby and S. M. Kerwin, *Bioorg. Med. Chem. Lett.*, 2009, **19**, 6293–6297.

296 J. Eswaran, M. Soundararajan and S. Knapp, *Cancer Metastasis Rev.*, 2009, **28**, 209–217.

297 J. Viaud and J. R. Peterson, *Mol. Cancer Ther.*, 2009, **8**, 2559–2565.
298 P. R. Rablen, *J. Am. Chem. Soc.*, 1997, **119**, 8350–8360.
299 H. S. Ban, T. Usui, W. Nabeyama, H. Morita, K. Fukuzawa and H. Nakamura, *Org. Biomol. Chem.*, 2009, **7**, 4415–4427.
300 D. J. Moshinsky, C. R. Bellamacina, D. C. Boisvert, P. Huang, T. Hui, J. Jancarik, S.-H. Kim and A. G. Rice, *Biochem. Biophys. Res. Commun.*, 2003, **310**, 1026–1031.
301 A. Martinez, M. Alonso, A. Castro, C. Pérez and F. J. Moreno, *J. Med. Chem.*, 2002, **45**, 1292–1299.
302 J. M. Domínguez, A. Fuertes, L. Orozco, M. del Monte-Millán, E. Delgado and M. Medina, *J. Biol. Chem.*, 2012, **287**, 893–904.
303 H. P. Morgan, M. J. Walsh, E. A. Blackburn, M. A. Wear, M. B. Boxer, M. Shen, I. W. Mcnae, M. W. Nowicki, P. A. M. Michels, D. S. Auld, L. A. Fothergill-Gilmore and M. D. Walkinshaw, *Biochem. J.*, 2012, **448**, 67–72.
304 D. Drennan and A. G. Ryazanov, *Prog. Biophys. Mol. Biol.*, 2004, **85**, 1–32.
305 A. K. Devkota, R. Edupuganti, C. Yan, Y. Shi, J. Jose, Q. Wang, T. S. Kaoud, E. J. Cho, P. Ren and K. N. Dalby, *ChemBioChem*, 2014, **15**, 2435–2442.
306 S. Meshinchi and F. R. Appelbaum, *Clin. Cancer Res.*, 2009, **15**, 4263–4269.
307 J. Xu, E. H. Q. Ong, J. Hill, A. Chen and C. L. L. Chai, *Bioorg. Med. Chem.*, 2014, **22**, 6625–6637.
308 F. Hausheer, S. Bain, M. Perry, L. Du, Y. Ohashi, Y. Ariyoshi and M. Fukuolca, *Asia-Pac. J. Oncol. Hematol.*, 2010, **2**, 1–13.
309 A. R. Parker, P. N. Petluru, V. L. Nienaber, M. Zhao, P. Y. Ayala, J. Badger, B. Chie-Leon, V. Sridhar, C. Logan, H. Kochat and F. H. Hausheer, *OncoTargets Ther.*, 2015, **8**, 375–383.
310 E. Anscombe, E. Meschini, R. Mora-Vidal, M. P. Martin, D. Staunton, M. Geitmann, U. H. Danielson, W. A. Stanley, L. Z. Wang, T. Reuillon, B. T. Golding, C. Cano, D. R. Newell, M. E. M. Noble, S. R. Wedge, J. A. Endicott and R. J. Griffin, *Chem. Biol.*, 2015, **22**, 1159–1164.
311 S.-H. Chen and G. Zhaori, *Eur. J. Clin. Invest.*, 2011, **41**, 221–232.
312 D. F. Mitcheson, A. R. Bottrill, K. Carr, C. R. Coxon, C. Cano, B. T. Golding, R. J. Griffin, A. M. Fry, C. Doerig, R. Bayliss and A. B. Tobin, *Malar. J.*, 2016, **15**, 535.
313 D. M. Lowery, D. Lim and M. B. Yaffe, *Oncogene*, 2005, **24**, 248–259.
314 Y. Chen, J. Zhang, D. Li, J. Jiang, Y. Wang and S. Si, *Oncotarget*, 2016, **8**, 1234–1246.
315 K. Normandin, J.-F. Lavallée, M. Futter, A. Beautrait, J. Duchaine, S. Guiral, A. Marinier and V. Archambault, *Sci. Rep.*, 2016, **6**, 37581.
316 H. L. Torney, J. K. Dulworth and D. L. Steward, *Antimicrob. Agents Chemother.*, 1982, **22**, 635–638.
317 M. Arita, *Microbiol. Immunol.*, 2014, **58**, 239–256.
318 M. Arita, G. Dobrikov, G. Pürstinger and A. S. Galabov, *ACS Infect. Dis.*, 2017, **3**, 585–594.
319 M. G. V. Heiden, L. C. Cantley and C. B. Thompson, *Science*, 2009, **324**, 1029–1033.
320 E. Saunier, C. Benelli and S. Bortoli, *Int. J. Cancer*, 2016, **138**, 809–817.
321 W. Sun, Z. Xie, Y. Liu, D. Zhao, Z. Wu, D. Zhang, H. Lv, S. Tang, N. Jin, H. Jiang, M. Tan, J. Ding, C. Luo, J. Li, M. Huang and M. Geng, *Cancer Res.*, 2015, **75**, 4923–4936.
322 Y. Liu, Z. Xie, D. Zhao, J. Zhu, F. Mao, S. Tang, H. Xu, C. Luo, M. Geng, M. Huang and J. Li, *J. Med. Chem.*, 2017, **60**, 2227–2244.
323 S. H. Francis, J. L. Busch and J. D. Corbin, *Pharmacol. Rev.*, 2010, **62**, 525–563.
324 K. A. Ahmed, T. Zhang, K. Ono, H. Tsutsuki, T. Ida, S. Akashi, K. Miyata, Y. Oike, T. Akaike and T. Sawa, *Biol. Pharm. Bull.*, 2017, **40**, 365–374.
325 R. A. Fairhurst, T. Knoepfel, C. Leblanc, N. Buschmann, C. Gaul, J. Blank, I. Galuba, J. Trappe, C. Zou, J. Voshol, C. Genick, P. Brunet-Lefeuvre, F. Bitsch, D. Graus-Porta and P. Furet, *Med. Chem. Commun.*, 2017, **8**, 1604–1613.
326 T. Knoepfel, P. Furet, R. Mah, N. Buschmann, C. Leblanc, S. Ripoche, D. Graus-Porta, M. Wartmann, I. Galuba and R. A. Fairhurst, *ACS Med. Chem. Lett.*, 2018, **9**, 215–220.
327 R. Mah, J. R. Thomas and C. M. Shafer, *Bioorg. Med. Chem. Lett.*, 2014, **24**, 33–39.
328 S. E. Dalton, L. Dittus, D. A. Thomas, M. A. Convery, J. Nunes, J. T. Bush, J. P. Evans, T. Werner, M. Bantscheff, J. A. Murphy and S. Campos, *J. Am. Chem. Soc.*, 2018, **140**, 932–939.
329 M. C. Wahl, C. L. Will and R. Lührmann, *Cell*, 2009, **136**, 701–718.
330 G. M. Hayes, P. E. Carrigan and L. J. Miller, *Cancer Res.*, 2007, **67**, 2072–2080.
331 A. Narayanan and L. H. Jones, *Chem. Sci.*, 2015, **6**, 2650–2659.
332 R. J. Pearson, D. G. Blake, M. Mezna, P. M. Fischer, N. J. Westwood and C. McInnes, *Cell Chem. Biol.*, 2018, **25**, 1107–1116.
333 J. P. Hughes, S. Rees, S. B. Kalindjian and K. L. Philpott, *Br. J. Pharmacol.*, 2011, **162**, 1239–1249.
334 C. H. Wong, K. W. Siah and A. W. Lo, *Biostatistics*, 2019, **2**(20), 273–286.
335 L. V. Sacks, H. H. Shamsuddin, Y. I. Yasinskaya, K. Bouri, M. L. Lanthier and R. E. Sherman, *JAMA*, 2014, **311**, 378–384.
336 T. J. Hwang, D. Carpenter, J. C. Lauffenburger, B. Wang, J. M. Franklin and A. S. Kesselheim, *JAMA Intern. Med.*, 2016, **176**, 1826–1833.
337 C. Printz, *Cancer*, 2015, **121**, 1529–1530.
338 S. Khozin, K. Liu, J. P. Jarow and R. Pazdur, *Nat. Rev. Drug Discovery*, 2015, **14**, 450–451.
339 M. Hay, D. W. Thomas, J. L. Craighead, C. Economides and J. Rosenthal, *Nat. Biotechnol.*, 2014, **32**, 40–51.
340 A. Lin, C. J. Giuliano, A. Palladino, K. M. John, C. Abramowicz, M. L. Yuan, E. L. Sausville, D. A. Lukow, L. Liu, A. R. Chait, Z. C. Galluzzo, C. Tucker and J. M. Sheltzer, *Sci. Transl. Med.*, 2019, **11**, eaaw8412.
341 R. Levi-Montalcini and V. Hamburger, *J. Exp. Zool.*, 1951, **116**, 321–361.
342 R. Levi-Montalcini and S. Cohen, *Proc. Natl. Acad. Sci. U. S. A.*, 1956, **42**, 695–699.

343 S. Cohen, *J. Biol. Chem.*, 2008, **283**, 33793–33797.
344 S. Cohen, *Dev. Biol.*, 1965, **12**, 394–407.
345 J. Bakker, M. Spits, J. Neefjes and I. Berlin, *J. Cell Sci.*, 2017, **130**, 4087–4096.
346 M. Scaltriti and J. Baselga, *Clin. Cancer Res.*, 2006, **12**, 5268–5272.
347 M. J. Wieduwilt and M. M. Moasser, *Cell. Mol. Life Sci.*, 2008, **65**, 1566–1584.
348 E. K. Rowinsky, *Annu. Rev. Med.*, 2004, **55**, 433–457.
349 R. S. Herbst, *Int. J. Radiat. Oncol., Biol., Phys.*, 2004, **59**, S21–S26.
350 T. Yamamoto, H. Hihara, T. Nishida, S. Kawai and K. Toyoshima, *Cell*, 1983, **34**, 225–232.
351 E. M. Bublil and Y. Yarden, *Curr. Opin. Cell Biol.*, 2007, **19**, 124–134.
352 P. M. Harari, *Endocr.-Relat. Cancer*, 2004, **11**, 689–708.
353 B. W. Ennis, M. E. Lippman and R. B. Dickson, *Cancer Invest.*, 1991, **9**, 553–562.
354 R. T. Curnow, *Cancer Immunol. Immunother.*, 1997, **45**, 210–215.
355 M. Schmidt, P. Reiser, D. Hills, W. J. Gullick and W. Wels, *Int. J. Cancer*, 1998, **75**, 878–884.
356 M. H. Cohen, J. R. Johnson, Y.-F. Chen, R. Sridhara and R. Pazdur, *Oncologist*, 2005, **10**, 461–466.
357 D. Saavedra and T. Crombet, *Front. Immunol.*, 2017, **8**, 269.
358 F. Ciardiello, R. Caputo, T. Troiani, G. Borriello, E. R. Kandimalla, S. Agrawal, J. Mendelsohn, A. R. Bianco and G. Tortora, *Int. J. Cancer*, 2001, **93**, 172–178.
359 N. G. Anderson, T. Ahmad, K. Chan, R. Dobson and N. J. Bundred, *Int. J. Cancer*, 2001, **94**, 774–782.
360 H. Patel, R. Pawara, A. Ansari and S. Surana, *Eur. J. Med. Chem.*, 2017, **142**, 32–47.
361 S. Wang, Y. Song and D. Liu, *Cancer Lett.*, 2017, **385**, 51–54.
362 C. M. Lovly and A. T. Shaw, *Clin. Cancer Res.*, 2014, **20**, 2249–2256.
363 J. Wang, B. Wang, H. Chu and Y. Yao, Intrinsic resistance to EGFR tyrosine kinase inhibitors in advanced non-small-cell lung cancer with activating EGFR mutations, https://www.dovepress.com/intrinsic-resistance-to-egfr-tyrosine-kinase-inhibitors-in-advanced-no-peer-reviewed-article-OTT, accessed February 3, 2019.
364 E. L. Kwak, R. Sordella, D. W. Bell, N. Godin-Heymann, R. A. Okimoto, B. W. Brannigan, P. L. Harris, D. R. Driscoll, P. Fidias, T. J. Lynch, S. K. Rabindran, J. P. McGinnis, A. Wissner, S. V. Sharma, K. J. Isselbacher, J. Settleman and D. A. Haber, *Proc. Natl. Acad. Sci. U. S. A.*, 2005, **102**, 7665–7670.
365 S. Kobayashi, H. Ji, Y. Yuza, M. Meyerson, K.-K. Wong, D. G. Tenen and B. Halmos, *Cancer Res.*, 2005, **65**, 7096–7101.
366 D. Li, L. Ambrogio, T. Shimamura, S. Kubo, M. Takahashi, L. Chirieac, R. Padera, G. Shapiro, A. Baum, F. Himmelsbach, W. Rettig, M. Meyerson, F. Solca, H. Greulich and K.-K. Wong, *Oncogene*, 2008, **27**, 4702–4711.
367 J. Marshall, J. Hwang, F. A. L. M. Eskens, H. Burger, S. Malik, M. Uttenreuther-Fischer, P. Stopfer, M. Ould-Kaci, R. B. Cohen and N. L. Lewis, *Invest. New Drugs*, 2013, **31**, 399–408.
368 P. Giordano, A. Manzo, A. Montanino, R. Costanzo, C. Sandomenico, M. C. Piccirillo, G. Daniele, N. Normanno, G. Carillio, G. Rocco, R. Bianco, F. Perrone and A. Morabito, *Crit. Rev. Oncol. Hematol.*, 2016, **97**, 143–151.
369 K. Park, E.-H. Tan, K. O'Byrne, L. Zhang, M. Boyer, T. Mok, V. Hirsh, J. C.-H. Yang, K. H. Lee, S. Lu, Y. Shi, S.-W. Kim, J. Laskin, D.-W. Kim, C. D. Arvis, K. Kölbeck, S. A. Laurie, C.-M. Tsai, M. Shahidi, M. Kim, D. Massey, V. Zazulina and L. Paz-Ares, *Lancet Oncol.*, 2016, **17**, 577–589.
370 A. Mullard, *Nat. Rev. Drug Discovery*, 2018, **17**, 81–85.
371 S. K. Rabindran, C. M. Discafani, E. C. Rosfjord, M. Baxter, M. B. Floyd, J. Golas, W. A. Hallett, B. D. Johnson, R. Nilakantan, E. Overbeek, M. F. Reich, R. Shen, X. Shi, H.-R. Tsou, Y.-F. Wang and A. Wissner, *Cancer Res.*, 2004, **64**, 3958–3965.
372 A. Chan, S. Delaloge, F. A. Holmes, B. Moy, H. Iwata, V. J. Harvey, N. J. Robert, T. Silovski, E. Gokmen, G. von Minckwitz, B. Ejlertsen, S. K. L. Chia, J. Mansi, C. H. Barrios, M. Gnant, M. Buyse, I. Gore, J. Smith, G. Harker, N. Masuda, K. Petrakova, A. G. Zotano, N. Iannotti, G. Rodriguez, P. Tassone, A. Wong, R. Bryce, Y. Ye, B. Yao and M. Martin, *Lancet Oncol.*, 2016, **17**, 367–377.
373 R. Di Lorenzo and M. S. Ahluwalia, *Ther. Adv. Med. Oncol.*, 2017, **9**, 781–796.
374 A. B. Hanker, M. R. Brewer, J. H. Sheehan, J. P. Koch, G. R. Sliwoski, R. Nagy, R. Lanman, M. F. Berger, D. M. Hyman, D. B. Solit, J. He, V. Miller, R. E. Cutler, A. S. Lalani, D. Cross, C. M. Lovly, J. Meiler and C. L. Arteaga, *Cancer Discovery*, 2017, **7**, 575–585.
375 A. Yver, *Ann. Oncol.*, 2016, **27**, 1165–1170.
376 C.-H. Yun, K. E. Mengwasser, A. V. Toms, M. S. Woo, H. Greulich, K.-K. Wong, M. Meyerson and M. J. Eck, *Proc. Natl. Acad. Sci. U. S. A.*, 2008, **105**, 2070–2075.
377 D. A. E. Cross, S. E. Ashton, S. Ghiorghiu, C. Eberlein, C. A. Nebhan, P. J. Spitzler, J. P. Orme, M. R. V. Finlay, R. A. Ward, M. J. Mellor, G. Hughes, A. Rahi, V. N. Jacobs, M. Red Brewer, E. Ichihara, J. Sun, H. Jin, P. Ballard, K. Al-Kadhimi, R. Rowlinson, T. Klinowska, G. H. P. Richmond, M. Cantarini, D.-W. Kim, M. R. Ranson and W. Pao, *Cancer Discovery*, 2014, **4**, 1046–1061.
378 T. S. Mok, Y.-L. Wu, M.-J. Ahn, M. C. Garassino, H. R. Kim, S. S. Ramalingam, F. A. Shepherd, Y. He, H. Akamatsu, W. S. M. E. Theelen, C. K. Lee, M. Sebastian, A. Templeton, H. Mann, M. Marotti, S. Ghiorghiu, V. A. Papadimitrakopoulou and AURA3 Investigators, *N. Engl. J. Med.*, 2017, **376**, 629–640.
379 S. Wang, S. T. Tsui, C. Liu, Y. Song and D. Liu, *J. Hematol. Oncol.*, 2016, **9**, 59.
380 M. Günther, J. Lategahn, M. Juchum, E. Döring, M. Keul, J. Engel, H. L. Tumbrink, D. Rauh and S. Laufer, *J. Med. Chem.*, 2017, **60**, 5613–5637.
381 J. A. Engelman, K. Zejnullahu, C.-M. Gale, E. Lifshits, A. J. Gonzales, T. Shimamura, F. Zhao, P. W. Vincent, G. N. Naumov, J. E. Bradner, I. W. Althaus, L. Gandhi, G. I. Shapiro, J. M. Nelson, J. V. Heymach, M. Meyerson, K.-K. Wong and P. A. Jänne, *Cancer Res.*, 2007, **67**, 11924–11932.

382 S.-H. I. Ou and R. A. Soo, *Drug. Des., Dev. Ther.*, 2015, **9**, 5641–5653.
383 Y.-L. Wu, Y. Cheng, X. Zhou, K. H. Lee, K. Nakagawa, S. Niho, F. Tsuji, R. Linke, R. Rosell, J. Corral, M. R. Migliorino, A. Pluzanski, E. I. Sbar, T. Wang, J. L. White, S. Nadanaciva, R. Sandin and T. S. Mok, *Lancet Oncol.*, 2017, **18**, 1454–1466.
384 A. Passaro and F. de Marinis, *Transl. Lung Cancer Res.*, 2018, **7**, S100–S102.
385 S. Pal Singh, F. Dammeijer and R. W. Hendriks, *Mol. Cancer*, 2018, **17**, 57.
386 A. J. Mohamed, L. Yu, C.-M. Bäckesjö, L. Vargas, R. Faryal, A. Aints, B. Christensson, A. Berglöf, M. Vihinen, B. F. Nore and C. I. E. Smith, *Immunol. Rev.*, 2009, **228**, 58–73.
387 S. Mahajan, A. Vassilev, N. Sun, Z. Ozer, C. Mao and F. M. Uckun, *J. Biol. Chem.*, 2001, **276**, 31216–31228.
388 D. A. Fruman, H. Chiu, B. D. Hopkins, S. Bagrodia, L. C. Cantley and R. T. Abraham, *Cell*, 2017, **170**, 605–635.
389 J. B. Petro and W. N. Khan, *J. Biol. Chem.*, 2001, **276**, 1715–1719.
390 A. Maas and R. W. Hendriks, *Dev. Immunol.*, 2001, **8**, 171–181.
391 J. S. Smolen and G. Steiner, *Nat. Rev. Drug Discovery*, 2003, **2**, 473–488.
392 S. Cheng, J. Ma, A. Guo, P. Lu, J. P. Leonard, M. Coleman, M. Liu, J. J. Buggy, R. R. Furman and Y. L. Wang, *Leukemia*, 2014, **28**, 649–657.
393 M. Spaargaren, M. F. M. de Rooij, A. P. Kater and E. Eldering, *Oncogene*, 2015, **34**, 2426–2436.
394 J. A. Woyach, E. Bojnik, A. S. Ruppert, M. R. Stefanovski, V. M. Goettl, K. A. Smucker, L. L. Smith, J. A. Dubovsky, W. H. Towns, J. MacMurray, B. K. Harrington, M. E. Davis, S. Gobessi, L. Laurenti, B. Y. Chang, J. J. Buggy, D. G. Efremov, J. C. Byrd and A. J. Johnson, *Blood*, 2014, **123**, 1207–1213.
395 S. E. M. Herman, A. L. Gordon, E. Hertlein, A. Ramanunni, X. Zhang, S. Jaglowski, J. Flynn, J. Jones, K. A. Blum, J. J. Buggy, A. Hamdy, A. J. Johnson and J. C. Byrd, *Blood*, 2011, **117**, 6287–6296.
396 H. Park, D. Zhao, G. Tsourdinis, Z. Ou, A. T. Tamayo, R. J. Ford, B. Fang, L. V. Pham, L. Zhang and M. Wang, *Blood*, 2014, **124**, 3028.
397 S. Mahajan, S. Ghosh, E. A. Sudbeck, Y. Zheng, S. Downs, M. Hupke and F. M. Uckun, *J. Biol. Chem.*, 1999, **274**, 9587–9599.
398 Z. Pan, H. Scheerens, S.-J. Li, B. E. Schultz, P. A. Sprengeler, L. C. Burrill, R. V. Mendonca, M. D. Sweeney, K. C. K. Scott, P. G. Grothaus, D. A. Jeffery, J. M. Spoerke, L. A. Honigberg, P. R. Young, S. A. Dalrymple and J. T. Palmer, *ChemMedChem*, 2007, **2**, 58–61.
399 L. A. Honigberg, A. M. Smith, M. Sirisawad, E. Verner, D. Loury, B. Chang, S. Li, Z. Pan, D. H. Thamm, R. A. Miller and J. J. Buggy, *Proc. Natl. Acad. Sci. U. S. A.*, 2010, **107**, 13075–13080.
400 R. H. Advani, J. J. Buggy, J. P. Sharman, S. M. Smith, T. E. Boyd, B. Grant, K. S. Kolibaba, R. R. Furman, S. Rodriguez, B. Y. Chang, J. Sukbuntherng, R. Izumi, A. Hamdy, E. Hedrick and N. H. Fowler, *J. Clin. Oncol.*, 2013, **31**, 88–94.
401 J. C. Byrd, R. R. Furman, S. E. Coutre, I. W. Flinn, J. A. Burger, K. A. Blum, B. Grant, J. P. Sharman, M. Coleman, W. G. Wierda, J. A. Jones, W. Zhao, N. A. Heerema, A. J. Johnson, J. Sukbuntherng, B. Y. Chang, F. Clow, E. Hedrick, J. J. Buggy, D. F. James and S. O'Brien, *N. Engl. J. Med.*, 2013, **369**, 32–42.
402 S. O'Brien, J. A. Jones, S. E. Coutre, A. R. Mato, P. Hillmen, C. Tam, A. Österborg, T. Siddiqi, M. J. Thirman, R. R. Furman, O. Ilhan, M. J. Keating, T. G. Call, J. R. Brown, M. Stevens-Brogan, Y. Li, F. Clow, D. F. James, A. D. Chu, M. Hallek and S. Stilgenbauer, *Lancet Oncol.*, 2016, **17**, 1409–1418.
403 J. C. Byrd, J. R. Brown, S. O'Brien, J. C. Barrientos, N. E. Kay, N. M. Reddy, S. Coutre, C. S. Tam, S. P. Mulligan, U. Jaeger, S. Devereux, P. M. Barr, R. R. Furman, T. J. Kipps, F. Cymbalista, C. Pocock, P. Thornton, F. Caligaris-Cappio, T. Robak, J. Delgado, S. J. Schuster, M. Montillo, A. Schuh, S. de Vos, D. Gill, A. Bloor, C. Dearden, C. Moreno, J. J. Jones, A. D. Chu, M. Fardis, J. McGreivy, F. Clow and D. F. James, and P. Hillmen, *N. Engl. J. Med.*, 2014, **371**, 213–223.
404 C. Grommes, S. S. Tang, J. Wolfe, T. J. Kaley, M. Daras, E. I. Pentsova, A. F. Piotrowski, J. Stone, A. Lin, C. P. Nolan, M. Manne, P. Codega, C. Campos, A. Viale, A. A. Thomas, M. F. Berger, V. Hatzoglou, A. S. Reiner, K. S. Panageas, L. M. DeAngelis and I. K. Mellinghoff, *Blood*, 2019, **133**, 436–445.
405 P. L. R. Nicolson, C. E. Hughes, S. Watson, S. H. Nock, A. T. Hardy, C. N. Watson, S. J. Montague, H. Clifford, A. P. Huissoon, J.-D. Malcor, M. R. Thomas, A. Y. Pollitt, M. G. Tomlinson, G. Pratt and S. P. Watson, *Haematologica*, 2018, **103**, 2097–2108.
406 J. C. Byrd, B. Harrington, S. O'Brien, J. A. Jones, A. Schuh, S. Devereux, J. Chaves, W. G. Wierda, F. T. Awan, J. R. Brown, P. Hillmen, D. M. Stephens, P. Ghia, J. C. Barrientos, J. M. Pagel, J. Woyach, D. Johnson, J. Huang, X. Wang, A. Kaptein, B. J. Lannutti, T. Covey, M. Fardis, J. McGreivy, A. Hamdy, W. Rothbaum, R. Izumi, T. G. Diacovo, A. J. Johnson and R. R. Furman, *N. Engl. J. Med.*, 2016, **374**, 323–332.
407 R. Famà, R. Bomben, S. Rasi, M. D. Bo, C. Ciardullo, S. Monti, F. Rossi, T. D'Agaro, A. Zucchetto, V. Gattei, G. Gaidano and D. Rossi, *Blood*, 2014, **124**, 3831–3833.
408 V. Patel, K. Balakrishnan, E. Bibikova, M. Ayres, M. J. Keating, W. G. Wierda and V. Gandhi, *Clin. Cancer Res.*, 2017, **23**, 3734–3743.
409 T. Barf, T. Covey, R. Izumi, B. van de Kar, M. Gulrajani, B. van Lith, M. van Hoek, E. de Zwart, D. Mittag, D. Demont, S. Verkaik, F. Krantz, P. G. Pearson, R. Ulrich and A. Kaptein, *J. Pharmacol. Exp. Ther.*, 2017, **363**, 240–252.
410 J. K. Park, J.-Y. Byun, J. A. Park, Y.-Y. Kim, Y. J. Lee, J. I. Oh, S. Y. Jang, Y. H. Kim, Y. W. Song, J. Son, K. H. Suh, Y.-M. Lee and E. B. Lee, *Arthritis Res. Ther.*, 2016, **18**, 91.
411 E. K. Evans, R. Tester, S. Aslanian, R. Karp, M. Sheets, M. T. Labenski, S. R. Witowski, H. Lounsbury, P. Chaturvedi,

H. Mazdiyasni, Z. Zhu, M. Nacht, M. I. Freed, R. C. Petter, A. Dubrovskiy, J. Singh and W. F. Westlin, *J. Pharmacol. Exp. Ther.*, 2013, **346**, 219–228.

412 A Study of Efficacy and Safety of M2951 in Subjects With Relapsing Multiple Sclerosis – Full Text View – ClinicalTrials.gov, https://clinicaltrials.gov/ct2/show/NCT02975349, accessed January 14, 2019.

413 C. L. Langrish, J. M. Bradshaw, T. D. Owens, R. L. Campbell, M. R. Francesco, D. E. Karr, S. K. Murray, R. C. Quesenberry, P. F. Smith, M. D. Taylor, J. Zhu, P. A. Nunn and S. G. Gourlay, *Blood*, 2017, **130**, 1052.

414 BMS-986195 Is a Highly Selective and Rapidly Acting Covalent Inhibitor of Bruton's Tyrosine Kinase with Robust Efficacy at Low Doses in Preclinical Models of RA and Lupus Nephritis, https://acrabstracts.org/abstract/bms-986195-is-a-highly-selective-and-rapidly-acting-covalent-inhibitor-of-brutons-tyrosine-kinase-with-robust-efficacy-at-low-doses-in-preclinical-models-of-ra-and-lupus-nephritis/, accessed January 14, 2019.

415 A Phase, Single-Ascending-Dose, Safety, Tolerability, Pharmacokinetic(PK), and Pharmacodynamic(PD) Study of BIIB068 in Healthy Participants – Full Text View – ClinicalTrials.gov, https://clinicaltrials.gov/ct2/show/NCT02829541, accessed January 14, 2019.

416 H. Pajouhesh and G. R. Lenz, *NeuroRx*, 2005, **2**, 541–553.

417 S. A. Hitchcock and L. D. Pennington, *J. Med. Chem.*, 2006, **49**, 7559–7583.

418 J. Jiang, M. Shen, C. J. Thomas and M. B. Boxer, *Curr. Top. Med. Chem.*, 2011, **11**, 800–809.

419 J. B. Baell and G. A. Holloway, *J. Med. Chem.*, 2010, **53**, 2719–2740.

420 J. B. Baell and J. W. M. Nissink, *ACS Chem. Biol.*, 2018, **13**, 36–44.

421 C. J. Martyniuk, A. Feswick, B. Fang, J. M. Koomen, D. S. Barber, T. Gavin and R. M. LoPachin, *Toxicol. Lett.*, 2013, **219**, 279–287.

422 S. Nijmeijer, H. Engelhardt, S. Schultes, A. C. van de Stolpe, V. Lusink, C. de Graaf, M. Wijtmans, E. E. J. Haaksma, I. J. P. de Esch, K. Stachurski, H. F. Vischer and R. Leurs, *Br. J. Pharmacol.*, 2013, **170**, 89–100.

423 Y. Liu, M. P. Patricelli and B. F. Cravatt, *Proc. Natl. Acad. Sci. U. S. A.*, 1999, **96**, 14694–14699.

424 D. Weichert and P. Gmeiner, *ACS Chem. Biol.*, 2015, **10**, 1376–1386.

425 S. G. Kathman and A. V. Statsyuk, *MedChemComm*, 2016, **7**, 576–585.

426 A. Jones, X. Zhang and X. Lei, *Cell Chem. Biol.*, 2017, **24**, 537–539.

427 J. Strelow, W. Dewe, P. W. Iversen, H. B. Brooks, J. A. Radding, J. McGee and J. Weidner, in *Assay Guidance Manual*, ed. G. S. Sittampalam, N. P. Coussens, K. Brimacombe, A. Grossman, M. Arkin, D. Auld, C. Austin, J. Baell, B. Bejcek, J. M. M. Caaveiro, T. D. Y. Chung, J. L. Dahlin, V. Devanaryan, T. L. Foley, M. Glicksman, M. D. Hall, J. V. Haas, J. Inglese, P. W. Iversen, S. D. Kahl, S. C. Kales, M. Lal-Nag, Z. Li, J. McGee, O. McManus, T. Riss, O. J. Trask, J. R. Weidner, M. J. Wildey, M. Xia and X. Xu, Eli Lilly & Company and the National Center for Advancing Translational Sciences, Bethesda (MD), 2004.

428 D. K. Nomura, M. M. Dix and B. F. Cravatt, *Nat. Rev. Cancer*, 2010, **10**, 630–638.

429 C. M. Harris, S. E. Foley, E. R. Goedken, M. Michalak, S. Murdock and N. S. Wilson, *SLAS Discovery*, 2018, **10**(23), 1040–1050.

430 J. M. Strelow, *SLAS Discovery*, 2017, **22**, 3–20.

431 B.-F. Krippendorff, R. Neuhaus, P. Lienau, A. Reichel and W. Huisinga, *J. Biomol. Screening*, 2009, **14**, 913–923.

432 I. Miyahisa, T. Sameshima and M. S. Hixon, *Angew. Chem., Int. Ed.*, 2015, **54**, 14099–14102.

433 P. Li, C. Lu, S. K. Balani and L.-S. Gan, *Drug Metab. Dispos.*, 2011, **39**, 1054–1057.

434 A. Zimmerlin, M. Trunzer and B. Faller, *Drug Metab. Dispos.*, 2011, **39**, 1039–1046.

435 P. A. Schwartz, P. Kuzmic, J. Solowiej, S. Bergqvist, B. Bolanos, C. Almaden, A. Nagata, K. Ryan, J. Feng, D. Dalvie, J. C. Kath, M. Xu, R. Wani and B. W. Murray, *Proc. Natl. Acad. Sci. U. S. A.*, 2014, **111**, 173–178.

436 Z. Fang, Y. Song, P. Zhan, Q. Zhang and X. Liu, *Future Med. Chem.*, 2014, **6**, 885–901.

437 R. S. Lo, *Pharmacogenomics*, 2012, **13**, 125–128.

438 D. S. Neel and T. G. Bivona, *npj Precis. Oncol.*, 2017, **1**, 3.

439 L. G. Ahronian and R. B. Corcoran, *Genome Med.*, 2017, **9**, 37.

440 J. M. Bradshaw, J. M. McFarland, V. O. Paavilainen, A. Bisconte, D. Tam, V. T. Phan, S. Romanov, D. Finkle, J. Shu, V. Patel, T. Ton, X. Li, D. G. Loughhead, P. A. Nunn, D. E. Karr, M. E. Gerritsen, J. O. Funk, T. D. Owens, E. Verner, K. A. Brameld, R. J. Hill, D. M. Goldstein and J. Taunton, *Nat. Chem. Biol.*, 2015, **11**, 525–531.

441 D. A. Shannon, R. Banerjee, E. R. Webster, D. W. Bak, C. Wang and E. Weerapana, *J. Am. Chem. Soc.*, 2014, **136**, 3330–3333.

442 A. M. Embaby, S. Schoffelen, C. Kofoed, M. Meldal and F. Diness, *Angew. Chem., Int. Ed.*, 2018, **57**, 8022–8026.

443 B. Wingelhofer, B. Maurer, E. C. Heyes, A. A. Cumaraswamy, A. Berger-Becvar, E. D. de Araujo, A. Orlova, P. Freund, F. Ruge, J. Park, G. Tin, S. Ahmar, C.-H. Lardeau, I. Sadovnik, D. Bajusz, G. M. Keserű, F. Grebien, S. Kubicek, P. Valent, P. T. Gunning and R. Moriggl, *Leukemia*, 2018, **32**, 1135–1146.

444 D. P. Ball, A. M. Lewis, D. Williams, D. Resetca, D. J. Wilson and P. T. Gunning, *Oncotarget*, 2016, **7**, 20669–20679.

445 A. G. Dossetter, E. J. Griffen and A. G. Leach, *Drug Discovery Today*, 2013, **18**, 724–731.